Cell adhesion and signalling at implantation

Youn-Jung Kang

Nuffield Department of Obstetrics and Gynaecology

St. Catherine's College

A thesis submitted for the degree of Doctor of Philosophy

April 2012

Supervised by:

Professor John Aplin

(Maternal and Fetal Health, University of Manchester)

Dr. Kevin Coward

(Nuffield Department of Obstetrics and Gynaecology, University of Oxford)

Acknowledgements

I am greatly indebted to my principal supervisor, Professor John Aplin, for supervising me with his instructive criticism, valuable advice and support throughout the last 2 years and for his careful feedback and comments on this thesis. His broad and enthusiasitic knowledge of reproductive biology and his logical way of thinking has inspired me throughout the years I spent in his laboratory. I also owe my deepest gratitude to my co-supervisor, Dr. Kevin Coward, for mentoring me to have confidence all the time, his bottomless support, precious advice and critical review of this thesis. His confidence in science and optimistic attitude in general encouraged me to believe in myself. I sincerely thank Professor Sue Kimber for her guidance, for critically analysing my work, and for full supporting the embryo work throughout my D.Phil. My special thanks go to Dr. Karen Forbes for encouraging me all the time to boost my capacity in the laboratory and for showing me the positive way to think every time I faced difficulties.

I am also deeply grateful to the Nuffield Department of Obstetrics and Gynaecology, especially Professor Ian Sargent, Ms. Pip Elphick, Ms. Janet Carver, and Mrs. Celine Jones, for supporting me to carry out my studies, both mentally and financially. An equal amount of gratitude is owed to my colleagues (Dr. Raja Nardif, Dr. Michelle Desforge, Dr. Lynda Harris, and Miss Sylvia Lui) in the Maternal and Fetal Health, University of Manchester, for sharing their invaluable knowledge with me and for always being helpful. I also would like to thank to Professor Helen Mardon for providing me an opportunity to start my D.Phil at the University of Oxford.

Last but the most, I would like to take this opportunity to express my profound gratitude to my beloved parents and little sister back home for their endless love and everlasting support, and for always being proud of me.

Table of contents

List of abbreviations…..viii

List of figures…..xii

List of tables.....xviii

Abstract…….....1

Chapter 1: General Introduction

1.1 Endometrium…….....2

1.2 The menstrual cycle…….…….....2

1.3 Development of the embryo…….…….....4

1.4 Implantation…….....6

1.5 Differences of implantation between species…….....8

1.6 Molecular factors…….....12

1.6.1 Anti-cellular adhesion molecule: MUC1……..…..…….....12

1.6.2 Cellular adhesion molecules: Integrins…….....19

1.6.2.1 Endometrial integrins and αvβ3……..…….....22

1.6.3 Extracellular matrix molecules: Osteopontin.....27

1.6.4 Growth factors …….....33

1.6.4.1 Insulin-like growth factor-I…….....33

1.6.4.2 Heparin-binding EGF-like growth factor.....38

1.7 *In vitro* models for the study of implantation…….....44

1.8 Ishikawa cells…….....48

1.9 Aims and approaches…….....49

Chapter 2: Materials & Methods

2.1 General reagents and solutions.....51

2.2 Antibodies…….....51

2.3 Cell culture…….....55

2.3.1 Endometrial epithelial cell line and maintenance……..….....55

2.3.2 Primary endometrial stromal cells and maintenance.....56

2.3.3 Sub-culturing of endometrial cells by trypsinisation.....56

2.3.4 Freezing and retrieving endometrial cells.....57

2.4 Embryo culture…….....57

2.4.1 Human embryos…….…….....58

2.4.2 Criteria used for the grading of human embryos.....…….....58

2.4.3 Mouse embryos (University of Oxford)….....61

2.4.4 Mouse embryos (University of Manchester).....61

2.4.4.1 Maintenance of animals…….....61

2.4.4.2 Mating and superovulation…….....62

2.4.4.3 Retrieval and culture of two-cell stage mouse embryos……..….....62

2.5 Co-culture of embryos with endometrial cells……..….....64

2.5.1 Two-dimensional (2D) culture.....64

2.5.2 Three-dimensional (3D) culture…….....64

2.6 Embryo attachment assay…….....65

2.7 Co-culture of growth factor-coated beads with endometrial cells.....66

2.7.1 Preparation of growth factor-coated beads.....66

2.7.2 Co-culture of beads on Ishikawa cell monolayers.....67

2.8 Immunocytochemistry……..…..…….....67

2.8.1 Immunocytochemical investigation of a 2-dimensional *in vitro* model…..….67

2.8.2 Immunocytochemical investigation of a 3-dimensional *in vitro* model.....…..68

2.8.3 Image analysis of immunocytochemical data…….…..69

2.9 Western blot analysis …….……..…….....69

2.9.1 Preparation of whole cell extracts..……...….....69

2.9.2 Quantification of protein levels…….……..….70

2.9.3 Preparation of protein lysate samples…….....…...70

2.9.4 SDS-polyacrylamide gel electrophoresis (SDS-PAGE)….……...…..…70

2.9.5 Electrophoretic transfer of proteins to PVDF membranes....……....72

2.9.6 Immunological detection of proteins……...72

2.9.7 Stripping and re-probing membrane……..……..……..….73

2.10 Cell adhesion assays…….……..…….....73

2.11 Cell-surface protein labeling with biotin……..…….….....74

2.12 Transfection of cells with short-interfering RNA..……..…….....75

2.13 Immunoprecipitation..…….……..…….….....79

2.14 Statistical analysis……...…….……..…….…....80

Chapter 3:

Establishment of an *in vitro* model of embryo implantation and investigation of molecular crosstalk between the attaching blastocyst and endometrial epithelial cells

3.1 Introduction.....81

3.2 Results……..…….....83

3.2.1 Establishment of an *in vitro* model of embryo implantation.....83

3.2.1.1 Verification of Ishikawa cells as an endometrial epithelial model..…83

3.2.1.2 Two-dimensional and three-dimensional models……..….....85

3.2.1.3 Attachment of embryos *in vitro*…….…….....86

3.2.1.4 Assessing the stability of embryo attachment.….....88

3.2.1.5 Heterologous vs. homologous *in vitro* models….....90

3.2.2 Molecular evidence for crosstalk between the attaching blastocyst and endometrial epithelial cells…….....….92

3.2.2.1 Clearance of MUC1 from Ishikawa cells after embryo attachment…92

3.2.2.1.1 MUC1 clearance in heterologous 2D culture…….....95

3.2.2.1.2 MUC1 clearance in heterologous 3D culture……..……..100

3.2.2.1.3 MUC1 clearance in homologous 2D culture…….....102

3.2.2.2 Up-regulation of integrin αvβ3 at the site of embryo attachment.....106

3.2.2.2.1 Integrin αvβ3 expression in 2D heterologous culture….....110

3.2.2.2.2 Integrin αvβ3 expression in 3D homologous gels……..…...114

3.2.2.2.3 Integrin αvβ3 expression in homologous 2D culture..….....119

3.2.2.2.4 Analysis of integrin β3 in 2D model by Western blotting ...124

3.2.2.3 Stable expression of integrin αvβ5 on Ishikawa cells after embryo attachment…….....….126

3.2.2.3.1 Integrin αvβ5 expression in heterologous 3D culture…….127

3.2.2.3.2 Integrin αvβ5 expression in homologous 2D culture….....129

3.2.2.4 Up-regulation of OPN at the site of embryo attachment.....….132

3.2.2.4.1 OPN expression in heterologous 2D culture...…….……132

3.2.2.4.2 Up-regulation of OPN protein in the presence of mouse embryos attachment at the protein level…….....136

3.2.2.5 Up-regulation of HB-EGF near the site of embryo attachment in heterologous 2D culture…..……..……..…….....…..138

3.2.2.6 Integrin αvβ3 knock-down suppresses mouse embryo attachment...142

3.2.2.7 OPN knock-down suppresses mouse embryo attachment…….....146

3.3 Discussion 149

3.3.1 General summary of main results.....149

3.3.2 Stages of embryo implantation.....150

3.3.3 Clearance of MUC1……..…….....152

3.3.4 Integrins of the αv family……..…….……154

3.3.5 OPN in embryo attachment…….……...…….……...……..158

3.3.6 HB-EGF in embryo attachment…..……....…….160

3.3.7 Concluding remarks…….....162

Chapter 4: Cell signalling at implantation

4.1 Introduction.....163

4.2 Results.....165

4.2.1 IGF-I and HB-EGF regulate the expression of integrin β3 and OPN in Ishikawa cells…..…….....…….....165

4.2.2 Cleaved OPN is localised on the apical surface of Ishikawa cells.....169

4.2.3 OPN promotes cell adhesion……..….172

4.2.4 Factors down-stream of IGF-I and HB-EGF…….…..…..…….....175

4.2.5 Protein-protein interaction in response to IGF-I.……..…..…..…..…....179

4.2.6 IGF-IR regulates embryo attachment…….....183

4.2.6.1 Up-regulation of IGF-IR at the site of embryo attachment in a 2D heterologous *in vitro* model..183

4.2.6.2 SiRNA-mediated knock-down of IGF-IR suppresses embryo attachment……187

4.2.7 SHP-2 regulates embryo attachment……190

4.2.7.1 Up-regulation of SHP-2 at the site of embryo attachment.....190

4.2.7.2 SiRNA-mediated knock-down of SHP-2 suppresses embryo attachment……193

4.2.8 Attachment of bead carrying proteins *in vitro*……196

4.2.8.1 SiRNA-mediated knock-down of integrin αvβ3 suppresses the attachment of beads bearing IGF-I, HB-EGF, or OPN.....199

4.2.8.2 SiRNA-mediated knock-down of OPN suppresses the attachment of beads bearing IGF-I or OPN but not beads bearing HB-EGF.....202

4.2.8.3 SiRNA-mediated knock-down of IGF-IR suppresses the attachment of beads bearing IGF-I, HB-EGF, or OPN…….....204

4.2.8.4 SiRNA-mediated knock-down of SHP-2 suppresses the attachment of beads bearing IGF-I, HB-EGF, or OPN……207

4.3 Discussion 210

4.3.1 General summary of main results……..…….....210

4.3.2 The role of OPN in embryo attachment…….....211

4.3.3 The role of IGF-I-integrin αvβ3-SHP-2 in embryo attachment……..….215

4.3.4 The role of HB-EGF-ErbB4-integrin αvβ3 in embryo attachment…….....217

4.3.5 The role of molecular crosstalk regulating embryo attachment……..….219

4.3.6 Concluding remarks.....221

Chapter 5: General discussion

5.1 General discussion…….....222

5.2 Recapitulation of the key phases of embryo attachment in vitro.....223

5.3 Embryo-uterine crosstalk.....224

5.4 A novel in vitro embryo attachment assay.....226

5.5 IGF-integrin αvβ3-HB-EGF signalling….....227

5.6 Clinical implications of integrin αvβ3-OPN as a potential biomarker for infertility…….....230

5.7 Future directives and general conclusion..….....231

References 234

Supplementary Appendices 270

List of publications 277

List of Abbreviations

The following is an explanation of commonly used abbreviations used throughout the text. Other, less commonly used abbreviations are explained within the text where appropriate.

2D	2-Dimensional
3D	3-Dimensional
ADAM 17	A Disintegrin And Metalloproteinase 17
ANOVA	Analysis of variance
AR	Amphiregulin
ART	Assisted Reproductive Technologies
BSA	Bovine Serum Albumin
BSP1	Bone Sialoprotein 1
BTC	β-cellulin
cAMP	Cyclic Adenosine Monophosphate
CSFM-3	Complex Serum-Free Medium
DAPI	4',6-diamidino-2-phenylindole
DKK-1	Dickkopf-1
DMEM-F12	Dulbecco's Modified Eagle Medium-Ham F12
DMSO	Dimethyl Sulfoxide
DOK	Docking protein
DTT	Dithiothreitol
ECC	Endometrial adenocarcinoma cell line
ECACC	European Collection of Cell Cultures
ECM	Extra Cellular Matrix
EDTA	Ethylenediaminetetraacetic acid

EGF	Epidermal Growth Factor
EGFR	Epidermal Growth Factor Receptor
EMT	Epithelial Mesenchymal Transition
EPR	Epiregulin
ERM	Ezrin/Radixin/Moesin
Eta 1	Early T-lymphocyte activation factor 1
FAK	Focal Adhesion Kinase
FCS	Fetal Calf Serum
FSH	Follicle Stimulating Hormone
GAPDH	Glyceraldehyde 3-phosphate dehydrogenase
HB-EGF	Heparin Binding Epidermal Growth Factor
hCG	Human Chorionic Gonadotropin
HER 1/4	Human epidermal growth factor receptor 1/4
HFEA	Human Fertilisation and Embryology Authority
HOXA	Homeobox gene
HRP	Horseradish Peroxidase
HSA	Human Serum Albumin
HSPG	Heparin Sulphate Proteoglycan
ICAM	Intracellular Adhesion Molecule
ICM	Inner Cell Mass
IGF-1	Insulin-like Growth Factor-1
IGF-II	Insulin-like Growth Factor-2
IGFR	Insulin-like Growth Factor Receptor
IGFBP	Insulin-like Growth Factor Binding Protein
IL	Interleukin
IRS	Insulin Receptor Substrate
IVF	In Vitro Fertilisation
LH	Luteinising Hormone

LIF	Leukemia Inhibitory Factor
MAPK	Mitogen Activated Protein Kinase
MMP	Matrix metalloproteinase
MUC1	Mucin 1
NRG-1,2	Neuregulin-1, 2
OPN	Osteopontin
PBS	Phosphate Buffered Saline
PCOS	Polycystic Ovary Syndrome
PDGF	Platelet-derived Growth Factor
PDGFR	Platelet-derived Growth Factor Receptor
PECAM-I	Platelet-Endothelial Cell Adhesion Molecule-1
PFA	Paraformaldehyde
PI3K	Phosphoinositide 3-Kinase
PMSG	Pregnant Mare Serum Gonadotropin
PTPs	Protein Tyrosine Phosphatases
PTPN 11	Tyrosine-protein Phosphatase Non-receptor Type 11
PTX-3	Pentraxin-3
PVDF	Polyvinylidene fluoride
QRT-PCR	Quantitative Reverse Transcriptase-Polymerase Chain Reaction
RGD	Arginine-glycine-aspartic acid
RIPA	Radioimmunoprecipitation assay buffer
RNA	Ribonucleic acid
SAHA	Suberoylanilide hydoxamic acid
SFK	Src Family Kinase
SH2	Src Homology 2
SHC	Src Homology Collagen
SHP2	Src-Homology 2 containing Phosphotyrosine phosphatase-2
SHPS1	Src-Homology 2 containing Phosphotyrosine phosphatase Substrate 1

SIBLING	Small Integrin Binding Ligand N-linked Glycoprotein
siRNA	Small Interfering RNA
SOX-4	Sry-related high mobility group-box 4
SPP1	Secreted phosphoprotein 1
TACE	Tumour Necrosis factor-A Converting Enzyme
TBS	Tris Buffered Saline
TE	Trophectoderm
TGF	Transforming growth factor
TIMP-3	Tissue Inhibitor of Metalloproteinase-3
VCAM	Vascular Cell Adhesion Molecule
VGF	Vaccinia virus growth factor

List of Figures

Chapter 1: General introduction

Figure 1.1: The menstrual cycle….....3

Figure 1.2: Development of the human embryo……..…….....5

Figure 1.3: Initial interactions between the embryo and endometrium….....7

Figure 1.4: Differences of implantation between species…….....10

Figure 1.5: Structure of MUC1…….....13

Figure 1.6: A schematic diagram of MUC1 and transport of MUC1-C receptor to thenucleus…….…….....15

Figure 1.7: Function of MUC1 as an anti-adhesion molecule acting as a barrier of endometrium during embryo attachment…….…….....17

Figure 1.8: A schematic diagram of α and β integrin subunits…….....21

Figure 1.9: Structure of OPN, integrin-binding sequences, cognate receptors, and sites for proteolytic cleavage……..……....28

Figure 1.10: Possible interaction between embryonic trophoblast and endometrial epithelium……..……..32

Figure 1.11: IGF-I and integrin αvβ3-linked signalling pathway….....37

Figure 1.12: Structure of proHB-EGF.....39

Figure 1.13: Process of HB-EGF signalling.....41

Figure 1.14: Paracrine and juxtacrine intercellular signal transduction via HB-EGF…….....43

Chapter 2: Materials & Methods

Figure 2.1: Grading criteria for human embryos…….....60

Figure 2.2: Process of retrieval for two-cell stage embryos from mouse oviducts….....63

Figure 2.3: Summary of cell surface protein isolation procedure……..….....75

Chapter 3:

Establishment of *in vitro* model of embryo implantation and investigation of molecular crosstalk between the attaching blastocyst and endometrial epithelial cells

Figure 3.1: Immunofluorescence staining for Cytokeratin and E-cadherin in Ishikawa cells…….....84

Figure 3.2: Schematic diagrams of 2D and 3D *in vitro* models.....…….....85

Figure 3.3: Attachment of embryos in *in vitro* gels……..……..….....87

Figure 3.4: Embryo attachment at each standardised stage used throughout this thesis……..…….....89

Figure 3.5: 2D and 3D *in vitro* models of embryo implantation…….....91

Figure 3.6: Localisation of MUC1 in Ishikawa cells……..…….....93

Figure 3.7: Qualification of MUC1 intensity profiling in Ishikawa cells.....94

Figure 3.8: MUC1 clearance in heterologous 2D culture…….....96

Figure 3.9: Quantification of MUC1 intensity profiling in heterologous 2D culture…….....97/98

Figure 3.10: Enlarged images of MUC1 clearance in heterologous 2D culture…....99

Figure 3.11: MUC1 clearance in heterologous 3D culture……..…...101

Figure 3.12: MUC1 clearance in homologous 2D culture.……..103/104

Figure 3.13: Quantification of MUC1 intensity profiling in homologous 2D culture……...…….105

Figure 3.14: Localisation of integrin αvβ3 in Ishikawa cells….……..…...107

Figure 3.15: Quantification of integrin αvβ3 intensity profiling in Ishikawa cells……...…..……..…...108

Figure 3.16: Localisation of integrin αvβ3 at higher magnification.……..…...109

Figure 3.17: Integrin αvβ3 staining of 2D culture…….…….....111

Figure 3.18: Quantification of integrin αvβ3 intensity profiling in heterologous 2D culture……..……..…….....112

Figure 3.19: Localisation of integrin αvβ3 and E-cadherin adjacent to mouse embryo attachment site…….....113

Figure 3.20: Localisation of integrin αvβ3 in the 3D gel…….……..115/116

Figure 3.21: Localisation of integrin αvβ3 in heterologous 3D gel.……..117/118

Figure 3.22: Integrin αvβ3 in homologous 2D culture…….…….....120

Figure 3.23: Actin (counter-stained to integrin αvβ3) in homologous 2D culture.……..……..…….....121

Figure 3.24: Quantification of integrin αvβ3 intensity profiling in homologous 2D culture.…….....122/123

Figure 3.25: Western blotting analysis of integrin β3 in Ishikawa control cells and cells with 5 attached mouse embryos ……...125

Figure 3.26: Localisation of integrin αvβ5 in Ishikawa cells……..…….....126

Figure 3.27: Integrin αvβ5 in heterologous 3D gel.. ..……..…….....127

Figure 3.28: Surface intensity of integrin αvβ5 in heterologous 3D gel.....…….....128

Figure 3.29: Localisation of integrin αvβ5 in homologous 2D culture…….....130

Figure 3.30: Quantification of integrin αvβ5 intensity profiling in homologous 2D culture……. …….....131

Figure 3.31: Localisation of OPN in Ishikawa cells…….……....133

Figure 3.32: OPN in homologous 2D culture…….…….....134

Figure 3.33: OPN in homologous 2D culture at higher magnification…….....135

Figure 3.34: Western blotting analysis of OPN on Ishikawa cells alone and Ishikawa cells including 5 attached mouse embryos…..…….....137

Figure 3.35: Localisation of HB-EGF on 2D heterologous gels....…….....139

Figure 3.36: Quantification of HB-EGF intensity profiling in homologous 2D culture……. …….....140

Figure 3.37: Localisation of HB-EGF in Ishikawa cells alone or near the mouse embryo attachment site.……..……..……....141

Figure 3.38: Knock-down of integrin αv mediated by siRNA…….…….....143

Figure 3.39: Knock-down of integrin β3 mediated by siRNA.....144

Figure 3.40: Knock-down of integrin αvβ3 reduced embryo attachment.....145

Figure 3.41: Knock-down of OPN mediated by siRNA.…….…….....147

Figure 3.42: Knock-down of OPN reduced embryo attachment.…….….....148

Chapter 4: Cell signalling at implantation

Figure 4.1: The effect of IGF-I or HB-EGF treatment upon integrin β3 and OPN expression.....166

Figure 4.2: Localisation of integrin αvβ3 in IGF-I or HB-EGF treated Ishikawa cells…….……167

Figure 4.3: Localisation of OPN in IGF-I or HB-EGF treated Ishikawa cells…....168

Figure 4.4: OPN on the surface of Ishikawa cells in response to IGF-I or HB-EGF.…….....169

Figure 4.5: Cleavage of OPN in response to AEBSF, NNGH, Leupeptin, and ZVAD-fmk treatment prior to IGF-I ……...……...171

Figure 4.6: OPN promoted the adhesion of Ishikawa cells and mouse embryos…….…….....173

Figure 4.7: Thrombin enhances OPN-mediated cell adhesion…….……....174

Figure 4.8: Phospho-IGF-IR expression in Ishikawa cells in response to IGF-I or HB-EGF…….....175

Figure 4.8 (continued): Phospho-ErbB4, and SHP-2 expression in Ishikawa cells in response to IGF-I or HB-EGF…….…….…….....176

Figure 4.9: Western blotting analysis of phospho-IGF-IR, IGF-IR β in Ishikawa cells co-cultured with mouse embryos….....177

Figure 4.9 (continued): Western blotting analysis of phospho-ErbB4 and SHP-2 in Ishikawa cells co-cultured with mouse embryos….....178

Figure 4.10: Protein-protein interaction in response to IGF-I.....180/181

Figure 4.11: Localisation of IGF-IR β in Ishikawa cells co-cultured with the mouse embryo in a 2D *in vitro* model ……...184

Figure 4.12: Localisation of IGF-IR β in Ishikawa cells co-cultured with the mouse

embryo in a 2D *in vitro* model with a higher magnification……185/186

Figure 4.13: Knock-down of IGF-IR mediated by siRNA transfection.…….……188

Figure 4.14: Knock-down of IGF-IR reduced embryo attachment…….……189

Figure 4.15: Locally increased SHP-2 in Ishikawa cells co-cultured with mouse embryos…….…….....191/192

Figure 4.16: Localisation of SHP-2 in Ishikawa cells…….…….....193

Figure 4.17: Knock-down of SHP-2 mediated by siRNA….....194

Figure 4.18: Knock-down of SHP-2 suppressed embryo attachment.…….……..195

Figure 4.19: Attachment of bead carrying growth factor.….....196

Figure 4.20: Bead attachment assay.…….……..…….....197

Figure 4.21: Western blotting analysis of integrin β3 on Ishikawa cells co-cultured with beads carrying IGF-I or HB-EGF….……...198

Figure 4.22: Attachment assays of beads carrying IGF-I, HB-EGF, or OPN after knock-down of integrin αv, β3, or αvβ3……..…….….200/201

Figure 4.23: Attachment assays of beads carrying IGF-I, HB-EGF, or OPN after knock-down of OPN……..…….....202/203

Figure 4.24: Attachment assay of beads carrying IGF-I, HB-EGF, or OPN on Ishikawa cells after knock-down of IGF-IR …….205/206

Figure 4.25: Attachment of beads carrying IGF-I, HB-EGF, or OPN after knock-down of SHP-2……..….....208/209

Chapter 5: General Discussion

Figure 5.1: Schematic summary of key findings from the present study.....229

List of Tables

Chapter 2: Materials and methods

Table 2.1: Primary antibodies used for immunocytochemistry….....52

Table 2.2: Secondary antibodies used for immunocytochemistry….....53

Table 2.3: Primary antibodies used for Western blotting…….....54

Table 2.4: Secondary antibodies used for Western blotting.…….....55

Table 2.5: Standard grades for assessing blastocyst development (Expansion grade, Inner cell mass and Trophectoderm grades)…….....59

Table 2.6: Composition of collagen gel mixture for three-dimensional embryo culture…….....65

Table 2.7: Standard criteria for scoring the stability of the embryo attachment…….....66

Table 2.8: Composition of resolving and stacking gels ….……..…71

Table 2.9: Sequences of siRNA (Integrin αv/β3, OPN, IGF-IR, and SHP-2)....77/78

Chapter 3:

Establishment of *in vitro* model of embryo implantation and investigation of molecular crosstalk between the attaching blastocyst and endometrial epithelial cells

Table 3.1: Standard criteria for measuring the stability of embryo attachment….....88

Abstract

Name: Miss Youn-Jung Kang **Degree: D.Phil in Obstetrics and Gynaecology**

Department: Nuffield Department of Obstetrics and Gynaecology

College: St. Catherine's College **Year/Term submitted: 2012/HT**

Implantation failure is one of the major causes of infertility and contributes a major barrier to assisted reproduction success. Establishing a detailed understanding of embryo implantation is critical to our basic knowledge of human reproduction. The initial embryo-endometrial interaction appears to be crucial in triggering the cascade of physiological and molecular events required to establish a stable maternal-conceptus relationship. I hypothesised that integrin αvβ3 and its ligand OPN mediate the initial interaction during implantation, and that this is modulated by growth factors secreted locally from the embryo. In order to overcome earlier difficulties in the investigation of implantation *in vivo*, *in vitro* models were established by transferring either mouse or human embryos onto confluent human uterine epithelial (Ishikawa) cells. Following 24 h of co-culture, embryos were loosely attached onto cells, with more stable attachment after 48 h. Embryo attachment stimulated local up-regulation of epithelial integrin αvβ3 and OPN as monitored by immunofluorescence. Furthermore, OPN was cleaved to produce an adhesion-active 45kDa fragment which translocated to the apical cell surface in response to IGF-I stimulation, but not to HB-EGF. In order to dissect associated mechanisms down to a single molecular interaction, ligand (IGF-I, HB-EGF, or OPN)-conjugated, embryo-sized microbeads were used in attachment assays. IGF-I/HB-EGF-coated beads enhanced levels of epithelial integrin αvβ3. Knock-down of αvβ3 reduced the rate of attachment of both embryos and beads carrying IGF-I, HB-EGF or OPN. Knock-down of OPN reduced the stability of embryo attachment and beads bearing IGF-I or OPN, but interestingly did not affect the rate of attachment of beads bearing HB-EGF. Additionally, knock-down of IGF-IR or SHP-2 reduced attachment rate of both embryo and protein-coated beads. I have thus demonstrated a role for αvβ3-OPN interaction in embryo attachment as an adhesion receptor and a mediator of intracellular signalling via two independent pathways. Two embryo-derived growth factors, IGF-I and HB-EGF, can mediate initial attachment to the epithelium. Experimental data suggest therapeutic applications to improve female infertility including the development of novel diagnostic markers for evaluating uterine receptivity.



CHAPTER 1

General Introduction

1.1 Endometrium

The endometrium is the innermost layer of a multi-layered dynamic organ composed of glandular and luminal epithelial cells, stroma with fibroblastic cells, immune-competent cells and blood vessels. As a lining for the uterus, the endometrium functions to maintain the patency of the uterine cavity. The endometrium is hormonally regulated and cyclically proliferates and differentiates to become an optimal structure for embryo implantation.

1.2 The menstrual cycle

The endometrium undergoes cyclic regeneration called the "menstrual cycle" in humans and great apes but is referred to as an "estrous cycle" in most other mammals. Each month, endometrial cells undergo transformation in terms of number, structure and function. Shedding during menstruation leads to regeneration from the basal layer overlaying the myometrium. The human menstrual cycle (Figure 1.1) is divided into three distinctive phases: the proliferative (follicular) phase, the secretory (luteal) phase, and the menstrual phase, which lasts for 28-30 days. During the proliferative phase, follicles in the ovary begin to develop under the influence of follicle stimulating hormone (FSH) while the endometrium starts proliferating under the influence of estrogen secreted by mature follicles. In addition, the endometrial glands increase in size and the arrangement of stromal cells becomes more compact. At the end of the proliferative phase on day 14, the endometrium is 5-6 mm thick. When the level of estrogen reaches its threshold, luteinising

hormone (LH) is secreted from the pituitary. Ovulation subsequently occurs 24-36 h after the LH surge.

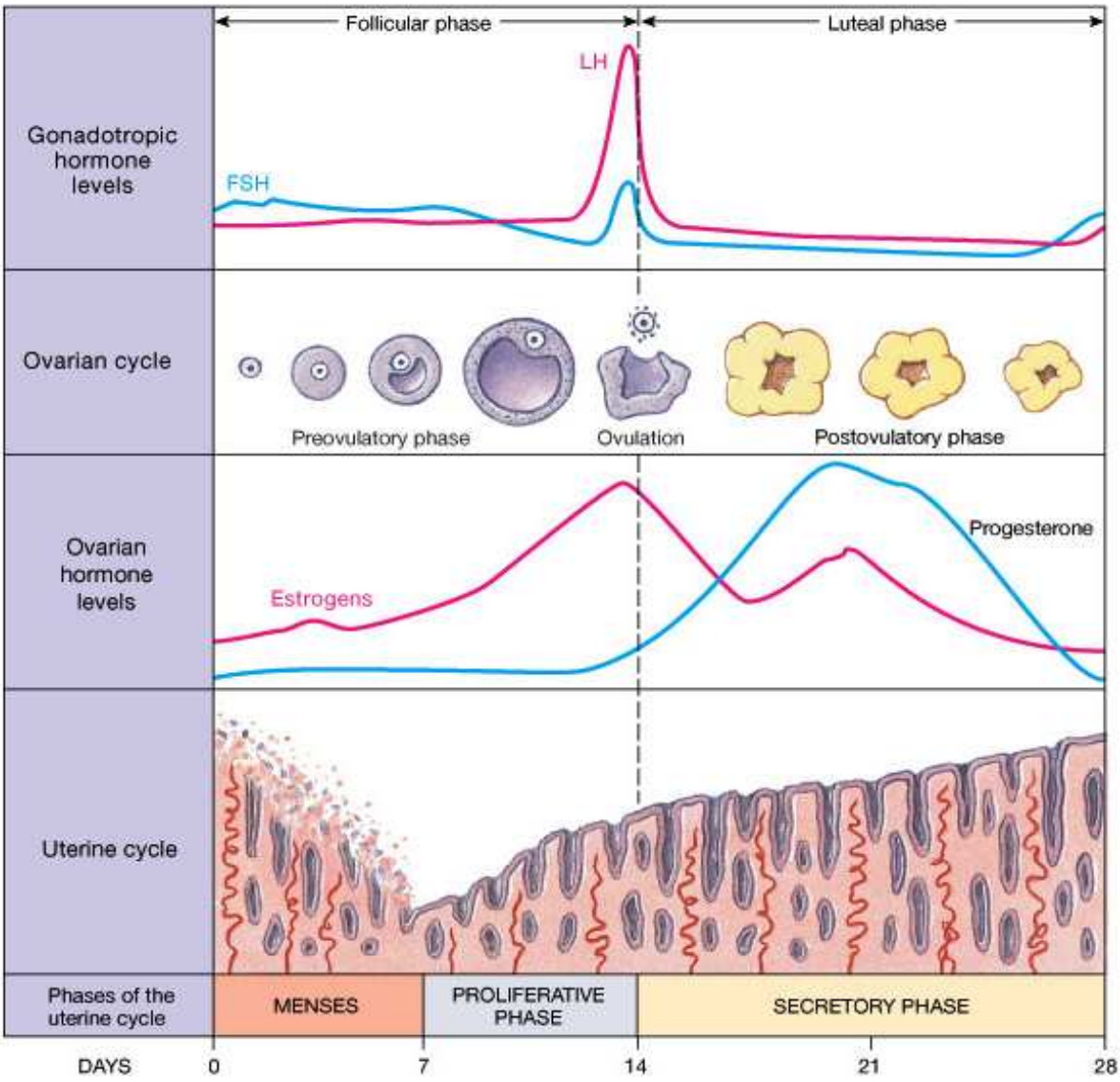


Figure 1.1: The menstrual cycle

The cycle of hormones (LH, FSH, estrogen, and progesterone), follicular development, ovulation, and the structure of endometrium during the menstrual cycle. Adapted from USMLElinks.com-Reproductive system, date accessed 03-02-2012.

After ovulation, and during the secretory phase, a corpus luteum, which is made from the remains of the dominant follicle in the ovary, produces large amounts of progesterone under the influence of FSH and LH. The endometrium then becomes receptive with a thick lining of uterine wall and blood vessels-rich with significantly increased levels of progesterone. Increased progesterone stimulates the increase of estrogen secretion, which is essential for embryo implantation. Successful implantation maintains the high level of progesterone and the receptive state of the endometrium. If implantation does not occur, the level of progesterone falls and the endometrium is shed, thus beginning the next cycle.

1.3 Development of the embryo

The preimplantation embryonic period in humans begins with fertilisation, which is referred to as embryonic day 1. When fertilisation occurs in the fallopian tube, a one-cell zygote is formed by the fusion of a haploid sperm with a haploid egg on day 1 and is surrounded by a membrane of glycoproteins, which is called the zona pellucida. A zygote undergoes several rounds of mitotic cell division by cleavage which increases the number of cells within the zona pellucida. After the 8-cell stage, the embryo undergoes cleavage and compaction, where the cells bind tightly to each other producing a cluster of cells until forming a ball of 32 cells, called a morula, on day 4. At the late morula stage, the embryo enters the uterine lumen undertaking more mitotic cell division and reaching the blastocyst stage which contains a blastocoel with two distinct cell populations, the inner cell mass (ICM) and the trophectoderm (TE) on day 5. The inner cell mass, which is located inside the blastocyst, gives rise to an embryo with pluripotency, while the trophectoderm, which

is the outer layer of the blastocyst, is the progenitor of trophoblast cells. At the late blastocyst stage on day 6, the blastocyst loses its zona pellucida and becomes implantation competent. The blastocyst attaches to the uterine epithelium to initiate implantation on day 7 while the trophoblast proliferates and differentiates into two different cell layers including cytotrophoblast, inner layer and syncytiotrophoblast, and outer layer, while the inner cell mass further differentiates into the epiblast and the primitive endoderm, The timeline of human embryo development is illustrated in Figure 1.2.

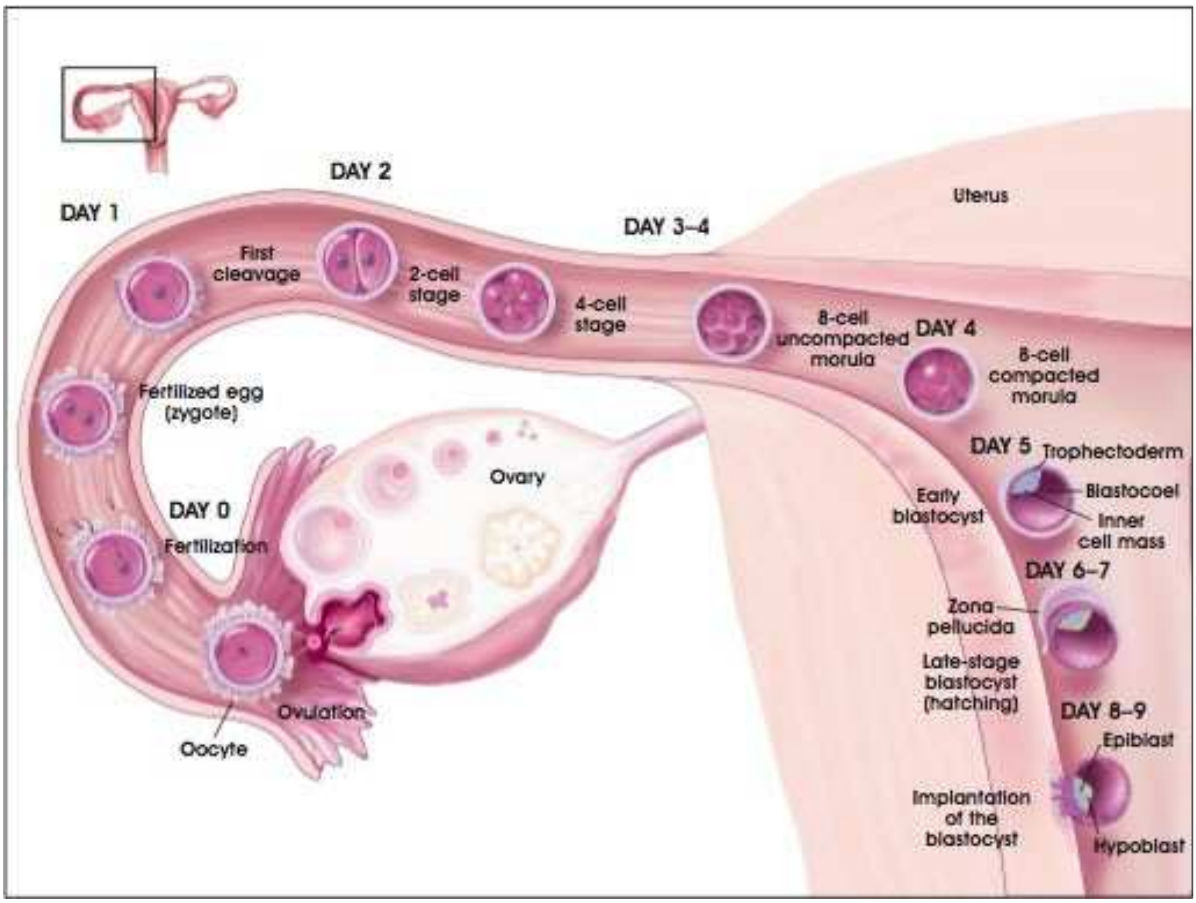


Figure 1.2: Development of the human embryo

A schematic diagram illustrating a timeline of human embryo development from fertilisation (day 1) to implantation (day 7-8). Adapted and modified from http://stemcells.nih.gov/info/scireport/appendixa, date accessed 15-02-2012.

1.4 Implantation

Embryo implantation is a pivotal step in reproduction. Sequential events involve complex signalling networks between the embryo and endometrium (Tabibzadeh, 1998; Dey et al., 2004; Nimbkar-Joshi et al., 2009). Due to the lack of a standard tool to examine the pre-implantation phase of pregnancy in humans, it is not possible to fully estimate the proportion of implantation failure (Wilcox et al., 1999; Diedrich et al., 2007). It has been reported that around 25% of embryos undergo successful implantation per IVF cycle, and the rate of embryonic loss at the implantation stage is higher than the rate of later fetal loss (de los Santos et al., 2003; de Mouzon et al., 2010). Thus, failure at the implantation stage is a major contributor to the low success rate of both spontaneous pregnancies and those resulting from ART (Margalioth et al., 2006). Increased understanding of implantation is critical to our basic knowledge of human development and may suggest key clues to solve problems of infertility and pregnancy failure. However, the molecular and cellular mechanisms of embryo implantation remain poorly understood (Singh et al., 2011).

Prior to implantation, the endometrium undergoes spatial and temporal changes, which are driven by ovarian steroid hormones to produce a period of uterine receptivity, referred to as the "window of implantation" (Psychoyos, 1973; Tabibzadeh, 1998; Dey et al., 2004). In humans, this lasts from approximately day 20 to day 24 of the menstrual cycle (Psychoyos, 1973; Enders, 1989; Achache and Revel, 2006). After the endometrium becomes receptive and the embryo reaches the blastocyst stage, implantation involves successive stages of apposition, adhesion and invasion processes (Enders and Schlafke, 1969; Norwitz et al., 2001). The process of embryo implantation is illustrated in Figure 1.3.

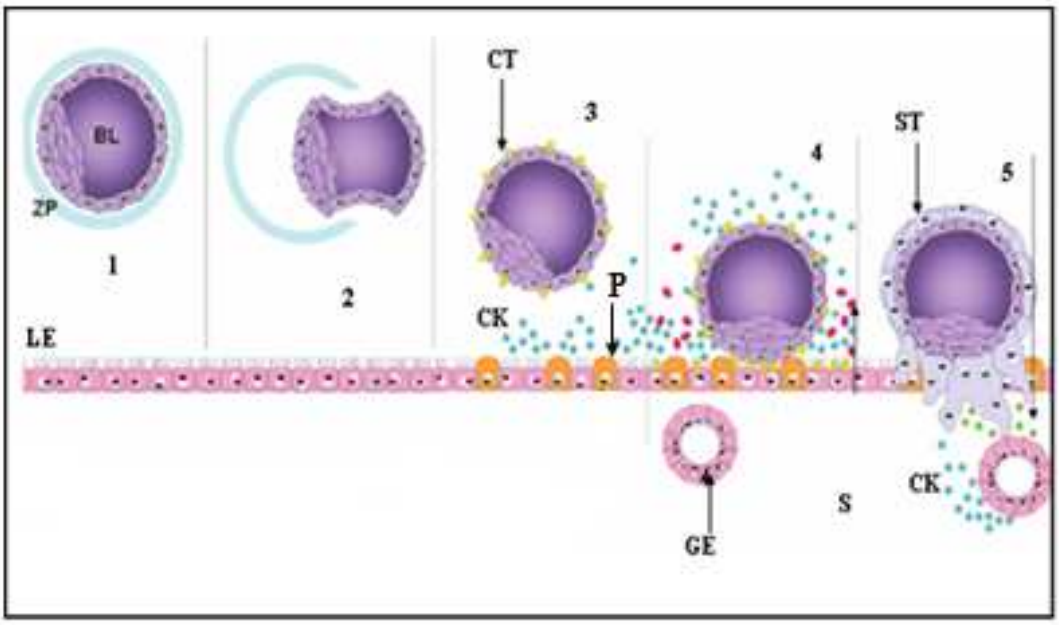


Figure 1.3: Initial interactions between the embryo and endometrium

A schematic diagram illustrating the process of embryo implantation, including apposition, adhesion, and invasion, **BL**: blastocyst, **ZP**: zona pellucida, **LE**: luminal epithelium, **CT**: cytotrophoblast, **ST**: syncytiotrophoblasts, **CK**: cytokine, **P**: pinopod, **GE**: glandular epithelium, **S**: stroma. Adapted and modified from Fitzgerald et al. (2008).

Around the sixth day following fertilisation, the embryo hatches from its zona pellucida, prior to initiation of implantation (Figure 1.3; Stage 1 and 2) (Banerjee and Fazleabas, 2010). During the apposition phase (Figure 1.3; Stage 3), the receptive luminal epithelium develops transient micro-protrusions known as pinopods (uterodome), localised on the apical surface of uterine epithelium which interdigitate with microvilli on the apical cytotrophoblast surface of the blastocyst (Bentin-Ley et al., 1999; Lopata et al., 2002). Once the embryo is positioned on the endometrium, it begins more direct and physical

interaction with the uterine epithelium for more stable adhesion (Figure 1.3; Stage 4). The inner cell mass is positioned on the endometrial side (Bentin-Ley and Lopata, 2000) and continues with penetration of syncytiotrophoblasts through the uterine epithelium and the underlying basement membrane to invade the endometrial stroma to establish a relationship with the maternal vasculature. Although this process is mainly controlled by trophoblasts in response to progesterone stimulation, the decidua, produced in the endometrium forming a new layer, restrains the invasion of trophoblasts (Figure 1.3; Stage 5) (Norwitz et al., 2001; Sharkey and Smith, 2003; Cakmak and Taylor, 2011). The endometrial stromal cells and extracellular matrix undergo decidualisation, which is defined as essential charateristics of the pregnant uterus showing increased glandular epithelial secretion, increased differentiation of uterine stromal cells, and increased stromal vascularity, which are essential for the establishment of successful pregnancy (Plaisier, 2011).

1.5 Differences of implantation between species

Most of the existing data relating to implantation are derived from *in vitro* or animal *in vivo* studies. This is due to the multitude of technical and ethical obstacles involved in studying the site of human implantation *in vivo*. Although animal studies may provide clues to human implantation, there are many differences between species (Figure 1.4) (Banerjee and Fazleabas, 2010). Based on the way the embryo contacts the uterine epithelium, there are three broad classifications in strategies of implantation: eccentric, centric, and interstitial (Wimsatt, 1975; Dey et al., 2004).

Murid rodents (Figure 1.4.A) undergo eccentric implantation, in which the luminal epithelium forms implantation chambers by invagination surrounding the trophoblast. The blastocyst induces the decidual responses and the endometrial epithelial cells above the decidua undergo apoptosis during the apposition stage. Subsequently, trophoblast cells penetrate into the stroma through the residual luminal epithelium (Enders, 1975; Dey et al., 2004; Li et al., 2006; Reese et al., 2008).

In interstitial implantation, blastocysts become embedded within the wall of the uterus. The manner of implantation of guinea pigs (Figure 1.4.B) is classified as the interstitial mode; when the blastocyst reaches the uterine lumen, the blastocyst develops an implantation cone at the opposite pole from the inner cell mass. The implantation cone, which is composed of syncytial trophoblast cells, penetrates the zona pellucida and attaches to the uterine epithelium. Subsequently, the blastocyst escapes from the zona pellucida and intrudes into the stroma by penetrating between uterine epithelial cells (Enders, 2000; Carter, 2007).

In rabbits (Figure 1.4.C), prior to penetration into the stroma, syncytial trophoblast cells adhere to the apices of the uterine epithelial cells and undergo fusion with apical ends of luminal epithelial cells. This manner of implantation is classified as centric implantation (Hoffman et al., 1998; Nicholls et al., 2011). Dogs, cows, pigs, sheep, and many marsupials exhibit centric implantation (Carson et al., 2000).

In primates (Figure 1.4.D), which adopt interstitial implantation, syncytial trophoblast formed near the inner cell mass adheres to the uterine epithelium and penetrates into the stroma by intruding between endometrial epithelial cells (Enders et al., 1983; Smith et al., 1987; Jones et al., 2001; Nimbkar-Joshi et al., 2009).

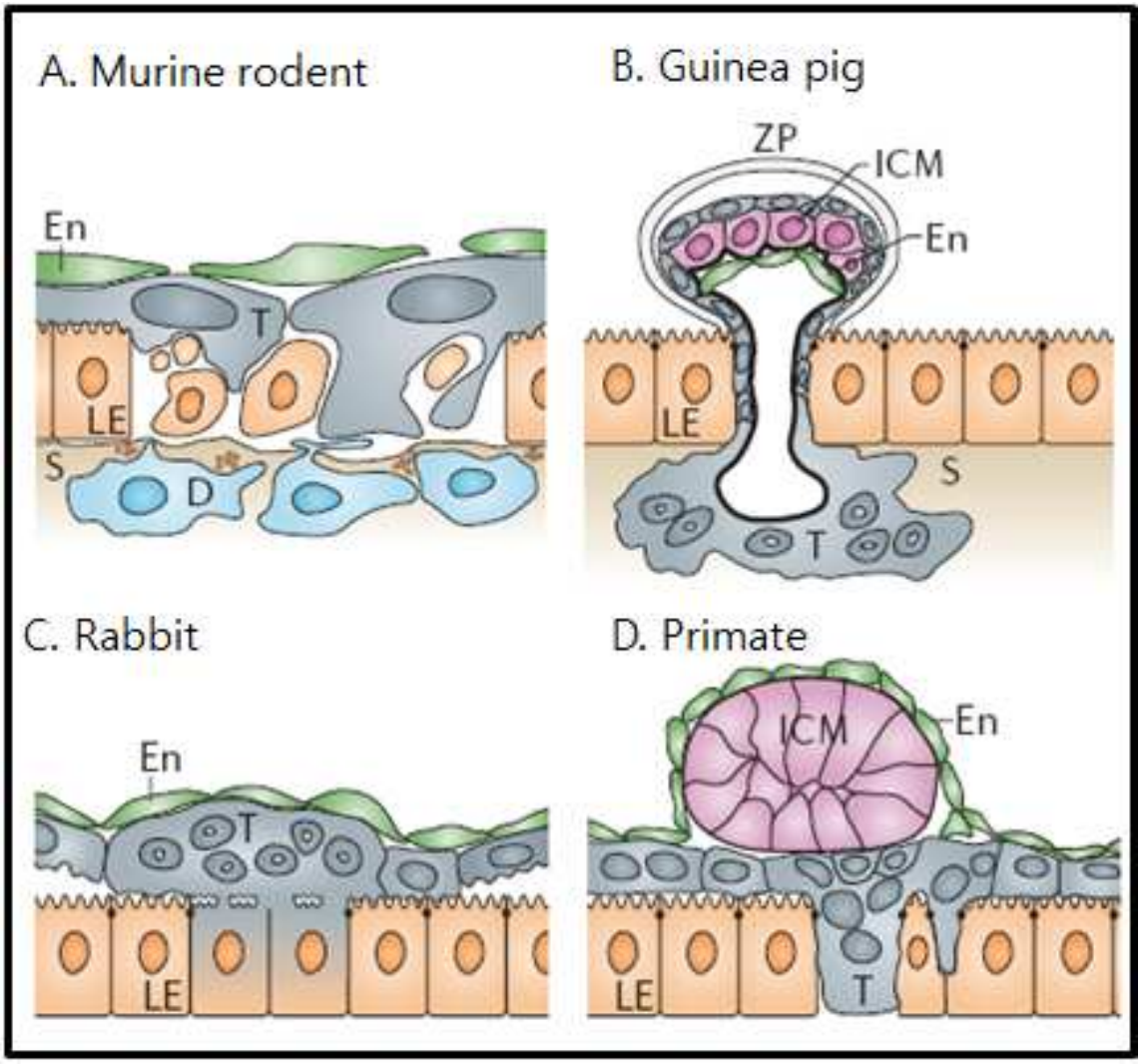


Figure 1.4: Differences of implantation in species

Schematic diagrams illustrating different manners of implantation in different species. Eccentric manner of implantation in mice and rats (**A**), interstitial mode in guinea pigs and primates (**B** and **D**), and centric implantation in rabbits (**C**), **En**: Embryonic Endoderm, **T**: Trophoblast, **LE**: Luminal Epithelium, **S**: Stroma, **ICM**: Inner Cell Mass, **D**: Decidua. Adapted from Wang and Dey (2006).

Regardless of the type of implantation, it can be considered that the purpose of implantation in all mammals is the same: to allow the conceptus to access maternally supplied nutrients and to protect the conceptus during early development. In interstitial implantation, this involves contacting the blood supply from the maternal tissue. Even though there are differences in the mechanism of implantation between species, *in vivo* studies using animal models are crucial to understand the molecular and mechanical events associated with implantation. Also, using different animal models provides greater chances to observe and understand the physiological mechanisms of each stage of implantation.

Pigs or sheep, which undergo centric implantation, are suitable models for the observation of the very initial stages of implantation, such as apposition and attachment phases, because in the centric manner of implantation the embryo sits on the uterine epithelium relatively longer and fuses with the luminal epithelial cells without penetration (Carson et al., 2000). Rabbits can be a good model to study embryo adhesion due to the precise timing of the window of implantation and distinctive morphological characteristics when the trophoblast cells adhere to the apical knob of luminal epithelial cells (Enders and Schlafke, 1971; Hoffman et al., 1998; Illera et al., 2003; Lee and DeMayo, 2004; Carter, 2007). Guinea pigs or non-human primates can serve as a good candidate for studying the penetration and invasion of trophoblast cells through the uterine epithelium to the stroma, while the mouse model can serve as a good candidate to study decidualisation (Enders and King, 1991; Enders et al., 1997; Dey et al., 2004; Nimbkar-Joshi et al., 2009). However, although many studies of the implantation have been performed using animal models, such studies remain of only limited value for understanding physiological mechanisms of human implantation. As a consequence, there is still a great deal of work required in order to identify factors and signalling pathways which modulate implantation in humans.

1.6 Molecular factors

Implantation is a complex sequential signalling process mediated by bi-directional crosstalk between the embryo and the endometrium, which is enabled by the synchronous development of the embryo and receptive endometrium (Simon et al., 2000b; Simon et al., 2000a; Garrido-Gomez et al., 2010). However, very little is known about the molecular events that establish endometrial receptivity prior to implantation, or the molecular mechanisms that control early dialogue between the embryo and endometrium during the window of implantation (Bazer et al., 2009; Cakmak and Taylor, 2011). Certain growth factors and adhesions molecules have been suggested to be involved, but functional data are still scarce (Aplin et al., 2001; Meseguer et al., 2001; Lessey et al., 2002; Johnson et al., 2003a; Aplin and Kimber, 2004; Dey et al., 2004; Aplin and Singh, 2008; Lim and Dey, 2009).

1.6.1 Anti-cellular adhesion molecule: MUC1

Prior to implantation, the uterine epithelial layer undergoes transition from a pre-receptive to a receptive state under the influence of ovarian hormones (Psychoyos, 1973; Psychoyos, 1986; Carson et al., 2000; Lessey, 2011). The apical surface of the uterine epithelial layer is shielded by a glycocalyx, which acts as a protective barrier against microbial and proteolytic attack, while at the same time allowing the uterus to become accessible to a prospective embryo (Aplin et al., 2001; Thathiah and Carson, 2002). The major component of apical glycocalyx is anti-cellular adhesion molecule, MUC1.

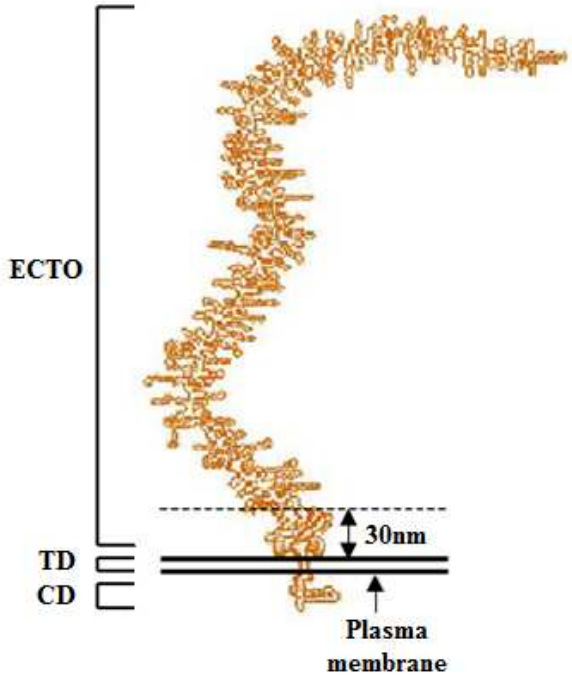


Figure 1.5: Structure of MUC1

A schematic diagram of the size and structure of the full-length MUC1 protein, **ECTO**: an N-terminal extracellular domain, **TD**: a transmembrane domain, and **CD**: a C-terminal cytoplasmic domain. Adapted and modified from Brayman et al. (2004).

MUC1 is an integral membrane glycoprotein (molecular weight >250kDa) with a large extracellular ectodomain containing a variable number of 20 amino acid tandem repeats, a hydrophobic transmembrane domain of 31 amino acids, and a short 56 amino acid intracellular non-glycosylated cytoplasmic tail (Figure 1.5) (Gendler et al., 1990; Ligtenberg et al., 1990; Meseguer et al., 1998; Meseguer et al., 2001; Kufe, 2008). MUC1 is abundantly expressed at the apical surface of secretory epithelial cells, including of the mammary glands, salivary glands, digestive tract, respiratory tract, kidney, bladder, prostate, and endometrium (Meseguer et al., 1998). Moreover, MUC1 as a proto-oncogene

is overexpressed in greater than 90% of human breast carcinomas and metastases (Zotter et al., 1988; Kufe, 2008). The structure of MUC1 is illustrated in Figure 1.5.

MUC1 is glycosylated by repeated intracellular endocytic recycling via the trans-Golgi network and fully glycosylated mature MUC1 is transferred to the cell surface, while the remainder is internalised and degraded following endocytosis (Litvinov and Hilkens, 1993; Hanisch and Muller, 2000). Two isoforms of MUC1 are known; MUC1/SEC that lacks transmembrane and cytoplasmic domains and may originate either from a proteolytic cleavage site in the proximal extracellular domain or by alternative splicing (Aplin et al., 1994), and MUC1/Y which lacks the tandem repeat domain and originates by alternative splicing. MUC1/SEC interacts with the extracellular domain of MUC1/Y resulting in MUC1/Y phosphorylation and cellular morphological alteration in various epithelial cells (Boshell et al., 1992).

In the epithelium, the extensively glycosylated extracellular domain of the MUC1 N-terminal subunit contributes to a barrier that protects the epithelial layer by shedding the cell surface in response to external stresses (Ligtenberg et al., 1992; Aplin et al., 1996a; Wesseling et al., 1996; Kufe, 2008). It has been reported that a transmembrane cleavage product of MUC1 acts as a growth factor receptor-like activity in undifferentiated human embryonic stem cells by associating with its ligand NM23 to activate down-stream MAP kinase signalling to eventually mediate cell growth (Hikita et al., 2008). Furthermore, this subunit is bound to the cell surface associating with the transmembrane of the MUC1 C-terminal subunit, which is capable of binding intercellular adhesion molecule (ICAM-1) (Regimbald et al., 1996). The MUC1-C extracellular domain acts as a binding site for galectin-3, which plays a bridging role between MUC1 and epidermal growth factor receptor (EGFR) and other receptor tyrosine kinases, including ErbB1/4 and platelet

derived growth factor receptor (PDGFR) (Schroeder et al., 2001; Pochampalli et al., 2007; Ramasamy et al., 2007).

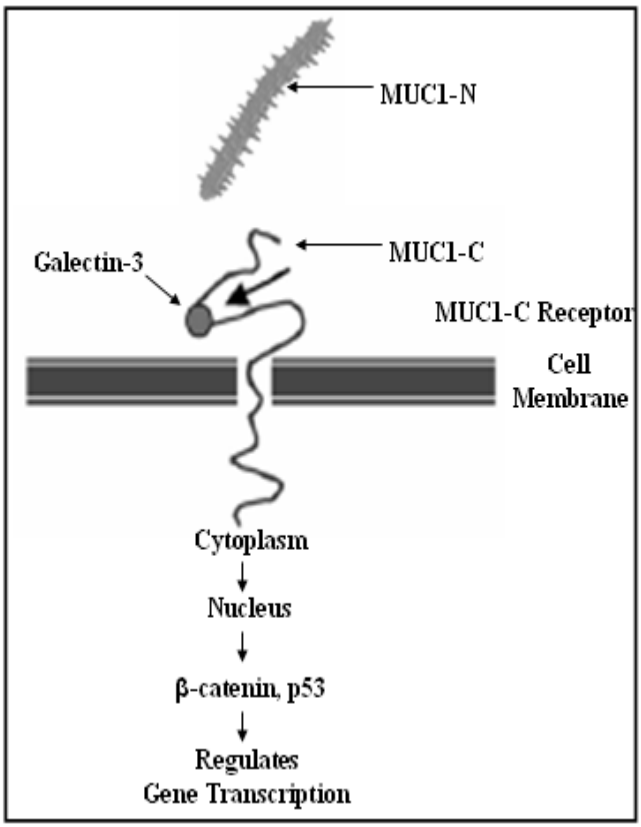


Figure 1.6. A schematic diagram of MUC1 and transport of MUC1-C receptor to the nucleus

MUC1 N-terminal subunit as a mucin component of MUC1 dimer can inhibit the interaction between cell surfaces by steric inhibition of other surface adhesion systems. Also this subunit is bound to cell surface associating with transmembrane of MUC1 C-terminal subunit which is capable of binding intracellular adhesion molecule, or may carry ligand for a selectin on endometrial luminal epithelium. MUC1 C-terminal cytoplasmic domain indirectly regulates Wnt target gene transcription by the interaction with β-catenin and associates with p53-mediated gene transcription. Adapted and Modified from Kufe D. Cancer Biol Ther. 2008

Several phosphorylated tyrosine residues in the cytoplasmic domain of the MUC1 C-terminal subunit serve as binding sites for the SH2 domain, a substrate for EGFR-mediated signalling. Additionally, overexpression of MUC1 C-terminal subunit blocks interaction between E-cadherin and β-catenin and directly interacts with β-catenin resulting in the disruption of cell-cell adhesion mediated by E-cadherin and loss of cell polarity. Association of MUC1 C-terminal subunit with β-catenin regulates Wnt and p53-mediated gene transcription (Figure 1.6) (Yamamoto et al., 1997; Huang et al., 2003; Wei et al., 2005; Kufe, 2008).

In the secretory phase of the menstrual cycle, at around the time of implantation, MUC1 is expressed at a higher rate at the apical surface of epithelial cells, as well as being detectable in the uterine fluid (Hey and Aplin, 1996). The involvement of MUC1 in implantation varies between different species. In mice, MUC1 is expressed at the surface of both luminal and glandular epithelium during pro-estrous, estrous, and meta-estrous phases. However, levels decline noticeably just prior to implantation and this pattern lasts until day 6 of pregnancy (Surveyor et al., 1995; Meseguer et al., 1998; Dharmaraj et al., 2010). During the pre- and peri- implantation period of rabbits, MUC1 level is elevated, though levels are significantly reduced or absent at sites of implantation (Hoffman et al., 1998). In humans, MUC1 expression is in contrast with that reported for mice. Human MUC1 is regulated by progesterone and exhibits moderate expression at the apical surface of both glandular and luminal epithelium during the proliferative phase. Levels are increased by the mid-secretory phase and are at maximal levels 7 days after the LH surge, the time of embryo implantation, showing accumulation of intracellular deposits (Hey et al., 1995; Meseguer et al., 1998). Furthermore, MUC1 is reported to be locally removed at the implantation site *in vitro* (Meseguer et al., 2001). Even if differences exist between species,

MUC1 is suggested to be an important factor in determining endometrial receptivity because it may be possible that intrinsic heterogeneity in MUC1 glycosylation may allow a local mechanism to recognise a receptive site within the endometrium, and that embryos could recognise MUC1-associated glycans or its protein backbone (Meseguer et al., 2001; Horne et al., 2006) .

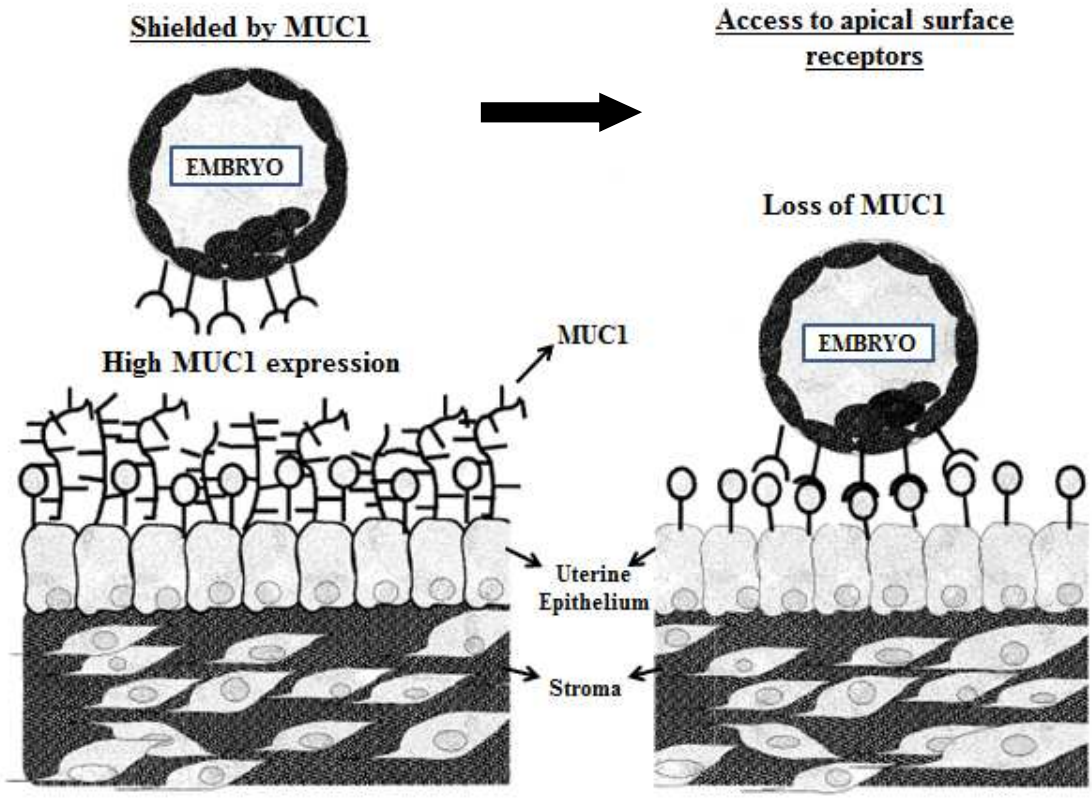


Figure 1.7: Function of MUC1 as an anti-adhesion molecule acting as a barrier of endometrium during embryo attachment.

The highly extended structure of MUC1 prevents the embryo from attaching to the apical surface of uterine epithelial cells. Loss of MUC1 permits access to apical cell surface receptors on the uterine epithelium that supports embryo attachment during the receptive phase. Adapted and modified from Hilkens et al. (1992), Aplin et al. (1994), Surveyor et al. (1995), Aplin et al. (1996a), and Meseguer et al. (1998).

In the endometrium, MUC1, including its extensively glycosylated ectodomain, is probably one of the first molecules that the embryo encounters prior to attachment to uterine epithelium. It may be postulated that MUC1 on the apical surface of epithelium inhibits cell-cell interaction between the embryo and endometrial epithelium by steric inhibition of receptor-ligand interactions mediated by other surface adhesion systems such as integrin-mediated adhesion (Ligtenberg et al., 1992; Aplin et al., 1996a; Wesseling et al., 1996). The function of MUC1 as an anti-adhesion molecule during embryo implantation is described as a schematic diagram in Figure 1.7.

However, a more complex role for MUC1 during implantation has been suggested in studies observing that MUC1 undergoes a change in glycosylation pattern during the receptive phase in humans (DeLoia et al. 1998). It has been demonstrated that highly sulphated lactosaminoglycan chains and sialokeratan sulphate epitopes are recognised in endometrial MUC1 (Aplin et al., 1998) and both glycans are hormonally regulated. Sulphated lactosaminoglycan epitopes are abundant in the proliferative phase but disappear during implantation, while sialokeratan sulphate epitopes are retained during implantation. It may be postulated that this unique glycosylation pattern is involved in the control of endometrial receptivity as well as playing a functional role as an anti-adhesion molecule (Aplin et al., 1998). Moreover, MUC1 carries sialyl Lewis^{x}, a ligand for selectin found in the endometrial luminal epithelium to mediate cell-cell adhesion between the embryo and epithelium (Hey and Aplin, 1996; Meseguer et al., 2001; Dharmaraj et al., 2010).

1.6.2 Cellular adhesion molecules: Integrins

Integrins are a family of heterodimeric transmembrane glycoproteins with non-covalently associated α and β subunits (Hynes, 1992), which function as receptors that mediate the attachment between cells and the tissues. In mammals, 18 α and 8 β subunits have been identified so far and 24 different α-β combinations have been reported. The ligand binding repertoire is determined, mostly by the specific combination of α and β subunits (Hynes, 1992; Takada et al., 2007; Barczyk et al., 2010). In general, each heterodimer contains an extracellular ligand binding site at the distal end and two leg regions from α and β subunit respectively, which go into the plasma membrane (Gilcrease, 2007). Both α and β subunits contain a large extracellular domain which is composed of more than 700 amino acids, a short transmembrane domain, and a cytoplasmic C-terminal domain that contains between 13 (β1 subunit) and 70 (β4 subunit) amino acids, but the length of each domain depends on the origin of integrin (Sastry and Horwitz, 1993; Kumar, 1998; Campbell and Humphries, 2011).

The extracellular part of both α and β subunits contains a divalent-cation-binding site which is crucial to determine both affinity and specificity to the ligand (Tozer et al., 1996). The relatively small size of the cytoplasmic domain contains important sequences for manipulating interactions with cytoskeletal molecules and signalling transduction. The cytoplasmic domain of the α subunit contains the GFFKR sequence, which is known as 'hinge domain' and forms a salt bridge with the corresponding membrane at the proximal region of the β subunit in the inactive integrin configuration (Hughes et al., 1996). Two NPXY sequences, which play an important part in acting as binding sites of many intracellular signalling proteins that have SH2 domains and thus exhibit phosphotyrosine binding, are located in the cytoplasmic domain of β subunit (Calderwood et al., 2000).

As a major adhesion molecule family, integrins recognise diverse extracellular matrix ligands including fibronectin (α5β1, αvβ3, and α4β1), collagen (α1β1 and α2β1), and laminin (α2β1, α3β1, and α6β1). Additionally, some integrins bind to cell surface receptors including the Ig superfamily members, intercellular adhesion molecule (ICAM-1) (αLβ2, αMβ2) or vascular cell adhesion molecule (VCAM-1) (α4β1) (Huttenlocher and Horwitz, 2011). Ultimately, integrins link to the actin cytoskeleton through a cytoplasmic tail to transmit signals intracellularly (Kumar, 1998, Hynes, 2002). Both subunits of integrin receptors contribute to recognise the RGD sequence (tripeptide arginine-glycine-aspartic acid (Arg-Gly-Asp)) in their matrix ligands and contain the potential binding sites for the ligand at or near a binding site for divalent cations to mediate specific biological activities (Ginsberg et al., 1990; Barczyk et al., 2010; Huttenlocher and Horwitz, 2011). In general, some integrins recognise more than one ligand, while some ligands are recognised by more than one integrin receptor. For example, 9 different integrins bind fibronectin and more than 5 integrins bind laminin (van der Flier and Sonnenberg, 2001). Diverse ligand bindings are associated with each other and mediate more dynamic and persistent cell-cell adhesion (Huveneers and Danen, 2009).

Due to the absence of intrinsic tyrosine kinase activity, which is intrinsic to tyrosine kinase receptors, such as the IGF receptors, integrins are required to undergo a distinct conformational change in the integrin extracellular segment in order to become activated in response to ligand occupancy and to mediate inside-out and outside-in signalling (Moiseeva, 2001; Xiong et al., 2002; Ross, 2004; Barczyk et al., 2010; Campbell and Humphries, 2011). The structure of integrin and its conformational change are illustrated in Figure 1.8.

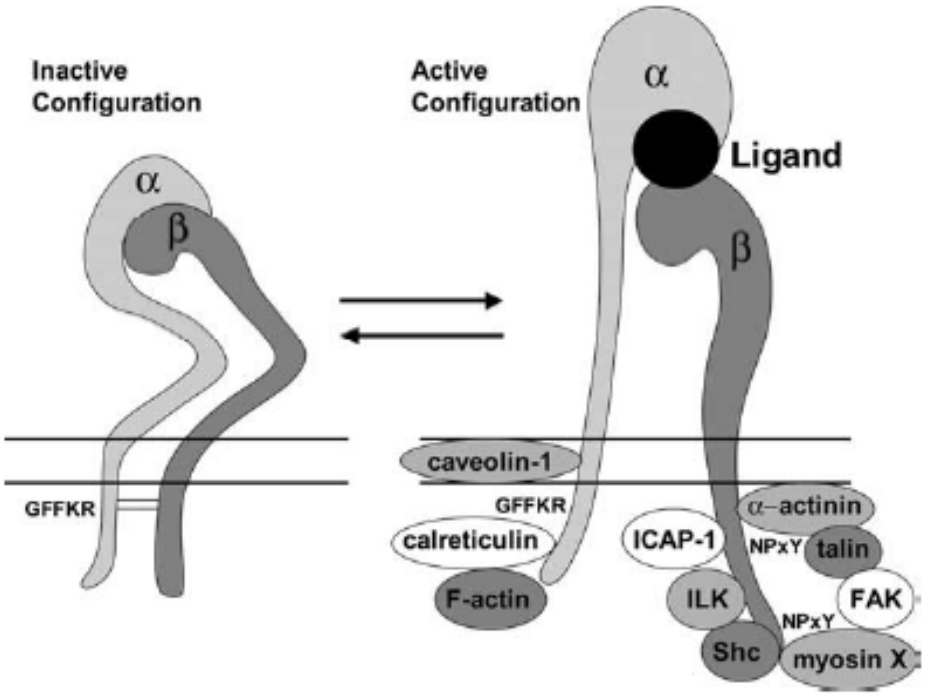


Figure 1.8: A schematic diagram of α and β integrin subunits

Each integrin heterodimer contains an extracellular ligand binding site at the distal end and two leg regions, one from the α and β subunits, that inserts into the plasma membrane. In an inactive or "OFF" state, two chains of integrin heterodimer are close together in the bent conformation and it does not bind ligand and transmit the signals. In an active or "ON" state upon a ligand binding, two chains become more extended shape and are in a separation of the legs and bind to other intracellular molecules to transduce the signals to further down-stream. Adapted from Gilcrease (2007).

The α subunit, in particular, contains one or more ligand binding sites to be involved in cell attachment and extracellular conformation, while the β subunit contains ligand binding sites localise at the divalent cation binding sequences, modulates gene expression, proliferation, migration, and differentiation with the association of cytoskeletal proteins (Kuhn and Eble, 1994; Geiger et al., 2009). After the extracellular domain of integrin binds to its specific ligand in the extracellular matrix, a conformational change

occurs to an active high affinity state. The cytoplasmic domain of the β subunit binds to several intracellular anchor proteins including talin, α-actin, and filamin (Tadokoro et al., 2003; Honda et al., 2009; Barczyk et al., 2010). Subsequently, these linkages are led to directly bind to actin or other anchor proteins, such as vinculin. This connection leads to a clustering of the integrins at the focal adhesion site. This process is called "outside-in signaling". The signalling mediated by integrin can also operate in the opposite direction. Signals generated inside the cell result in the conformational change of integrins leading to the modulation of integrin binding to their ligands outside the cell. This process is referred to "inside-out signalling" (Tozer et al., 1996; Hynes, 2002; Askari et al., 2009; Gahmberg et al., 2009).

Integrin-mediated adhesion is manipulated by the synergistic effect of interaction with anchoring proteins. The initial adhesion is mediated with talin, whose N-terminal domain interacts with the cytoplasmic domain of the integrin β subunit and the C-terminal domain binds actin. The subsequent activation of integrin is achieved by cooperation of kindlin, which also binds to the β subunit of integrin. Additionally, the assembly of integrin-mediated adhesion is enhanced by the binding of vinculin to talin, which promotes the clustering of integrin-actin complexes and focal adhesion interaction (Galbraith et al., 2002; Humphries et al., 2007; Askari et al., 2009; Anthis and Campbell, 2011).

1.6.2.1 Endometrial integrins and αvβ3

Integrins are expressed in most cell types in multicellular animals, such as epithelial cells, endothelial cells, and erythrocytes. Most cells express more than one integrin receptor (Barczyk et al., 2010). In particular, a large variety of integrins have been identified in endometrial cells (Lessey et al., 1992; Singh and Aplin, 2009). Integrin-

mediated adhesion, migration, and invasion in response to intracellular and extracellular signals make integrins potential participants in complex reproductive events, including implantation and placentation. Some integrins are regulated spatially and temporally within the uterus during the menstrual cycle, whereas others show consistent expression. Integrins whose expression is increased during the mid-luteal phase of cycle are suggested as markers for uterine receptivity. Mainly, integrins including the β1 or αv subunit are expressed in the endometrium; integrin α1β1, α2β1, α3β1, α4β1, α6β1, α6β4, α9β1, αvβ1, αvβ3, αvβ5, and αvβ6 are known to be particularly expressed at the uterine luminal surface of epithelium and widely considered as potential endometrial markers for mediating implantation (Lessey et al., 1992; Bowen and Hunt, 2000; Aplin and Kimber, 2004).

Integrin α2β1, α3β1, and α9β1 are constitutively expressed on the luminal epithelium during the menstrual cycle, while integrin α1β1 and α4β1 are expressed during the mid- to late-secretory phase (Lessey et al., 1996; Bowen and Hunt, 2000; Singh and Aplin, 2009). The important role of integrin α4β1 has been suggested in mouse *in vivo* studies demonstrating intrauterine blocking of integrin α4 using a specific antibody, which led to implantation failure or delayed implantation (Basak et al., 2002). Furthermore, immunohistochemical analysis revealed the low expression of integrin α4β1 in endometrial stroma during implantation, a finding that correlated with recurrent miscarriage (Skrzypczak et al., 2001). Moreover, the integrin family, including the αv subunit, recognises specific extracellular matrix components through the RGD peptide motif. In particular, integrin αvβ3, as a receptor of several different ECM ligands, including fibronectin, vitronectin, osteopontin, and thrombospondin through RGD sequences, has been considered as a marker of uterine receptivity. In human endometrium, integrin αvβ3 appears abruptly in the luminal and glandular epithelium on day 20 of the menstrual cycle

and its maximal expression on the uterine epithelium overlaps with the window of implantation (Lessey et al., 1992; Lessey and Castelbaum, 2002). In mice, the apical localisation of integrin αvβ3 on luminal and glandular epithelium has been observed throughout early pregnancy and expression increases at the time of implantation (Aplin et al., 1996b). Regulation of integrin β3 subunit expression during the cycle, especially an increase in abundance during mid-secretory phase, is influenced by ovarian hormone signalling, using the transcription factor HOXA10 as an intermediary (Daftary et al., 2002). Furthermore, cycle-independent integrin αvβ5, a receptor for fibronectin, vitronectin and osteopontin, is expressed at the apical surface of both luminal and glandular epithelial cells in humans throughout the menstrual cycle (Aplin et al., 1996b), while αvβ6 is present, but with reduced expression during the mid-secretory phase of the cycle (Bowen and Hunt, 2000).

At the time of implantation, the expression of integrin is increased on embryonic trophoblast cells by the differentiation of cytotrophoblast cells to an invasive extra-villous phenotype. During the initial stages of apposition and adhesion, trophectoderm expresses integrin α5β1, αvβ3, αvβ5 and αvβ6 (Sutherland et al., 1993; Bloor et al., 2002) and integrin α1β1, α6β1, and α7β1 in the later stages of the invasion phase (Bowen and Hunt, 2000). Integrin α5β1 is expressed by cells localised between the inner cell mass and the cavity rather than the external trophectoderm surface of early expanded blastocysts. As the trophectoderm undergoes differentiation, integrin α5β1 is translocated to the apical surface of trophoblast cell membranes which are the first to contact the uterus when the implantation commences (Clark et al., 2005). Integrin αvβ3 has been known to translocate to the apical membrane of trophoblast cells from the rat embryo when it attaches to uterine epithelial cells *in vitro* suggesting its important role during initial embryo-endometrial

interaction (Kaneko et al., 2011a).

Female mice lacking the integrin β1 gene develop embryos normally to the blastocyst stages, but it fails to implant due to the inability to adhere to or invade the endometrial basement membrane (Brakebusch et al., 1997), while integrin αv gene null mice are fertile, embryonic development is lethal due to defects of development including vasculogenesis and angiogenesis (Bader et al., 1998; McCarty et al., 2002).

Due to the appearance of integrin αvβ3 on both the embryo and endometrial epithelium in human (Lessey, 1994; Lessey et al., 1995) as well as other mammalian species (Aplin et al., 1996b; Illera et al., 2000; Johnson et al., 2001; Garcia et al., 2004; Kaneko et al., 2011b), integrin αvβ3 has been extensively studied to investigate its roles in the early implantation. Additionally, the presence of ligands for integrin αvβ3-binding on both the embryo and endometrial epithelium have been reported (Kimmins et al., 2004; Casals et al., 2012b).

The functional significance of integrin β3 subunit has been demonstrated with the absence or late expression of integrin β3 in menopausal endometrium and patients with unexplained infertility (Lessey et al., 1995). Additionally, the aberrant expression of integrin αvβ3 is associated with infertility, endometriosis (Lessey et al., 1994), luteal phase deficiency (Lessey et al., 1992; Castelbaum et al., 1994) and polycystic ovarian syndrome (Apparao et al., 2002). Also, studies using intrauterine injection of RGD peptide or disintegrin echistatin, or functional neutralising antibody against integrin αvβ3 have been shown to significantly reduce the number of implantation sites in mouse endometrium, and the same effect has also been revealed in rabbit endometrium (Illera et al., 2000; Illera et al., 2003). However, it should be noted that integrin αv or β3 null mice are fertile but

undergo fetal mortality despite successful implantation (Graham et al., 1990; Bader et al., 1998). Recently, mRNA level of integrin β3 on day 21 has been suggested as an indicator to predict success rate after IVF treatment with the consideration of integrin αvβ3 as a clinical and research marker for human implantation (Elnashar and Aboul-Enein, 2004).

Integrin αvβ3 interacts with various ECM components by recognising RGD sequences to mediate cell adhesion, migration and to regulate the balance between cell proliferation and differentiation (Horton, 1997). A large cysteine loop between residues 177 and 184 (^{177}CYDMKTTC^{184}) of the extracellular domain of integrin β3 subunit determines the specificity of integrin αvβ3 controlling affinity to the ligand depending on IGF-I stimulation (Maile et al., 2006). The β3 subunit has been known to play an important role in the connection between integrins and the cytoskeleton (Gahmberg et al., 2009). Outside-in binding of the engagement of extracellular matrix ligand to integrin β3 subunit results in further activation and tyrosine phosphorylation of the tyrosines in the two NPXY sequences (Gilcrease, 2007). This phosphorylation induces signalling transduction via talin and docking protein 1 (DOK1) activating focal adhesion kinase (FAK) at a critical tyrosine residue, Tyr-397, initiating an SH2 domain-dependent association with c-Src mediating the further down-stream intracellular signalling transduction (Sastry and Horwitz, 1993; Schlaepfer et al., 1997; Ling et al., 2005a; Oxley et al., 2008). Within the cytoplasmic domain of the β3 subunit, two tyrosines (Tyr^{747} and Tyr^{759}) are required for cell spreading and transfer of the integrins to focal adhesion sites (Ylanne et al., 1995). The β3 subunit of the integrin αvβ3 heterodimer is phosphorylated upon binding to vitronectin but not to fibronectin suggesting ligand binding may affect tyrosine phosphorylation (Datta et al., 2002; Butler et al., 2003; Gahmberg et al., 2009).

1.6.3 Extracellular matrix molecules: Osteopontin

Osteopontin (OPN) is a member of the small integrin binding ligand N-linked glycoprotein (SIBLING) family of ECM proteins and cytokines mediating various physiological and pathological events including the maintenance of tissue integrity, bone mineralisation, cancer metastasis and angiogenesis (Johnson et al., 2003a; Standal et al., 2004). OPN, which is also known as secreted phosphoprotein 1 (SPP1), bone sialoprotein (BSP) (Franzen and Heinegard, 1985) and early T-lymphocyte activation factor 1 (Eta-1) (Patarca et al., 1989), is present in various epithelial cells of the gastrointestinal tract (Imano et al., 2009), kidneys (Xie et al., 2001), thyroids (Briese et al., 2010), breast (Senger et al., 1989a), uterus (Johnson et al., 2000; Apparao et al., 2001; Quenby et al., 2007; Singh and Aplin, 2009), placenta (Briese et al., 2005), and testes (Brown et al., 1992; Luedtke et al., 2002) and also expressed by smooth muscle cells (Liaw et al., 1994), leukocytes (Ihnen et al., 2010), highly metastatic tumour cells (Hotte et al., 2002), and body fluids as a secreted form (Johnson et al., 2003a). In health, OPN is mostly observed at a low level of expression but it is dramatically elevated under the conditions of inflammation and tissue remodelling (Murry et al., 1994; Ramaiah and Rittling, 2008).

A native form of OPN which is 70kDa in size with 301 (human) amino acids as a monomer contains two glutamines targetting transglutaminases, a thrombin cleavage site, tripeptide arginine-glycine-aspartic acid sequences, and a calcium phosphate apatite binding region (Johnson et al., 2003a; Ahmed et al., 2011). The roles of OPN, including cell-cell adhesion and migration, are mediated by interaction with various cell surface receptors (Chakraborty et al., 2006). OPN enables the formation of homotypic polymers via transglutaminase cross-linking. Its self-assembly provides multiple integrin binding sites to promote cell-cell and cell-matrix interactions (Kaartinen et al., 2002; Erikson et al.,

2009). The N-terminal region of OPN contains an ELVTDEP sequence providing a binding site for integrin α4β1 (Bayless et al., 1998). Additionally, it contains the GRGDS motif, which plays an important role of an adhesion molecule by acting as a binding site for integrin αvβ1 (Hu et al., 1995b), αvβ3 (Liaw et al., 1995a; Liaw et al., 1995b), αvβ5 (Hu et al., 1995a), αvβ6 (Yokosaki et al., 2005), α5β1 (Barry et al., 2000), and α8β1 (Denda et al., 1998). Mutation of RGD site disrupts cell adhesion and migration in various cells (Miyauchi et al., 1991).

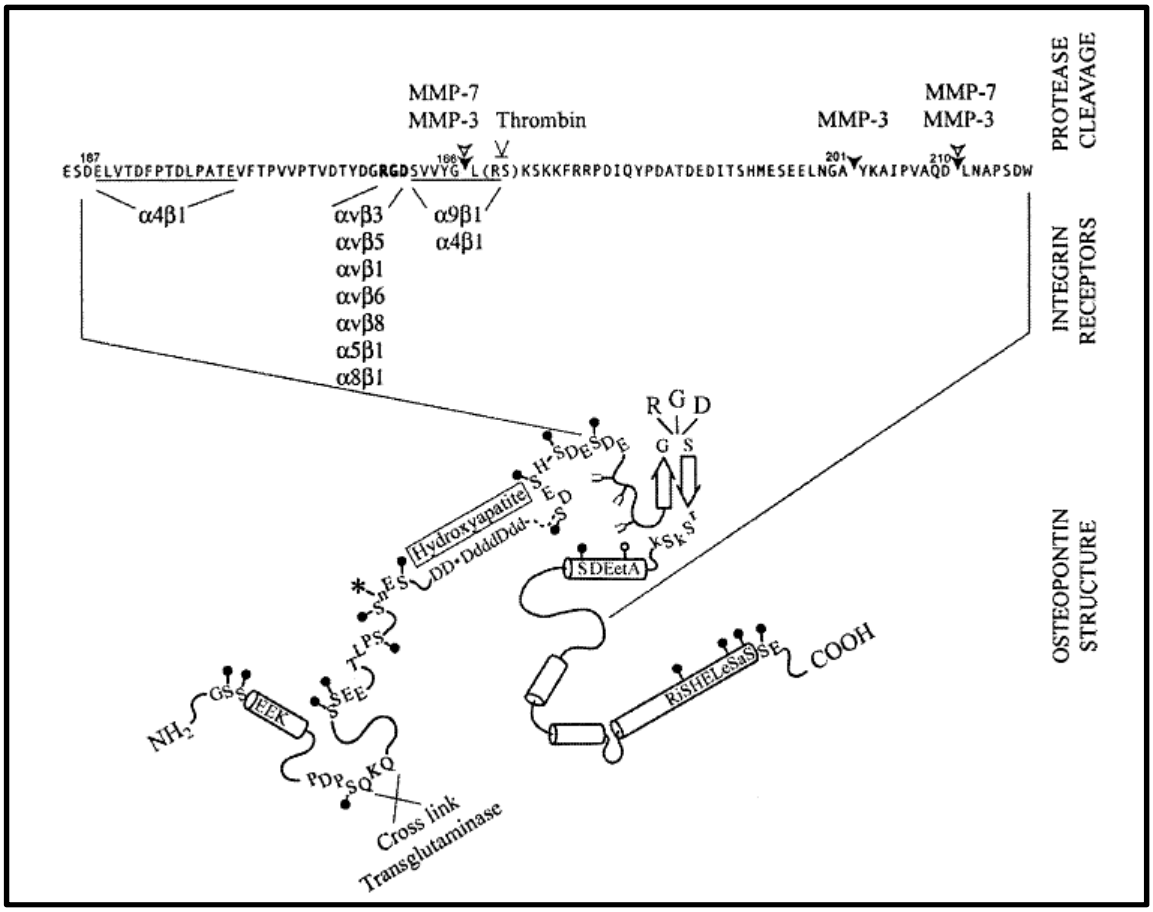


Figure 1.9: Structure of OPN, integrin-binding sequences, cognate receptors, and sites for proteolytic cleavage.

A hypothetical structure of OPN based on the amino acids and secondary structure prediction of functional domains of ECM components and positions of post-translational modifications. Adapted and modified from Sodek et al. (2000) and Johnson et al. (2003a).

Furthermore, OPN contains the SVVYGLR sequence for binding of integrin α9β1, α4β1, and α4β7 to promote leukocyte adhesion (Yokosaki et al., 1999; Johnson et al., 2003a). Functional consequences are dependent on the occupancy of OPN. For example, the occupancy with integrin αvβ1, αvβ3, or αvβ5 mediates cell adhesion while occupancy with only integrin αvβ3 supports cell migration in smooth muscle cells (Liaw et al., 1995b).

Moreover, the COOH- terminal fragment of OPN interacts with cell surface proteoglycan CD44 splice variants isoforms (CD44v3-v6) to recruit leukocytes and trigger integrins to active adherence configurations (Weber et al., 1996). The interaction between OPN and CD44 may require the cooperation of integrin β1 in order to stimulate cell migration and chemotaxis (Katagiri et al., 1999). OPN is a part of the attachment complex hyaluronan-CD44-ERM (ezrin/radixin/moesin). This complex mediates fibroblast, macrophage, and tumour cell migration (Zohar et al., 2000). Binding to receptors either extracellularly or intracellularly leads OPN to mediate cell-cell interaction and cell-ECM interaction by activating cellular signalling pathways in either a direct or indirect manner (Sodek et al., 2000; Johnson et al., 2003a; Ahmed et al., 2011).

OPN undergoes extensive post-translational modifications including phosphorylation, proteolytic cleavage, and glycosylation in order to mediate cell-matrix and cell-cell interactions thereby regulating various signalling pathways leading to cell adhesion, migration, and suppression of cell apoptosis (Sodek et al., 2000; Johnson et al., 2003a; Christensen et al., 2005; Ahmed et al., 2011). Due to various post-translational alterations, different forms of OPN are detected in normal as well as tumour cells giving rise to molecular mass variants ranging from 25kDa to 70kDa (Johnson et al., 2003b; Rangaswami et al., 2006).

Proteolytic cleavage is believed to be important to the biological function of OPN. OPN is cleaved at the RSK (arginine^{168}-serine^{169} in human) site by thrombin or a secreted serine protease, generating two fragments at the N-terminal and C-terminal (Senger and Perruzzi, 1996; Kon et al., 2002). There is evidence that a thrombin generated OPN N-terminal fragment of 45kDa is strongly involved in cell attachment, adhesion, and migration due to increased access to integrins via the RGD domain at its NH_2-terminal region (Senger and Perruzzi, 1996). Other groups have suggested that thrombin generated C-terminal domain of OPN promotes both cell migration and adhesion in breast cancer cells (Mi et al., 2007). Blockade of the thrombin cleavage site in OPN using an inhibitor for thrombin, Argatroban, specifically reduces the adhesion and migration of breast cancer cells in both *in vitro* and *in vivo* (Schulze et al., 2008). Additionally, OPN is cleaved by matrix metalloproteinases (MMPs), MMP-3 and MMP-7. Following cleavage by MMPs, the OPN fragment binds to integrin receptors to initiate cell adhesion and migration in tumour cell lines *in vitro* as well as *in vivo* in remodelling tissues such as the postpartum uterus (Agnihotri et al., 2001). The structure of OPN, its integrin receptors and proteolytic cleavage sites are illustrated in Figure 1.9.

In human endometrial epithelium, OPN is weakly expressed inside the cell, specifically adjacent to the cell surface membrane in the early-secretory phase and gradually increases in response to progesterone on day 16-17 of the menstrual cycle (Apparao et al., 2001; Carson et al., 2002; Quenby et al., 2007). This increase of OPN following the LH surge has been demonstrated by comparative global gene expression studies in human endometrial tissues between the LH surge and the late-proliferative phase of the cycle (Kao et al., 2002). Following the LH surge, and during the mid- to late-secretory phase of the menstrual cycle, OPN persists on the apical surface of uterine

luminal and glandular epithelial cells, and expression is particularly prominent in and adjacent to pinopods (Quenby et al., 2007). During implantation, OPN expression is extended to the decidualising stroma and embryonic trophectoderm (Omigbodun et al., 1997; Quenby et al., 2007). Similar patterns of OPN expression has been observed in pigs and sheep. In pregnant pigs, OPN expression reaches maximum levels on both the apical surface of endometrial luminal epithelium and trophectoderm on day 14 of pregnancy, a period that corresponds to early implantation and the embryo attachment phase (Garlow et al., 2002; White et al., 2005). In pregnant sheep, progesterone-dependent OPN is secreted between day 11 and 17, coincident with the initial attachment phase of implantation and is highly expressed on trophectoderm between day 14 and 19 of pregnancy, especially on the interface between the luminal epithelium and trophectoderm (Johnson et al., 1999; Johnson et al., 2003b). Furthermore, in rabbit uteri, OPN is dramatically elevated on day 4 to 7 of pregnancy, corresponding to the rise of progesterone and the time of initial implantation and embryo attachment (Apparao et al., 2003). There is evidence to suggest a functional role for OPN during mouse pregnancy. OPN null mice are fertile but show reduced pregnancy rates during mid-gestation suggesting peri-implantation pregnancy loss (Weintraub et al., 2004). In pregnant mouse uteri, estrogen-dependent OPN appears on the luminal epithelium on day 4.5 of pregnancy and is co-localised with immune cells, such as leukocytes and macrophages in stroma (White et al., 2006).

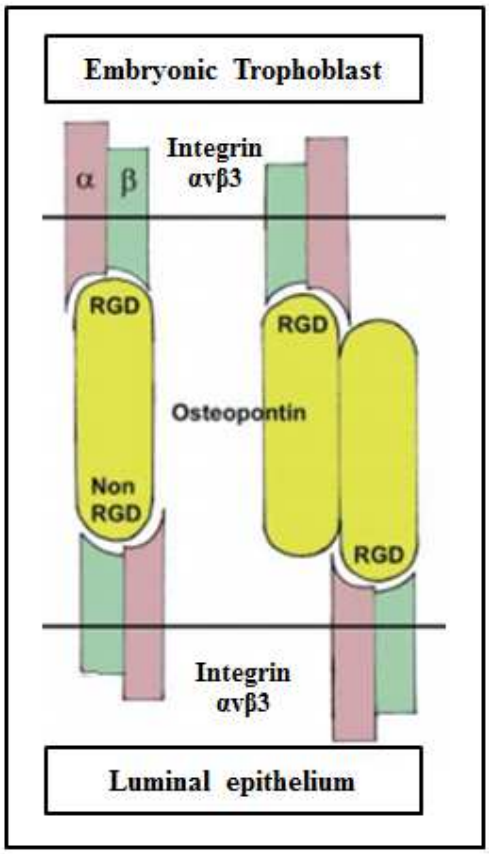


Figure 1.10: Possible interaction between embryonic trophoblast and endometrial epithelium

A schematic diagram illustrating that two populations of integrin αvβ3 expressed on the embryo and endometrium respectively, bind to each other via OPN, a bi-functional bridging molecule. Adapted from Spencer et al. (2004).

Both OPN and integrin αvβ3, a primary ligand for OPN via the RGD sequence, show increased expression during the mid- to late-secretory phases in endometrial epithelium and have been proposed as markers for distinguishing receptive from non-receptive endometrium in clinics (Apparao et al., 2001; Lessey, 2002a; Lessey and Castelbaum, 2002; Quenby et al., 2007; Erikson et al., 2009). Moreover, embryos express both molecules on the surface of trophoblast cells (Omigbodun et al., 1997; Johnson et al.,

2003a). Binding of OPN to integrins activates integrin receptors and cytoskeletal proteins and subsequently promotes focal adhesions in the trophectoderm of embryos. This may suggest that both integrin αvβ3 and OPN may be related to endometrial receptivity for implantation and that OPN binds to two populations of integrin αvβ3; on the embryo and endometrium respectively to facilitate bi-directional bridging between these surfaces for embryo attachment to the uterine epithelium (Figure 1.10) (Apparao et al., 2001).

Aberrant expression of OPN is associated with infertility caused by isolated polycystic ovary syndrome (PCOS) (DuQuesnay et al., 2009), but remains controversial in endometriosis (Cho et al., 2009; Wei et al., 2009; Casals et al., 2012b). Although the functional significance of increased OPN expression in secretory-phase endometrium remains to be explored further, its temporal and spatial patterns of expression suggest an important role during implantation and placentation.

1.6.4 Growth factors

During implantation, temporally and spatially coordinated activation of the functional blastocyst and the receptive uterus are regulated by several growth factors (Duc-Goiran et al., 1999; Dey et al., 2004; Guzeloglu-Kayisli et al., 2009). These factors bind to their specific cell surface receptors and initiate signalling cascades by phosphorylating various down-stream components (Singh et al., 2011).

1.6.4.1 Insulin-like growth factor-I

Insulin-like growth factors (IGFs) are known as potent mitogenic growth factors

involved in cell proliferation and differentiation having 45% sequence homology with insulin (Blundell and Humbel, 1980; Rechler and Nissley, 1985). Insulin-like growth factor I (IGF-I) and II (IGF-II) exert their biological effects by binding to transmembrane receptors (IGFRs) on the surface of target cells (Lammers et al., 1989). It has been shown that the action of IGFs in cellular and molecular mechanisms is regulated by a family of high-affinity IGF binding proteins (IGFBPs). IGFs are key growth factors in many reproductive events in human and other mammalian species, acting as mediators of steroid hormones in a paracrine and/or autocrine manner (Giudice et al., 1993; Giudice et al., 1998).

IGF-I plays important roles at the maternal-fetal interface including oocyte maturation (Gomez et al., 1993), uterine endometrial proliferation (Rutanen, 1998), placental function (Murata et al., 1994), and pre-implantation embryo development (Humbel, 1990). During early pregnancy (day 4 to 6) in mice, higher levels of IGF-I mRNA expression have been detected in the uterus (Kapur et al., 1992). Enhanced levels of IGF-I in the early-secretory phase suggest the potential role of IGF-1 in endometrial receptivity (Fluhr et al., 2008). In ovariectomised rats, levels of IGF-I transcription is abruptly elevated in response to exogenous estrogen or progesterone treatments, compared to low expression at basal levels (Kapur et al., 1992). Regulation of IGF-I upon estrogen and progesterone stimulation has also been observed in pigs showing up-regulation of IGF-I mRNA in the endometrium in response to estrogen (Simmen et al., 1990). Additionally, IGF-I has shown to act synergistically with estrogen to induce DNA synthesis in uterine organ cultures (Ghahary et al., 1990). It may be assumed that IGF-I plays a role in regulating implantation by acting as a mediator of estrogen. *In vivo* human studies have shown that IGFs are predominantly expressed in endometrial stromal cells; IGF-I is

expressed during the mid- to late-proliferative and early-secretory phase of the menstrual cycle primarily under estrogenic stimulation, while IGF-II is abundantly expressed during the mid- to late-secretory phase and acts as a mediator of progesterone (Zhou et al., 1994; Fluhr et al., 2008). Thus, it has been hypothesised that IGF-I is produced predominantly in endometrial stromal cells and mediates biological mitogenesis upon stimulus of estrogen by binding to IGF-IR on the epithelium in a paracrine manner (Oner and Oner, 2007). However, results from *in vivo* studies have yielded conflicting data by showing up-regulation of IGF-I and suppression of IGF-II during implantation (Gao et al., 1995).

Furthermore, there is evidence to show that IGF-I is produced from the blastocyst to mediate local mechanisms of implantation as shown by the secretion of IGF-I from the mouse embryo on day 8 of pregnancy in the culture medium (Spaventi et al., 1990). Embryonic carcinoma cells (PC13) express IGF-IR and secrete IGFBP, while mouse embryo organ explants including liver, intestine, heart, brain, and kidney secrete IGF-I (D'Ercole et al., 1980). Moreover, IGF-I enhances embryonic development and embryo quality by increasing the number of cells in the trophectoderm and inner cell mass (Kim et al., 2005). Other studies report the involvement of IGFs in the proliferation of cytotrophoblast cells and syncytial formation via the MAP kinase pathway, thus suggesting an important role in implantation and placentation (Forbes et al., 2008).

This is further supported by studies in mice lacking the IGF-I gene which are infertile and exhibit abnormal development of follicles beyond the secondary stage, and ovulatory defects (Louhio et al., 2000). IGF-I null mice result in increased pre- and post-natal mortality with loss of embryotrophic activity (Lackey et al., 1999) and multiple defects including underdevelopment of muscle tissues, a significantly reduced number of auditory neurons, and increased rates of apoptosis in cochlear neurons (Baker and Lyons,

1996; Camarero et al., 2001). The precise role that IGF-I plays in the mechanism of embryo implantation remains to elucidate.

The cellular response to IGF-I stimulation is modulated by ECM proteins, such as collagen I and IV, fibronectin, thrombospondin-1, and osteopontin (Nam et al., 2000; Woodward et al., 2000). ECM molecules play roles in the alteration of IGF-I down-stream signalling either in a direct way by modifying cellular adherence, or in an indirect way by binding to cell surface receptors, such as integrins (Woodward et al., 2000). In response to IGF-I, IGF-IR is auto-phosphorylated, resulting in the activation of IGF-IR intrinsic kinase activity allowing recruitment of various signaling molecules including insulin receptor substrate-I (IRS-I) and Src-homology containing (Shc) domain (Jones et al., 1996; Nolan et al., 1997; Petley et al., 1999). Changes in ligand occupancy of integrin αvβ3 have shown to directly modulate responsiveness to IGF-I stimulation (Jones et al., 1996; Ross, 2004). Blocking integrin αvβ3 ligand occupancy using a neutralising antibody or disintegrin echistatin has led the inhibition of IGF-I stimulated cell migration by reducing the phosphorylation of IGF-IR in response to IGF-I stimulation and the activation of the intrinsic kinase molecules of IGF-IR including IRS-I and PI3 kinase (Jones et al., 1996; Zheng and Clemmons, 1998).

Furthermore, occupancy of integrin αvβ3 with ligand has been shown to regulate the activity of protein tyrosine phosphatases, especially SHP-2 (PTPN 11), which is a down-stream factor of IGF-I signalling. In general, protein tyrosine phosphatase (PTP) molecules, such as SHP-1 and SHP-2 are important in growth factor and cytokine signal transduction pathways (Maile et al., 2002). Of the PTPs, SHP-2 is a non-transmembrane protein tyrosine phosphatase involved in various intracellular signalling pathways in response to growth factors such as insulin, IGF-I, PDGF, and EGF (Fujioka et al., 1996).

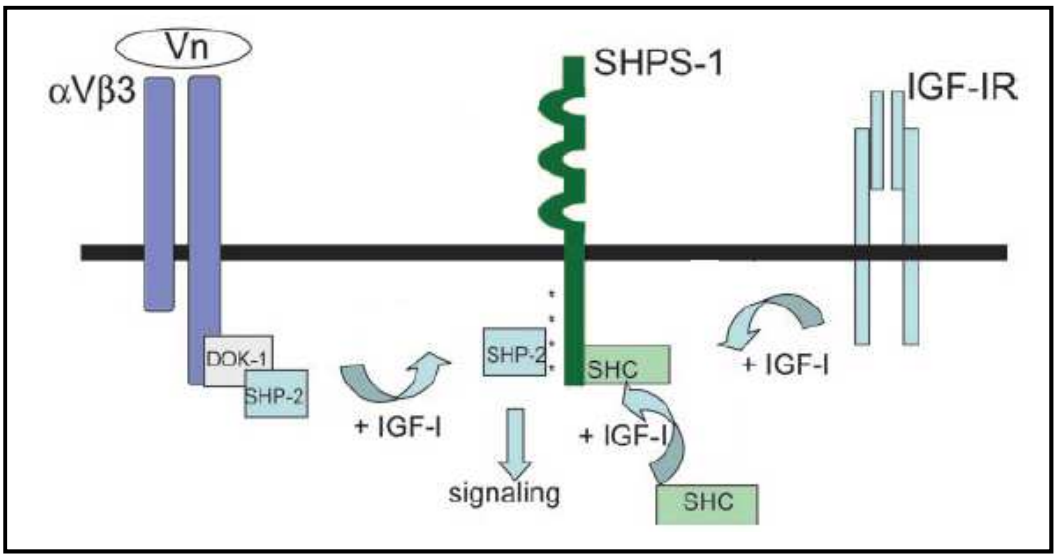


Figure 1.11: IGF-I and integrin αvβ3-linked signalling pathway

Upon the activation of integrin αvβ3 in response to engagement with its ligand, phosphorylated β3 integrin is associated with SHP-2. After the activation of IGF-IR in response to IGF-I stimulation, SHPS-1 is activated and exhibits high affinity to SHP-2. Recruitment of SHP-2 to SHPS-1 induces the phosphorylation of Shc to activate further down-stream mitogenic signalling components, such as MAPK. Adapted and modified from Clemmons and Maile (2005).

The importance of SHP-2 in the interaction between IGF-I and integrin αvβ3 linked signalling pathways has been demonstrated in studies in which IGF-I induces the phosphorylation of IGF-1 receptors and subsequently enhances the activation of integrin αvβ3 by increasing the affinity of its ligand-binding and the recruitment of SHP-2 in smooth muscle cells. To activate integrin function SHP-2 must be localised to the membrane and transferred to SHPS-1 (Maile and Clemmons, 2002). In smooth muscle cells, the membrane localisation of SHP-2, and its transfer to SHPS-1, are correlated with the association of phosphorylated integrin β3 with SHP-2 mediated by adaptor molecules including DOK-1, subsequently regulating IGF-I-dependent down-stream signalling

(Figure 1.11) (Ling et al., 2005a). Complexes of SHP-2 and SHPS-1 mediate cell adhesion and migration, regulating integrin function by phosphorylation of focal adhesion kinase (FAK) which is indirectly induced by the activation of Src family kinases (SFK) (Maile and Clemmons, 2002; Ling et al., 2005b). SHP-2 expression in the endometrium has not been characterised and its role is currently unknown. However, it is interesting to hypothesise that it may be important in mediating the interaction between growth factors, receptors and adhesion molecules in the embryo and endometrium during the early stage of implantation.

1.6.4.2 Heparin-binding EGF-like growth factor

Heparin-binding epidermal growth factor-like growth factor (HB-EGF), a 20-22kDa glycoprotein, is a member of the epidermal growth factor (EGF) family (Raab and Klagsbrun, 1997) and has structural features in common with EGF, transforming growth factor-α (TGF-α), vaccinia virus growth factor (VGF), amphiregulin (AR), β-cellulin (BTC), epiregulin (EPR), and neuregulin-1, 2 (NRG-1, 2) (Elenius et al., 1997). The precursor of HB-EGF is synthesised as a transmembrane form (proHB-EGF) containing signal peptide, heparin-binding, EGF-like, juxtamembrane, transmembrane, and cytoplasmic domains (Nishi and Klagsbrun, 2004).

In the transmembrane form, precursor HB-EGF transduces its signal via activation of receptors on adjacent cells in a juxtacrine manner and enhances its juxtacrine activity within associations via the tetraspanin protein (CD9), or integrin α3β1 (Higashiyama et al., 1995; Nakamura et al., 1995; Iwamoto and Mekada, 2000). Its membrane-anchored localisation at cell-cell contact sites may support its juxtacrine mitogenic activity in

regulating intercellular interactions. Additionally, precursor HB-EGF can undergo a process called 'ectodomain shedding' by which the precursor form is enzymatically cleaved at the plasma membrane by matrix metalloproteinases (MMPs) or a disintegrin and metalloproteinase (ADAM) to remove the prodomain and yield a soluble form (sHB-EGF) and a C-terminal fragment containing transmembrane and cytoplasmic domains (Goishi et al., 1995; Izumi et al., 1998; Iwamoto and Mekada, 2000; Hieda et al., 2008). The secreted form (sHB-EGF) acts as a potent mitogen in various types of cells, including epithelial cells by binding to receptors on the same cell in an autocrine manner or distant cells in a paracrine manner. The heparin-binding domain, which is unique in the EGF-like growth factor family, modulates biological activity (Shishido et al., 1995). The structure of the precursor form of HB-EGF is illustrated in Figure 1.12.

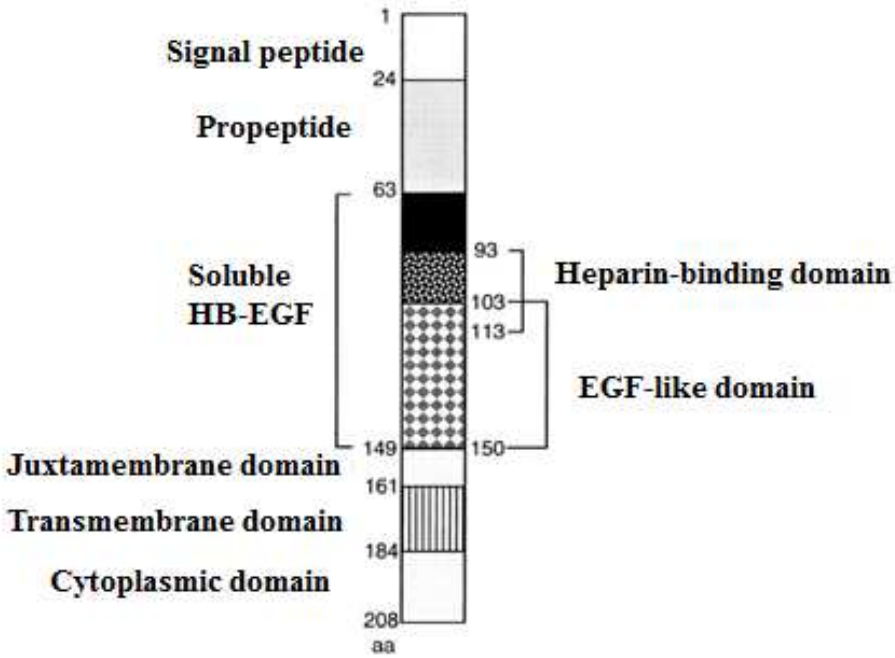


Figure 1.12: Structure of proHB-EGF

A schematic diagram illustrating the structure of proHB-EGF, including propeptide, heparin-binding domain, EGF-like domain, juxtacrine domain, transmembrane domain, and cytoplasmic domain. Adapted from Iwamoto and Mekada (2000).

HB-EGF acts as a juxtacrine, paracrine, or autocrine signalling mediator by primarily binding to ErbB1 (HER1) (Higashiyama et al., 1991) and ErbB4 (HER4) in either a direct or indirect manner, leading to different phenotypes (Elenius et al., 1997). Juxtacrine binding causes suppression of cell growth and inhibits apoptosis (Iwamoto et al., 1999), while autocrine and/or paracrine activity of HB-EGF mediates cell proliferation and migration (Yahata et al., 2006; Prince et al., 2010). ErbB receptors exist as inactive monomers with folded configuration to prevent dimerisation in normal conditions (Burgess et al., 2003; Tsujioka et al., 2011). They begin conformational rearrangement upon binding to HB-EGF, thereby forming both homodimers (ErbB1/1 and ErbB4/4) and heterodimers (ErbB1/4) (Olayioye et al., 2000). Dimerisation consequently induces stimulation of intrinsic receptor tyrosine kinases and results in auto-phosphorylation, leading to the recruitment and activation of down-stream components including MAP kinase and PI3 kinase pathways (Raab et al., 1996; Nishi and Klagsbrun, 2004; Holbro and Hynes, 2004; Tsujioka et al., 2011).

In addition, binding of both transmembrane and soluble forms of HB-EGF to ErbB receptors requires interaction with heparan sulfate proteoglycan (HSPG) molecules on the cell surface (Shishido et al., 1995; Iwamoto and Mekada, 2000). HSPG functions as a co-receptor for HB-EGF and also mediates cell adhesion by interacting with the heparin binding domain of extracellular matrix proteins, such as fibronectin (Iwamoto and Mekada, 2000; Xu et al., 2007). Thus, HB-EGF, containing binding sites for both HSPG and ErbB receptors, mediates cell adhesion by interacting with HSPG, while binding with ErbB receptors induces down-stream signalling. The processes of ectodomain shedding of HB-EGF and its juxtacrine and paracrine modes of signalling are illustrated in Figure 1.13.

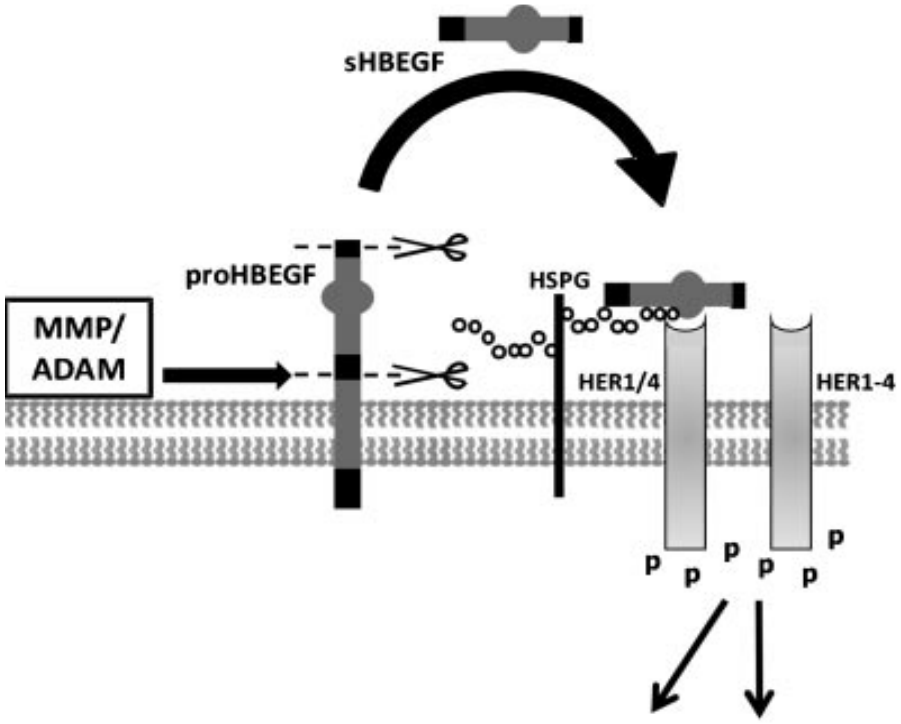


Figure 1.13: Process of HB-EGF signalling

A schematic diagram showing how the transmembrane form of HB-EGF is enzymatically cleaved to release sHB-EGF, which interacts with receptor tyrosine kinases, such as HER1 (ErbB1) or HER4 (ErbB4) to induce receptor auto-phosphorylation and initiate down-stream intracellular signalling. Adapted and modified from Jessmon et al. (2009).

The study of uterine HB-EGF expression began with the elucidation of its action as either a paracrine or autocrine factor in order to stimulate the proliferation of stromal cells during decidualisation in pregnant mice (Zhang et al., 1994a; Zhang et al., 1994b). In mice, HB-EGF appears around 6-7 hours before embryo attachment onto the uterine epithelium and exhibits local expression at the blastocyst apposition site where the earliest events of implantation occur, and expression continues during early pregnancy (Das et al., 1994). The appearance of HB-EGF prior to implantation has also been observed in the

baboon and Rhesus monkey (Yue et al., 2000; Leach et al., 2001). In humans, HB-EGF is highly expressed on the apical surface of the receptive luminal epithelium during the mid-secretory phase of the menstrual cycle, which is immediately prior to the window of implantation and this apical localisation of HB-EGF persists during the secretory phase. This consistent pattern of HB-EGF expression has also been observed at the mRNA level in humans (Birdsall et al., 1996; Yoo et al., 1997; Chobotova et al., 2002; Stavreus-Evers et al., 2002). The pre-implanting embryo expresses HB-EGF itself (Hamatani et al., 2004a). In addition, both the cytotrophoblast and syncytiotrophoblasts of the chorionic villi between 6 and 8 weeks express HB-EGF in human pregnancy (Leach et al., 1999). Moreover, HB-EGF increases the rates of both mouse and human embryo hatching and development and promotes the outgrowth of trophoblasts *in vitro* suggesting the involvement of HB-EGF during early embryo-endometrial interaction (Das et al., 1994; Martin et al., 1998).

A more defined role of HB-EGF in implantation has been suggested based on *in vivo* evidence which showed that embryo-sized HB-EGF-soaked beads transferred to pseudopregnant mouse uteri induced local implantation-like responses including HB-EGF expression on the luminal epithelium, increased vascular permeability, decidualisation, and of the expression of implantation markers (Paria et al., 2001). Furthermore, in ovariectomised hamsters, a species in which implantation can occur in the presence of progesterone alone; maternal estrogen is not essential for implantation (unlike mice or humans), uterine HB-EGF was not induced in the presence of progesterone alone. HB-EGF secreted from the blastocyst may induce its own expression in the luminal epithelium locally during implantation (Wang et al., 2002).

When HB-EGF is expressed in the luminal epithelium during implantation, ErbB

receptors and HSPGs are available for interaction with HB-EGF on the blastocyst surface (Nishi and Klagsbrun, 2004). ErbB1 is localised in the inner cell mass (Paria et al., 1999), while ErbB4 is expressed on the surface of trophoblast cells, particularly, adjacent to the inner cell mass of peri-implanting blastocyst. Localisation of ErbB4 may suggest interaction with HB-EGF in either a juxtacrine or paracrine manner mediates early events of implantation (Figure 1.14) (Chobotova et al., 2002). In addition, differential localisation of two ErbB receptors may indicate distinct functional roles during implantation.

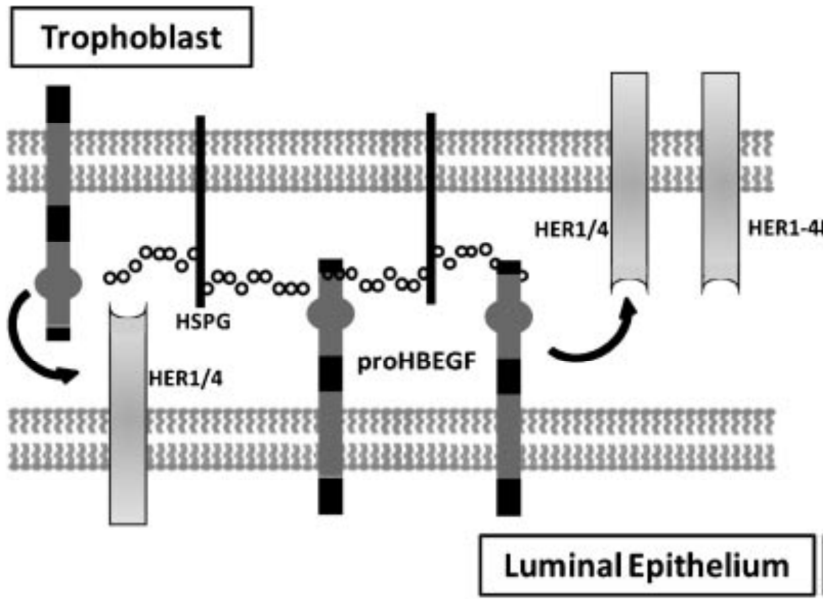


Figure 1.14: Paracrine and juxtacrine intercellular signal transduction via HB-EGF

A schematic diagram illustrating that the transmembrane form of HB-EGF which is expressed on both embryonic trophoblast and endometrial epithelium mediates embryo attachment onto uterine luminal epithelium. Adapted and modified from Jessmon et al. (2009).

Furthermore, as stated earlier, the blastocyst expresses HB-EGF on the surface of trophoblast, and ErbBs are expressed on the surface of luminal epithelium (Hamatani et al., 2004a). HSPG is also expressed on both the exterior surface of blastocyst trophectoderm and uterine epithelial cells during the initial stage of implantation (Raab et al., 1996). It may be postulated that HB-EGF is involved in the mechanism of implantation by serving as a two-way signalling bridge between the embryo and endometrium (Figure 1.14). However, mice lacking the HB-EGF gene are sub-fertile with delayed implantation and reduced litter size owing to defects in ovarian and uterine function which suggests that the deficiency of HB-EGF may be partially compensated by prolonged amphiregulin expression resulting from reduced estrogen secretion from defective ovaries. Blastocysts lacking the HB-EGF gene were successfully implanted on the uteri of wild-type mice (Xie et al., 2007).

1.7 *In vitro* models for the study of implantation

Due to the inaccessible nature of the human implantation site *in vivo*, efforts to obtain samples of human embryos at the site of implantation have been largely unsuccessful. Thus, there is a distinct lack of knowledge regarding the specific mechanisms underlying the early stage of implantation, such as apposition, adhesion, and the early penetration of the embryo through the endometrial epithelium.

Various *in vitro* models of embryo-endometrium interaction have been established over recent years in order to overcome the difficulties of *in vivo* study in human and differences between animal and human implantation. Kliman et al. (1990) developed an *in vitro* model of implantation using purified trophoblast cells from first, second, and third

trimester villous tissues and endometrial tissues obtained from hysterectomy or curettage. Tissues were first minced and co-cultured in polypropylene tubes on a rotator. The attachment of trophoblast cells on endometrial tissues was confirmed by hCG-positive staining and some trophoblast cells were shown to have penetrated the endometrial explant. Landgren et al. (1996) further established an *in vitro* model using endometrial tissues from day 4, 5, and 6 following the LH peak. Tissues were obtained via biopsy from healthy women with normal menstrual cycles and co-cultured with human embryos. This study demonstrated that the embryo was positioned on the lining of the epithelium within 3 h and subsequently penetrated the endometrial epithelium. Both types of model were established in order to mimic the *in vivo* endometrial environment by maintaining endometrial tissue explants in an appropriate culture medium. However, explant models are associated with a major problem, that of extensive tissue necrosis.

In order to investigate the late phase of implantation, human trophoblast cells obtained from early pregnancy terminations were co-cultured with human endometrial stromal cells derived from patients with benign disease. Microarray data after 24 h of co-culture using two different cell types demonstrated a significant increase in metalloproteinase inhibitor-3 (TIMP-3), dickkopf-1 (DKK-1), insulin-like growth factor binding protein 1 (IGFBP-1), pentraxin-3 (PTX-3), and interleukin-8 (IL-8), and a significant reduction of matrix metalloproteinase (MMP-11) and sry-related high mobility group-box 4 (SOX-4) upon contact with trophoblast cells (Popovici et al., 2000). This group postulated that a network induced by the contact of endometrial stromal cells with trophoblast cells might be related to inflammatory, immune, hematological and developmental mechanisms (Popovici et al., 2000). In a subsequent study, Carver et al. (2003) focused upon the invasion stage of implantation. An *in vitro* model was established

by co-culturing day 6 human blastocysts on monolayers of human primary endometrial stromal cells obtained via biopsy and immediately purified and decidualised by cyclic adenosine monophosphate (cAMP). This group demonstrated that when attached to decidualised stromal cells, human blastocysts showed outgrowth and further invasion into the stromal layer. Using this *in vitro* model, this research group also revealed potential modulators of trophoblast invasion to the stromal cells during implantation (Carver et al., 2003; Grewal et al., 2008). While *in vitro* models demonstrating interaction between the embryo and stromal cells have provided a significant opportunity with which to understand the invasion phase of implantation, this type of *in vitro* model overlooks the initial events of implantation, such as apposition, attachment, and adhesion, which are essential for successful implantation.

In order to overcome limitations of such models, and the lack of knowledge regarding multi-interactions between the different layers of endometrium, Bentin-Ley's' group established a 3-dimensional *in vitro* model composed of reconstituted endometrial stromal cells with collagen separated by basement membrane from the epithelial layer. This model, which closely resembled the structure of the human endometrium *in vivo,* has the potential to allow visualisation of all three different stage of implantation; embryo attachment and adhesion, and penetration of the embryo through the epithelial layer to the stromal layer. These authours demonstrated that the inner cell mass was located on the endometrial side when the embryo invaded to the stroma, which is very different to how mouse implantation occurs (Bentin-Ley and Lopata, 2000).

Another *in vitro* model focused on the initial attachment and adhesion of the embryo to the endometrial epithelium. This model was established by co-culturing day 5 mouse embryos on monolayers of immortalised human endometrial epithelial cells. This

demonstrated the initial attachment of embryos to the endometrial epithelium either in the presence or absence of hormones suggesting steroid treatment increases the incidence of stable attachment. Additionally, MUC-1 expression was removed at sites adjacent to the site of embryo attachment, while the sialomucin CD 164 was not affected by the presence of embryo (Singh et al., 2010).

Recently, a high-throughput and reproducible attachment assay was developed using an *in vitro* model. This model involved co-culturing trophoblast spheroids prepared from trophoblast choriocarcinoma (BeWo) cells, size-selection, and immortalisation with human endometrial epithelial (RL-95-2 and AN3-CA) cells. The authours suggested that the methodology used in this *in vitro* model can be applied for specific studies using various cell types and also provide significant opportunities to improve screening techniques for potential mediators of embryo attachment by demonstrating the rapid fluorometric assessment of BeWo spheroid attachment to endometrial epithelial cells (Ho et al., 2012).

Furthermore, Uchida et al. (2012) established an *in vitro* model by co-culturing trophoblast spheroids prepared from trophoblast choriocarcinoma (jAR) cells with human endometrial epithelial (Ishikawa) cells. This demonstrated that the stimulation with ovarian steroid hormones and treatment of a histone deacetylase inhibitor, suberoylanilide hydroxamic acid (SAHA) enhanced the attachment and adhesion of jAR spheroids to Ishikawa cells as well as induced the epithelial-mesenchymal transition (EMT) (Uchida et al., 2012). Using this model, other group investigated that large-conductance calcium-activated potassium channels (BK_{Ca} channels) play an important role in embryo implantation by regulating the activity of NG-kB and homeostasis of Ca^{2+} in human endometrial cells (Zhang et al., 2012).

As yet, no *in vitro* model has been developed which completely mimics the complex *in vivo* endometrial environment. However, i*n vitro* models using epithelial cells or a combination of epithelial and stromal layers can provide significant opportunities to study implantation at stages encompassing the sequential events of apposition, adhesion and invasion.

1.8 Ishikawa cells

The first endometrial cell line, HEC-1, was established by Kuramoto in 1968 (Kuramoto et al., 1972), and while Clarke et al. (1987) established an endometrial adenocarcinoma cell line, ECC-1, in 1987. ECC-1 has not been well characterised yet but is known to maintain estrogen and progesterone receptors. Furthermore, these cells appear to have similar phenotypes to luminal and surface epithelial cells, which provides useful advantages with which to study initial embryo-endometrial interaction. RL95-2 has been extensively used for implantation study but has also been criticised due to lack of apico-basal polarity, tight and adherens junctions, and cytoskeleton organisation. HEC-1A cells have not been selected as a good model for illustrating the potential mechanisms of implantation, despite maintaining epithelial polarity because it does not allow the adherence of trophoblast cells.

Although many endometrial cell lines have been investigated and characterised, Ishikawa cells appear to be an excellent model with which to study the normal endometrial epithelium and explore potential crosstalk between the embryo and endometrial epithelium, as well as identify candidate factors which possibly mediate implantation. Ishikawa cells, firstly described by Nishida et al. (1985), were originally derived from human endometrial

adenocarcinoma cells from a 39-year-old-Asian woman. This cell line maintains estrogen and progesterone receptors and these receptors respond readily to steroid hormones. Furthermore, the Ishikawa cell line exhibits the common milieu of enzymes and structural proteins found in normal endometrial epithelium. Even though this cell line undergoes morphological changes during long periods of culture, it grows stably, forms a monolayer, and maintains epithelial polarity (Singh et al., 2010). Castelbaum et al. (1997) reported that Ishikawa cells are an excellent model to investigate the regulation of endometrial integrins (Lessey et al., 1992), and their hormonal responses, by demonstrating the expression of two cycle-dependent integrins. Ishikawa cells express integrin α1β1 and αvβ3 which have been observed in normal endometrial epithelial tissues and appear to regulate endometrial receptivity and mediate cell adhesion during implantation. Estrogen-primed progesterone treatment induces the increased expression of integrin α1β1 but suppressed expression of integrin αvβ3 (Castelbaum et al., 1997).

1.9 Aims and approaches

This study focused upon three predominant aims in order to address specific molecular mechanisms regulating embryo implantation. The major aims of this study were:

1. To establish an *in vitro* model of interaction between the embryo and endometrium in 2-dimensional and 3-dimensional configurations and find evidence for crosstalk between the blastocyst and receptive endometrial epithelial cells.

2. To investigate the IGF-I-integrin αvβ3-OPN and HB-EGF-integrin αvβ3-OPN axes in regulating embryo attachment.

These particular problems were approached broadly in the following ways:

a) a 2-dimensional *in vitro* model was developed involving co-culture of either mouse or human embryos with Ishikawa cells, **b)** a 3-dimensional *in vitro* model was developed involving co-culture of mouse embryos on Ishikawa cells maintained on a collagen gel containing human endometrial stromal cells, **c)** immunofluorescence analysis was used to confirm distributional changes of adhesion molecules (MUC1, integrin αvβ5 and integrin αvβ3), an extracellular glycoprotein ligand (OPN), growth factor (HB-EGF), growth factor receptor (IGF-IR), and protein tyrosine phosphatase (SHP-2) following embryo attachment, **d)** Western blotting was used to investigate alterations in molecular profile of the epithelium in response to embryo attachment or stimulation by growth factors, **e)** co-immunoprecipitation was used to investigate for interaction between respective molecules, **f)** a novel *in vitro* model was developed by replacing the embryo with growth factor-loaded embryo-sized beads, **g)** the functionality of ligand-loaded beads was confirmed by performing bead attachment assays, and **h)** small interfering RNA knock-down was applied to elucidate the role of specific gene products in embryo attachment and ligand-loaded bead attachment.



CHAPTER 2

Materials & Methods

2.1 General reagents and solutions

All materials and chemical reagents for this study were supplied from Sigma Aldrich Chemical Company Ltd. (Dorset, UK) unless otherwise stated.

2.2 Antibodies

In total, 18 primary and 7 secondary antibodies were utilised for immunocytochemistry or Western blotting analysis in this study. Antibody specificity and cross-reactivity were confirmed by manufacturers unless otherwise stated specifically. A summary of antibody type, source, working dilution and incubation time are described in Tables 2.1 and 2.2, and Tables 2.3 and 2.4, respectively.

Table 2.1: Primary antibodies used for immunocytochemistry

Primary Antibody (Clone)	Supplier	Stock Conc.	Dilution (1%BSA /PBS)	Isotype	Source	Incubation Time
Cytokeratin (CY-90)	Santa Cruz, UK	200 µg/ml	1:100	IgG_1	Mouse	Overnight 4°C
E-cadherin (67A4)	Santa Cruz, UK	200 µg/ml	1:80	IgG_1	Rabbit	Overnight 4°C
MUC1 (BC-2)	Chemicon, UK	100 µg/ml	1:100	IgG_1	Mouse	Overnight 4°C
Integrin αvβ5 (15F11)	Chemicon, UK	100 µg/ml	1:100	IgG_{2a}	Mouse	Overnight 4°C
Integrin αvβ3 (LM609)	Chemicon, UK	100 µg/ml	1:100	IgG_1	Mouse	Overnight 4°C
HB-EGF (C-18)	Santa Cruz, UK	200 µg/ml	1:50	IgG	Goat	Overnight 4°C
ErbB4	Gift from Dr. Katya Chovotoba	100 µg/ml	1:100	IgG	Rabbit	Overnight 4°C
OPN (53)	Enzo Lifescience, UK	1 mg/ml	1:100	IgG_{2a}	Mouse	Overnight 4°C
SHP-2	Santa Cruz, UK	200 µg/ml	1:100	IgG	Rabbit	Overnight 4°C
IGF-IR β	Invitrogen, UK	100 µg/ml	1:100	IgG	Rabbit	Overnight 4°C

Table 2.2: Secondary antibodies used for immunocytochemistry

Secondary Antibody	Supplier	Stock Conc.	Dilution (0.1% BSA/PBS)	Epitope	Incubation Time
Goat anti-mouse Alexafluor 488	Invitrogen, UK	2 mg/ml	1:400	All mouse IgG subclasses	1 h, RT
Goat anti-mouse Alexafluor 568	Invitrogen, UK	2 mg/ml	1:400	All mouse IgG subclasses	1 h, RT
Goat anti-rabbit Alexafluor 488	Invitrogen, UK	2 mg/ml	1:400	All rabbit IgG subclasses	1 h, RT
Goat anti-rabbit Alexafluor 568	Invitrogen, UK	2 mg/ml	1:400	All rabbit IgG subclasses	1 h, RT
Donkey anti-goat Alexafluor 488	Invitrogen, UK	2 mg/ml	1:400	All donkey IgG subclasses	1 h, RT
Phalloidin (Texas Red-X dye)	Invitrogen, UK	100units/ml (20μM)	1:80		1 h, RT

RT: Room Temperature

Table 2.3: Primary antibodies used for Western blotting

Primary Antibody	Supplier	Molecular weight (kDa)	Stock Conc.	Dilution	Species/ Ig class	Incubation Time
Integrin αv	Cell Signalling, UK	135/140	201 µg/ml	1:1000	Rabbit/ IgG	Overnight 4°C
Integrin β3	Cell Signalling, UK	97/110/130	180 µg/ml	1:1000	Rabbit/ IgG	Overnight 4°C
OPN	Enzo Lifescience, UK	20~70	1 mg/ml	1:2000	Mouse/ IgG	Overnight 4°C
SHP-2	Santa Cruz, UK	70	200 µg/ml	1:2000	Rabbit/ IgG	Overnight 4°C
SHP-2	Santa Cruz, UK	70	200 µg/ml	1:2000	Mouse/ IgG	Overnight 4°C
IGF-IR β	Santa Cruz, UK	97	200 µg/ml	1:1000	Rabbit/ IgG	Overnight 4°C
P-IGF-IR	Biosource, UK	97	100 µg/ml	1:1000	Rabbit/ IgG	Overnight 4°C
P-ErbB4	Millipore, UK	180	100 µg/ml	1:1000	Rabbit/ IgG	Overnight 4°C
GAPDH	Santa Cruz, UK	35	200 µg/ml	1:500	Mouse/ IgG	Overnight 4°C
β-ACTIN	Cell Signalling, UK	44	11 µg/ml	1:1000	Rabbit/ IgG	Overnight 4°C

Table 2.4: Secondary antibodies used for Western blotting

Primary Antibody	Supplier	Stock Conc.	Dilution	Target Specificity	Incubation Time
Polyclonal Goat Anti-rabbit Immunoglobulins/HRP	Dako Cytomation, Denmark	1.1g/lit	1:1250	All rabbit IgG	1 h, RT
Polyclonal Goat Anti-mouse Immunoglobulins/HRP	Dako Cytomation, Denmark	1.1g/lit	1:1250	All mouse IgG	1 h, RT

RT: Room Temperature

2.3 Cell culture

2.3.1 Endometrial epithelial cell line and maintenance

Ishikawa cells, originating from human endometrial adenocarcinoma cells of a Japanese woman, were obtained from the European Collection of Cell Cultures (ECACC) and maintained in a 1:1 combination of Phenol-red Dullbecco's Modified Eagle Medium (DMEM) (Invitrogen, UK) with Ham 12 (Invitrogen, UK) supplemented with 10% Fetal Calf Serum (FCS) (Sigma, UK), 50 U/ml penicillin and 50 µg/ml streptomycin (Sigma, UK). Cells were incubated with 5% CO_2 at 37°C.

2.3.2 Primary endometrial stromal cells and maintenance

All samples of human endometrial tissue were obtained with informed consent in accordance with the requirements of the Central Oxford Research Ethics Committee and all experiments were performed with appropriate ethical approval from the Oxford Research Ethics Committee.

Human primary endometrial stromal cells were obtained from fertile patients aged 20-49 years undergoing hysterectomy for benign indications or sterilisation. Following a dissociation procedure (Carver et al., 2003), primary stromal cells were maintained in Phenol-red DMEM supplemented with 10% FCS, 50 U/ml penicillin and 50 µg/ml streptomycin and incubated with 5% CO_2 at 37°C. Stromal cells, verified by immunofluorescent staining using an antibody raised against stromal cell marker Thy-1 (Santa Cruz, UK) following dissociation, between passage 2 and 10 were used for studies.

2.3.3 Sub-culturing of endometrial cells by trypsinisation

Both endometrial epithelial and stromal cells grown in 75-cm^2 culture flasks were passaged at 90% confluence using 3 ml of 0.1% trypsin with 0.53mM EDTA (Invitrogen, UK). Following trypsinisation, detached cells were neutralised with 7 ml of DMEM-F12 culture media including FCS. Subsequently, cells were collected in 15 ml falcon tubes and centrifuged at 1300 rpm for 3 min to wash cells and remove dead cells and debris. Supernatants were discarded and pellets were resuspended in 1 ml of DMEM-F12 culture media including FCS. $1x10^6$ cells were counted using a hemocytometer (details are

described in Supplementary Appendix 2) and plated in 75-cm^2 culture flask for maintenance. Cells were plated in various sizes of plates for further experiments.

2.3.4 Freezing and retrieving endometrial cells

Cells were trypsinised at 90% confluence and neutralised with DMEM-F12 culture medium including FCS. Cell pellets were then resuspended in 1 ml of freezing medium (90% FCS and 10% Dimethyl Sulfoxide (DMSO)) and transferred into a cryovial (Nunc, UK) for overnight storage at -80°C. The next day, pellets were transferred into a liquid nitrogen container for long term storage.

Frozen cells were thawed at 37°C in a water bath and washed with DMEM-F12 culture medium to remove DMSO. Cell pellets were resuspended in DMEM-F12 culture medium including 10% FCS and incubated at 37°C in 5% CO_2. Cells were maintained as described in Section 2.3.1.

2.4 Embryo culture

Initially studies were carried out at the Nuffield Department of Obstetrics and Gynaecology, University of Oxford (from Jan, 2009 to Aug, 2010) and subsequently all experimental work was transferred to the University of Manchester (from Sep, 2010 to Dec 2011).

2.4.1 Human embryos

All human embryo work was carried out at the Nuffield Department of Obstetrics and Gynaecology, University of Oxford. Ethical approval for this study was obtained from the Oxfordshire Research Ethics Committee and a research license was obtained from the Human Fertilisation and Embryology Authority (HFEA). Human embryos were donated for research with informed written consent from patients attending the Oxford Fertility Unit, John Radcliffe Hospital, for IVF treatment. Ovarian stimulation, oocyte retrieval, insemination and grading for Day 2 embryos were performed in accordance with routine clinical procedures as described in Supplementary Appendix 3. Embryos were assessed according to morphology and those displaying ≥50% blastomere survival were donated for research and were transferred to 100µl of a complex serum-free medium (CSFM3) supplemented with 1 mmol/l HB-EGF (Heparin Binding Epidermal Growth Factor-like Growth Factor) and 2.5% human serum albumin (HSA) (Bio Products Laboratory, Elstree, UK) and overlaid with 1ml of mineral oil (Sigma, UK). Embryos were maintained in culture to the hatched blastocyst stage and those selected as Grade A and B in both trophectoderm and inner cell mass (Table 2.5 and Figure 2.1) were transferred onto *in vitro* 2D and 3D models for further research. Standard criteria for grading embryos are described in Section 2.4.2.

2.4.2 Criteria used for the grading of human embryos

As the human embryo is composed of two different cell types (inner cell mass and trophectoderm), and a fluid cavity, the standardised grading of embryos is normally assigned to three separate quality scores for each composition, such as blastocyst

development stage, inner cell mass score, and trophectoderm score. Standard criteria for scoring human embryos are described in Table 2.5 and Figure 2.1.

Table 2.5: Standard grades for assessing blastocyst development

-Expansion grade-

Expansion grade	Development of embryo
1	Volume of blastocoel cavity is less than half of embryo
2	Volume of blastocoel cavity is more than half of embryo
3	Full blastocyst
4	Expanded blastocyst
5	Hatching
6	Hatched

-Inner cell mass (ICM) and Trophectoderm (TE) grades-

ICM grade	Quality of inner cell mass	TE grade	Quality of trophectoderm
A	Many cells and tightly packed	**A**	Many cells and forming a cohesive layer
B	Several cells and loosely grouped	**B**	Several cells and loosely formed epithelium
C	Very few cells	**C**	Very few large cells

(All criteria were adapted and modified from the website of IVF of Advanced Fertility Centre of Chicago, date accessed 05-03-2012)

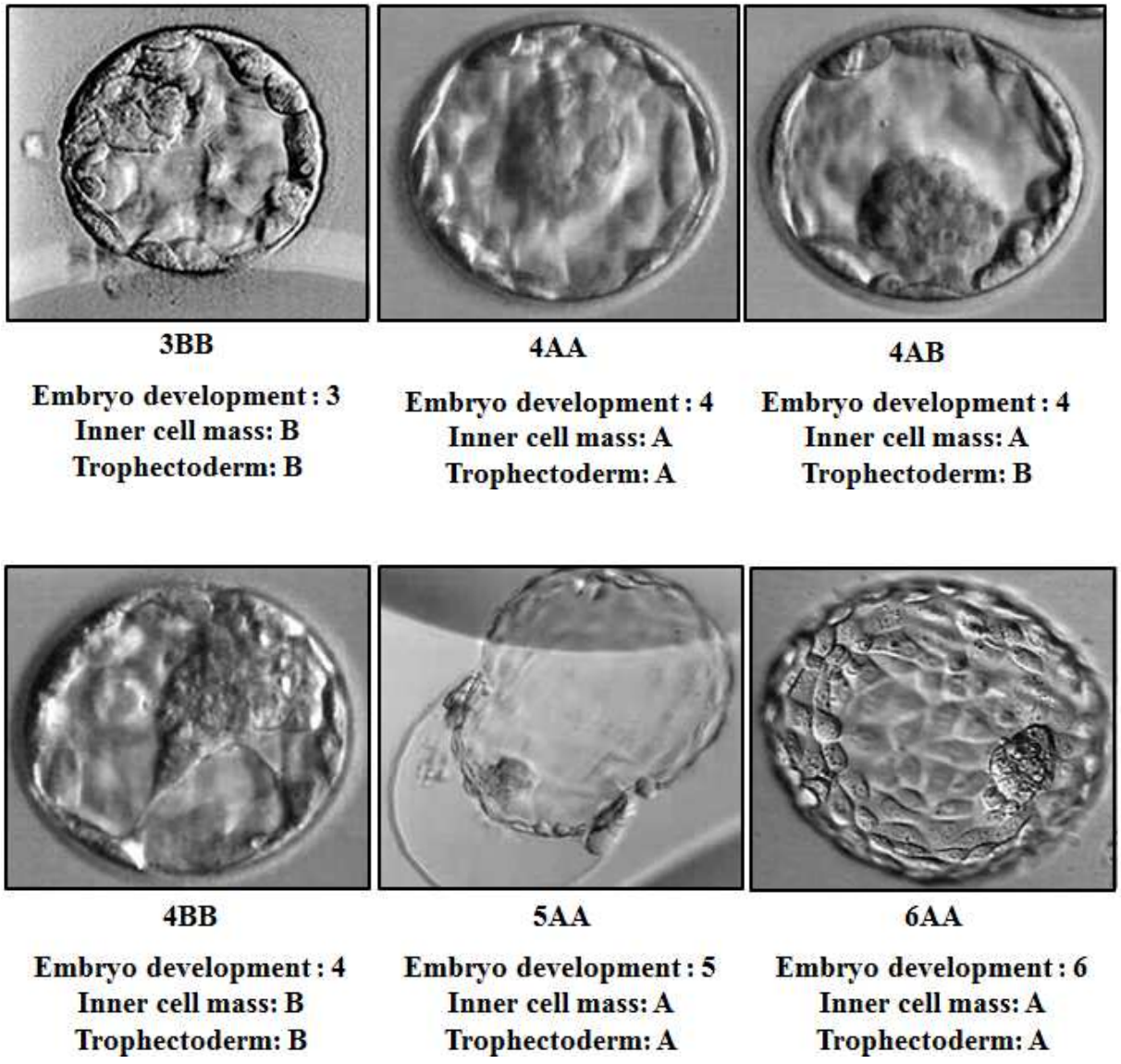


Figure 2.1: Grading criteria for human embryos

Phase contrast microscopy images of human embryos in grades between 3 and 5. All images were adapted and modified from the website of IVF of Advanced Fertility Centre of Chicago, date accessed 05-03-2012.

2.4.3 Mouse embryos (University of Oxford)

Female CBAB6F1 mice were injected with pregnant mare serum gonadotrophin (PMSG, at 5 weeks) and chorionic gonadotrophin (47 h later than the first injection) and mated with CBAB6F1 males (Maintained by Biomedical Services, John Radcliffe Hospital). Two-cell embryos were obtained from the oviduct by flushing at day 1.5 post coitum, transferred to M2 medium (Sigma, Dorset, UK), and subsequently placed into a 30 µl drop of pre-equilibrated DMEM supplemented with 10% FCS covered with mineral oil and incubated at 37°C, 6% Oxygen. Two-cell embryo flushing from mice was carried out by Biomedical Services at the John Radcliffe Hospital.

2.4.4 Mouse embryos (University of Manchester)

All mouse work was transferred to the University of Manchester in September 2010.

2.4.4.1 Maintenance of animals

Female C57BL/6 mice were maintained by the Biomedical Services Unit at the University of Manchester. 6-8 week old male and female mice were used throughout all experiments. All mice were kept under standard conditions of 12 h light and 12 h dark at 20-22°C, 40-60% humidity with free access to food and water.

2.4.4.2 Mating and superovulation

Female C57BL/6 mice were injected via an intraperitoneal route with 0.1 ml of 5 IU PMSG and 0.1 ml of 5 IU hCG (47 h later than the first injection). Eight hours after hCG injection female mice were mated with C57BL/6 males. On the following morning, female mice were examined for presence of a vaginal plug as an indicator of successful mating.

2.4.4.3 Retrieval and culture of two-cell stage mouse embryos

On day 2, pregnant mice were sacrificed 48 h following hCG injection. Using sterilised scissors and forceps the lower abdominal cavity of mice was incised and both oviducts dissected following removal of both uterine horns using fine forceps. Two-cell embryos were obtained from the oviduct either by flushing using a 34G blunt-ended stainless steel needle (Cooper Needleworks, Birmingham, UK) and syringe or by chopping (mincing) using fine forceps under a microscope. Flushed embryos were washed with M2 media supplemented with 4 mg/ml bovine serum albumin (BSA) and subsequently transferred into a 60 µl drop of KSOM for further washing and finally cultured in a drop of 30 µl KSOM covered with mineral oil and incubated at 5% CO_2, 37°C until the blastocyst stage. The procedure of retrieval for two-cell stage mouse embryos from the oviduct is described in Figure 2.2. On day 5, mouse embryos were transferred onto confluent Ishikawa cells.

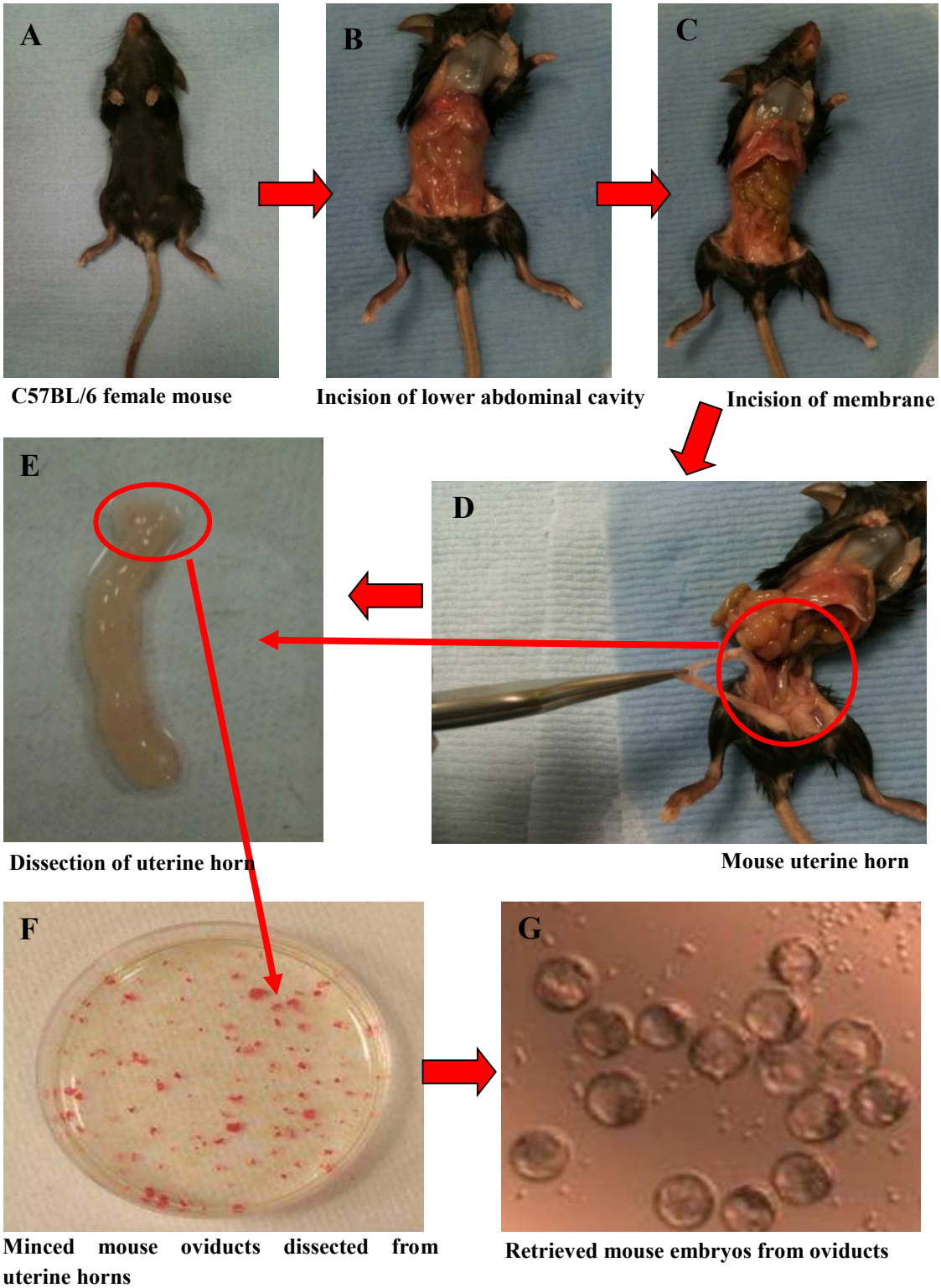


Figure 2.2: Process of retrieval for two-cell stage embryos from mouse oviducts

2.5 Co-culture of embryos with endometrial cells

2.5.1 Two-dimensional (2D) culture

13 mm coverslips were coated with matrigel (BD Science, Oxford, UK) diluted 15 times with ice-cold serum free phenol-red DMEM-F12 for 1 h at room temperature. After being coated, $5x10^4$ Ishikawa cells were seeded per coated coverslip in a 24 well plate. Ishikawa cells were maintained in DMEM-F12 culture media supplemented with 10% FCS and incubated in 5% CO_2 at 37°C. Once cells were confluent on the coverslip, they were starved overnight and day 5 mouse blastocysts or day 6 human blastocysts were transferred onto the monolayer of Ishikawa cells.

2.5.2 Three-dimensional (3D) culture

$1.2x10^6$ endometrial stromal cells were mixed in neutralised collagen solution before gelation within a membrane transwell insert (Millipore, Watford, UK) in a single well of from a 24-well plate (16.28mm in a diameter) and incubated for 30-40 min at 37°C to set. The collagen gel preparation is described in Table 2.6. The top of the collagen gel was then coated with 100µl matrigel (1 in 15 dilution) for 30 min at 37°C. Finally, $3x10^4$ Ishikawa cells were seeded and maintained in DMEM-F12 medium supplemented with 10% FCS and incubated in 5% CO_2 at 37°C.

Table 2.6: Composition of collagen gel mixture for three-dimensional embryo culture

Components	Source	Volume (µl)
10x DMEM	Sigma Aldrich, Dorset, UK	30
-HCO_3 (7.5%)	Sigma Aldrich, Dorset, UK	15
HEPES (1M)	Sigma Aldrich, Dorset, UK	6
Glutamine (200mM)	Sigma Aldrich, Dorset, UK	3
10x Folic acid	Sigma Aldrich, Dorset, UK	3
Collagen type I	Sigma Aldrich, Dorset, UK	243
Total		300

2.6 Embryo attachment assay

Day 5 mouse embryos were transferred onto confluent Ishikawa cells in independent microwells of a 96-well plate. After 24-48 h of co-culture, the stability of embryo attachment was determined. Before measurement, the plate was shaken three times from side to side and back and forth, respectively and each measurement was performed manually under a microscope examining the stability of each mouse embryo upon tapping the plate. Standardised criteria for scoring the stability of embryo attachment is described

in Table 2.7.

Table 2.7: Standard criteria for scoring the stability of embryo attachment (adapted and modified from Carver et al. (2003))

Score	Standard of scoring the stability
1	Floating
2	Weakly attached but detached after tapping
3	Weakly attached and still attached after tapping
4	Strongly attached
5	Strongly attached and some parts of trophoblast cells were invaded

2.7 Co-culture of growth factor-coated beads with endometrial cells

2.7.1 Preparation of growth factor-coated beads

Embryo-sized beads (BioRad, Hertfordshire, UK; 80-150μm) were washed with PBS six times by repeat centrifugation and resuspension. 30 μl drops of IGF-I, HB-EGF, OPN, or BSA were overlaid with 2 ml of mineral oil and equilibrated in an incubator at 37°C for 30 min. Washed beads were then transferred to growth factor drops and incubated

for 2 h at 37°C.

2.7.2 Co-culture of beads on Ishikawa cell monolayers

A 13mm coverslip was coated with matrigel (BD Science, Watford, UK) diluted 15 times with ice-cold serum free phenol-red DMEM-F12 for 1 h at room temperature. After coating, $5x10^4$ Ishikawa cells were seeded onto a coated coverslip in a single well of a 24 well plate and maintained in DMEM-F12 supplemented with 10% FCS in 5% CO_2 at 37°C. Once cells were confluent on the coverslip, growth factor-coated beads were transferred.

2.8 Immunocytochemistry

2.8.1 Immunocytochemical investigation of a two-dimensional *in vitro* model

Ishikawa cells were prepared as described in Section 2.5.1 on matrigel-coated coverslips and either mouse or human blastocysts were transferred onto Ishikawa cells at confluence. After 24-48 h of co-culture, media was removed and cells were gently washed with PBS (x2) before fixing with 4% PFA (BDH Chemicals, Poole, UK) for 15 min at room temperature. After fixation, cells were rinsed with PBS (x3) and permeablised with 0.5% Triton X-100 (Sigma, Dorset, UK) for 15 min at room temperature. When the permeablisation was not required to exclude intracellular expression, this step was not carried out. Following three further PBS washes, cells including embryos were blocked

with 3% BSA in PBS for 1 h at room temperature to minimise non-specific binding and subsequently indirect immunofluorescence staining was performed by incubating at 4°C overnight with respective primary antibodies using dilutions and conditions indicated in Table 2.1. The next day, cells were washed with PBS for 5 min (x3) to remove primary antibody and depending on the primary antibody host, incubated with either goat anti-mouse or goat anti-rabbit Alexafluor 488 (FITC) / 568 (RED) secondary antibodies (Molecular Probes, Eugene, Oregon, USA) for 1 h at room temperature in darkness. For the negative control, cells were incubated only with secondary antibody omitting incubation with primary antibody, or replacing primary antibody with the same isotype of IgG. Cells, including embryos, were rinsed with PBS for 5 min (x3) and mounted in Vectashield mountant containing 4',6-diamidino-2-phenylindole (DAPI) (Vector Laboratories, Peterborough, UK) for nuclear staining.

2.8.2 Immunocytochemical investigation of a three-dimensional *in vitro* model

Endometrial cells were co-cultured with mouse embryos on 3D gels as described in Section 2.5.2. After the embryo had implanted onto the layer of epithelial cells, the gel was fixed with 4% PFA for 45 min and soaked in embedding solution (Polyscience, Eppelheim, Germany) at 4°C overnight. The gel was removed from the insert and frozen at -20°C. Serial sectioning was carried out using a cryostat by Ms. Janet Carver (Nuffield Department of Obstetrics and Gynaecology, University of Oxford) for immunofluorescence staining. Four sections were spaced out on each slide and were checked using light microscopy to find the attached embryos. A border line was drawn between sections using a DAKO pen to prevent mixing between sections. Sections were

permeablised with 0.5% Triton X-100 for 15 min and washed with PBS for 5 min (x3). Sections were blocked with 3% BSA in PBS for 1 h at room temperature and subsequently incubated with primary antibodies at 4°C overnight. The next day, sections were washed with PBS for 5 min (x3) and incubated with the appropriate secondary antibodies for 1 h at room temperature in darkness and then re-washed in the same manner. After the final washing, sections were covered with a glass coverslip using Vectashield mounting medium containing DAPI (Vector Laboratories, Peterborough, UK).

2.8.3 Image analysis of immunocytochemical data

Images were captured using 10X, 20X, 40X and oil immersion 40X objectives of a Leica DMRBE microscope, a Hamamatsu Orca C4742-95 digital camera and analyzed with Openlab software Invitrovision (University of Oxford) and Zeiss AxioObserver Inverted Microscope (Carl Zeiss Inc., Jena, Germany) (University of Manchester).

2.9 Western blot analysis

2.9.1 Preparation of whole cell extracts

Cells cultured to 95% confluence on 6-well plates were washed with ice-cold PBS (x2) on ice to stop cellular activity. Radioimmunoprecipitation assay (RIPA) buffer (100 µl) including protease inhibitor cocktail set I and phosphatase inhibitor cocktail set II and III (Sigma, Dorset, UK) was added to each well. Cells were scraped and collected in 1.5 ml microcentrifuge tubes. Extracts were homogenised using a sterile 27G needle and 1 ml

syringe and kept in ice for 30 min to reduce viscosity. Extracts were subsequently stored at -20°C prior to Western blotting.

2.9.2 Quantification of protein levels

The concentration of protein extracted from Ishikawa cells was quantified using the established Bradford assay (Bio-rad, Hertfordshire, UK). A serial standard dilution series (1.0, 0.5, 0.25, 0.125 and 0 mg/ml) was prepared using BSA dissolved in distilled water. All samples were diluted 1 in 10. 10 µl of each diluted sample was added per well to a 96-well plate. 200 µl of diluted Bradford reagent (1 in 5 dilution with distilled water) was added to each sample. All assays, for each sample, were carried out in triplicate. After 15 min of incubation at room temperature, the plate was read at 595 nm using a Versamax microplate reader (Molecular Devices, East Sussex, UK).

2.9.3 Preparation of protein lysate samples

Prior to loading, protein lysates were thawed and 30 µg of protein prepared by diluting with water and sample volume of 2x sample buffer and 10% (v/v) β-mercaptoethanol was added to all samples. Prior to loading, protein samples were heated at 95°C for 5 min.

2.9.4 SDS-polyacrylamide gel electrophoresis (SDS-PAGE)

Proteins were separated electrophoretically by molecular weight on SDS-containing PAGE using the manufacturer's recommended protocol but with some modifications. 10% SDS-polyacrylamide gels of 1.5 mm thickness were prepared using

Mini-Protean II casting apparatus (BioRad Laboratories, Hertordshire, UK). The composition of resolving and stacking gels are provided in Table 2.8. After gels were set up in a vertical electrophoresis system, the tank was filled with 1x electrophoresis/electrode buffer. The composition of electrophoresis/electrode buffer is described in Supplementary Appendix 1. 30 µg of proteins were loaded onto each well and protein molecular weight kaleidoscope prestained standard marker (BioRad Laboratories, Hertordshire) was loaded onto a well and electrophoresis was performed for the first 20 min at a constant voltage of 90V until the samples reached resolving gel and then at a constant voltage of 110V.

Table 2.8: Composition of resolving and stacking gels (volume given for 2 mini-gels)

	Resolving gel	**Stacking gel**
% of gel	10 %	3 %
dH_2O	4.7 ml	6.5 ml
30% Bis-Acrylamide	3.3 ml	1.0 ml
Separating gel buffer	2 ml	-
Stacking gel buffer	-	2.5 ml
10% APS	150 µl	100 µl
TEMED	10 µl	15 µl

APS: Ammonium Persulfate

TEMED: Tetramethylethylenediamine

2.9.5 Electrophoretic transfer of proteins to PVDF membranes

Separated proteins were transferred to polyvinylidene fluoride (PVDF) membranes (Millipore, Watford, UK) using a BioRad wet transfer system. Prior to transfer, the PVDF membrane was activated by soaking in methanol for 2 min. In addition, 2 sponges and 2 filter papers were also prepared for each cassette and soaked in transfer buffer. The composition of transfer buffer is described in Supplementary Appendix 1. Following electrophoresis, the stacking gel was discarded and the resolving gel was removed from the glass plate and transferred onto PVDF membrane. Filter paper was overlaid on each gel. Air bubbles were removed by rolling a pipette tube over the filter paper. Transfer buffer was filled to the top of the tank and electrophoretic wet transfer was performed for 80 min at a constant 110V. Once the transfer was complete, the membrane was removed from the cassette and blocked with 5% BSA in 0.05% TBS-Tween 20 at room temperature for 1 h on a platform shaker at room temperature.

2.9.6 Immunological detection of proteins

After blocking, membranes were probed with respective primary antibodies (Table 2.3) on a platform shaker at 4°C overnight. The next day, membranes were washed for 5 min (x5) with 0.05% TBS-Tween 20 and incubated with peroxidase-labelled goat anti-rabbit and goat anti-mouse IgG secondary antibody (Table 2.4) at 1:1250 dilutions at room temperature for 1 h, and then re-washed in the same manner.

Membranes were exposed to the enhanced chemiluminescence system and then to Amersham or Kodak film. The exposure time was optimised depending on the signal.

Films were developed by Kodak D19 developer for 1 min, washed with tap water for 1 min, fixed with Kodak fixer for 1 min and finally washed with tap water. When films were dry, the size of protein bands was determined by reference to the molecular weight marker.

2.9.7 Stripping and re-probing membranes

In order to detect other proteins using different primary antibodies on the same blot, membranes were heated to 55°C for 30 min in stripping buffer as described in Supplementary Appendix 1 within a shaker and washed thoroughly with 0.05% TBS-Tween 20 for 15 min (x5). Membranes were then incubated with the respective primary antibody overnight at 4°C after 1 h of blocking in 5% BSA in 0.05% TBS-Tween 20 at room temperature. The immunological detection process was performed in the same manner as described in Section 2.9.6.

2.10 Cell adhesion assays

Prior to seeding cells, the microwells of a 96-well plate were coated with OPN (5ng/µl, 20ng/µl), OPN (5ng/µl, 20ng/µl) + Thrombin (10NIH units/µg), BSA (5ng/µl, 20ng/µl) for the negative control and FCS for the positive control for 2 h at 37°C. After being coated, wells were washed thoroughly with PBS. $3x10^3$ Ishikawa cells were plated in serum-free DMEM-F12 media and each treatment was performed in triplicate. Cell adhesion was examined at 2 h, 4 h and 24 h after cell seeding followed by removing the culture media and washing with PBS. Phase contrast images of attached cells were taken. In order to investigate the mechanism of OPN cleavage, cells were treated with serine

protease inhibitor (AEBSF (10 μM)), potent broad MMPs inhibitor (NNGH (50 μM)), serine and cysteine inhibitor (Leupeptin (50 μM)), or broad caspase inhibitor (ZVAD-fmk (50 μM)).

2.11 Cell-surface protein labelling with biotin

In order to isolate the cell surface protein, confluent Ishikawa cells maintained in a 75-cm^2 flask were cooled down by washing twice with ice-cold PBS. Washing was not more than 5 sec to avoid cells being detached. Subsequently, cells were labelled with EZ-link Sulfo-NHS-SS-Biotin by incubating with a thiol-cleavage amine-reactive biotinylation reagent for 30 min at 4°C on a rocking platform to ensure an even coverage of cells with the labelling solution. After quenching, cells were harvested with mild detergent. Biotin-labelled cells on the apical cell surface were immunoprecipitated with NeutrAvidin Agarose in the column which was capped both bottom and top. After 1 h incubation at room temperature with end-over-end mixing using a rotator, cell lysates which were immunoprecipitated with avidin gel were centrifuged for 1 min at 1000g. Flow-through was discarded and the contents left in the column were washed with washing buffer including protease inhibitors. In order to elute pure protein from the lysates immunoprecipitated with avidin gel and recover NeutrAvidin protein monomer, SDS-PAGE sample buffer including 50mM DTT was added to the column and heated for 5 min at 95°C. Isolated protein was collected in a fresh tube after the centrifuge for 2 min at 1000g. Samples were then analysed by Western blotting as described in Section 2.9. A summary of procedures is illustrated in Figure 2.3

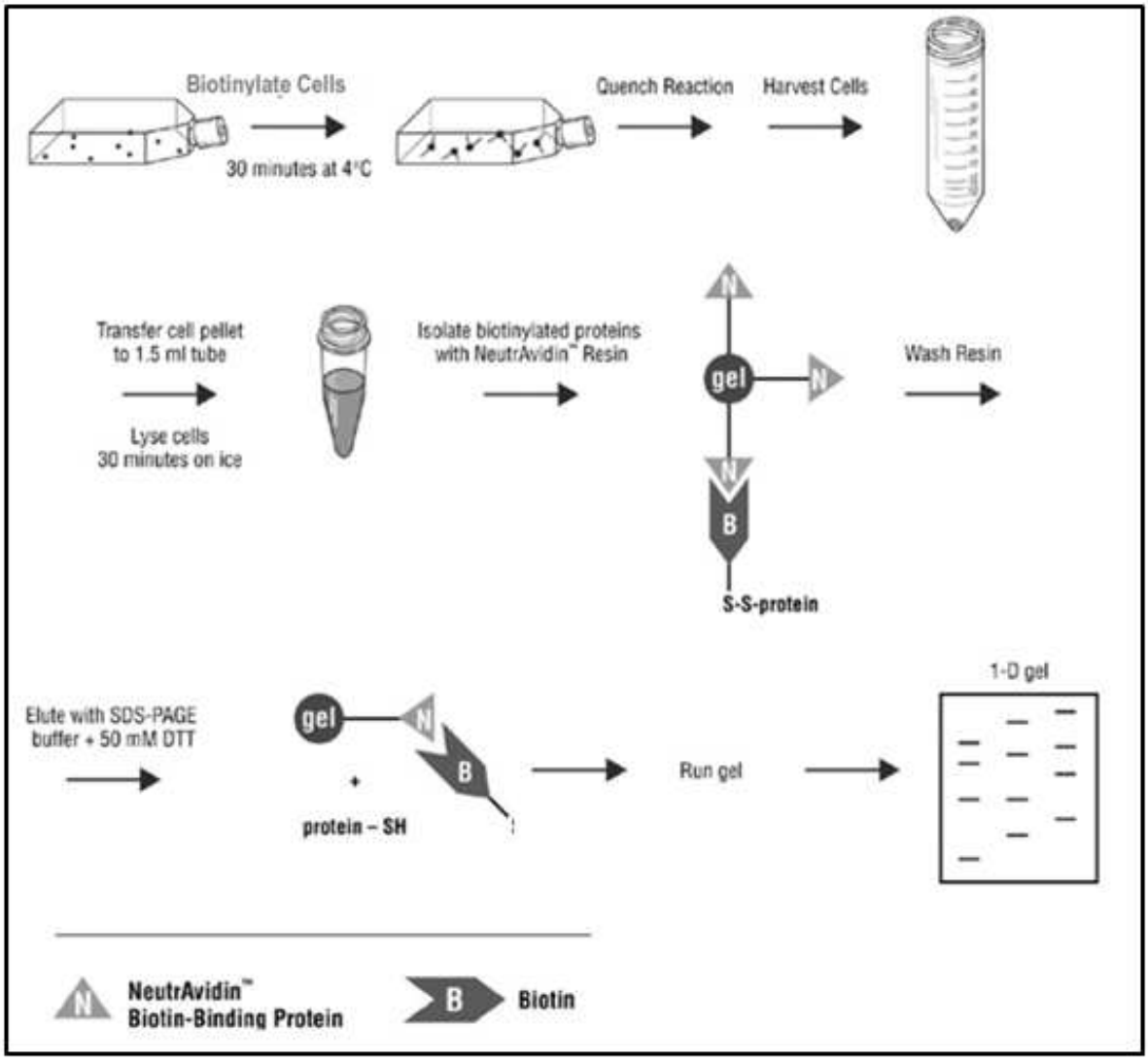


Figure 2.3: Summary of cell surface protein isolation procedure

A schematic diagram illustrating a procedure that glycoproteins from biotinylated apical cell membranes were affinity purified (adapted from http://www.piercenet.com/instructions/2161511, date accessed 09-04-2012)

2.12 Transfection of cells with short-interfering RNA

$3x10^4$ Ishikawa cells were plated onto 96-well plates and cultured in DMEM-F12 supplemented with 10% FCS, 50U/ml penicillin and 50μg/ml streptomycin. At 70% confluence, the medium was changed to DMEM-F12 without FCS, penicillin and streptomycin and cells were incubated overnight at 37°C. Knock-down of integrin αvβ3 was performed using two different siRNA sequences (Thermo Scientific, Northumberland, UK) which target the integrin αv (ITGAV) and β3 (ITGB3) genes respectively. Knock-down of OPN, IGF-IR, or SHP-2 was performed using siRNA sequences targeting the OPN (Thermo Scientific, Northumberland, UK), IGF-IR (Ambion, Paisley, UK), or PTPN11 (Invitrogen, Paisley, UK) gene respectively (Table 2.9). All siRNA reagents were pools of sequences targeting each gene. An siRNA which does not target any known sequence in the human genome was used for control experiments. Ishikawa cells were transfected with integrin αv, β3, OPN, IGF-IR, SHP-2 or non-targeting siRNA (100nM in total concentration) using the DharmaFECT 2 transfection reagent (Thermo Scientific, Northumberland, UK) for 48 h before mouse embryos or beads were transferred onto Ishikawa cells, as recommended by the manufacturer but with some modifications. Briefly, 5 μM of stock siRNA solution was dissolved in RNase free water and was prepared prior to transfection. In tube 1, 5 μM of siRNA was diluted down to an appropriate concentration with serum-free and antibiotic-free culture media and in tube 2, DharmaFECT 2 transfection reagent was diluted down to an appropriate concentration as recommended by the manufacturer. After 5 min of incubation at room temperature, solutions from both tube 1 and 2 were mixed gently and incubated for 20 min at room temperature. Mixed solutions were diluted with serum-free and antibiotic-free culture media to the total concentration required. Following gentle mixing, solutions including siRNA were added to cells.

Ishikawa cells without transfection or transfection with only reagent were used for control experiments.

Table 2.9 Sequences of siRNA (Continued on page 77)

Gene		Source	CAT#	Sequences
Integrin αv : ITGAV On-Target plus smart pool	siRNA 1	Thermo Scientific, Northumberland, UK	J-004565-07	CCUCUGACAUUGAUUGUUA
	siRNA 2	Thermo Scientific, Northumberland, UK	J-004565-08	CCGAAACAAUGAAGCCUUA
	siRNA 3	Thermo Scientific, Northumberland, UK	J-004565-09	GAACAUGUCCUCCUUAUAC
	siRNA 4	Thermo Scientific, Northumberland, UK	J-004565-10	GUUCACGCCUGCUAACAUU
Integrin β3 : ITGB3 On-Target plus smart pool	siRNA 1	Thermo Scientific, Northumberland, UK	J-004124-08	GCAGUGAAUUGUACCUAUA
	siRNA 2	Thermo Scientific, Northumberland, UK	J-004124-09	GAAGAACGCGCCAGAGCAA
	siRNA 3	Thermo Scientific, Northumberland, UK	J-004124-10	GCCAACAACCCACUGUAUA
	siRNA 4	Thermo Scientific, Northumberland, UK	J-004124-11	CCAGAUGCCUGCACCUUUA

Gene		Source	CAT#	Sequences
OPN : SPP1 On-Target plus smart pool	siRNA 1	Thermo Scientific, Northumberland, UK	J-012558-09	CCAAGUAAGUCCAACGAAA
	siRNA 2	Thermo Scientific, Northumberland, UK	J-012558-10	CAUCUUCUGAGGUCAAUUA
	siRNA 3	Thermo Scientific, Northumberland, UK	J-012558-11	UGAACGCGCCUUCUGAUUG
	siRNA 4	Thermo Scientific, Northumberland, UK	J-012558-12	GAUGAACUGGUCACUGAUU
IGF-IR : IGFIR	siRNA	Ambion, Paisley, UK	Sense	GGAAUACAGGAAGUAUGGATT
			Antisense	UCCAUACUUCCUGUAUUCCTG
SHP-2: PTPN11	siRNA	Invitrogen, Paisley, UK	10620312-112409-B08	UUUCUGCUCUUCUUCAAUCCUGCGC

2.13 Immunoprecipitation

Cells were washed twice with ice-cold PBS at 90% confluence and harvested with RIPA buffer without reducing agents. Cell extracts were clarified by centrifugation and quantified. In order to reduce non-specific binding of proteins to protein A coated Sepharose beads (GE Healthcare, Buckinghamshire, UK), 250 µg of protein was incubated with the beads for 20 min at room temperature and centrifuged for 20 sec at 13000 rpm (60461 g). Pre-washed protein A coated beads with RIPA buffer were added to pre-cleared cell lysates. An optimised volume (15 µl) of integrin αvβ3, OPN, or SHP-2 primary antibody was added to the mixture of cell lysates and beads. The top cap of the tube was sealed with Parafilm to avoid leaking and placed on a rotary wheel overnight at 4°C. The next day, supernatant was collected in a fresh tube centrifugation at 13000 rpm (60461 g) for 1 min and the pellet was washed with RIPA buffer (x3) to reduce non-specific binding. Both the supernatant and pellet were resuspended in 2x sample buffer, heated for 5 min at 95°C and spun for 2 min at 13000 rpm (60461 g). The immunoprecipitate bound with integrin αvβ3, OPN, or SHP-2 was collected in the supernatant eluted from the pelleted beads. Samples were then analysed by Western blotting. In co-immunoprecipitation studies, samples were probed with additional primary antibodies to investigate the association between two chosen molecules and also probed with primary antibody which was used for immunoprecipitation to control the amount of protein loaded as well as confirm that the immunoprecipitation was successful.

2.14 Statistical analysis

Data on the embryo attachment assay scored by the standard criteria described in Section 2.6 and bead attachment assay assessed by scoring the number of attached beads against the total number of beads originally transferred, are presented as means ± the standard error of the mean (SEM). All proportions (represented as %) were arcsine transformed prior to statistical analysis using Prism software 5.0 (Graph-Pad, USA). Statistical significance was determined by one-way analysis of variance (ANOVA) followed by Tukey's Multiple Comparison post-hoc test. A P value that was <0.05 was considered statistically significant. The students' t-test was also utilised to determine statistical significance between two groups (for example, to analyse attachment rate on transformed cells vs. on control cells).



CHAPTER 3

Establishment of an *in vitro* model of embryo implantation and investigation of molecular crosstalk between the attaching blastocyst and endometrial epithelial cells

3.1 Introduction

Due to the inaccessible nature of the human embryo implantation site, much of the existing information regarding implantation has been obtained from animal models and *in vitro* studies. To overcome the limitation of *in vivo* studies, various types of *in vitro* models have been established over recent years (Kliman et al., 1990; Landgren et al., 1996; Popovici et al., 2000; Bentin-Ley and Lopata, 2000; Carver et al., 2003; Singh et al., 2010; Ho et al., 2012), as described in Chapter 1.

Even if *in vitro* studies cannot completely mimic the uterine environment, they can provide the opportunity to investigate potential interactions that might occur *in vivo* and allow manipulation of the various parameters that may affect the mechanism of implantation (Teklenburg and Macklon, 2009). Unraveling the mechanisms of implantation may suggest key clues to solve problems of infertility and pregnancy failure.

Although there are inter-species differences in terms of both implantation timing and mechanisms (Hoffman et al., 1998; Enders, 2000; Dey et al., 2004; Wang and Dey, 2006), reciprocal interaction between the embryo and the endometrium is always essential for implantation. Given the scarcity of human embryos for research, *in vitro* modelling using mouse embryos seems a highly appropriate method with which to study implantation.

In order to focus on the initial interaction between the embryo and endometrium, I have established two different *in vitro* models of implantation. Firstly, a two-dimensional *in vitro* model in which either mouse or human embryos were co-cultured on confluent endometrial epithelial cells, an environment which would mimic the endometrium surface where the embryo begins interaction with maternal tissues as previously described by

Singh et al. (2010). This also provides a platform to investigate the initial interaction between the embryo and endometrial epithelium, which is not possible to observe *in vivo*. Secondly, a three-dimensional *in vitro* model in which embryos were co-cultured on an endometrial epithelial layer grown on collagen mixture with endometrial stromal cells. This is likely to allow investigation beyond the initial epithelial phase of attachment to the invasion to the stroma. The basic principal behind the establishment of the three-dimensional *in vitro* model followed by Bentin-Ley et al (2000), however earlier limitations of reproducibility were overcome by applying immortalised human endometrial epithelial cells (Castelbaum et al., 1997; Uchida et al., 2012) to establish an epithelial monolayer. Development of these new models allowed intricate investigation of the mechanism of embryo implantation.

I hypothesised that the embryo may secrete signals that alter the epithelial phenotype via local pathways based upon earlier evidence showing elevated levels of growth factors in culture media surrounding developing mouse embryo (Spaventi et al., 1990; Fluhr et al., 2008), and the fact that growth factor-loaded beads transferred into mouse uterine horns induced local responses elicited by the embryo (Paria et al., 2001). In this thesis, MUC1, integrin αvβ5, αvβ3, OPN and HB-EGF were tested as components that might mediate, sense or report such changes (Aplin et al., 1996b; Das et al., 1994; Illera et al., 2000; Johnson et al., 2001; Lim and Dey, 2009; Singh et al., 2010). Furthermore, in order to investigate the role of epithelial integrin αvβ3 or OPN in embryo attachment, gene expression within the endometrial cells was manipulated by short interfering RNA (siRNA) transfection. If successful, these experiments would make possible further mechanistic investigations that are simply not possible *in vivo*.

3.2 Results

3.2.1 Establishment of an *in vitro* model of embryo implantation

Immortalised human endometrial Ishikawa cells (Castelbaum et al., 1997; Singh et al., 2010; Uchida et al., 2012) provided an epithelial monolayer and substrates, including collagen mixture with human endometrial stromal cells, mimicked the endometrial stroma within an *in vitro* model. Either mouse or human embryos were transferred and the sequential phases of implantation to the epithelial layer were examined.

3.2.1.1 Verification of Ishikawa cells as an endometrial epithelial model

Ishikawa cells were immunostained for Cytokeratin 18 (CY-90) and E-cadherin as markers for epithelial cells (Jiang et al., 2010; Strauss et al., 2011). Cytokeratin was strongly expressed in the cytoplasm, while E-cadherin was distributed as expected at the lateral plasma membrane (Figure 3.1).

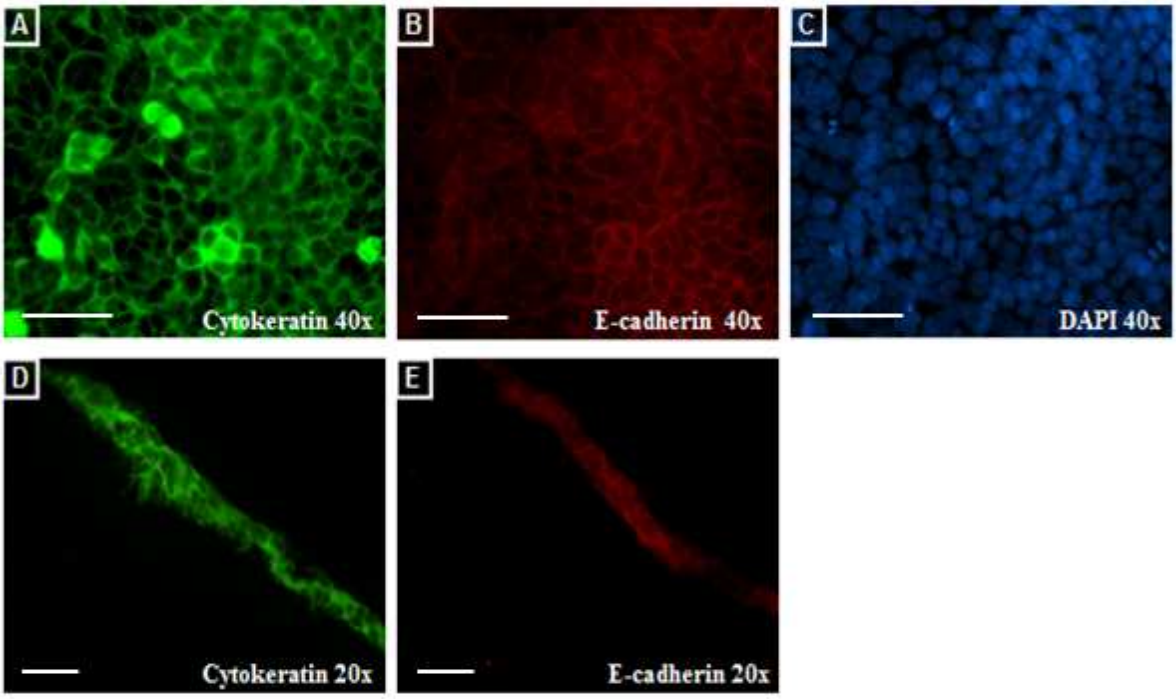


Figure 3.1: Immunofluorescence staining for Cytokeratin and E-cadherin in Ishikawa cells

Immunofluorescence staining for cytokeratin (**A**), E-cadherin (**B**), and nuclear staining (**C**) in Ishikawa cells grown on a matrigel coated coverslip. Cytokeratin (**D**) and E-cadherin (**E**) staining of Ishikawa cells grown on a collagen gel containing human endometrial stromal cells. Images were captured at a magnification of 40X (**A**, **B**, and **C**) or 20X (**D** and **E**), Green: Cytokeratin, Red: E-cadherin, Blue: Nucleus (DAPI (4',6-diamidino-2-phenylindole)), Scale bar = 50 µm

3.2.1.2 Two- and three-dimensional *in vitro* models

Two-dimensional (2D) and three-dimensional (3D) *in vitro* models of embryo-epithelial interaction were successfully established. For 2D investigations, Ishikawa cells (between passages 3-25) were grown for 3 days on coverslips with a matrigel coating. For the 3D model, human primary endometrial stromal cells (between passages 3-6) were prepared in a gel of bovine dermis collagen type I, plated onto cell culture insert membrane, and then immediately after gel formation, coated with matrigel to simulate an epithelial basement membrane. Ishikawa cells were then added onto pre-made collagen gel mixture with stromal cells and incubated for 3 days to allow a surface monolayer to form. Test embryos were transferred onto gels for further investigation. Schematic diagrams of the 2D and 3D *in vitro* models are illustrated in Figure 3.2.

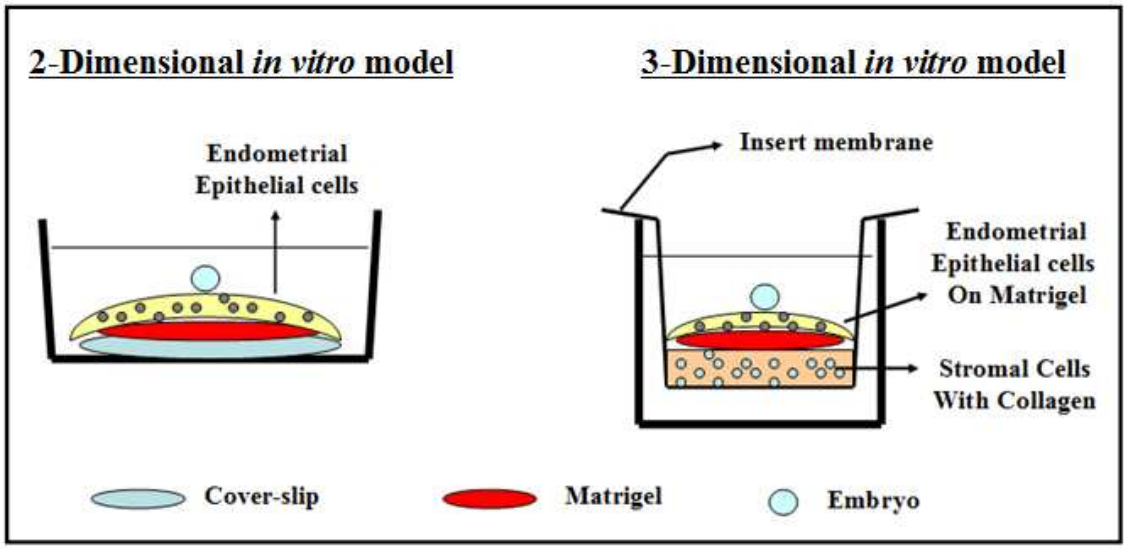


Figure 3.2: Schematic diagrams of 2D and 3D *in vitro* models

In the 2D *in vitro* gel, a mouse or human embryo was co-cultured on a monolayer of Ishikawa cells maintained on a matrigel-coated coverslip for 48 h or 60 h, respectively. Ishikawa cells were seeded onto the collagen mixture of endometrial stromal cells in the 3D *in vitro* gel. After the gel was formed, a mouse embryo was transferred and co-cultured for 60 h.

3.2.1.3 Attachment of embryos *in vitro*

Randomly selected mouse (n=367) or human (n=58) embryos were transferred to 106 independent 2D gels and 3 independent 3D gels. Twenty four hours after transfer, observations of embryo attachment were performed. At this initial stage, both mouse and human embryos showed tenuous, but clearly visible, attachment which could be easily lost by external stresses introduced by fixation or tapping the plate. No disruption was observed of the epithelial cells surrounding the attachment site (Figure 3.3.A). At 48 h of co-culture, increases in the number of attached mouse and human embryos were observed compared to 24 h. At 48 h after transfer, 72% of mouse embryos (n=264) had stably attached to the cells so that they were retained after fixation or tapping the plate. Displacement or disruption of cells surrounding the attached mouse embryo, and marked outgrowth of trophoblast cells were observed (Figure 3.3.B). Human embryos required 60 h to reach a stage of stable attachment in 2D gel. 45% of human embryos (n=26) had attached and caused disruption of underlying Ishikawa cells (Figure 3.3.C). For the 3D gel, mouse embryos were co-cultured for 60 h to reach a stable adhesion and initial invasion stage through the epithelial layer into the stroma (Figure 3.3.D).

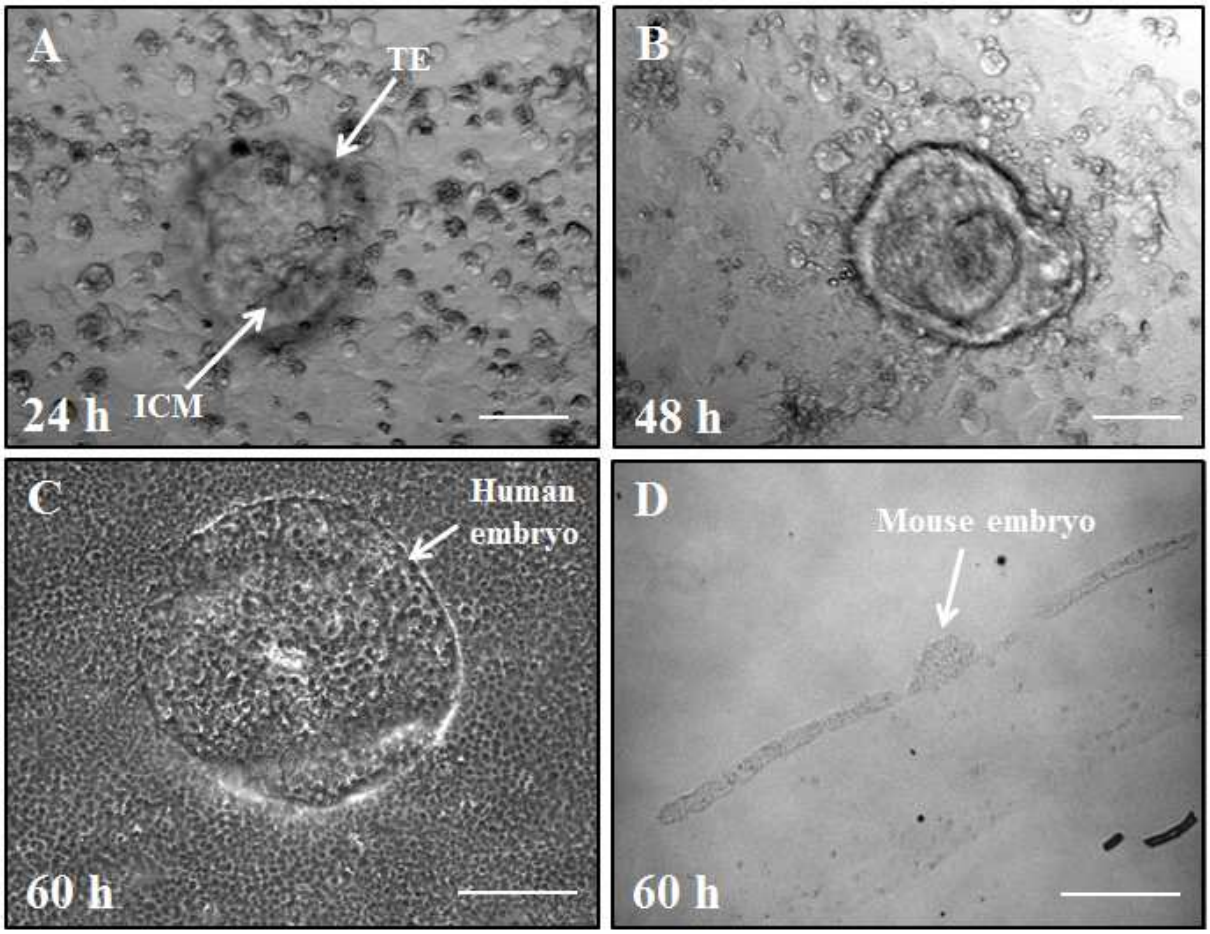


Figure 3.3: Attachment of embryos in *in vitro* gels

Phase contrast images of mouse embryo attached on confluent Ishikawa cells after 24 h (**A**) and 48 h (**B**) of co-culture in 2D *in vitro* gels, an attached human embryo (white arrow) on Ishikawa cells at 60 h after co-culture **(C**), and mouse embryo (white arrow) attached on a frozen section of 3D gel (**D**), ICM: Inner cell mass, TE: Trophectoderm, Images were captured at a magnification of 20X (**A** and **B,** Scale bar = 50 µm) and 10X (**C** and **D,** Scale bar = 200 µm).

3.2.1.4 Assessing the stability of embryo attachment

Multiple observations of attaching embryos throughout the 48 h time period of experimental observation allowed distinct stages of attachment to be identified. A standardised scale (Table 3.1) was devised for use in all subsequent experiments. Initial observations were made 24 h after embryo transfer. Before examining the stability of embryo attachment, the plate was shaken from the side to side, and back and forth, three times respectively, and each embryo was examined by tapping the plate. Five standard stages of attachment were defined and used as a measurement scale (Table 3.1) and each stage is illustrated in Figure 3.4. In stage 1, embryos were unattached (data not shown). Stage 2 embryos (Figure 3.4; Stage 2) had found the site of attachment and tenuously attached, but detached after tapping. Embryos at stage 3 (Figure 3.4; Stage 3) did not lose their attachment position after tapping and disrupted epithelium underneath the attached embryos (white arrows of Figure 3.4; Stage 3). Embryos at stage 4 (Figure 3.4; Stage 4) were stably attached after tapping with no lateral displacement but clearer disruption underneath the embryo (white arrows of Figure 3.4; Stage 4), while those at stage 5 exhibited spreading, suggesting the outgrowth of trophectoderm (black arrow with ★ of Figure 3.4; Stage 5).

Table 3.1: Standard criteria for measuring the stability of embryo attachment

Stage	Status
1	Floating
2	Weakly attached but detached after tapping
3	Weakly attached but stuck at the attachment site after tapping
4	Stably attached
5	Stably attached and showed the outgrowth

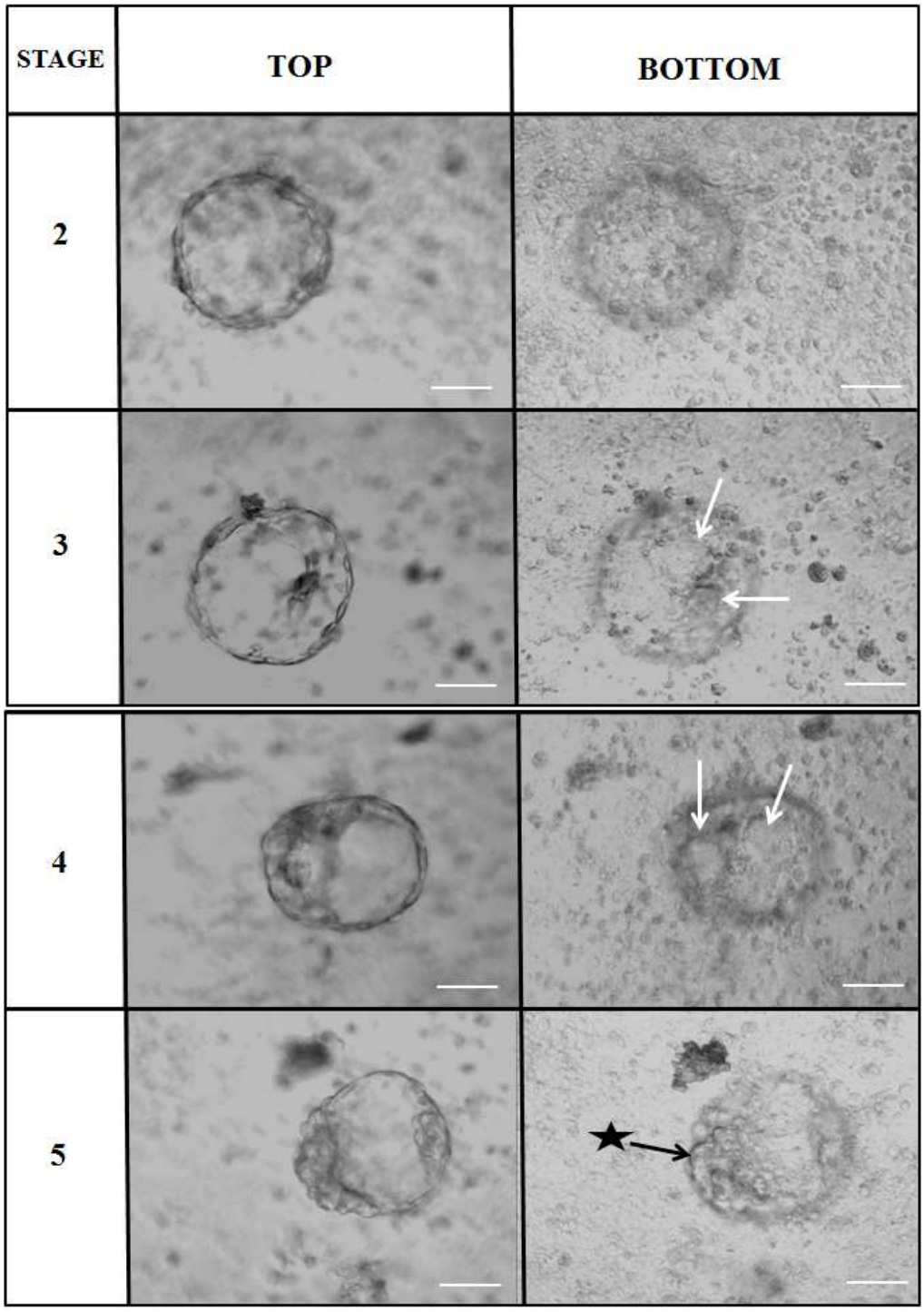


Figure 3.4: Embryo attachment at each standardised stage used throughout this thesis

Phase contrast images captured in upper or lower planes of mouse embryos attached to Ishikawa cells between 24 h and 48 h. White arrows marks disruption of epithelial cells and black arrow with ★ marks outgrowth of trophoblast. Images were captured at a magnification of 20X, Scale bar = 50 μm

3.2.1.5 Heterologous vs. homologous *in vitro* models

-Heterologous *in vitro* model-

In light of the scarcity of human embryos for research, mouse embryos were transferred to human epithelial cells as described in Section 2.5. 2D gels containing stably attached mouse embryos were fixed, permeablised and immunostained as described in Section 2.8.1 (Figure 3.5.A). The 3D cultures were fixed after 60 h of co-culture and subsequently frozen at -20°C. Attached embryos were identified by serial sectioning. Sections containing an attached embryo were immunostained for specific molecules for further study as described in Section 2.8.2 (Figure 3.5.B).

-Homologous *in vitro* model-

Human embryos were transferred to Ishikawa cells, or endometrial stromal cells, cultured on matrigel-coated coverslips in serum-free medium to observe their attachment and invasion. After 60 h of co-culture, 2D gels were fixed and immunostained for several adhesion molecules and growth factors as described in Section 2.8.1 (Figure 3.5.C).

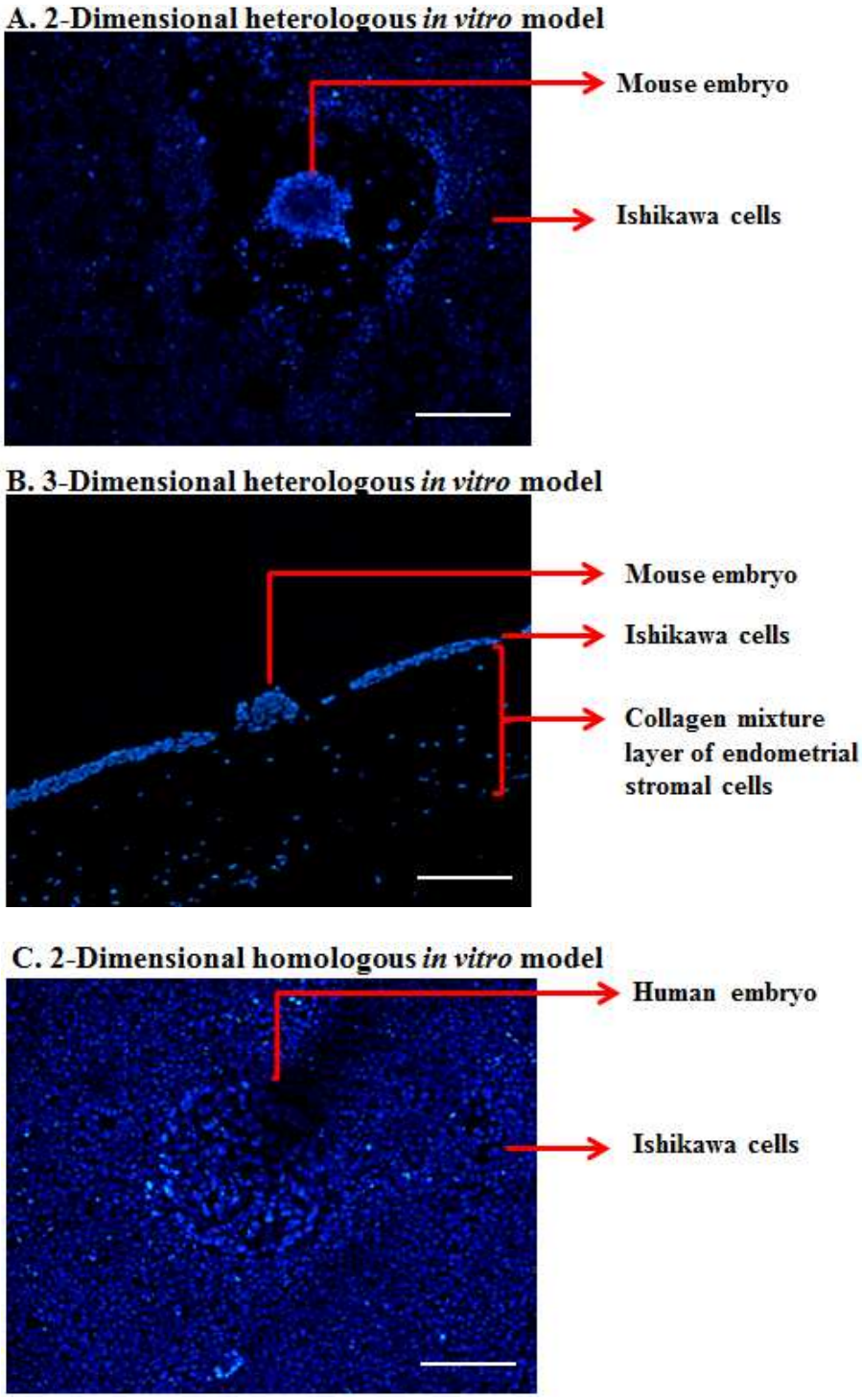


Figure 3.5: 2D and 3D *in vitro* models of embryo implantation

Nuclear staining (DAPI) demonstrating a mouse embryo attached on Ishikawa cells in 2D *in vitro* model (**A**), a section containing an attached mouse embryo on the Ishikawa cell layer above the collagen gel containing endometrial stromal cells within a 3D model (**B**), and a human embryo attached on Ishikawa cells in 2D *in vitro* model (**C**). All images were captured at a magnification of 10X, Scale bar = 200 µm.

3.2.2 Molecular evidence for crosstalk between the attaching blastocyst and endometrial epithelial cells

In order to investigate the local pathways involved with embryo attachment, immunocytochemistry or Western blotting was used to test MUC1, integrin αvβ3, αvβ5, OPN and HB-EGF in models with or without embryo attachment. A detailed plan of study on each molecule is referred to Supplementary Appendix 4. Gene silencing technique using siRNA transfection was also applied to investigate the role of integrin αvβ3 and OPN in embryo attachment.

3.2.2.1 Clearance of MUC1 from Ishikawa cells after embryo attachment

To investigate MUC1 regulation in Ishikawa cells upon embryo attachment, 37 mouse embryos (heterologous model) and 9 human embryos (homologous model) were used in 2D and 3D cultures. MUC1 expressed as a mosaic pattern at the apical surface of control Ishikawa cells and DAPI (nuclear staining) was uniformly stained. Intensity of MUC1 in each image was profiled (Figure 3.6). Mosaic pattern of expression is clearly demonstrated by quatified intensity profiling graphs from two representative sets of gels (Figure 3.7-Set I and II).

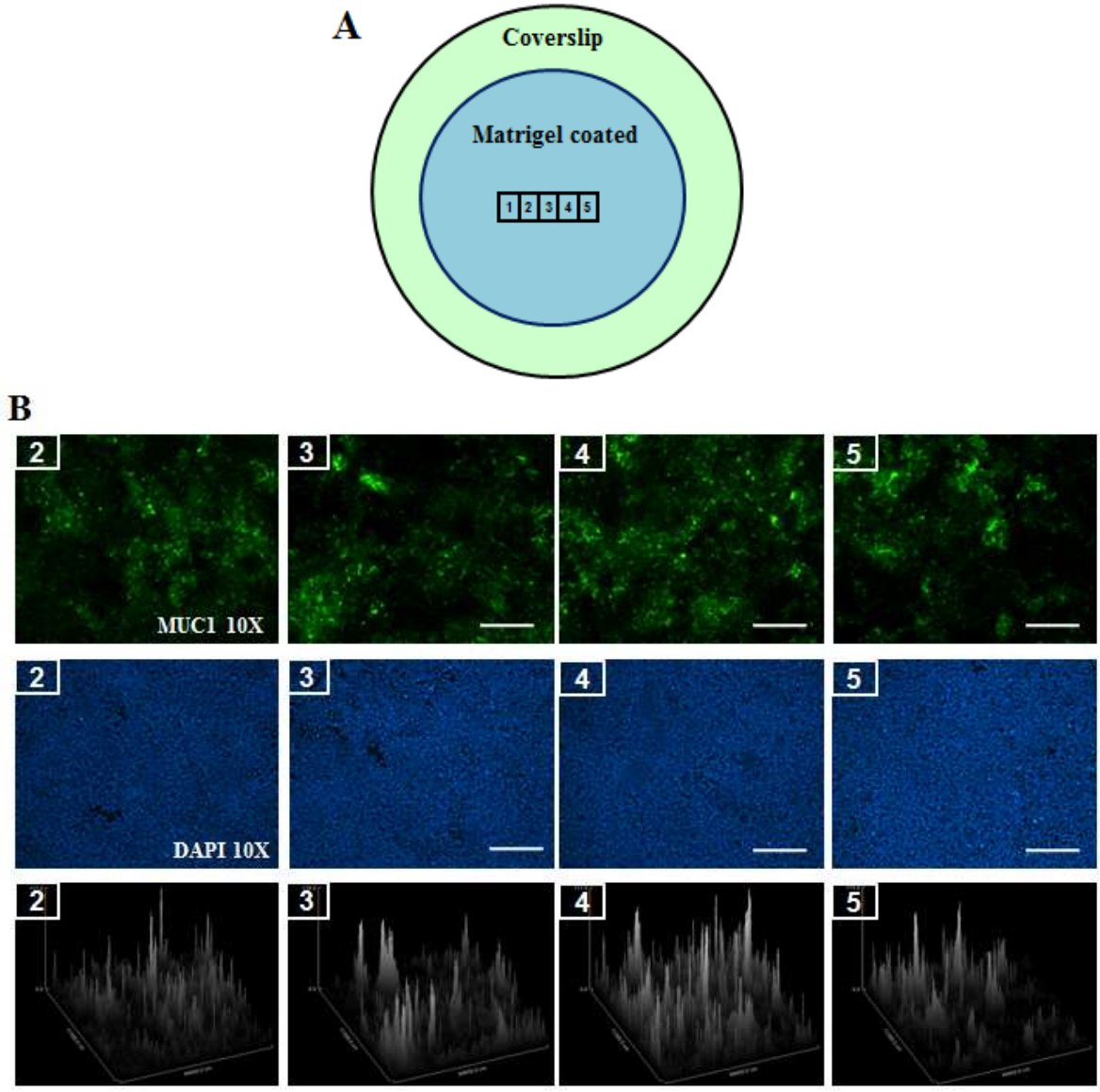
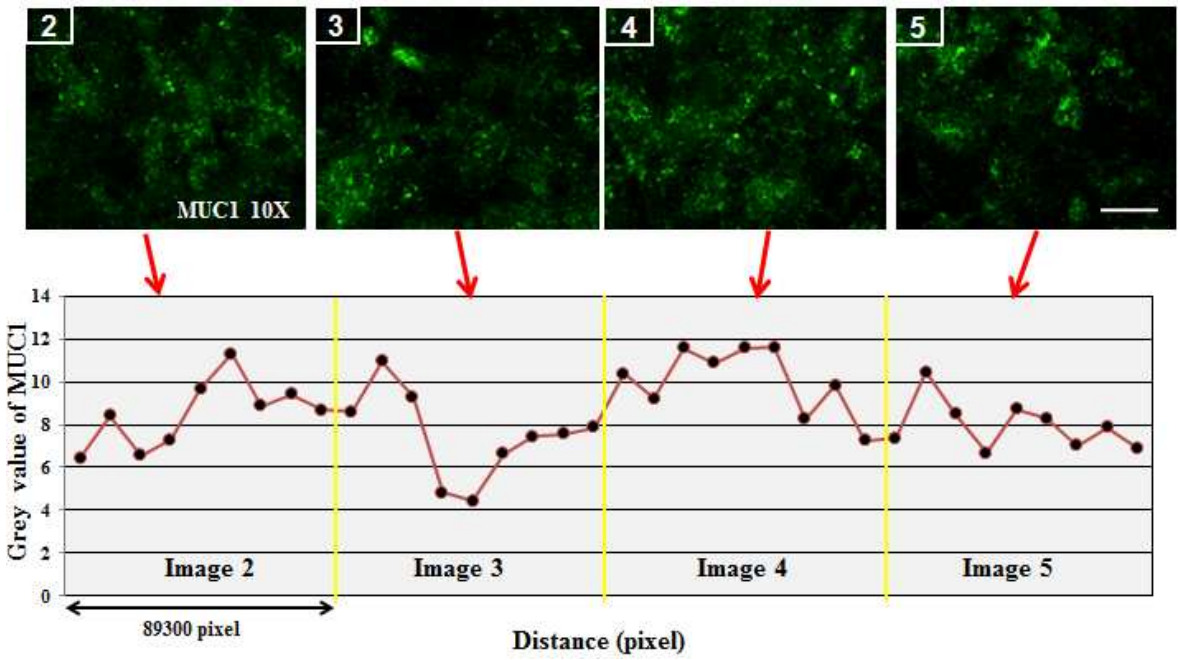


Figure 3.6: Localisation of MUC1 in Ishikawa cells

Immunofluorescence staining for human MUC1 with a mouse monoclonal antibody (BC-2) and nuclei with DAPI in Ishikawa cells (**B**). Images were obtained from 5 different regions (only 4 images are displayed) of coverslip as illustrated (**A**). Intensity of MUC1 in each image was profiled. Images were captured at a magnification of 10X.Green: MUC1, Blue: Nucleus staining (DAPI), Scale bar = 200 µm

Set I



Set II

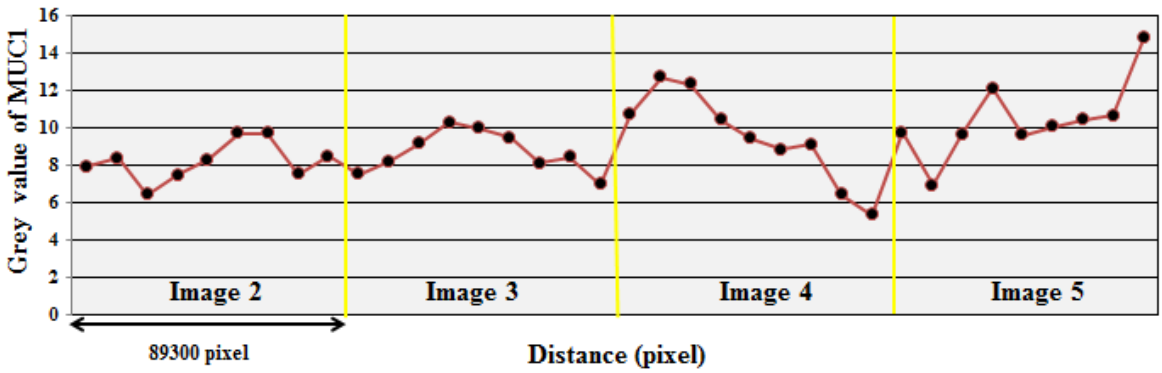


Figure 3.7: Quantification of MUC1 intensity profiling in Ishikawa cells

Surface intensity of MUC1 captured from 5 different areas (only 4 images are displayed) from each coverslip of two representative 2D gels was profiled in grey scale. The X-axis indicates the distance (pixel) of each image while the Y-axis shows grey value of MUC1 expression of Ishikawa cells. Each point on the graph shows the average of MUC1 at every 10000 pixel of each image (Each image was 89300 pixels in width). Quantified intensity profiling showed the mosiac expression of MUC1, Scale bar = 200 µm.

3.2.2.1.1 MUC1 clearance in heterologous 2D culture

For immunofluorescence analysis, 31 day 5 mouse embryos were co-cultured with Ishikawa cells in 13 independent wells. Prior to transferring embryos, Ishikawa cells were starved for 24 h. Co-culture with mouse embryos was carried out in serum-free medium. At 48 h after co-culture, both embryos were determined as Stage 5 of standardised criteria for measuring the stability of embryo attachment (Table 3.1), demonstrating stable attachment and outgrowth from the trophectoderm. Wells including the attached embryos and cells were fixed and immunostained.

Images were obtained from 5 different regions of the 2D co-cultures and surface intensity of MUC1 was profiled. As shown in Figure 3.8, there was a reduction of MUC1 near the embryo, creating a clear boundary around the site of attachment. Away from the embryo attachment site apical MUC1 showed a mosaic expression. This is clearly demonstrated by a quantified intensity profiling; profiling of Set I showed that MUC1 was gradually reduced near the attachment sites and the extent of MUC1 clearance from epithelial cells was approximately 1.402 mm in diameter from the embryo, profiling of Set II demonstrated similar pattern of reduction near mouse embryo, however, profiling of Set III showed the mosaic pattern of MUC1 expression without reduction near the embryo (Figure 3.9-Set I, II and III). The clearance of MUC1 around the site of mouse embryo attachment (Figure 3.8, image 3) and the unaffected mosaic expression of MUC1 (Figure 3.8, image 4) are shown with enlarged images in Figure 3.10.

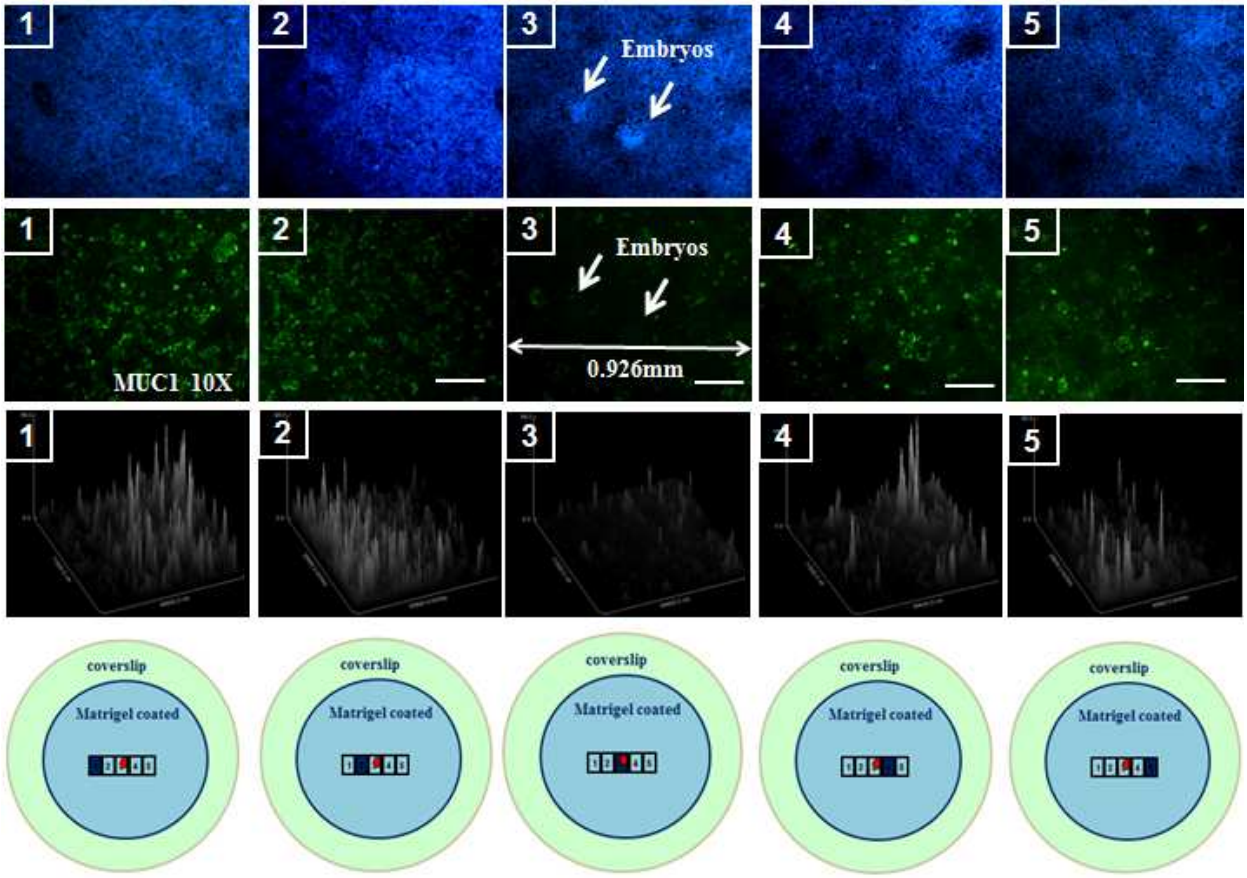
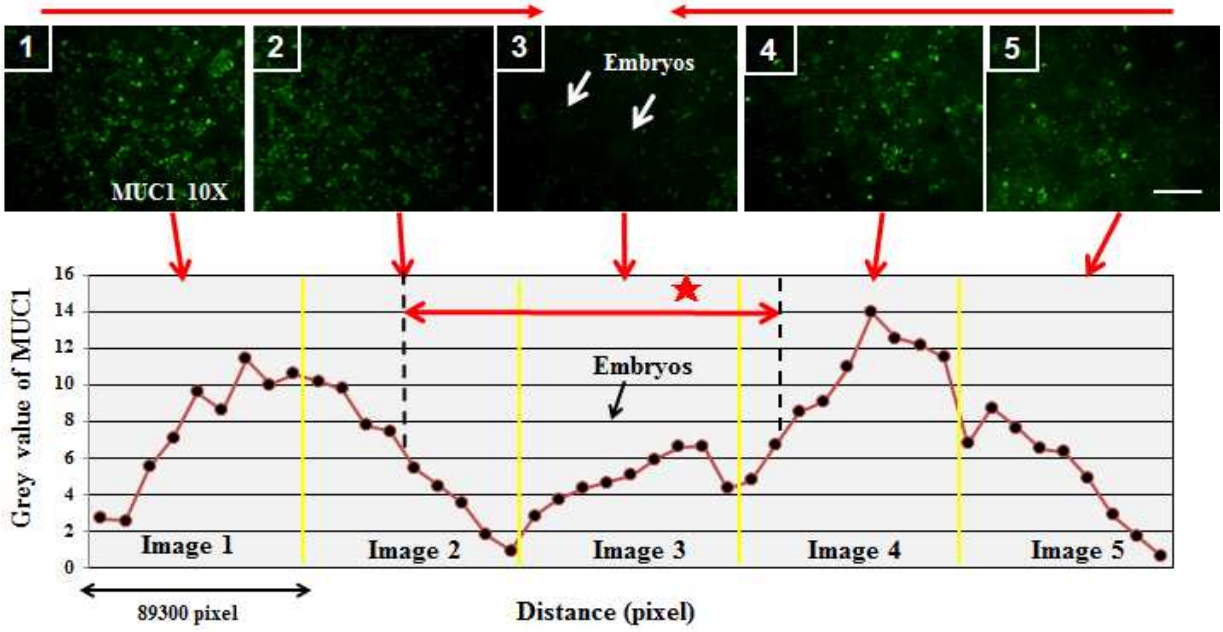


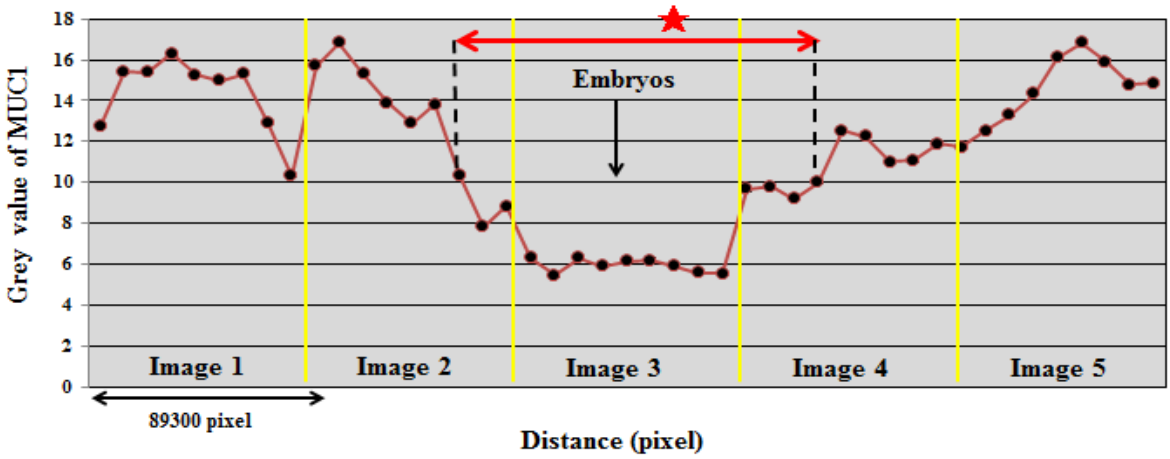
Figure 3.8: MUC1 clearance in heterologous 2D culture

Immunofluorescence staining for human MUC1 in Ishikawa cells co-cultured with mouse embryos (white arrows). Images were obtained from 5 different regions of coverslip as illustrated in diagrams at the foot of each figure. Images were captured at a magnification of 10X. Intensity of MUC1 was profiled. Green: MUC1, Scale bar = 200 μm

Set I


1
2
3
4
5
Embryos
MUC1 10X
Grey value of MUC1
16
14
12
10
8
6
4
2
0
Embryos
Image 1
Image 2
Image 3
Image 4
Image 5
89300 pixel
Distance (pixel)

Set II


Grey value of MUC1
18
16
14
12
10
8
6
4
2
0
Embryos
Image 1
Image 2
Image 3
Image 4
Image 5
89300 pixel
Distance (pixel)

Set III

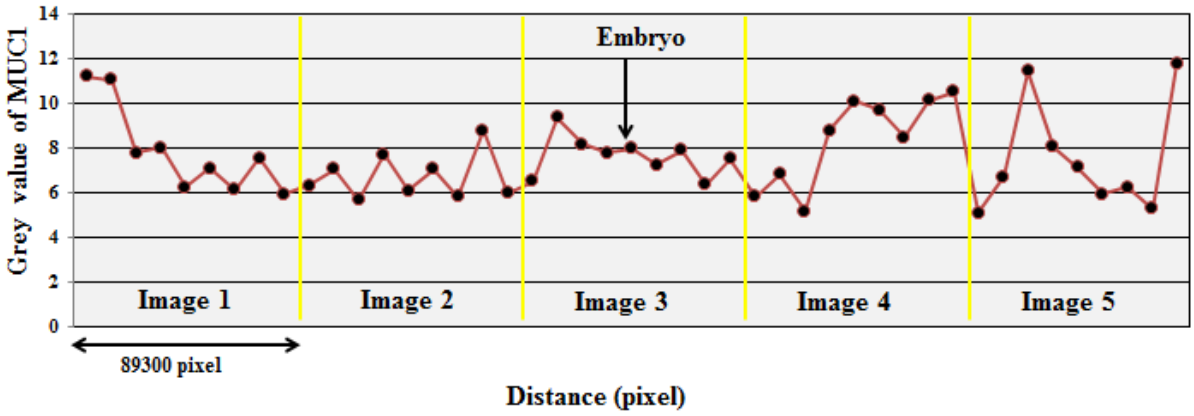


Figure 3.9: Quantification of MUC1 intensity profiling in heterologous 2D culture

Surface intensity of MUC1 captured from 5 different areas from each coverslip of three representative sets of experiments was profiled in grey scale. The X-axis indicates the distance (pixel) of each image while the Y-axis shows grey value of MUC1 expression. Each point on the graph shows the average of MUC1 at every 10000 pixel of each image (Each image was 89300 pixels in width). Set I and II: Quantified intensity profiling showed that MUC1 was gradually reduced towards the embryo attachment sites (white arrows) from the outside of coverslip. Clearance of MUC1 was observed in the area (★), Set III: Quantified intensity profiling showed unaffected mosaic pattern of MUC1 expression, Scale bar = 200 µm.

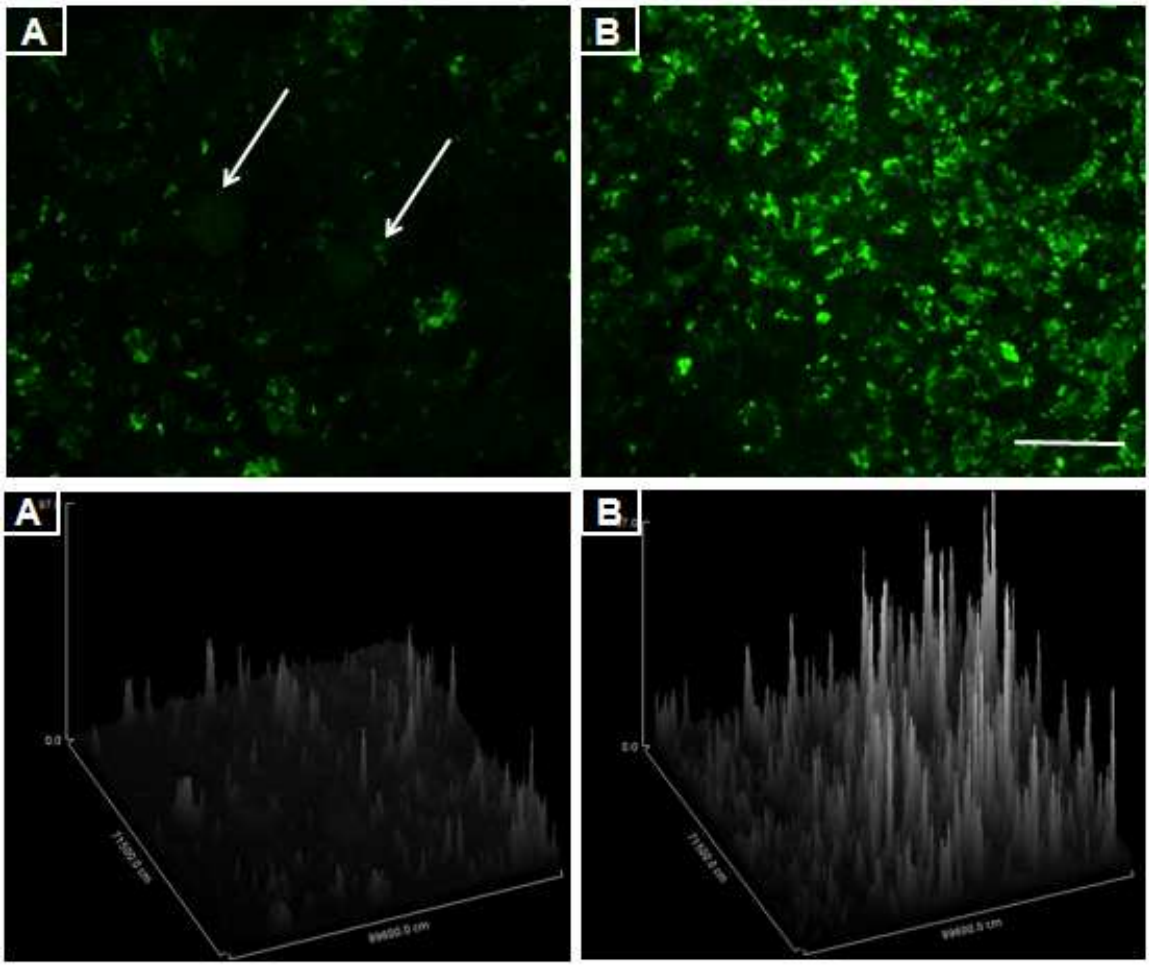


Figure 3.10: Enlarged images of MUC1 clearance in heterologous 2D culture

An image taken from Figure 3.8 (image #3) with cleared MUC1 staining adjacent to the attachment sites of two embryos (white arrows) (**A)**, an image taken from Figure 3.8 (image #4) with unaffected MUC1 staining away from the embryo attachment site (**B)**. Images were captured at an optical magnification of 10x and enlarged digitally. Intensity of MUC1 in each image was profiled. Green: MUC1, Scale bar = 200 µm

3.2.2.1.2 MUC1 clearance in heterologous 3D culture

For the analysis of MUC1 in the 3D model, 6 day 5 mouse embryos were transferred to Ishikawa cells cultured on the top of a collagen gel containing human endometrial stromal cells for 60 h. After embryos were stably attached, the gel was fixed and frozen at -20°C for sectioning. Frozen sections (some including the embryo attachment site) were subsequently immunostained for MUC1.

Three different images were captured from the 3D gel. A mouse embryo was located in the centre of the gel (white arrow) and stably attached after 60 h. MUC1 generally appeared as a mosaic as observed in the 2D gel and clearance was observed adjacent to the mouse embryo and surface intensity of MUC1 was profiled. E-cadherin showed even expression across the whole epithelium (Figure 3.11).

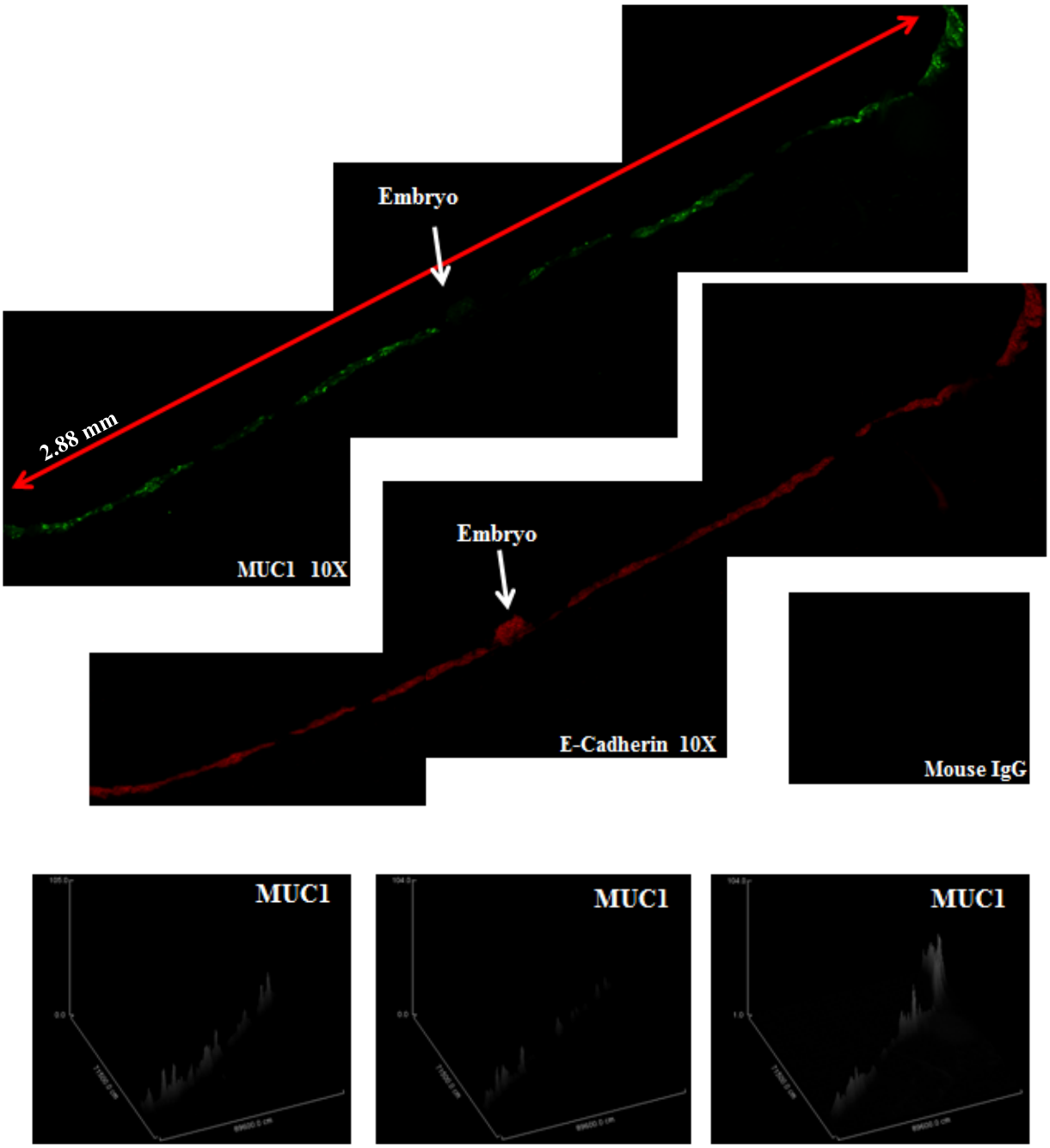


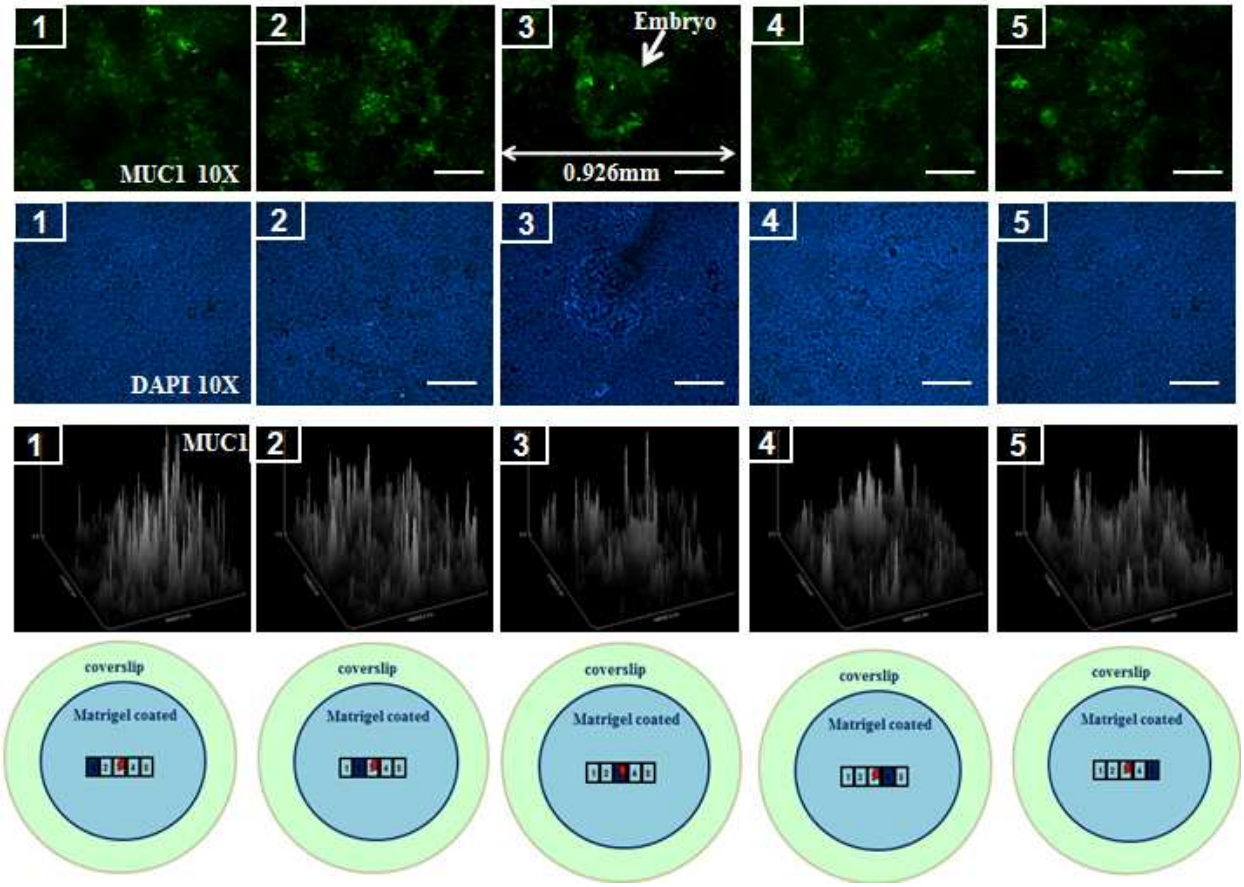
Figure 3.11: MUC1 clearance in heterologous 3D culture

Immunofluorescence staining for MUC1 and E-cadherin in Ishikawa cells co-cultured with a mouse embryo (white arrow) in 3D gel. Three images demonstrated the entire gel (2.88 mm in length). Images were captured at a magnification of 10X. Surface intensity of MUC1 of each image was profiled. Mouse IgG staining represents a negative control for MUC1 staining. Green: integrin αvβ3, Red: E-cadherin

3.2.2.1.3 MUC1 clearance in homologous 2D culture

Nine day 6 human blastocysts were transferred to confluent Ishikawa cells on 9 independent 2D cultures. MUC1 clearance was detected near the site of attachment, but the area was smaller in size than that detected on 2D gels with mouse embryo (Figure 3.12-Set I and II). Areas further away from the attachment site displayed an unaffected mosaic pattern of MUC1. According to nuclear staining, this clearance pattern was not affected by the initial seeding density of Ishikawa cells. This was clearly demonstrated by a quantified intensity profiling. MUC1 was rapidly reduced adjacent to the attachment site of the human embryo and the extent of MUC1 clearance from epithelial cells was approximately 0.849 mm (Set I) and 0.876 mm (Set II) in diameter from the embryo (Figure 3.13-Set I and II).

Set I


1
2
3
Embryo
4
5
MUC1 10X
0.926mm
1
2
3
4
5
DAPI 10X
1
MUC1
2
3
4
5
coverslip
Matrigel coated
coverslip
Matrigel coated
coverslip
Matrigel coated
coverslip
Matrigel coated
coverslip
Matrigel coated

Set II

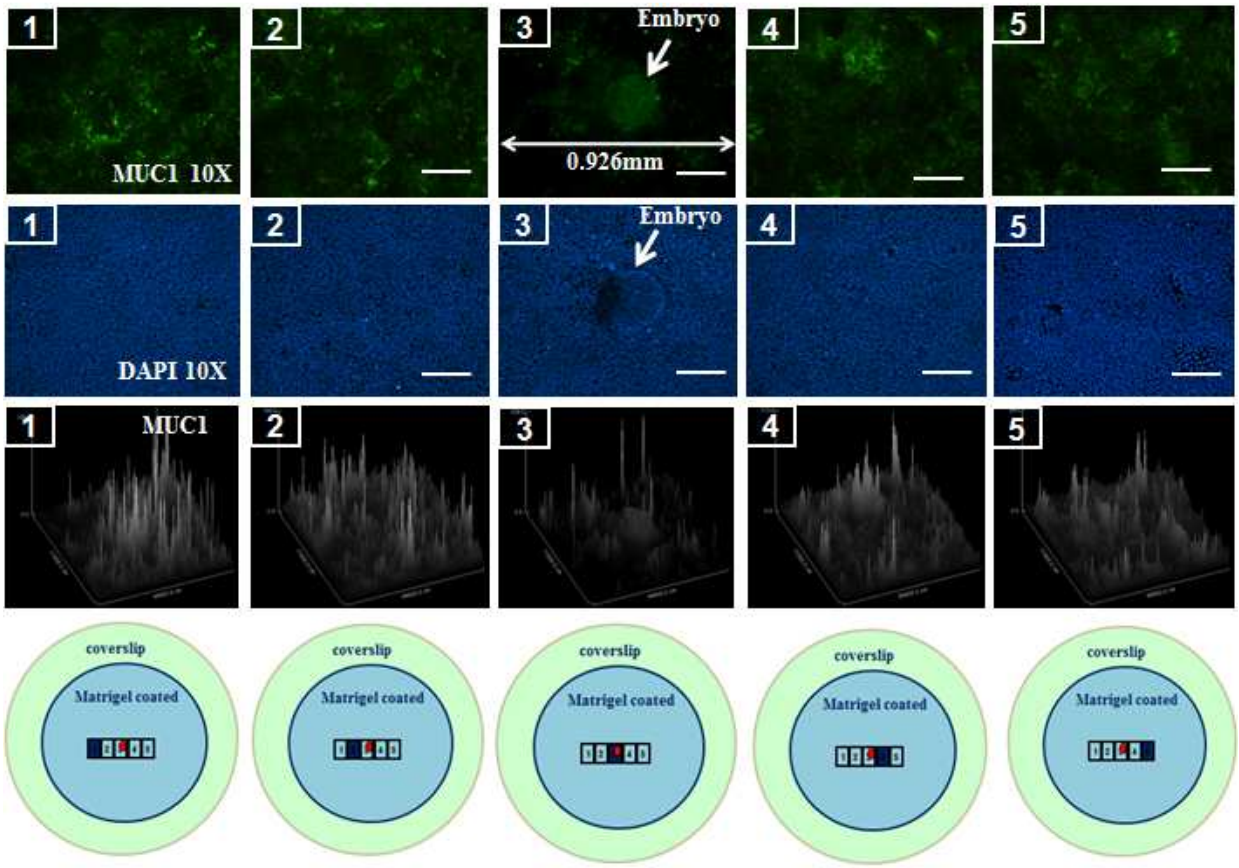
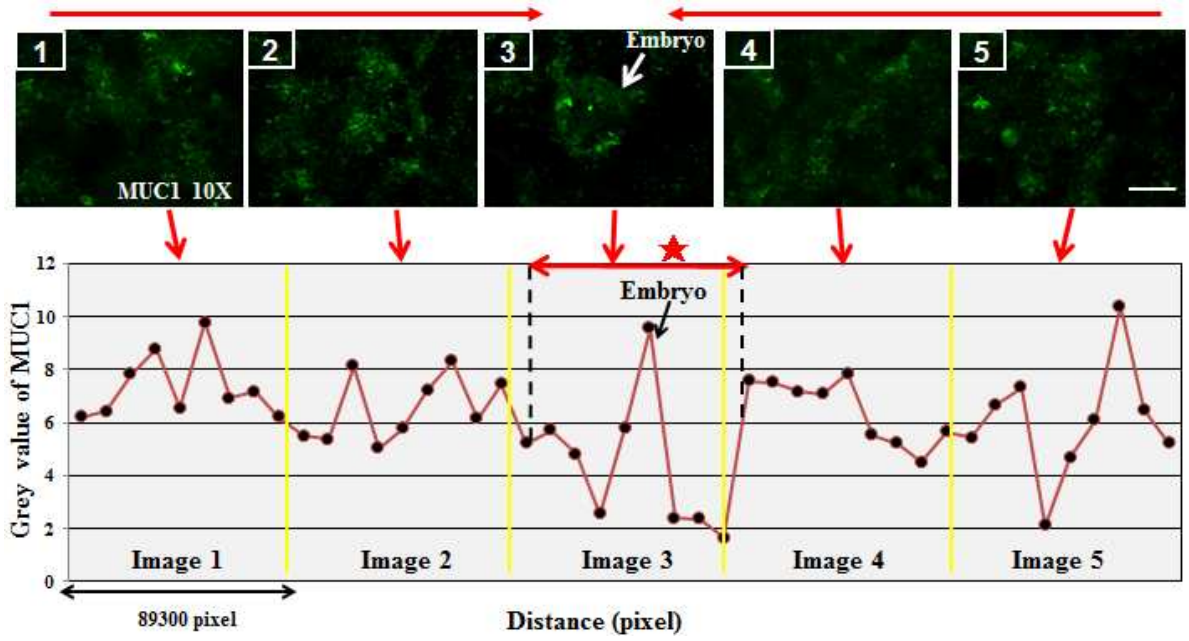


Figure 3.12: MUC1 clearance in homologous 2D culture

Two representative immunofluorescence staining for human MUC1 with a mouse monoclonal antibody (BC-2) in Ishikawa cells co-cultured with a human embryo (white arrow). Images were obtained from 5 different regions of each coverslip from two representative homologous 2D gels as illustrated in diagrams at the foot of each figure. Images were captured at a magnification of 10X. Intensity of MUC1 was profiled quantitatively. Green: MUC1, Blue: Nucleus (DAPI), Scale bar = 200 μm

Set I



Set II

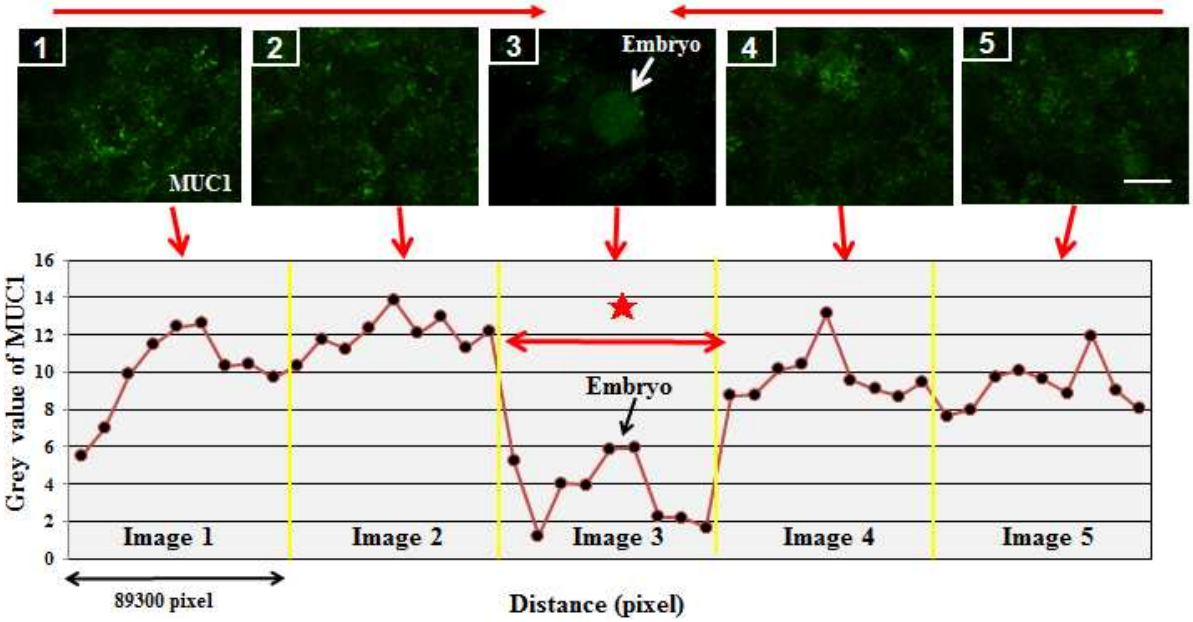


Figure 3.13: Quantification of MUC1 intensity profiling in homologous 2D culture

Surface intensity of MUC1 captured from 5 different areas from each coverslip from Set I and II of Figure 3.12 was profiled in grey scale. The X-axis indicates the distance (pixel) of each image while the Y-axis shows grey value of MUC1 expression. Each point on the graph shows the average of MUC1 at every 10000 pixel of each image (Each image was 89300 pixels in width). Quantified intensity profiling showed that MUC1 was rapidly reduced at the embryo attachment sites (white arrow) from the outside of coverslip. Clearance of MUC1 was observed in the area (★), Scale bar = 200 µm.

3.2.2.2 Up-regulation of integrin αvβ3 at the site of embryo attachment

Integrin αvβ3 was examined in Ishikawa cells adjacent to the sites of embryo attachment by immunocytochemistry, and Western blotting was used to examine global expression in microwells containing confluent Ishikawa cells exposed to mouse embryos. 178 mouse embryos and 8 human embryos were used in total.

Integrin αvβ3 was weakly expressed in the absence of embryos, displaying evenly low intensity and E-cadherin was expressed uniformly. Comparing to the expression of mouse IgG and rabbit IgG as negative controls for integrin αvβ3 (anti-mouse) and E-cadherin (anti-rabbit) respectively, the signal from integrin αvβ3 was greater than from negative controls (Figure 3.14) and surface intensity of integrin αvβ3 in Ishikawa cells of two independent gels was profiled (Figure 3.15). It was clearly observed at higher magnification that integrin αvβ3 was present predominantly at cellular borders at the areas of cell-cell contact and relatively weakly at the apical and basal membrane of cells. E-cadherin was distributed predominantly on the lateral plasma membrane (Figure 3.16).

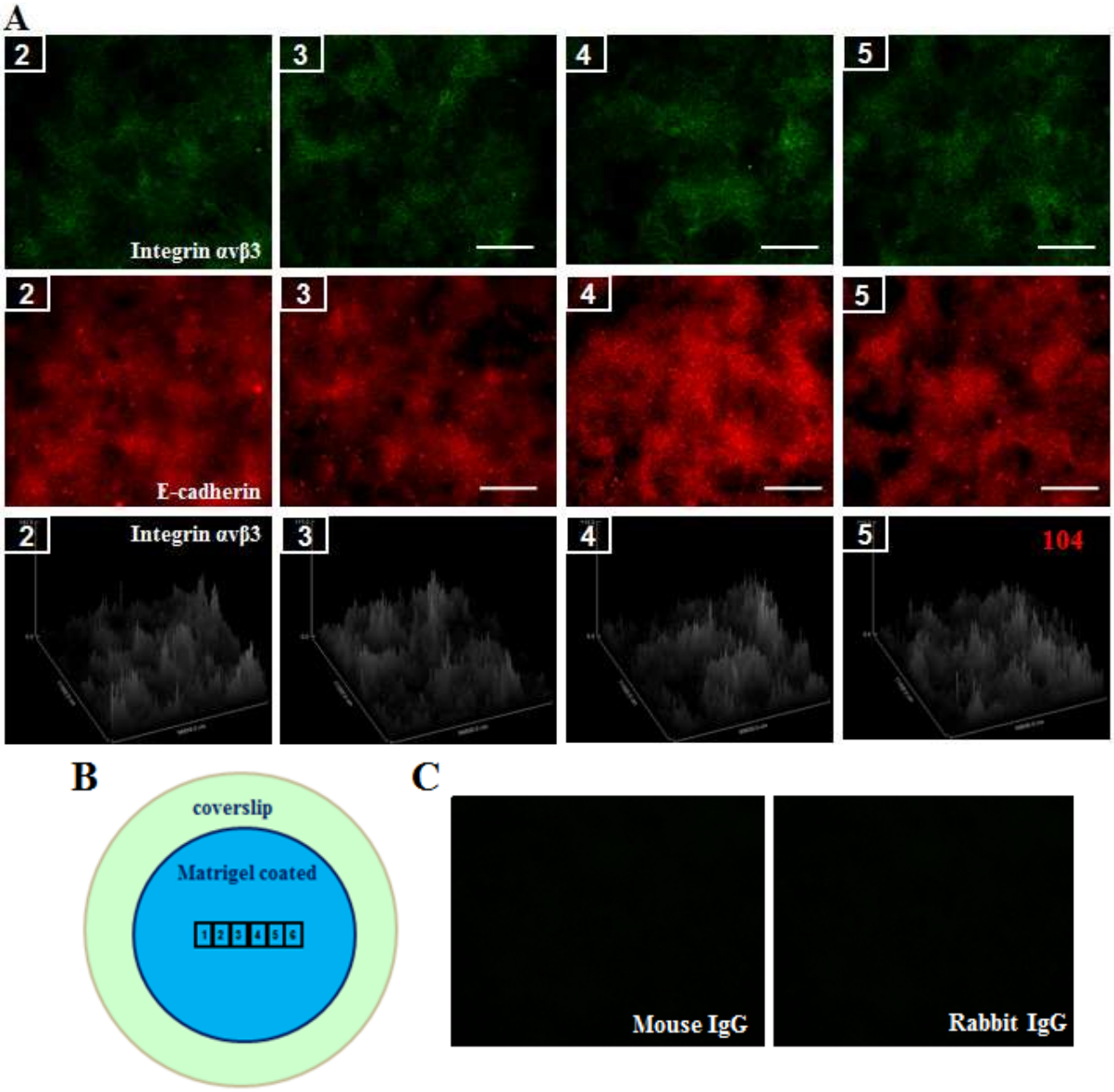


Figure 3.14: Localisation of integrin αvβ3 in Ishikawa cells

Immunofluorescence staining for human integrin αvβ3 using LM609 antibody which detects both αv and β3 together, and E-cadherin in Ishikawa cells (**A**). Images were obtained from 6 different regions of the coverslip as illustrated (**B**) (4 images are displayed). Intensity of integrin αvβ3 in each image was profiled. Note that the number (104) on schematic diagrams for profiling indicates the maximum pixel number of all images. Negative controls for both integrin αvβ3 and E-cadherin (**C**), images were captured at a magnification of 10X. Green: integrin αvβ3, Red: E-cadherin, Scale bar = 200 µm

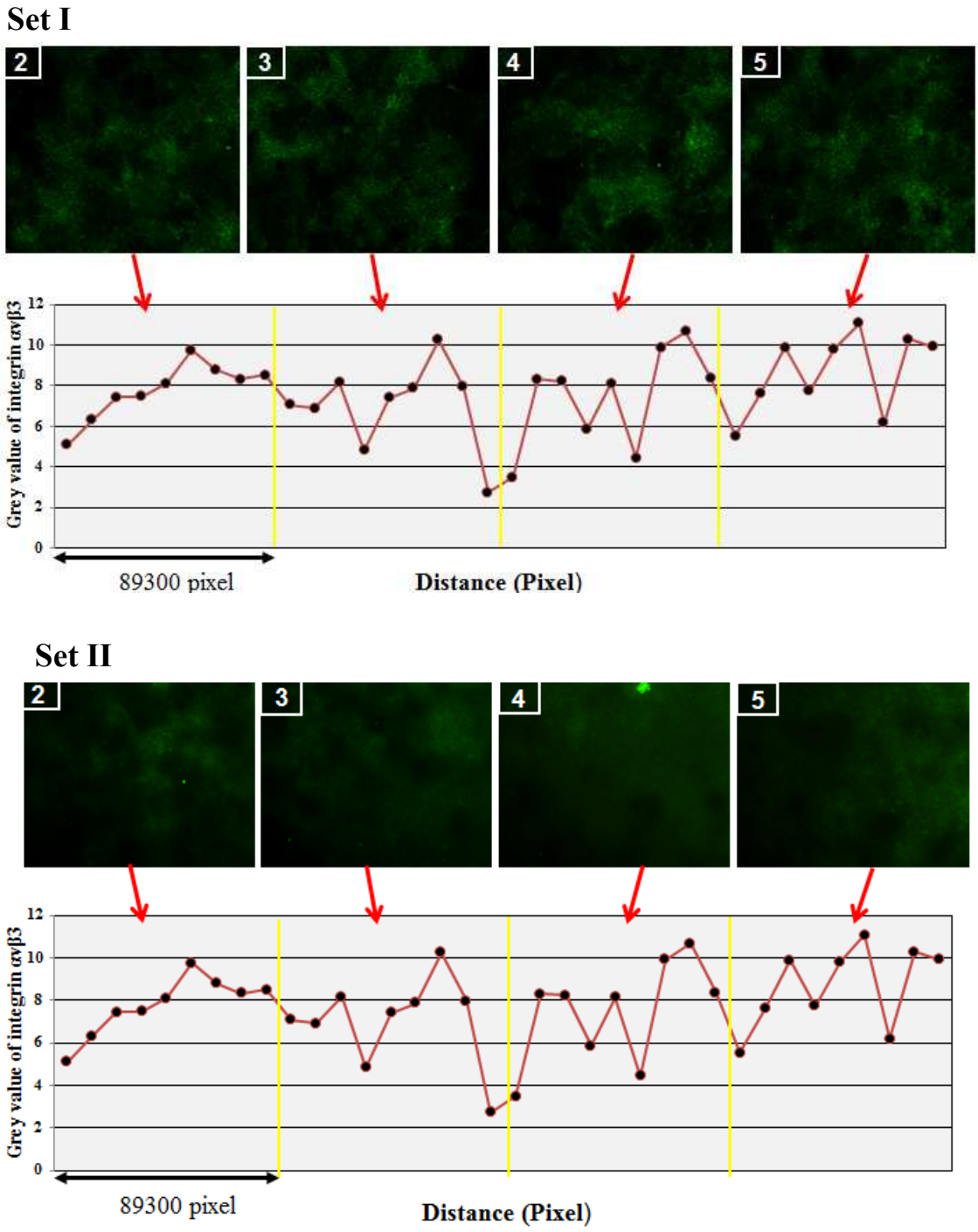
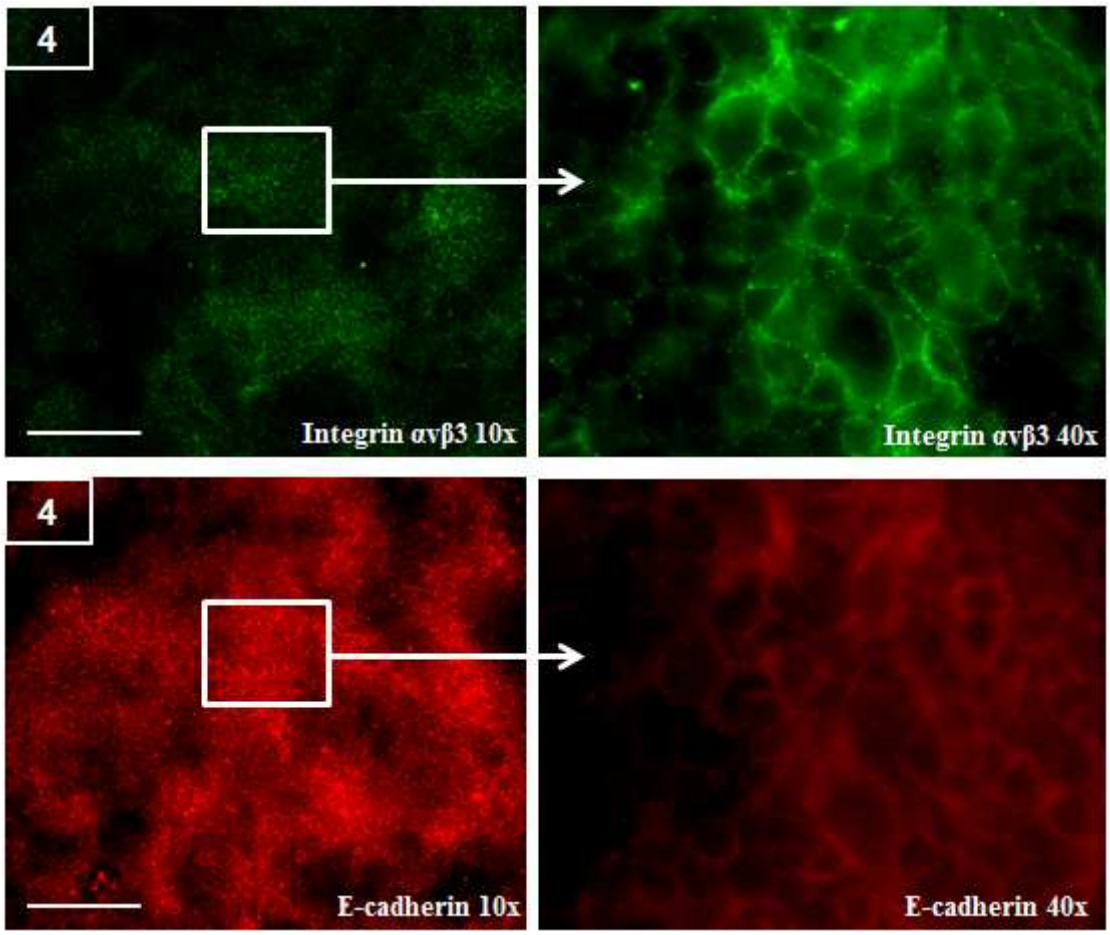


Figure 3.15: Quantification of integrin αvβ3 intensity profiling in Ishikawa cells

Surface intensity of integrin αvβ3 captured from each coverslip from two representative 2D gels (Set I and II) was profiled in grey scale. The X-axis indicates the distance (pixel) of each image while the Y-axis shows grey value of integrin αvβ3 expression. Each point on the graph shows the average of intensity of αvβ3 at every 10000 pixel of each image (Each image was 89300 pixels in width). Quantified intensity profiling showed that integrin αvβ3 was uniformly expressed across the whole coverslip.



Overlay:

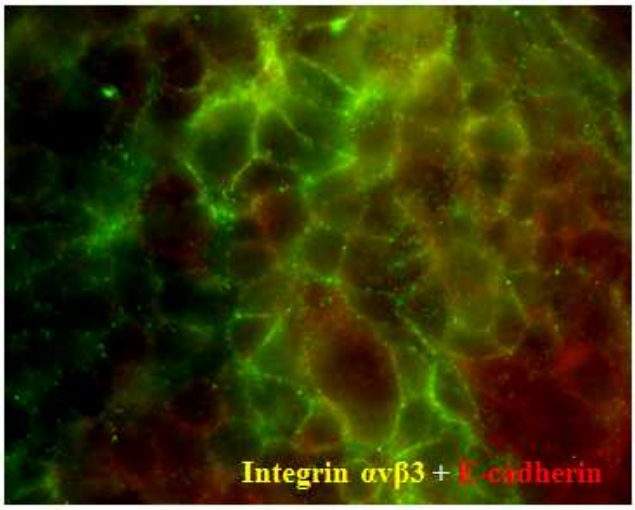


Figure 3.16: Localisation of integrin αvβ3 at higher magnification

Localisation of integrin αvβ3 and E-cadherin in Ishikawa cells. Images obtained from image # 4 from Figure 3.14 were magnified with an optical magnification of 40X and enlarged digitally. Green: integrin αvβ3, Red: E-cadherin, Scale bar = 200 µm

3.2.2.2.1 Integrin αvβ3 expression in 2D heterologous culture

For immunofluorescence analysis on 2D heterologous *in vitro* cultures, 55 day 5 mouse embryos were transferred to confluent Ishikawa cells cultured on matrigel-coated coverslips within 31 independent wells. After 48 h of co-culture, wells were fixed, permeablised, and immunostained for integrin αvβ3 (LM609).

Integrin αvβ3 was locally elevated at the site of embryo attachment (Figure 3.17), while staining was unaffected further away from the attachment site. This was clearly demonstrated by intensity profiling. Integrin αvβ3 was gradually elevated towards the attachment with a steep drop at the site of embryo attachment due to the displacement of Ishikawa cells from beneath the attachment site (Figure 3.18-Set I and II). Integrin αvβ3 expressed by cells adjacent to the site of mouse embryo was observed at higher magnification (Figure 3.19). Integrin αvβ3 was mostly localised to the peri-cellular borders and areas of cell-cell contact, while E-cadherin was distributed on embryonic cells and adherens junctions at the lateral side of cell plasma membrane.

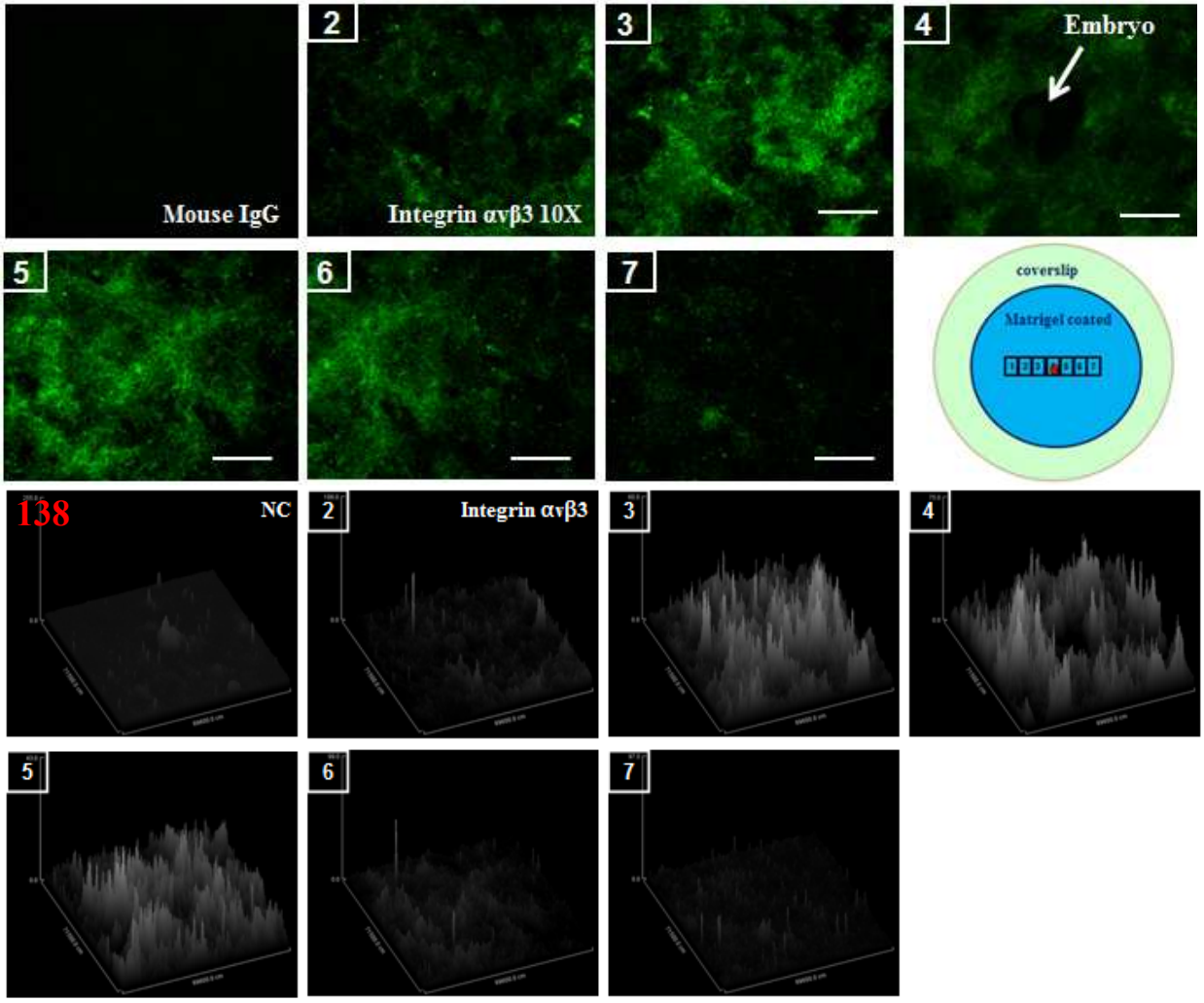


Figure 3.17: Integrin αvβ3 staining of 2D culture

Immunofluorescence staining for integrin αvβ3 with LM609 antibody in Ishikawa cells co-cultured with a mouse embryo (white arrow). Images were obtained from 7 different regions of coverslip as illustrated. The first image depicts the expression of mouse IgG as a negative control. Images were captured at a magnification of 10X. Intensity of integrin αvβ3 was profiled. Note that the number (138) on schematic diagrams for profiling indicates the maximum pixel number of all images. Green: integrin αvβ3, Scale bar = 200 µm

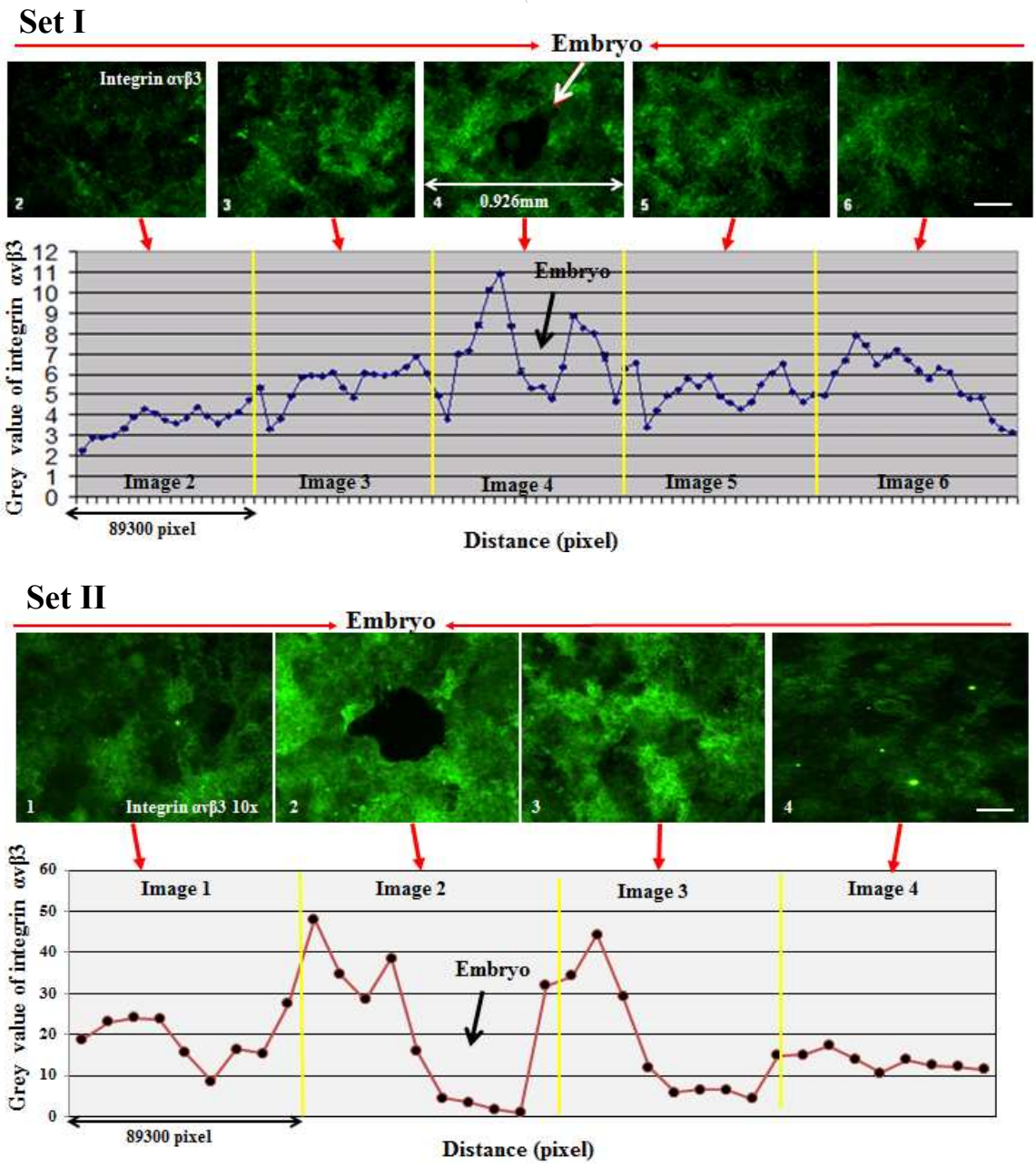


Figure 3.18: Quantification of integrin αvβ3 intensity profiling in heterologous 2D culture

Surface intensity of integrin αvβ3 captured from each coverslip of two representative 2D gels (Set I and II) was profiled in grey scale. The X-axis indicates the distance (pixel) of each image while the Y-axis shows grey value of integrin αvβ3 expression. Each point on the graph shows the average of intensity of αvβ3 at every 5000 pixel of each image (Each image was 89300 pixels in width). Quantified intensity profiling showed that integrin αvβ3 was gradually elevated towards the embryo attachment site (white arrow) from the outside of coverslip with a marked reduction at the site of attachment due to the displacement of Ishikawa cells surrounding the mouse embryo, Scale bar = 200 µm.

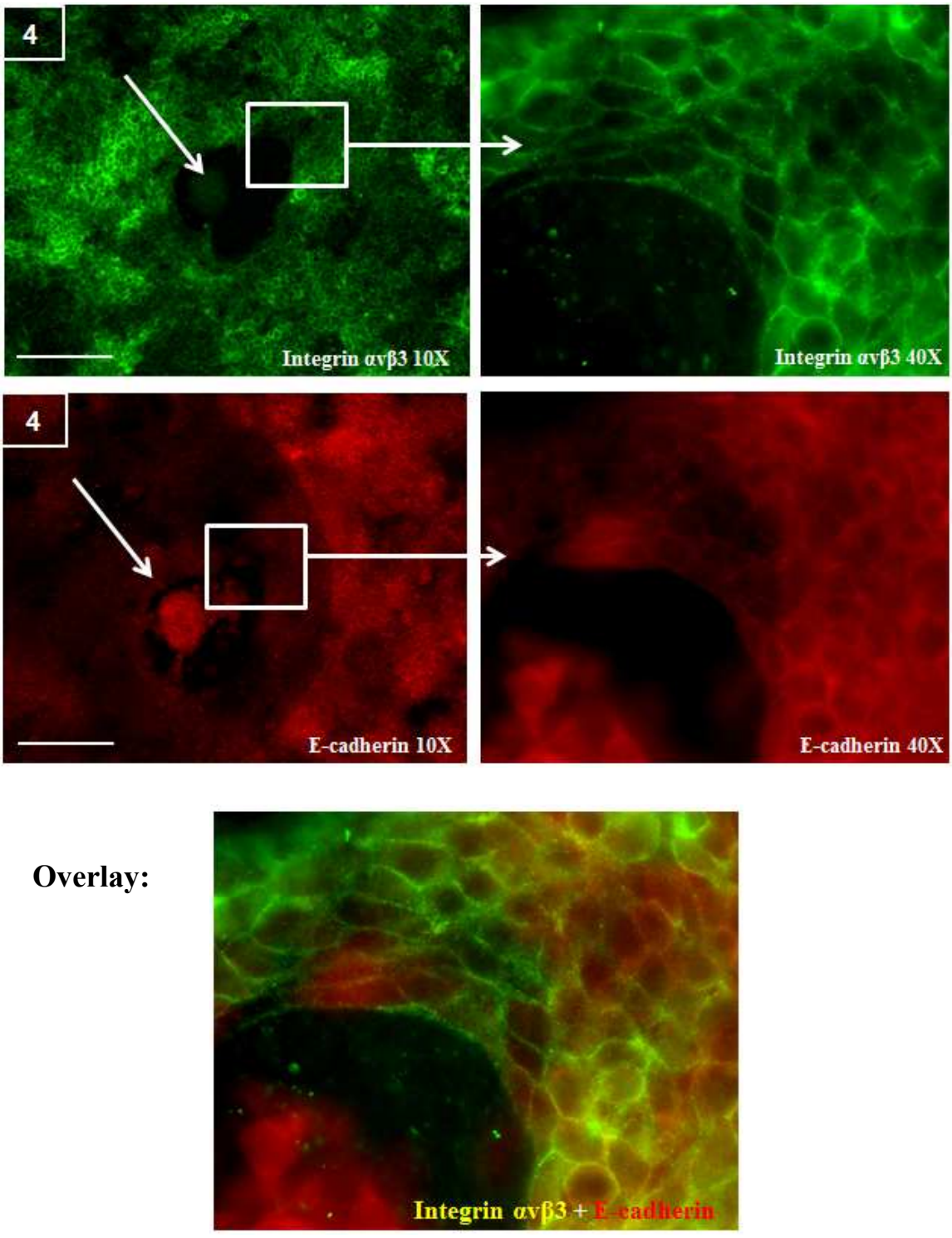


Figure 3.19: Localisation of integrin αvβ3 and E-cadherin adjacent to the mouse embryo attachment site

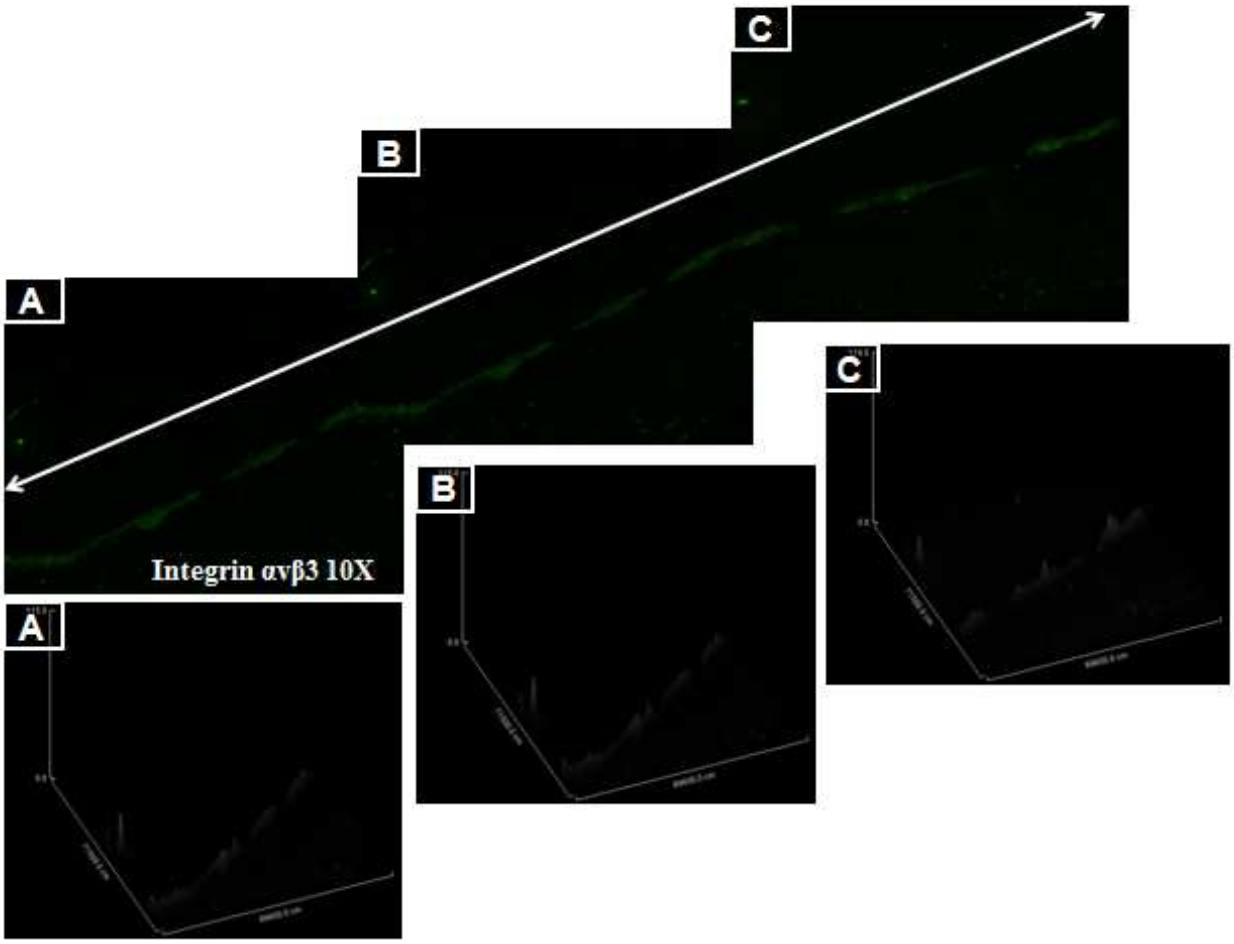
The region of image # 4 from Figure 3.16 were captured at an optical magnification of 40X and enlarged digitally. The dark trace was caused from a cracked element in the fluorescence light path on red staining. Green: integrin αvβ3, Red: E-cadherin, Scale bar = 200 µm

3.2.2.2.2 Integrin αvβ3 expression in 3D homologous gels

For 3D *in vitro* cultures, 6 mouse embryos were transferred to confluent Ishikawa cells grown on a collagen gel containing human primary endometrial stromal cells for 60 h. After the embryo had become stably attached, the gel was fixed with 4% PFA for 1 h at room temperature and frozen at -20°C. Frozen sections including embryo attachment sites, were subsequently immunostained for integrin αvβ3.

As observed with the expression of integrin αvβ3 in 2D *in vitro* culture, integrin αvβ3 was only weakly stained on the whole layer of Ishikawa cells on the top of the gel and only weakly stained in some stromal cells in a collagen gel mixture in the absence of the embryo. Intensity of integrin αvβ3 was profiled (Figure 3.20-Set I and II).

Set I



Set II

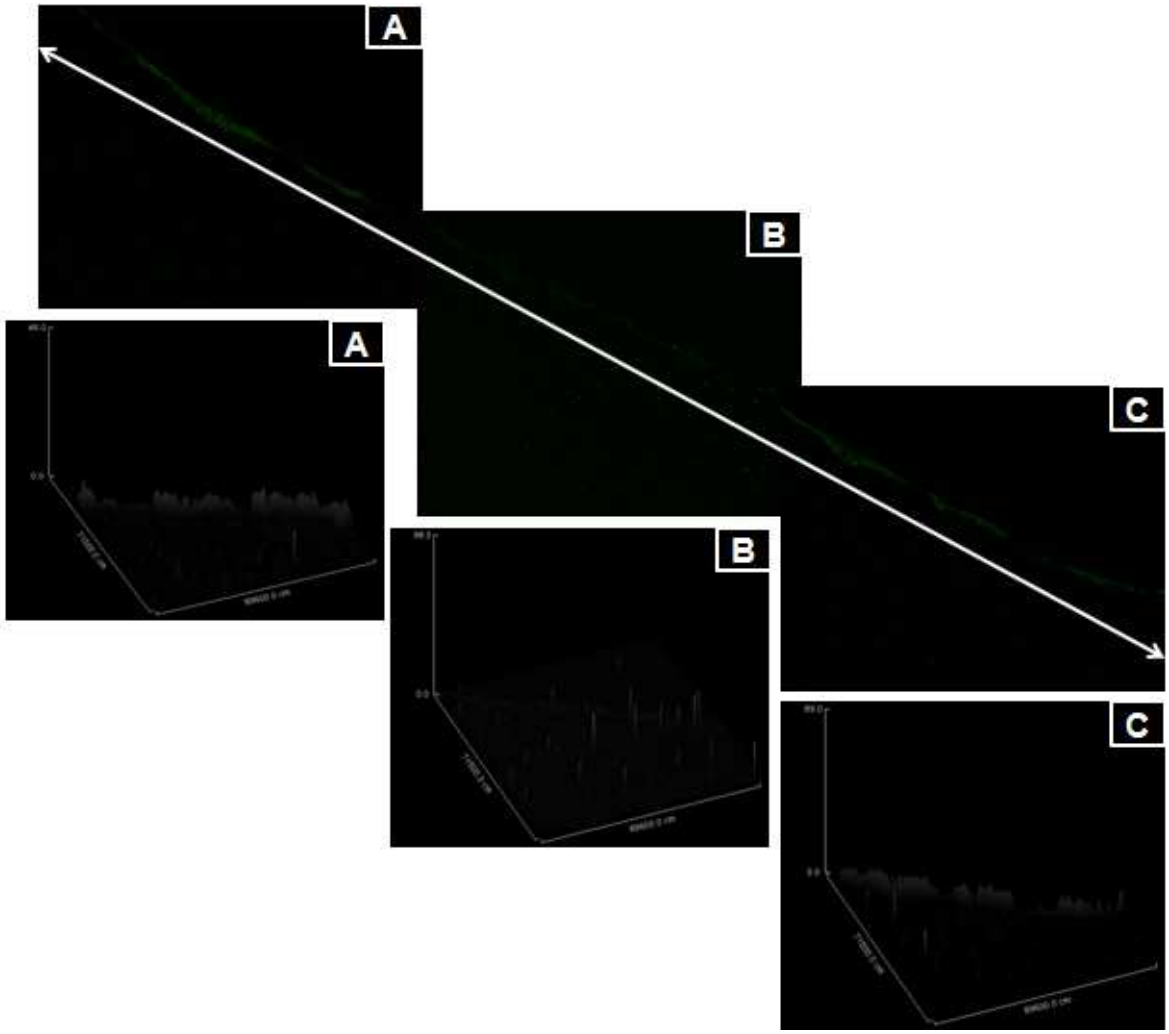
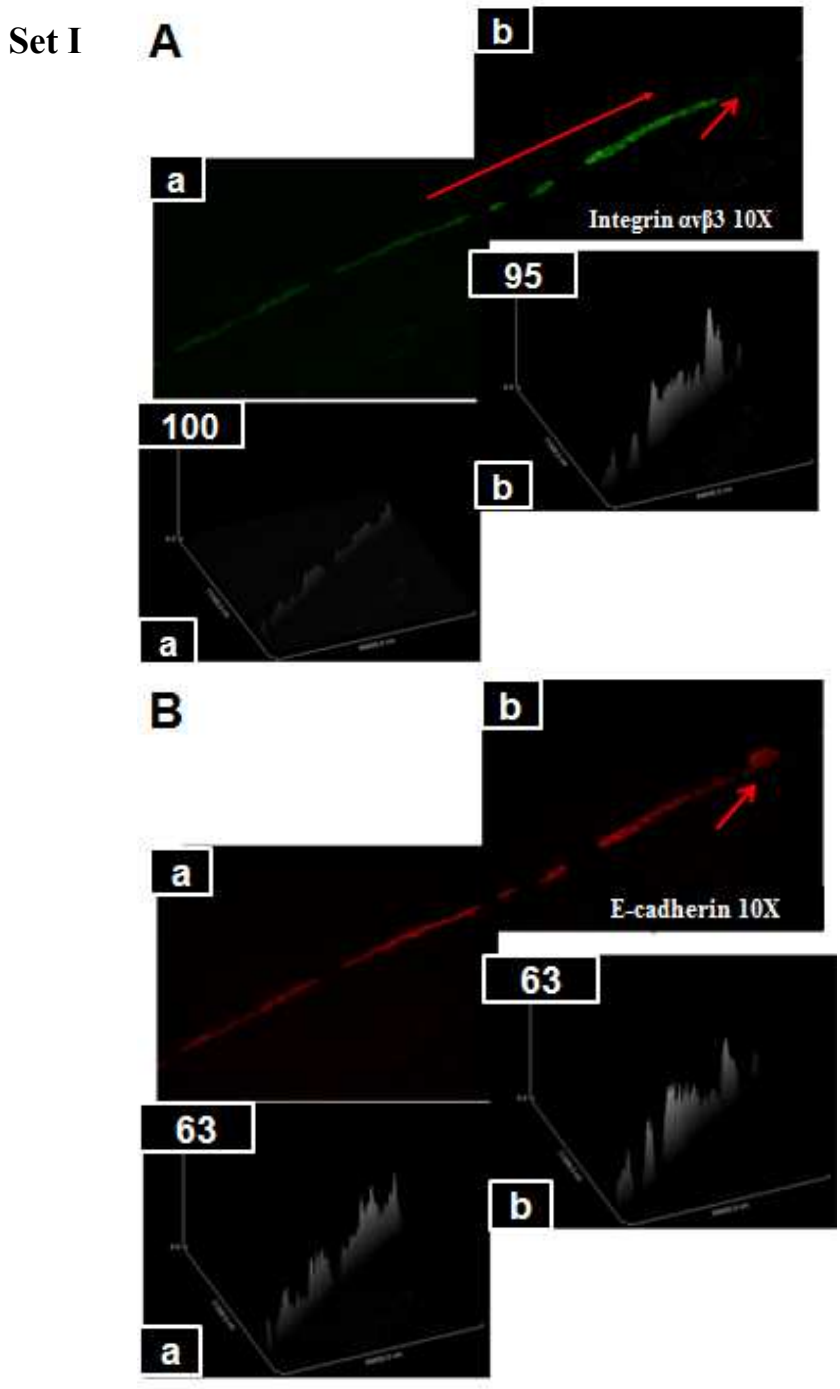


Figure 3.20: Localisation of integrin αvβ3 in the 3D gel

Immunofluorescence staining for integrin αvβ3 in two representative 3D gels. Three images (**A**, **B**, and **C**) from each gel demonstrated the entire gel (2.88 mm in length). Images were captured at a magnification of 10X. Intensity of integrin αvβ3 in each image was profiled. Green: integrin αvβ3

The intensity of integrin αvβ3 gradually increased towards the mouse embryo attachment site from the edge of the section from 3D *in vitro* gel, while E-cadherin was evenly stained across the half of gel. The intensity of integrin αvβ3 and E-cadherin of two independent 3D gels including mouse embryo were profiled in Figure 3.21-Set I and II.



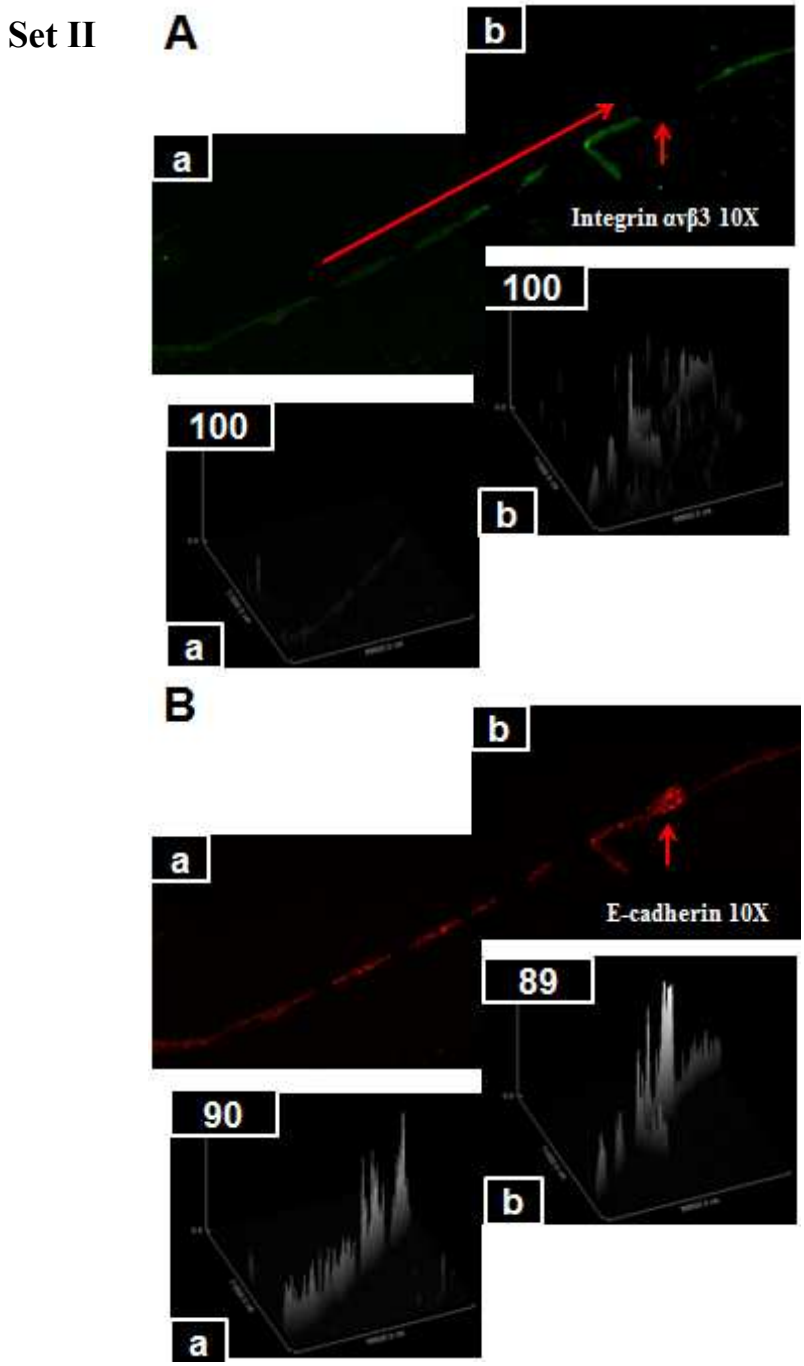


Figure 3.21: Localisation of integrin αvβ3 in heterologous 3D gel

Immunofluorescence staining for integrin αvβ3 with LM609 antibody (**A**) and E-cadherin with 67A4 antibody (**B**) in Ishikawa cells co-cultured with mouse embryos (red arrows) in two representative 3D gels (Set I and II). Image (**a**) and (**b**) displayed the half of gel. Images were captured at a magnification of 10X. Distribution of each molecule on each image was quantified by surface intensity profiling. Note that the number on schematic diagrams for profiling indicates the maximum pixel number of each image. Green: integrin αvβ3, Red: E-cadherin

3.2.2.2.3 Integrin αvβ3 expression in homologous 2D culture

Eight day 6 human embryos were co-cultured on confluent Ishikawa cells for 60 h. 2D gels including attached human embryos were fixed and permeabilised. As shown in Figure 3.22, the intensity of integrin αvβ3 staining gradually increased towards the site of human embryo attachment (white arrow) but further away from the attachment site integrin αvβ3 staining was unaffected, while actin was uniformly expressed (Figure 3.23). The surface intensity of integrin αvβ3 and actin staining was profiled (Figure 3.22, 3.23). Profiled intensity of integrin αvβ3 and actin of two representative 2D gels including human embryo was quantified in a graph illustrating the distributional change of integrin αvβ3 and uniformly stained actin across the whole region (Figure 3.24-Set I and II).

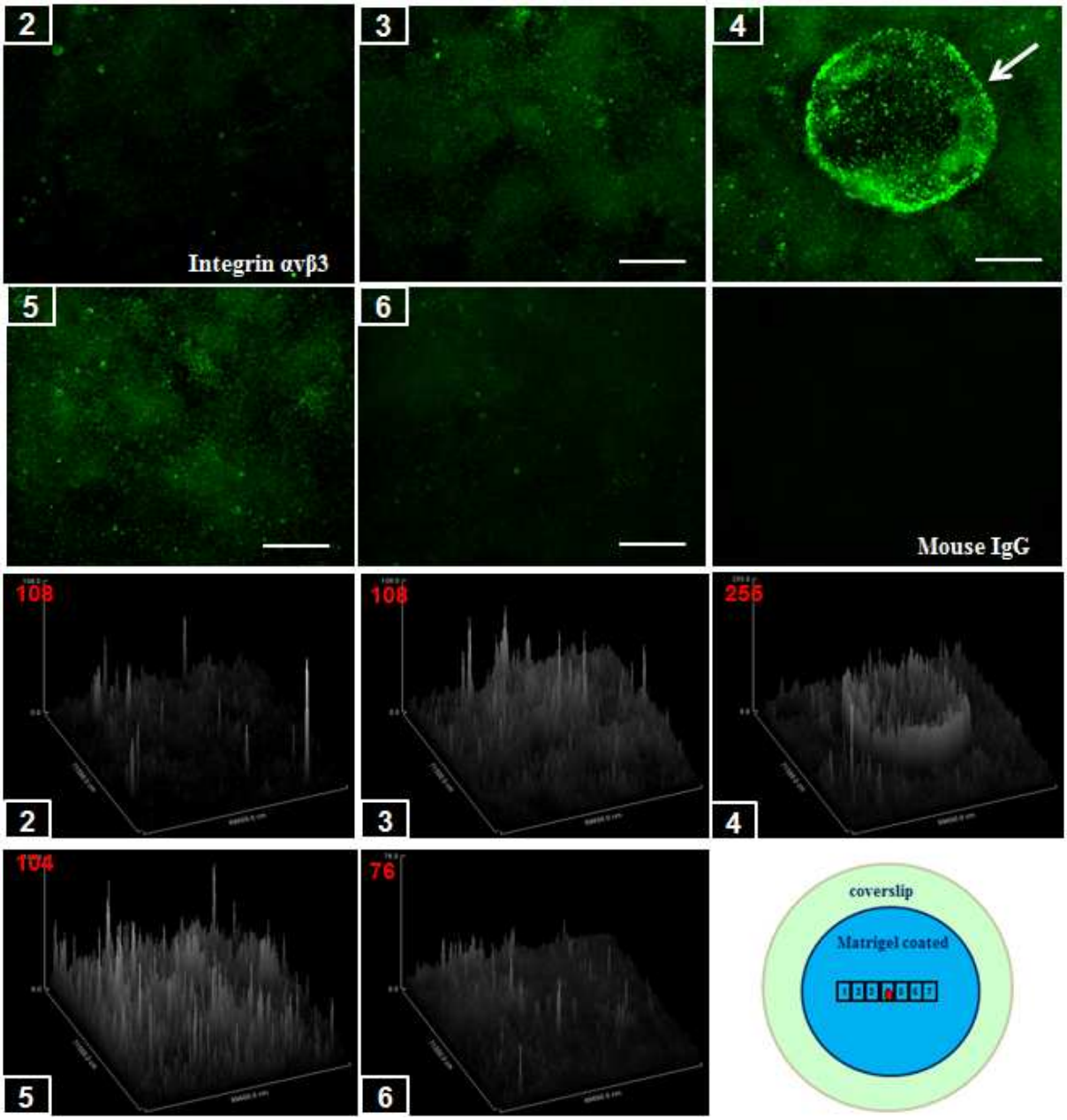


Figure 3.22: Integrin αvβ3 in homologous 2D culture

Immunofluorescence staining for integrin αvβ3 with LM609 antibody in Ishikawa cells co-cultured with one human embryo (white arrow). Images were obtained from 7 different regions of coverslip as illustrated in a diagram at the bottom of the figures (5 images are displayed). Images were captured at a magnification of 10X. Distribution of integrin αvβ3 on each image was quantified by surface intensity profiling. Note that the number on schematic diagrams for profiling indicates the maximum pixel number of each image. Green: integrin αvβ3, Scale bar = 200 μm

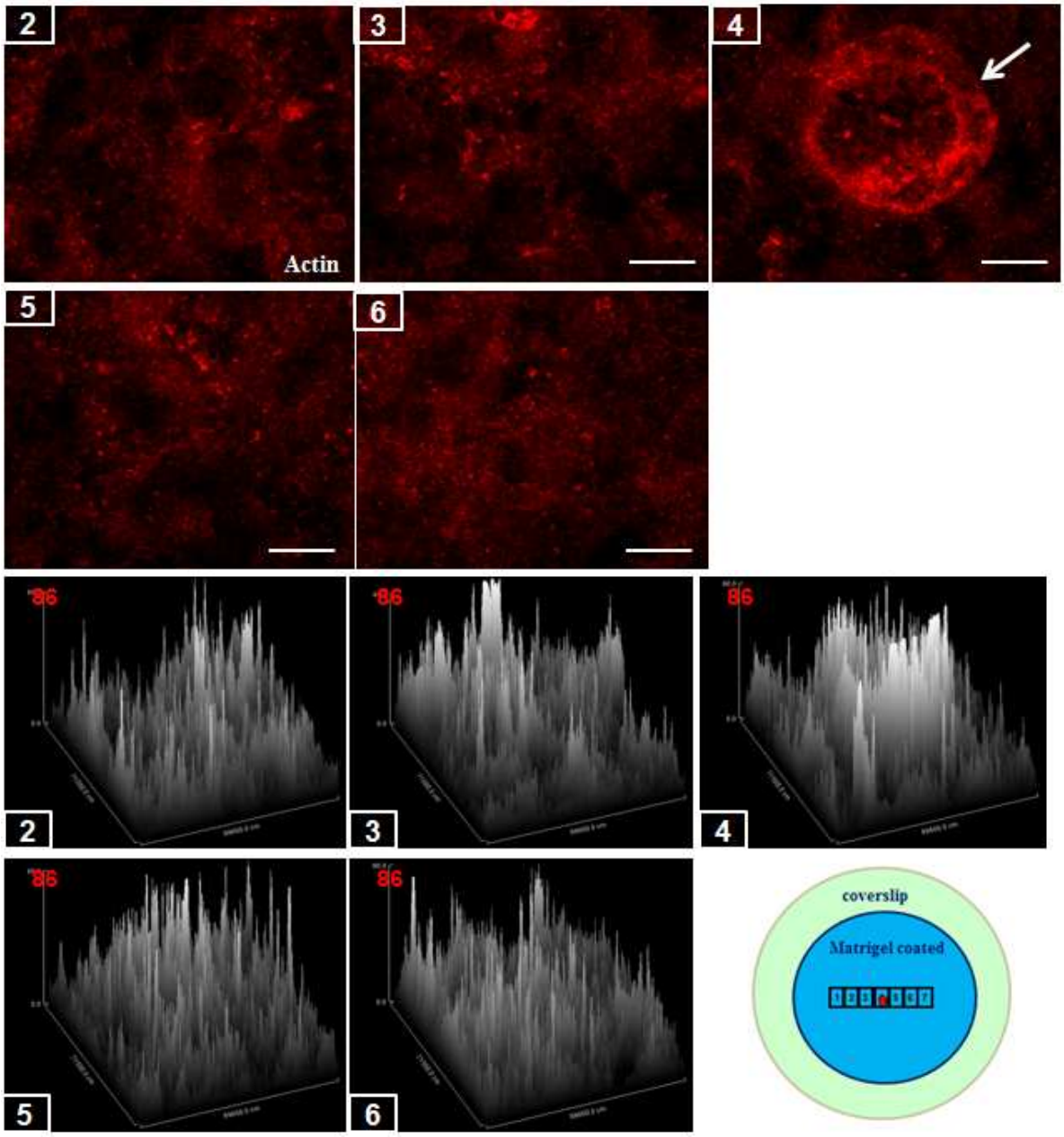
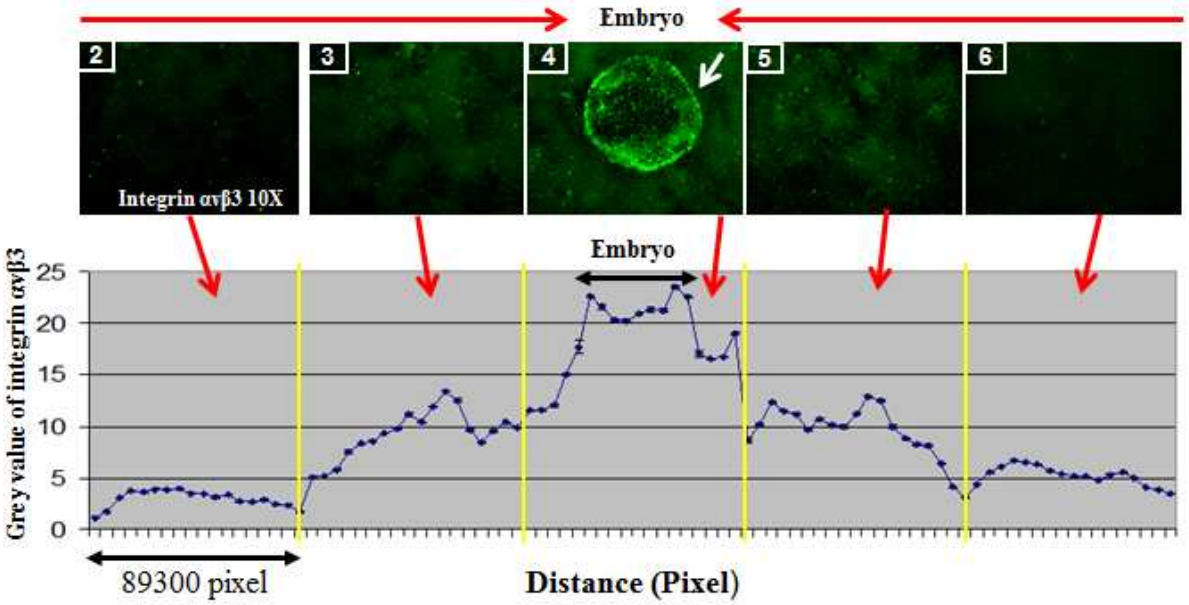


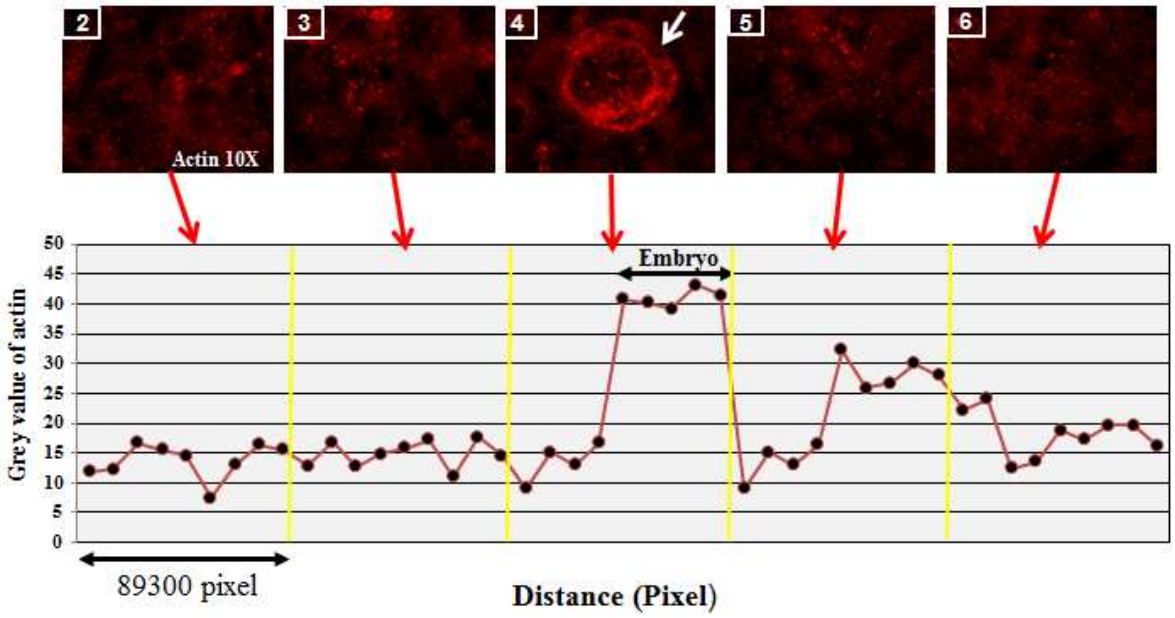
Figure 3.23: Actin (counter-stained to integrin αvβ3) in homologous 2D culture

Immunofluorescence staining for actin (counter-stained to integrin αvβ3) with phalloidin in Ishikawa cells co-cultured with a human embryo (white arrow). Images were obtained from 7 different regions of coverslip as illustrated in a diagram at the bottom of the figures (5 images are displayed). Images were captured at a magnification of 10X. Distribution of actin on each image was quantified by surface intensity profiling. Note that the number on schematic diagrams for profiling indicates the maximum pixel number of each image. Red:Actin, Scale bar = 200 μm

Set I- Integrin αvβ3



Set I- Actin



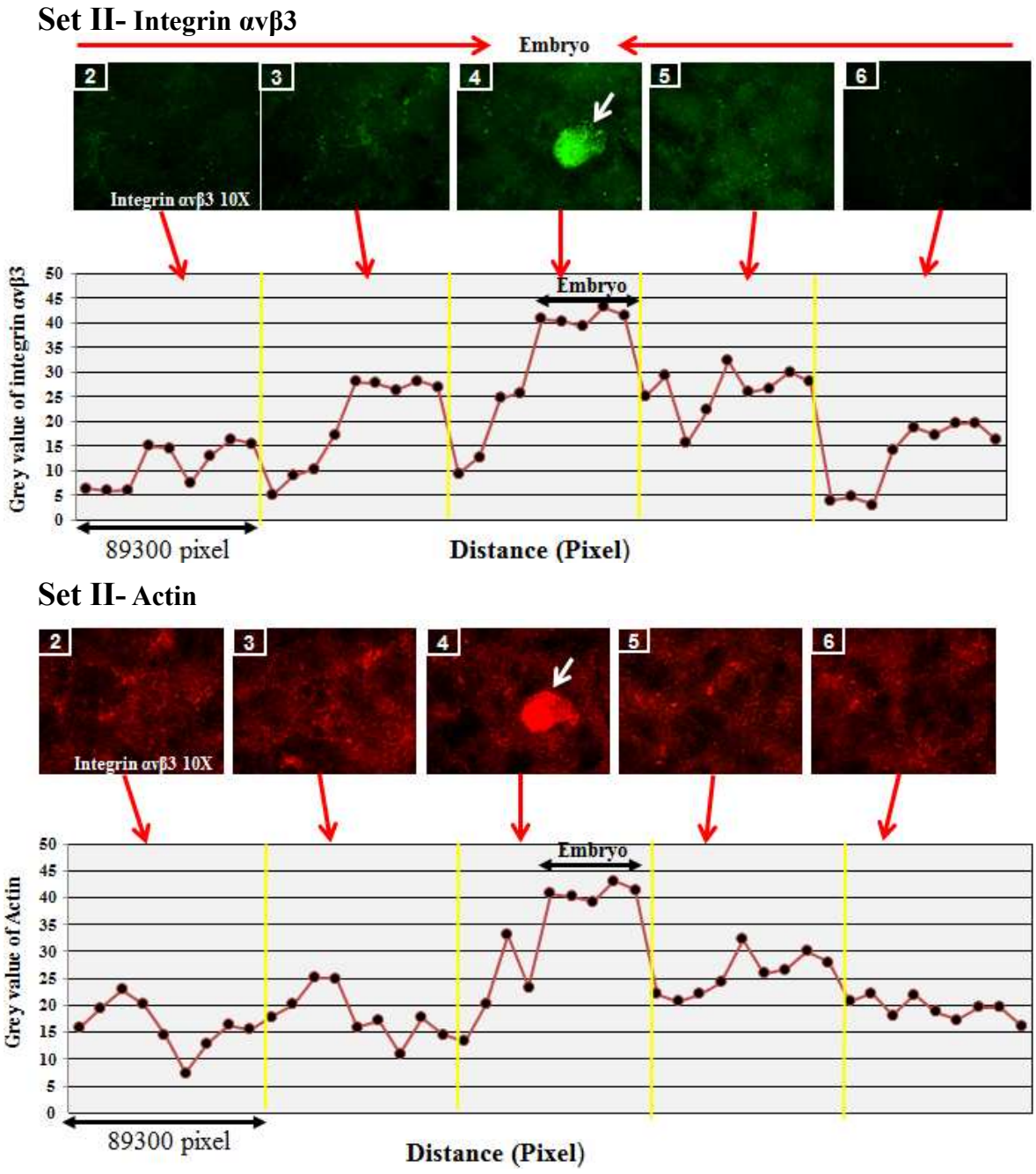


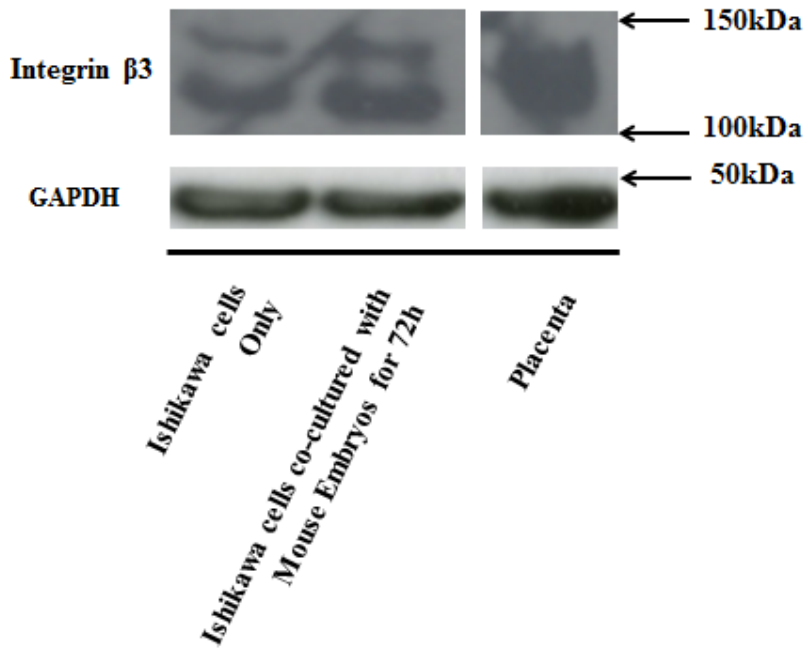
Figure 3.24: Quantification of integrin αvβ3 intensity profiling in homologous 2D culture

Surface intensity of integrin αvβ3 captured from 5 different areas from each coverslip of two independent 2D gels (Set I and II) was profiled in grey scale. The X-axis indicates the distance (pixel) of each image, while the Y-axis shows grey value of integrin αvβ3 expression. Each point on the graph shows the average of intensity of αvβ3 at every 5000 pixel of each image (Each image was 89300 pixels in width). Quantified intensity profiling showed that integrin αvβ3 was gradually elevated towards the human embryo attachment site (white arrow) from the outside of coverslip, while actin was evenly expressed across the coverslip.

3.2.2.2.4 Analysis of integrin β3 in 2D model by Western blotting

Seventy five mouse embryos were transferred to 15 independent 2D *in vitro* cultures (5 embryos per well) and co-cultured on confluent Ishikawa cells. Seventy two hours after co-culture, lysates were extracted from the Ishikawa cells themselves for a control experiment, or from Ishikawa cells including 5 attached mouse embryos in one confluent well of a 24-well plate, respectively. Western blot analysis using a polyclonal integrin β3 antibody, demonstrated increased expression when 5 attached mouse embryos were present, compared to control cells without embryos (Figure 3.25). Antibody specificity was tested with protein extracted from the placenta as a positive control.

A **Integrin β3 subunit expression at the protein level**



B

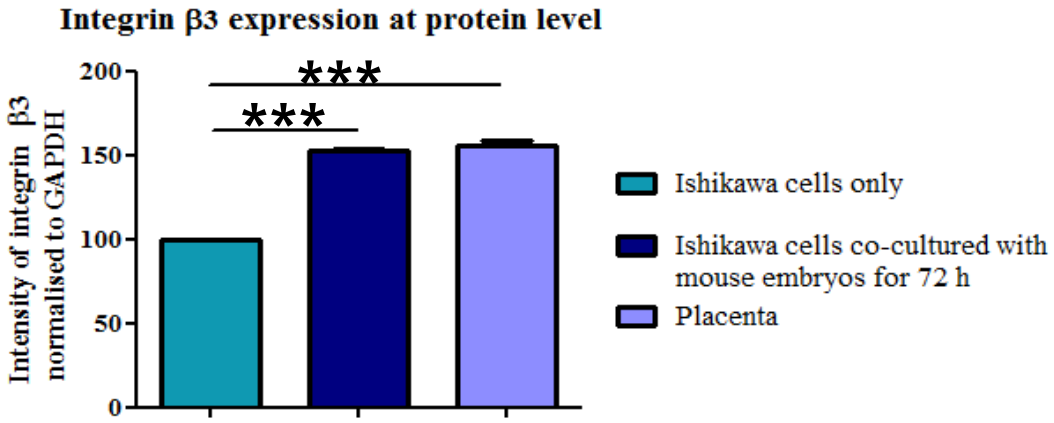


Figure 3.25: Western blotting analysis of integrin β3 in Ishikawa control cells and cells with 5 attached mouse embryos

Representative immunoblots using an anti-integrin β3 antibody with purified samples from control cells, cells co-cultured with mouse embryos for 72 h, and placenta tissues (positive control). Bands corresponding to 110~130kDa were successfully detected, which were the expected size for the expressed integrin β3 protein (**A**). Relative densitometry values illustrating the intensity of bands obtained for control or co-cultured cells. Asterisk (***) denotes a statistically significant difference ($P \leq 0.0001$) as determined by the student's t-test. Data are represented as mean ± S.E.M (**B**).

3.2.2.3 Stable expression of integrin αvβ5 in Ishikawa cells after embryo attachment

In order to investigate the distribution of integrin αvβ5 upon embryo attachment on endometrial epithelium, 17 day 5 mouse embryos were co-cultured on 2D and 3D gels and 5 day 6 human embryos were used for 5 independent 2D *in vitro* cultures.

Integrin αvβ5 expressed at the apical and lateral side of Ishikawa cells without embryos (Figure 3.26).

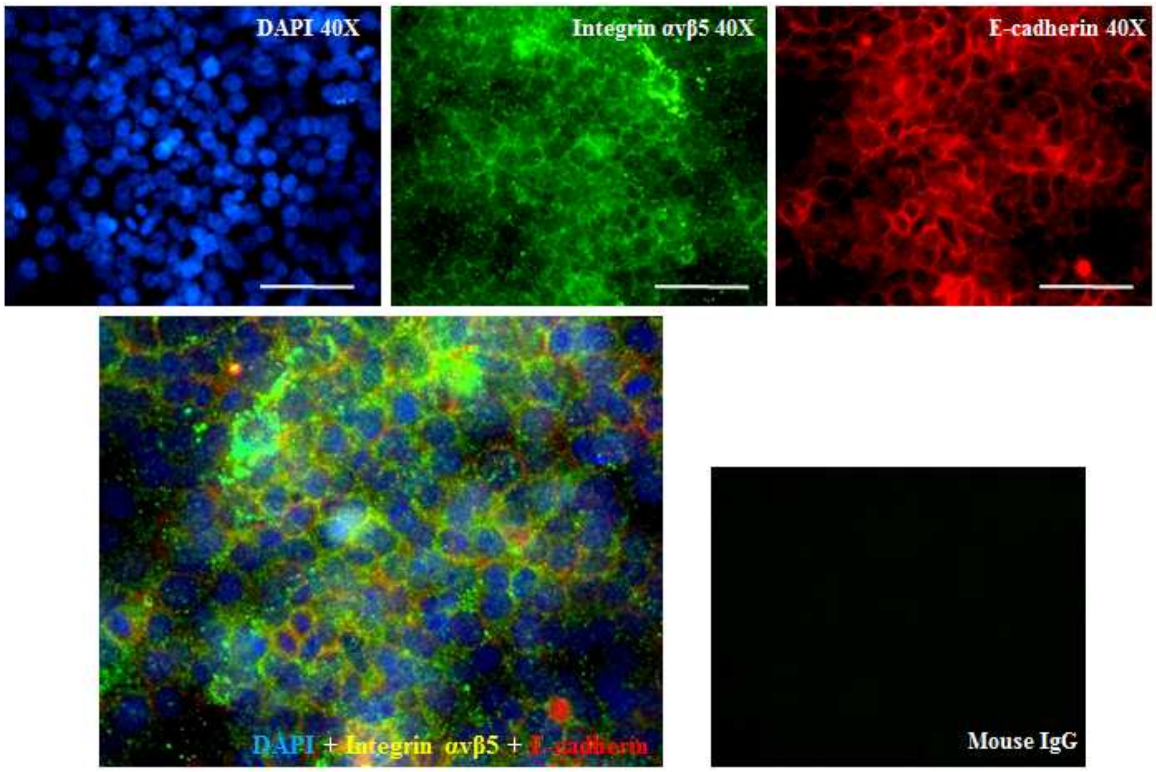


Figure 3.26: Localisation of integrin αvβ5 in Ishikawa cells

Localisation of integrin αvβ5 using a mouse monoclonal integrin αvβ5 antibody which detects the complex of αv and β5 subunits, no reactivity with other complexes, and E-cadherin (counter-stained) in Ishikawa cells. Images were captured with a magnification of 40X and enlarged digitally. Mouse IgG was used as a negative control. Blue: Nucleus (DAPI), Green: integrin αvβ5, Red: E-cadherin, Scale bar = 50 µm

3.2.2.3.1 Integrin αvβ5 expression in heterologous 3D culture

After 60 h of co-culture, gels were fixed and immunostained for human integrin αvβ5 using a mouse monoclonal antibody which detects the αvβ5 complex. As shown in Figure 3.27, integrin αvβ5 and E-cadherin were both expressed at similar levels in cells close to, and more distant from the attached mouse embryo and each image was profiled (Figure 3.28).

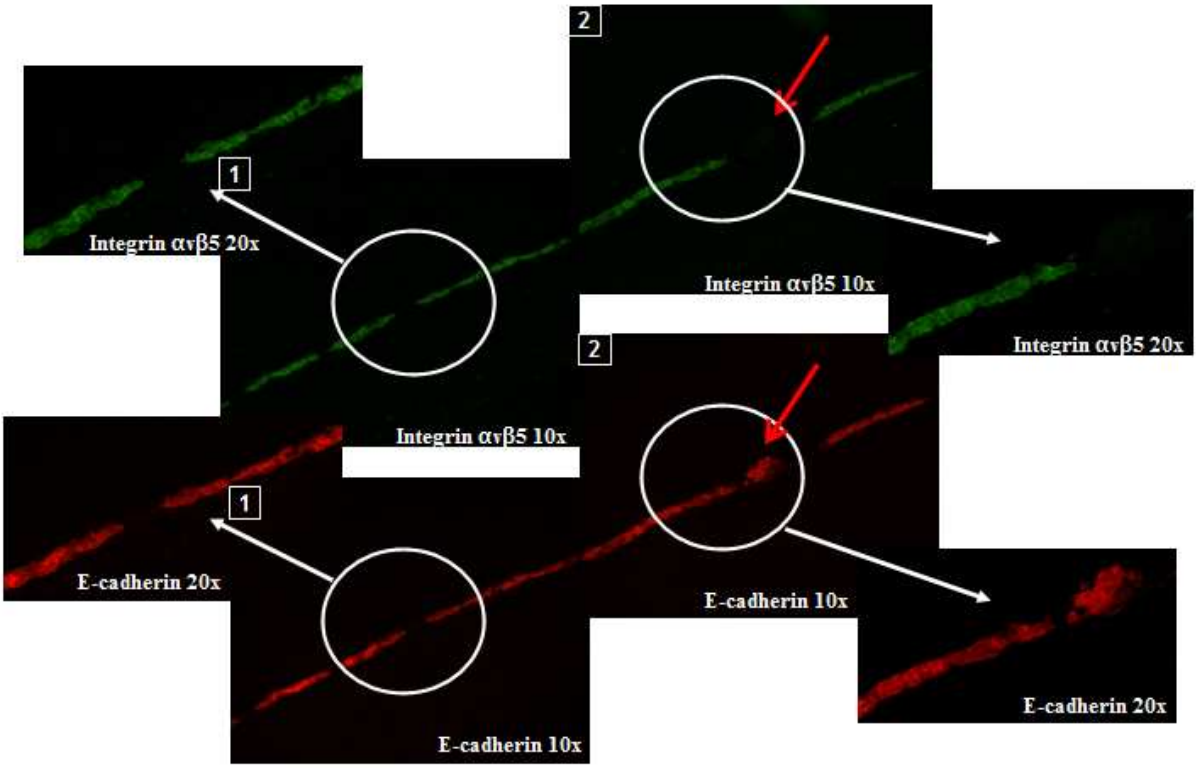


Figure 3.27: Integrin αvβ5 in heterologous 3D gel

Immunofluorescence staining for integrin αvβ5 and E-cadherin (counter-stained) in Ishikawa cells co-cultured with mouse embryo (red arrow) in 3D gel. Images were captured at a magnification of 10X and specific regions in circles were magnified with an optical magnification of 20X. Green: integrin αvβ5, Red: E-cadherin

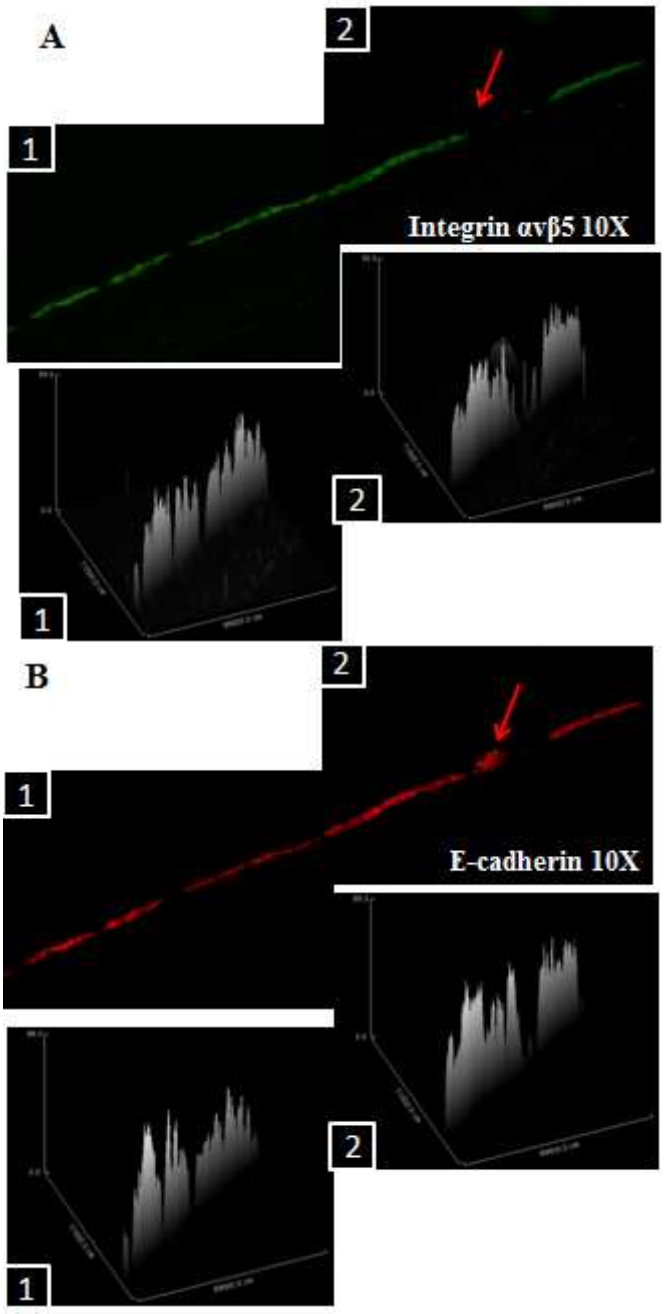


Figure 3.28: Surface intensiy of integrin αvβ5 in heterologous 3D gel

Surface intensity of integrin αvβ5 and E-cadherin (counter-stained) in each image of Figure 3.25. Images were captured at a magnification of 10X. Green: integrin αvβ5, Red: E-cadherin

3.2.2.3.2 Integrin αvβ5 expression in homologous 2D culture

Five human embryos were co-cultured on Ishikawa cells in 5 independent gels for 60 h after which the 2D gels were fixed and permeabilised. The surface intensity of integrin αvβ5 was profiled (Figure 3.29) and even expression was observed in epithelial cells. Integrin αvβ5 immunoreactivity was also observed on the attached human blastocyst. Actin was stained evenly across the coverslip. Mosaic pattern of integrin αvβ5 was clearly demonstrated by a quantified intensity profiling of two independent 2D gels including human embryos (Figure 3.30).

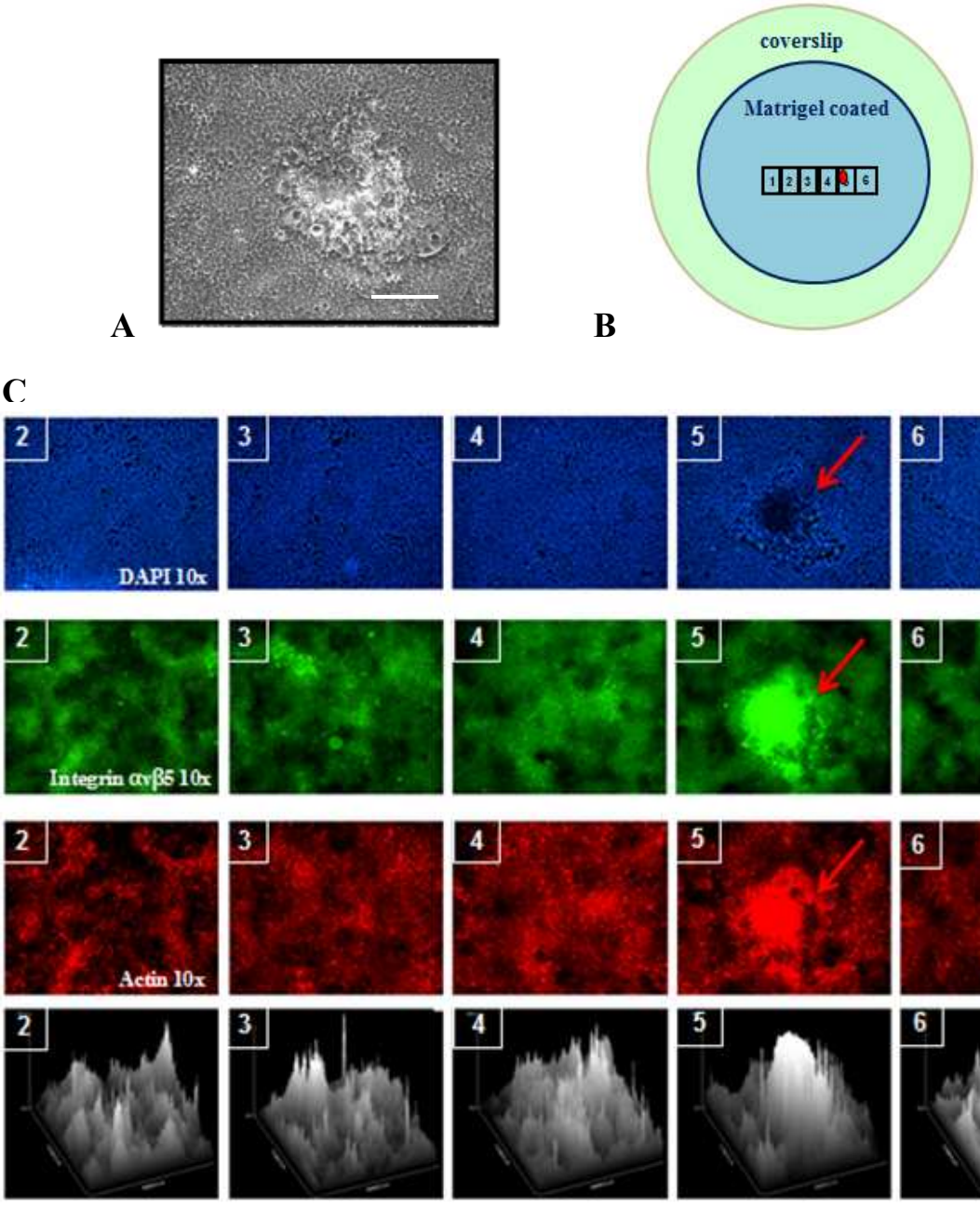
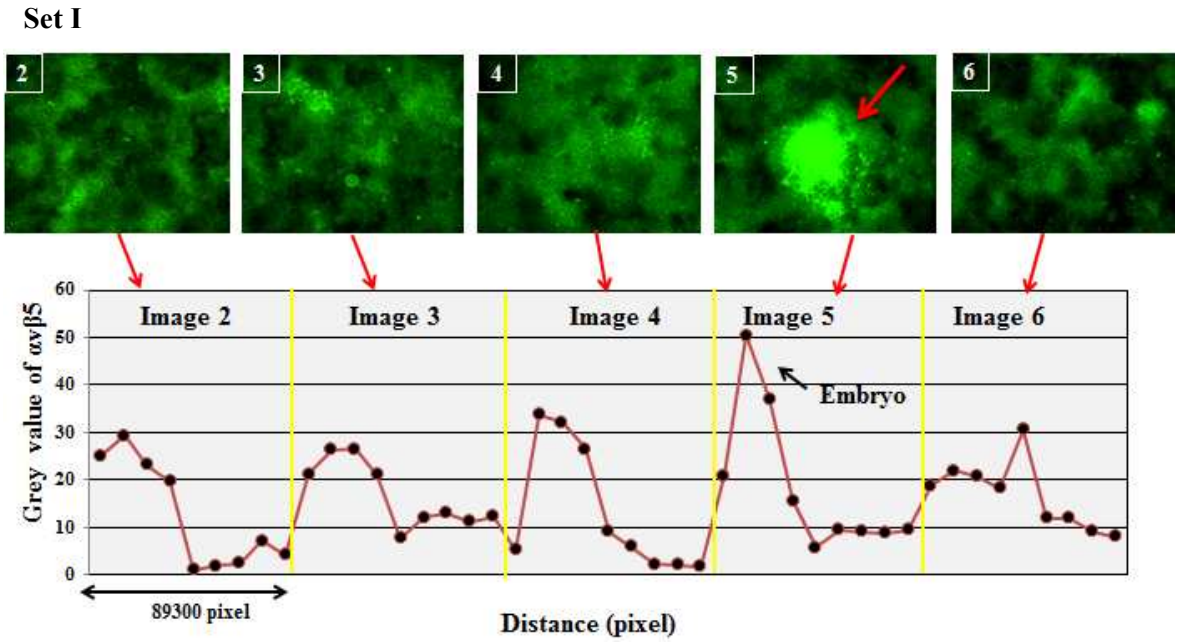


Figure 3.29: Localisation of integrin αvβ5 in homologous 2D culture

Phase contrast image of 2D culture of Ishikawa cells co-cultured with human embryo (**A**). A diagram of coverslip illustrating the location of each image from the coverslip and human blastocyst (red spot in image 5) (**B**). Immunofluorescence staining for integrin αvβ5 and actin (counter-stained) with phalloidin in Ishikawa cells co-cultured with human embryo (red arrows) (**C**). Images were obtained from 6 different regions of coverslip as illustrated (**B**) (5 images are displayed). Images were captured at a magnification of 10X. Distribution of integrin αvβ5 on each image was quantified with surface intensity profiling. Blue: Nucleus (DAPI), Green: integrin αvβ5, Red: Actin, Scale bar = 200 μm



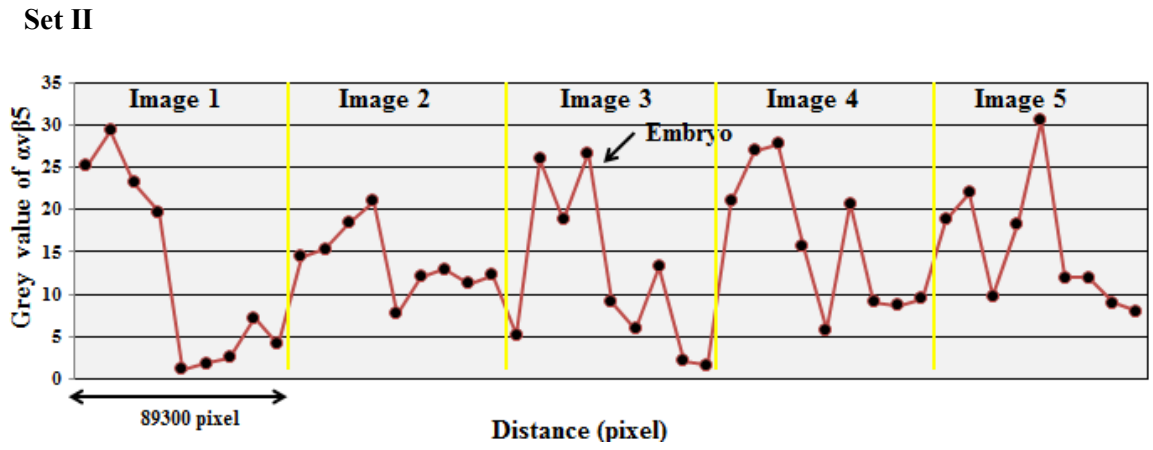


Figure 3.30: Quantification of integrin αvβ5 intensity profiling in homologous 2D culture

Surface intensity of integrin αvβ5 captured from 5 different areas from each coverslip from two representative 2D gels with human embryo was profiled in grey scale. The X-axis indicates the distance (pixel) of each image, while the Y-axis shows grey value of integrin αvβ5 expression. Each point on the graph shows the average of intensity of αvβ5 at every 10000 pixel of each image (Each image was 89300 pixels in width). Quantified intensity profiling showed repeated pattern showing the mosaic expression of integrin αvβ5 across the whole gel.

3.2.2.4 Up-regulation of OPN near the site of embryo attachment

OPN was examined in Ishikawa cells in the presence of a mouse embryo by immunocytochemistry, and Western blotting was used to examine global expression in microwells containing confluent Ishikawa cells exposed to mouse embryos. Eighty one mouse embryos were used in total.

OPN was weakly expressed in the cytoplasm of the cells exhibiting a mosaic expression. Comparing to the expression of mouse IgG as a negative control, OPN signal was greater than from negative control. Cytoplasmic staining of OPN was clearly observed at higher magnification (Figure 3.31).

3.2.2.4.1 OPN expression in heterologous 2D culture

Six randomly selected mouse embryos were transferred to confluent Ishikawa cells of 6 independent gels. Forty eight hours later gels were fixed, permeabilised, and immunostained for OPN.

Images were obtained from 5 different regions of the 2D co-cultures and surface intensity of OPN was profiled. As shown in Figure 3.30, OPN was increased near the embryo, while nuclei were uniformly stained. This is clearly demonstrated by a quantified intensity profiling showing that OPN was gradually increased near the attachment sites (Figure 3.32).

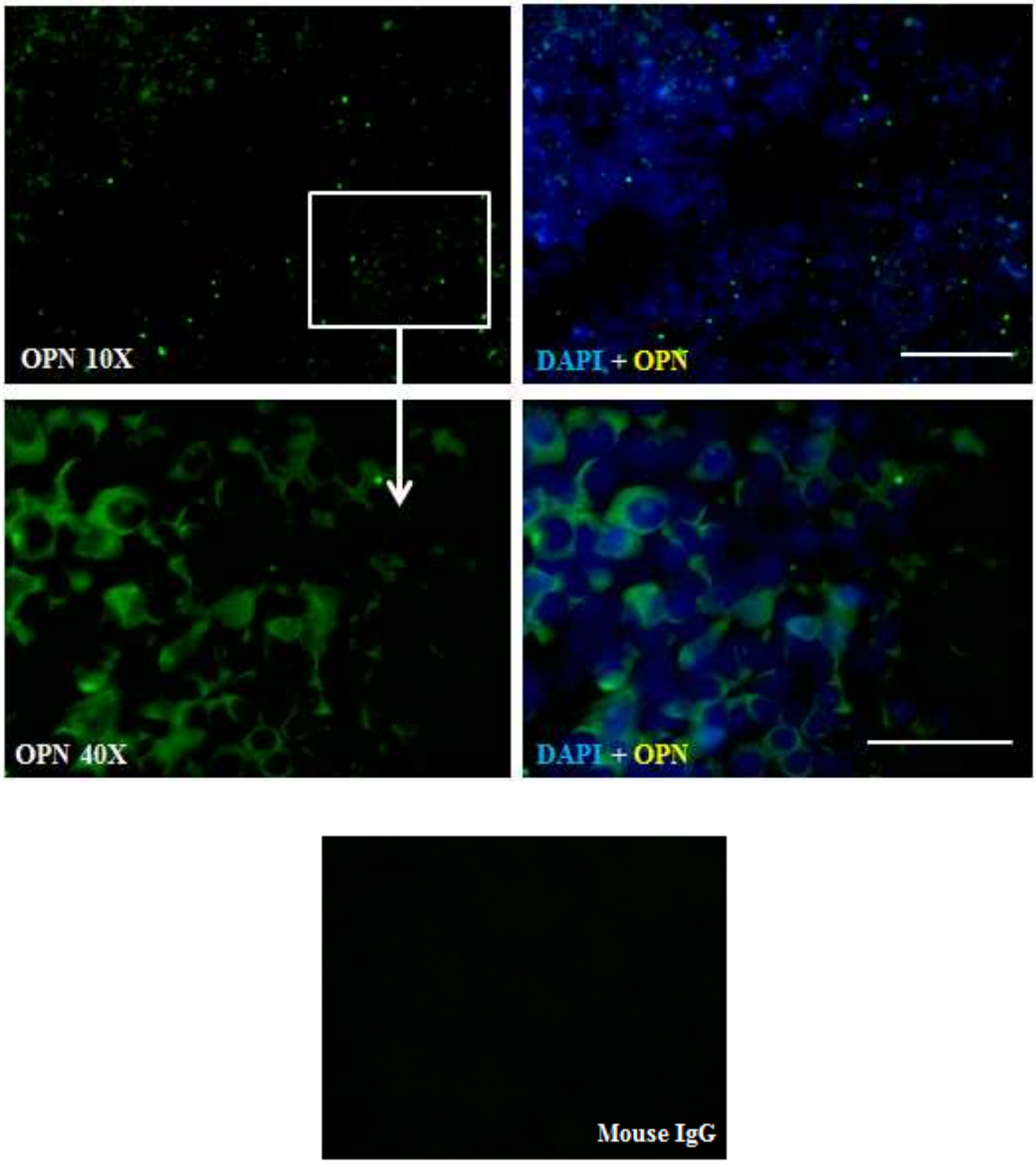


Figure 3.31: Localisation of OPN in Ishikawa cells

Immunofluorescence staining for OPN in Ishikawa cells. Images were captured at a magnification of 10X (Scale bar = 200 µm) or 40X (Scale bar = 50 µm) and enlarged digitally. Green: OPN, Blue: Nucleus (DAPI)

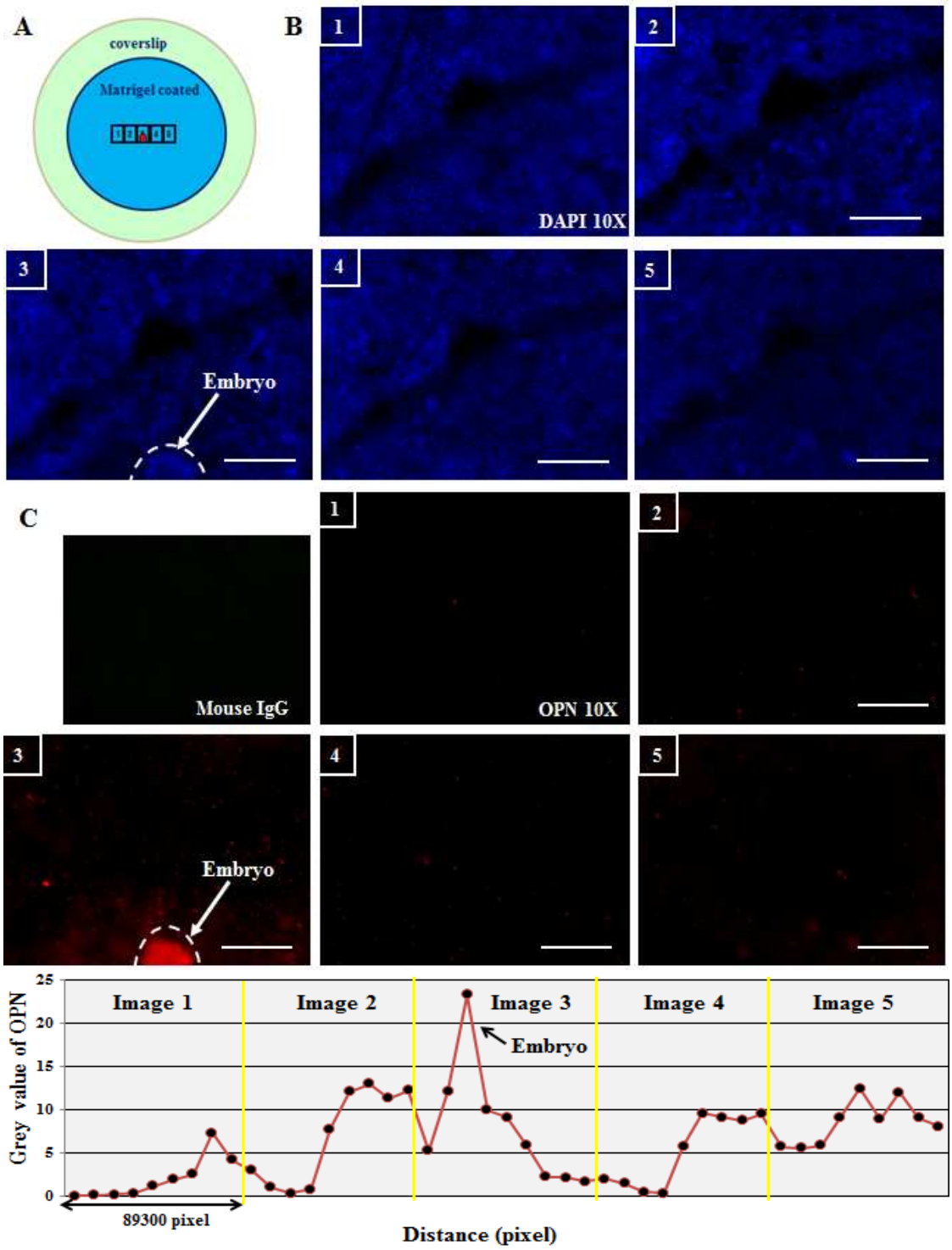


Figure 3.32: OPN in homologous 2D culture

Immunofluorescence staining (Set I) for OPN (**C**) and nuclei (**B**) in Ishikawa cells co-cultured with a mouse embryo (white circle, arrow). Images were obtained from 5 different regions of a coverslip as illustrated (**A**). The diagonal black stripe on images was caused from a cracked element in the fluorescence light path. Each image of OPN staining was profiled. Images were captured at a magnification of 10X. Blue: Nucleus (DAPI), Red: OPN, Scale bar = 200 µm

Three different regions were selected by distance from the attachment site. OPN was strongly expressed on both the mouse embryo and surrounding Ishikawa cells with strong expression at the top of the cell layer, some of which was associated with vesicular deposits. Much stronger expression of OPN was observed adjacent to the embryo than in more distal areas of the epithelial monolayer (Figure 3.33).

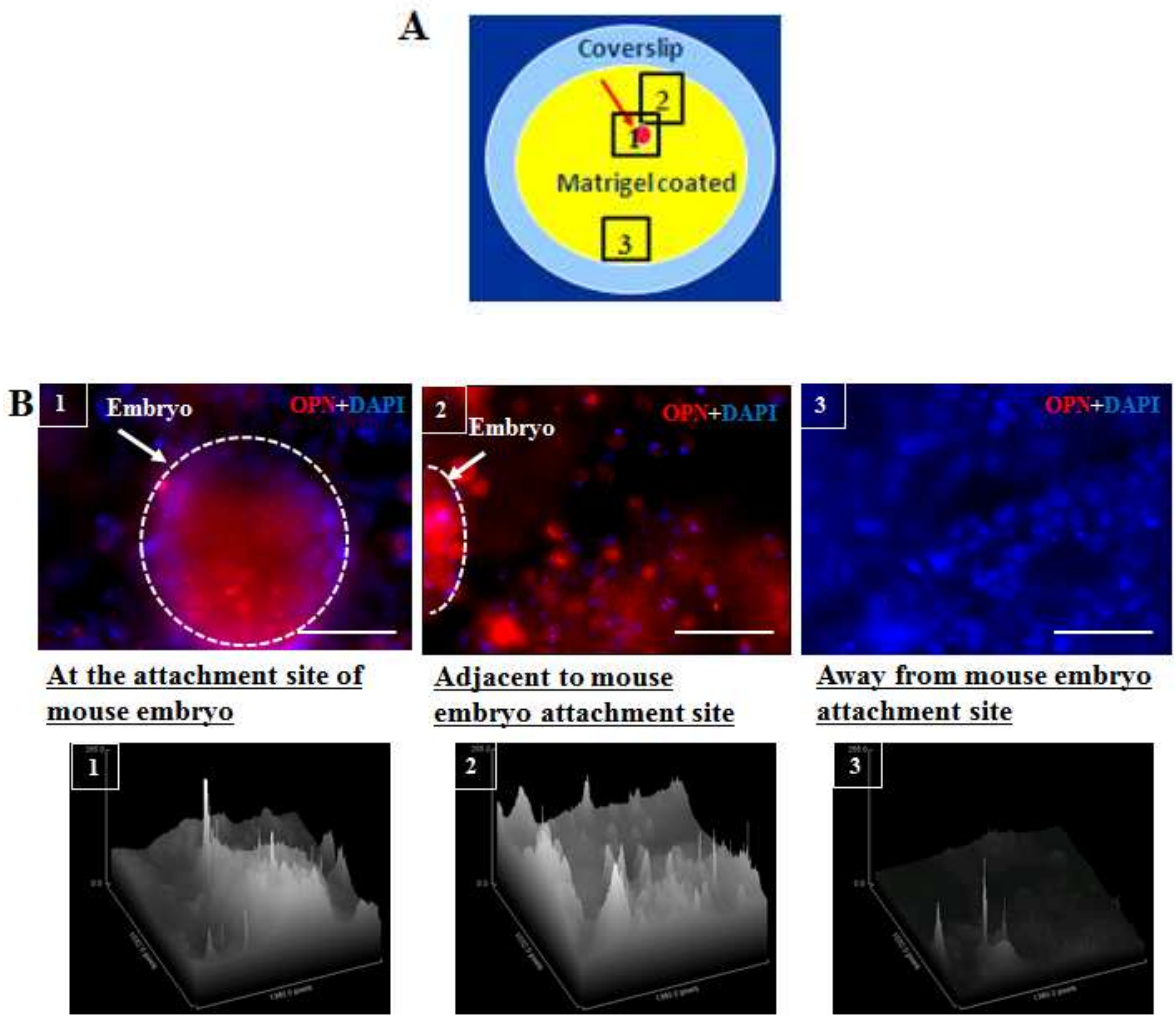


Figure 3.33: OPN in homologous 2D culture at higher magnification

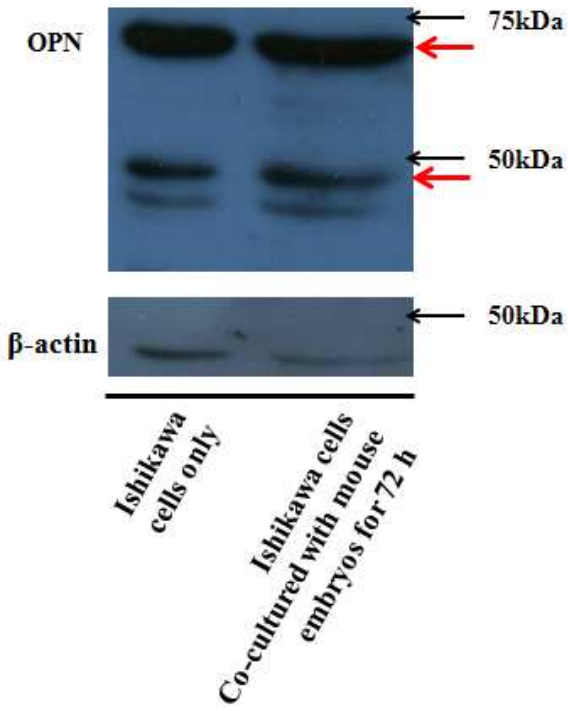
Immunofluorescence staining for OPN and nuclei (**B**) in Ishikawa cells co-cultured with a mouse embryo (white circle, arrow). Images were obtained from 3 different regions of a coverslip as illustrated (**A**). The diagonal black stripe on images was caused from a cracked element in the fluorescence light path. Images were captured at a magnification of 40X. Blue: Nucleus (DAPI), Red: OPN, Scale bar = 50 µm

3.2.2.4.2 Up-regulation of OPN protein in the presence of attached mouse embryos

Five mouse embryos were transferred to each individual 2D *in vitro* culture and co-cultured for 72 h. Cell lysates were prepared from Ishikawa cells and co-cultures. Immunoblots were probed for monoclonal OPN antibody.

OPN showed predominant bands at 70, 45, and 25kDa. Increased OPN was detected after 72 h of co-culture. In particular, the 45kDa fragment was slightly elevated (1.4x) after 72 h of co-culture with 5 mouse embryos in one confluent well from a 24 well plate (Figure 3.34)

A **OPN expression at the protein level**



B



Figure 3.34: Western blotting analysis of OPN in Ishikawa cells alone and Ishikawa cells including 5 attached mouse embryos

Representative immunoblots using anti-OPN antibody with purified samples from control cells and cells co-cultured with mouse embryos for 72 h. Bands corresponding to ~70kDa were successfully detected, which were the expected size for the expressed OPN protein (**A**). Relative densitometry values illustrating the intensity of 70kDa and 45kDa fragments of OPN bands obtained for control or co-cultured cells. Asterisk (***) denotes a statistically significant difference ($P \leq 0.0001$) as determined by the student's t-test. Data are represented as mean ± S.E.M (**B**).

3.2.2.5 UP-regulation of HB-EGF near the site of embryo attachment in heterologous 2D culture

Thirty five mouse embryos were randomly selected and transferred to 16 independent 2D gels. Forth eight hours after transfer, gels were fixed and immunostained for HB-EGF with an antibody which detects both transmembrane and soluble forms.

HB-EGF was weakly expressed at the lateral side of Ishikawa cells alone (Figure 3.37.A). However, expression was locally elevated at the site of embryo attachment, while its staining was unaffected further away from the attachment site. This is clearly demonstrated by quantified intensity profiling of HB-EGF in grey scale (Figure 3.35 and Figure 3.36-Set I and II). HB-EGF was strongly expressed at the apical and lateral sides of cells adjacent to embryo attachment site displaying evident vesicular stainings (Figure 3.37.B) compared to weak expression in the membrane.

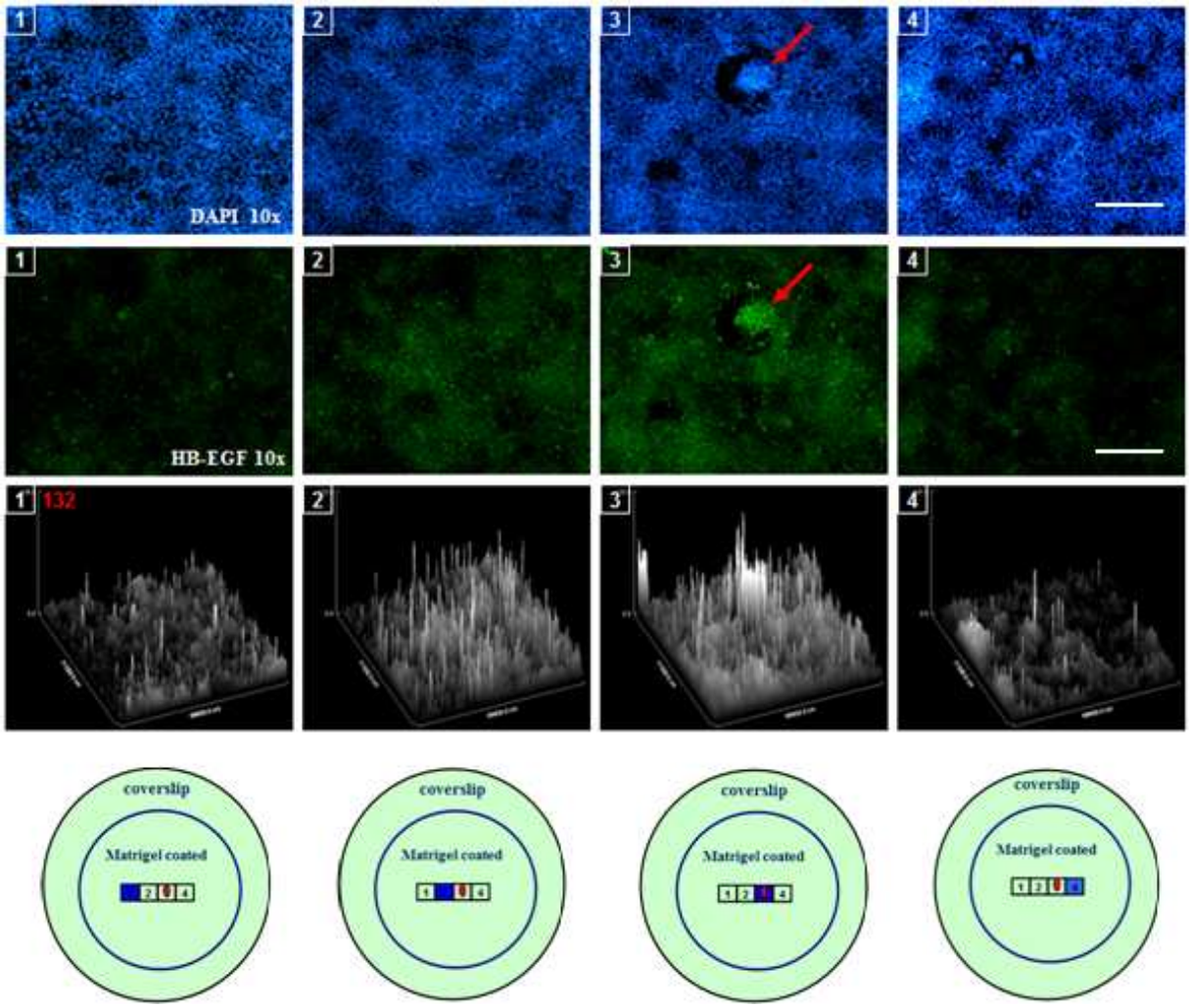


Figure 3.35: Localisation of HB-EGF on 2D heterologous gels

Representative immunofluorescence microscopy images taken for HB-EGF in Ishikawa cells co-cultured with a mouse embryo (red arrow). Images were obtained from 4 different regions of coverslip as illustrated in diagrams at the foot of the figures. Images were captured at a magnification of 10X. Intensity of HB-EGF staining across the gel was profiled. Blue: Nucleus (DAPI), Green: HB-EGF, Scale bar = 200 µm

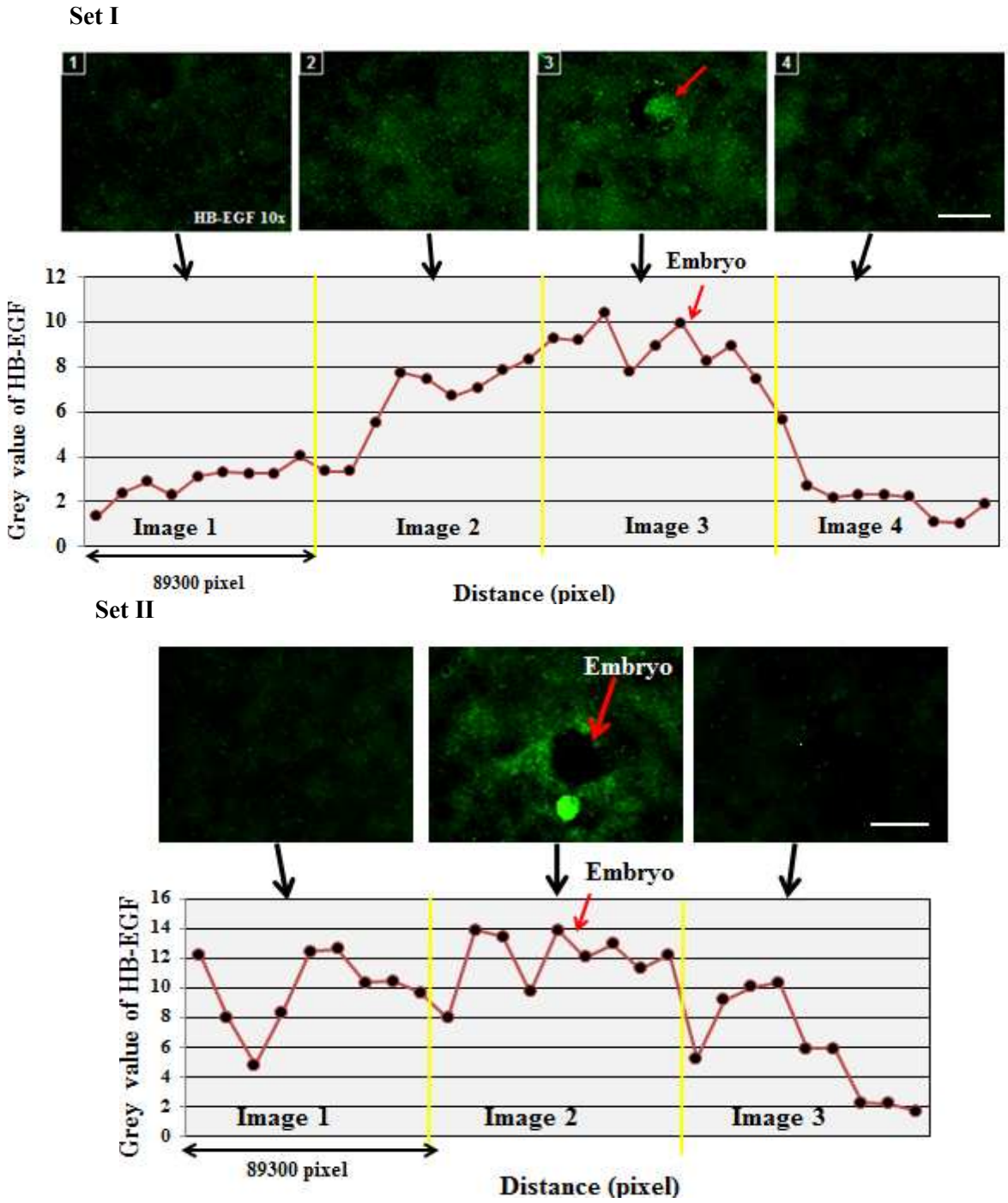


Figure 3.36: Quantification of HB-EGF intensity profiling in heterologous 2D cultures

Surface intensity of HB-EGF captured from each coverslip from two separate representative sets of gels was profiled in grey scale. The X-axis indicates the distance (pixel) of each image, while the Y-axis shows grey value of HB-EGF expression. Each point on the graph shows the average of HB-EGF at every 10000 pixel of each image (Each image was 89300 pixels in width). Quantified intensity profiling showed similar pattern in which HB-EGF was gradually elevated towards the mouse embryo attachment site (red arrow) from the outside of coverslip, Scale bar = 200 µm.

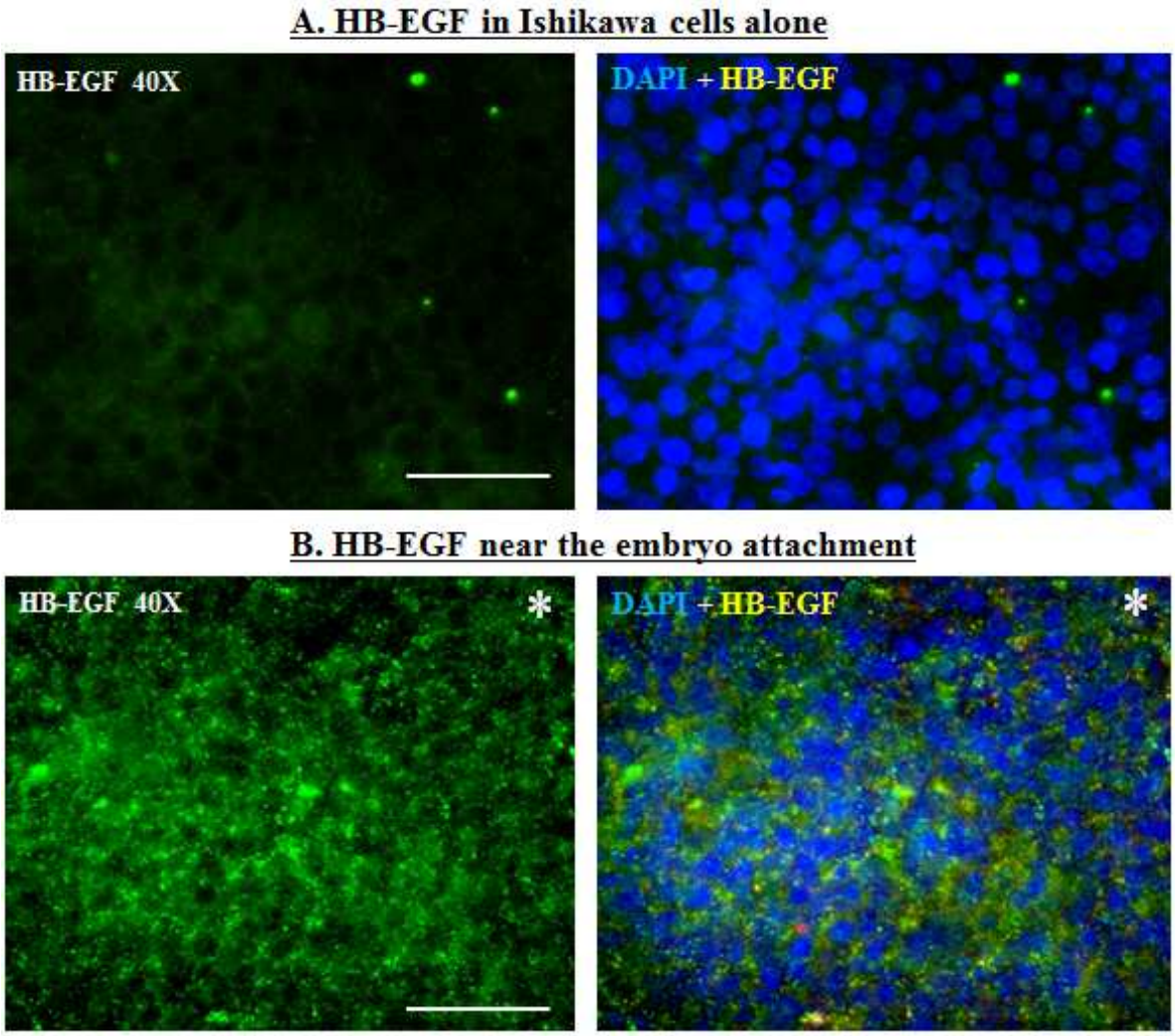


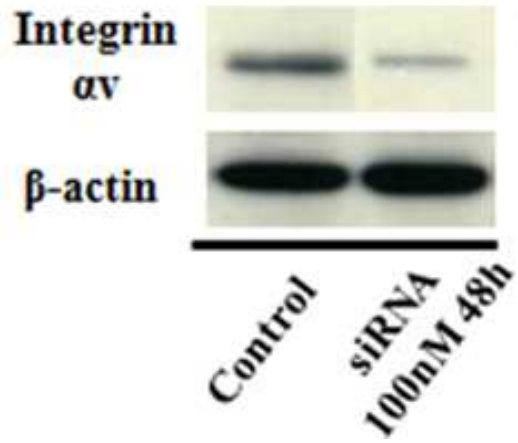
Figure 3.37: Localisation of HB-EGF in Ishikawa cells alone or near the mouse embryo attachment site

Representative immunofluorescence staining for HB-EGF in Ishikawa cells alone **(A)** or cells co-cultured with a mouse embryo (located at the area marked with white *) (**B**). Images were captured at a magnification of 40X. Blue: Nucleus (DAPI), Green: HB-EGF, Scale bar = 50 µm.

3.2.2.6 Integrin αvβ3 knock-down suppresses mouse embryo attachment

In order to investigate the roles of integrin αvβ3 in embryo attachment, Ishikawa cells were transfected with integrin subunit αv or β3 siRNA separately or in combination. Various concentrations (25, 50, and 100nM) of four RNA sequences that target different regions of integrin αv and β3 were used and transfection times were tested up to 72 h. Western blotting of cell lysates showed significant knock-down by 48 h after transfection. Ishikawa cells transfected with integrin αv siRNA at 100nM for 48 h showed approximately 85% reduction in protein expression compared to control cells and Ishikawa cells transfected with integrin β3 siRNA at 100nM for 48 h showed approximately 90% reduction in protein expression compared to control cells (Figure 3.38, 3.39). However, after 72 h of transfection, alterations were evident in the morphology of cells, which pulled apart from each other. This disturbed cell-cell adhesion and resulted in defects in the monolayer (Supplementary Appendix 5). Therefore, the duration of transfection used was 48 h.

A **Integrin αv expression at the protein level**



B

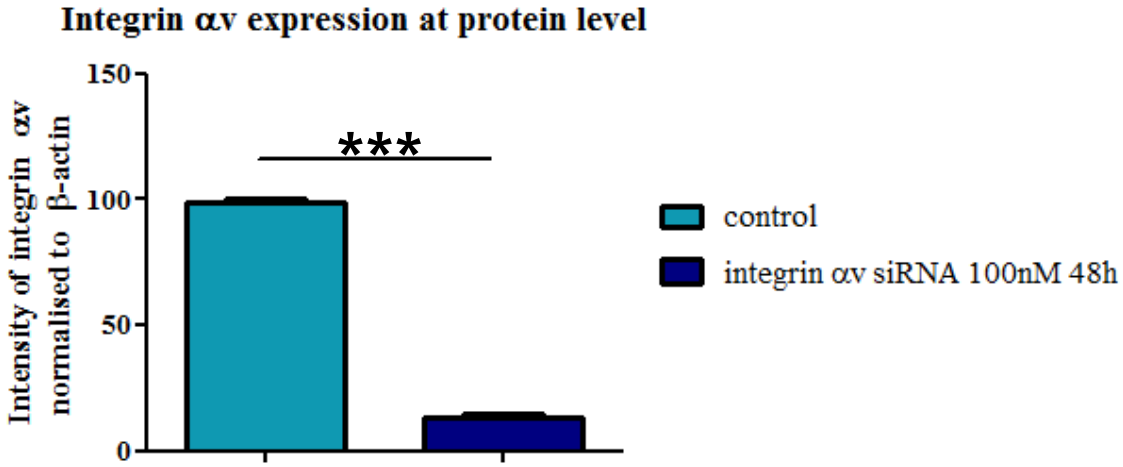
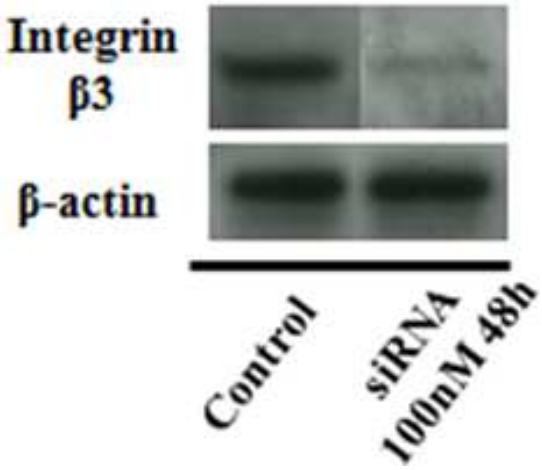


Figure 3.38: Knock-down of integrin αv mediated by siRNA

Immunoblot using anti-integrin αv antibody with purified samples from control and integrin αv siRNA (100nM, 48 h) transfected Ishikawa cells. The ~135kDa band corresponded to the expected size for integrin αv protein (**A**). Relative densitometry values illustrating the intensity of integrin αv bands obtained for control or cells transfected with integrin αv siRNA. Asterisk (***) denotes a statistically significant difference ($P \leq 0.0001$) as determined by the student's t-test. Data are represented as mean ± S.E.M (**B**).

A **Integrin β3 expression at the protein level**



B

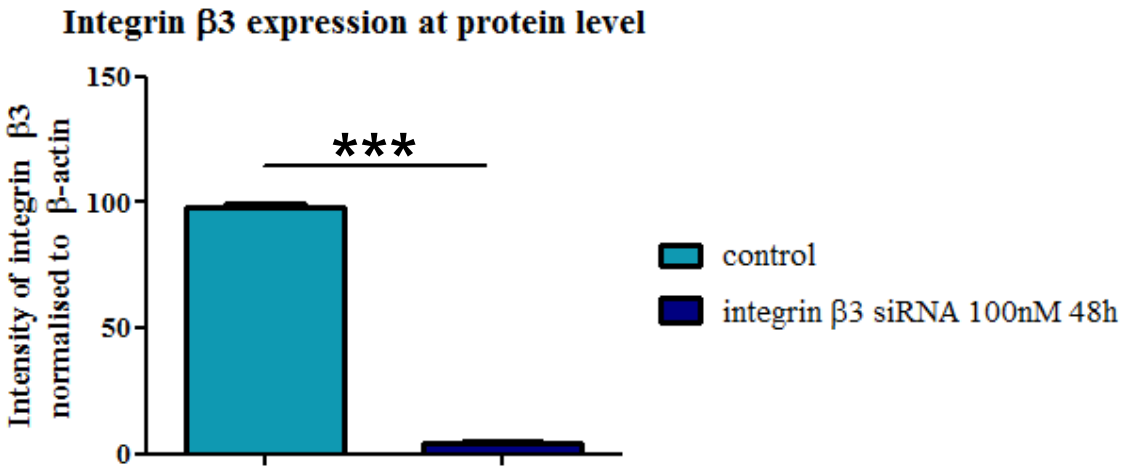


Figure 3.39: Knock-down of integrin β3 mediated by siRNA

Immunoblot using anti-integrin β3 antibody with purified sample from control and integrin β3 siRNA (100nM, 48 h) transfected Ishikawa cells. The ~110kDa band corresponded to the expected size for integrin β3 protein (**A**). Relative densitometry values illustrating the intensity of integrin β3 bands obtained for control cells or cells transfected with integrin β3 siRNA. Asterisk (***) denotes a statistically significant difference ($P \leq 0.0001$) as determined by the student's t-test. Data are represented as mean ± S.E.M (**B**).

The mouse embryo attachment assay was performed following after knock-down. Ishikawa cells were plated onto a microwell plate and upon 80% of confluence, cells were starved overnight and then transfected with integrin subunit αv, β3, αv and β3 and non-target siRNA. Day 5 mouse embryos (three independent sets of embryo attachment assays using 68 mouse embryos) were transferred following three washes with serum-free culture medium after 48 h of transfection and the stability of embryo attachment was measured after 24 h of co-culture. The assessment was performed by scoring the stability of embryo attachment described in Section 3.2.1.4 (Table 3.1). It was observed that embryos on normal Ishikawa cells and Ishikawa cells transfected with non-targeting siRNA were significantly more stably attached than embryos co-cultured with Ishikawa cells transfected with integrin αv (P=0.0236), β3 (P=0.0002) or αv+β3 (P<0.0001) siRNA (Fig 3.40). However, after 48 h of co-culture, all embryos were stably attached.

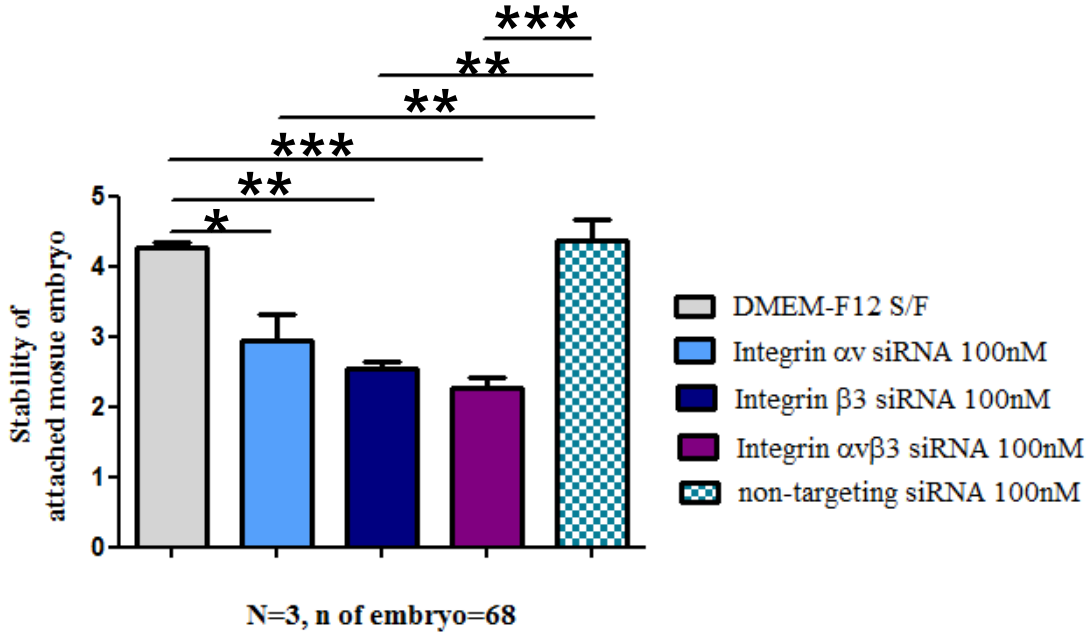


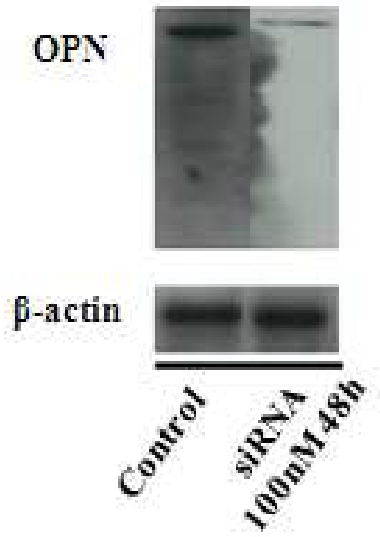
Figure 3.40: Knock-down of integrin αvβ3 reduced embryo attachment

Mean proportions of the stability of three independent sets of embryo attachment assays using 68 mouse embryo after 24 h of co-culture on control, integrin αv, β3, αvβ3 and non-target siRNA (100nM, 48h) transfected cells. Asterisks (*, **, ***) on the histograms denote statistically significant differences (p<0.05). Data are shown as mean ± SEM.

3.2.2.7 OPN knock-down suppresses mouse embryo attachment

In order to allow optimal reduction of OPN expression in Ishikawa cells, various concentrations (25, 50, and 100nM) and transfection times (up to 72 h) of an siRNA pool containing a combination of four different RNA sequences that target OPN mRNA were exposed to Ishikawa cells. Western blotting of cell lysates demonstrated significant knock-down by 72 h after transfection and especially cell lysates from Ishikawa cells transfected with OPN siRNA with 100nM concentration for 48h or 72 h showed approximately 85% of reduction in OPN protein expression compared to OPN of controlled cells (Figure 3.41). However, after 72 h of transfection, alterations were evident in Ishikawa cell morphology. Therefore, the duration of transfection used was 48 h.

A **OPN expression at the protein level**



B

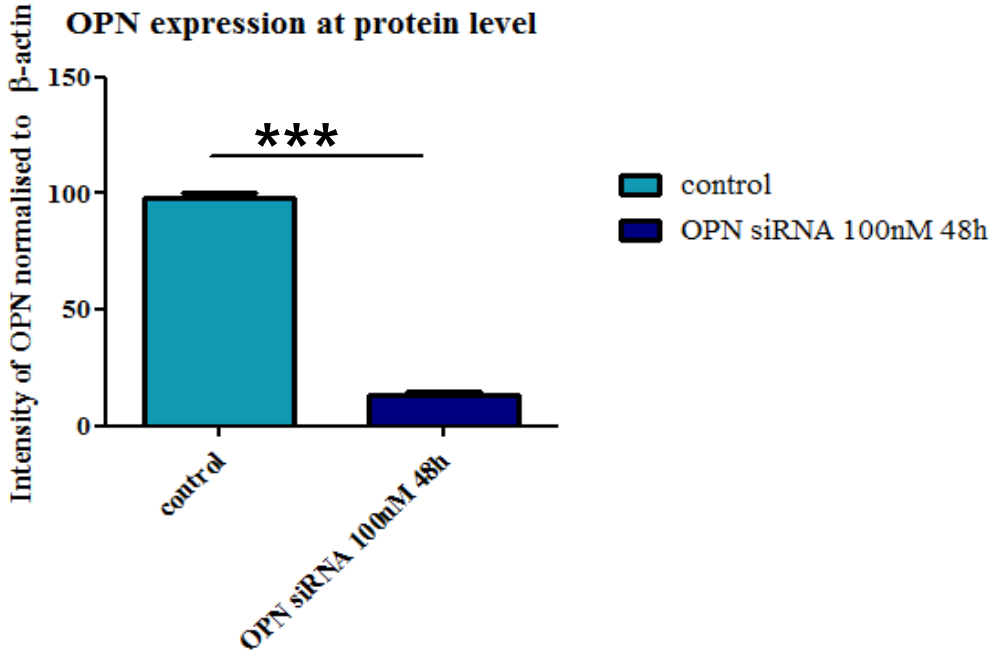


Figure 3.41: Knock-down of OPN mediated by siRNA

Immunoblot using anti-OPN antibody with purified sample from control and OPN siRNA (100nM, 48 h) transfected Ishikawa cells. A band at ~70kDa was detected that had the expected size for the expressed OPN protein (**A**). Relative densitometry values illustrating the intensity of OPN bands obtained for control or cells transfected with OPN siRNA. Asterisk (***) denotes a statistically significant difference ($P \leq 0.0001$) as determined by the student's t-test. Data are represented as mean ± S.E.M (**B**).

Twenty eight day 5 mouse embryos were transferred after 48 h of transfection. The stability of embryo attachment was assessed described in Section 3.2.1.4 (Table 3.1). It was observed that embryos on normal Ishikawa cells (P=0.0003) and Ishikawa cells transfected with non-targeting siRNA (P=0.0007) were significantly more stably attached than embryos co-cultured with Ishikawa cells transfected with OPN siRNA (Figure 3.42). However, after 48 h of co-culture, all mouse embryos were stably attached on all wells.

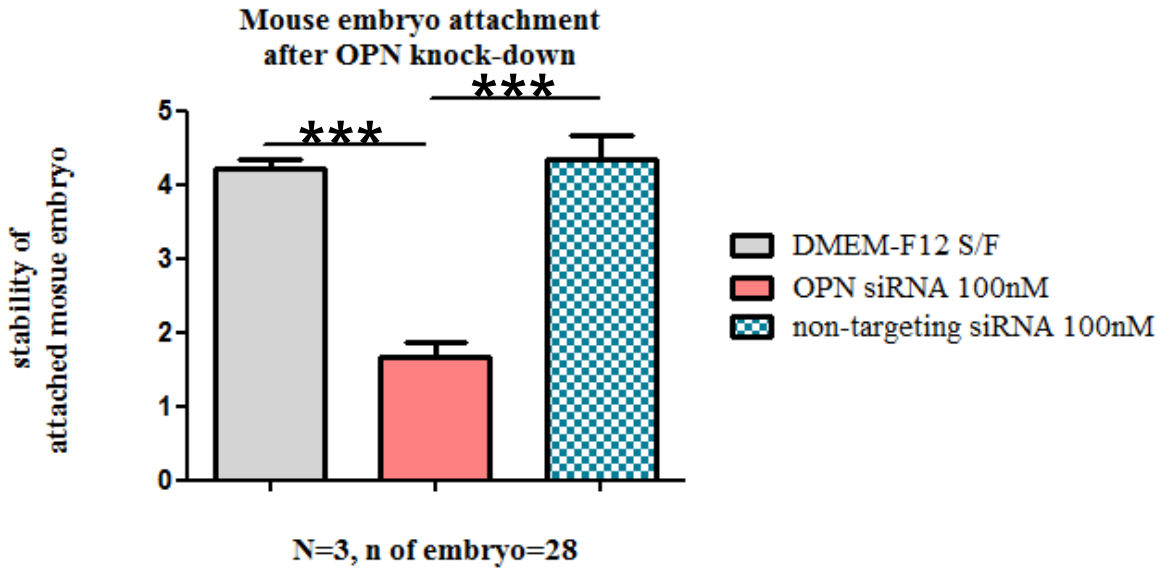


Figure 3.42: Knock-down of OPN reduced embryo attachment

Mean proportions of the stability of three independent sets of embryo attachment assays using 28 mouse embryos after 24 h of co-culture on control, OPN and non-target siRNA (100nM, 48h) transfected cells. Asterisks (***) on the histograms denote statistically significant differences (P<0.0001). Data are shown as mean ± SEM.

3.3 Discussion

3.3.1 General summary of main results

Both mouse and human embryos showed weak, tenuous, but visible attachment at 24 h of co-culture without any disruption or displacement of Ishikawa cells surrounding the attachment site. Forty eight hours after co-culture, mouse embryos were stably attached and retained their original attached location after external stresses, such as fixation or plate tapping, exhibiting displacement and disruption at the apical and lateral side of Ishikawa cells surrounding the attached embryo. Human embryos required 60 h to reach the stable adhesion stage.

As I hypothesised that embryo-derived signals induce local phenotype alteration in endometrial epithelium during embryo attachment, MUC1, integrin αvβ3, αvβ5, OPN, and HB-EGF were examined as candidates that mediate or are involved in such alterations. Data arising from these investigations showed that MUC1 expression was reduced adjacent to both mouse and human embryo attachment sites. The extent of clearance induced by the human embryo was smaller than that of the mouse embryo. Integrin αvβ3 was up-regulated near both mouse and human embryo attachment sites exhibiting predominantly punctuate expression at the lateral side of cells, while integrin αvβ5 showed stable expression at the apical and lateral side of cells with or without an embryo. Furthermore, intracellularly localised OPN was up-regulated and demonstrated vesicular deposition near the attached embryo at the apical surface of Ishikawa cells. Western blot analysis of OPN expression

revealed that 45kDa cleaved OPN was increased in cell lysates including attached mouse embryos compared to control cells without the embryo. Moreover, HB-EGF expression was elevated adjacent to the embryo attachment site.

In order to investigate the roles of integrin αvβ3 or OPN in embryo attachment, mouse embryo attachment assays were performed on Ishikawa cells transfected integrin αv or β3 separately, or in combination, or OPN, respectively. Knock-down of integrin αvβ3 or OPN suppressed embryo attachment exhibiting a significant reduction in the stability of embryo attachment compared to embryo attachment in control cells or cells transfected with non-targeting or mock transfected cells.

3.3.2 Stages of embryo implantation

The initial stages of embryo implantation *in vivo* have been classified as apposition, adhesion, and invasion (Enders and Schlafke, 1969). Apposition and the early attachment of the embryo to the uterine epithelium has not been observed in either humans or other primates, presumably due to the tenuous and transient nature of this fundamental interaction (Hertig et al., 1959; Enders, 2000).

Observations made in the present study, using heterologous and homologous *in vitro* models, revealed that both human and mouse embryos were competent to undergo attachment and reach the stable adhesion stage. Singh et al. (2010) described the initial and tenuous interaction between the embryo and epithelial cells *in vitro* referring as “attachment 1” and the subsequent stable adhesion stage as “attachment 2”. Consistent with this, the 2D and 3D *in vitro* models developed during the present study, allowed

visualisation of the highly unstable initial interaction between the embryo and epithelial cells occurring in the first 24 h of co-culture. Subsequently at 48-60 h, both 2D and 3D models demonstrated the stable adhesion and initial invasion stages.

The original purpose of establishing the 3D *in vitro* model was to study the later stage of adhesion and penetration to the stroma. However penetration beyond the stable adhesion stage was not clearly observed, perhaps because an observation period of longer than 60 h may be required to observe it *in vitro,* or the collagen mixture with stromal cells may be not enough to be receptive.

Adhesion of embryonic trophoblast cells, first to the apical and then to the lateral side of endometrial epithelial cells, along with breaching of the epithelial barrier, have been shown to occur in both the mouse and human (Lopata et al., 2002; Pampfer and Donnay, 1999), but it is not known how this occurs *in vivo*. Pampfer et al. (1999) demonstrated that epithelial apoptosis occurred during mouse implantation. Based on *in vitro* evidence, Galan et al. (2000) suggested that embryo-induced juxtacrine apoptosis occurs in human endometrium after the adhesion stage. Carver et al. (2003) described the nature and extent of human embryo invasion into the stromal cell layer, exhibiting initial weak attachment and subsequent elongation of the embryo showing two leading edges of invasion and penetration. Collectively, these studies provide evidence that may explain the morphological differences of embryo attachment between heterologous and homologous models. In the heterologous model, a wide area of displacement, which created a hole, was observed near mouse embryos, while displacement induced by the human embryo did not create any gap between the embryo and epithelial cells. This suggests that there are key differences in the manner of implantation between the human and mouse. Further work will be required to clarify the relation of apoptotic mechanism with embryo attachment

during implantation and differences in apoptotic/displacement pathway between the human and mouse.

3.3.3 Clearance of MUC1

MUC1 has roles in regulating endometrial receptivity and embryo implantation by acting as an anti-adhesion molecule, however, regulation of mechanisms differ among species. In the human endometrium, progesterone-responsive MUC1 is increased during the mid-secretory phase of the menstrual cycle showing continuous apical expression in the luminal epithelium, but is reduced in the implantation phase in other species during this period (Aplin and Hey, 1995; Hey et al., 1995; Surveyor et al., 1995; Hoffman et al., 1998; Meseguer et al., 1998; Meseguer et al., 2001) .

Consistent with the *in vitro* findings of Meseguer et al. (2001) and Singh et al. (2010), immunofluorescence analysis of 2D cultures in the present study demonstrated local clearance of MUC1 at the site of both mouse and human blastocyst attachment suggesting that removal of MUC1 appears to be accomplished by direct regulation by the embryo rather than maternal hormones. This was supported by Western blot analysis which showed that MUC1 was down-regulated in lysates of cells exposed to mouse embryos in a single well from a 24-well plate compared to controls. However, the surface area of MUC1 clearance observed at human embryo attachment sites was smaller than at mouse embryo attachment sites. This may indicate that human MUC1 regulation is distinct to the regulatory mechanism in mice. In 3D cultures, MUC1 clearance near the mouse embryo was not clearly observed because epithelial cells on each section were limited to a thin

layer. Thus, it is difficult to clarify whether the clearance of MUC1 near the attachment site was induced by the embryo or its original mosaic expression. Since not all embryos transferred onto Ishikawa cells induced MUC1 clearance, even if they were attached stably, as previously described (Singh et al., 2010), it appears that MUC1 clearance is not an essential prerequisite for attachment. This may be due to the intrinsic variation of embryo capacity or delayed clearance following a delayed attachment.

MUC1 appears to be regulated by paracrine signals from the embryo, possibly growth factors including IGFs (Spaventi et al., 1990; Fluhr et al., 2008) and HB-EGF (Paria et al., 2001; Lim and Dey, 2009) to alter local epithelial phenotypes. Pochampalli et al. (2007) reported that MUC1 interacts with ErbB1 (EGFR/HER1), one of the receptors for HB-EGF or EGF, regulating stability of ErbB1 upon EGF, or HB-EGF-stimulated activation and degradation, to control the growth of human mammary epithelial cells via activation of the MAP kinase pathway. This may suggest that MUC1 in the epithelium regulates receptors for embryo-derived HB-EGF or EGF by regulating ligand-mediated ubiquitination and degradation of ErbB1 in order to mediate cell proliferation and migration via activating down-stream components.

Moreover, there is a possibility that several embryo-derived proteases including MMP 14 or TACE (ADAM 17) cleave MUC1 into two fragments and that the extracellular domain of MUC1 re-associates to the endometrial cell membrane mediating anti-adhesion in the apical epithelium (Thathiah and Carson, 2002; Thathiah et al., 2003; Aplin, 2006; Mahanta et al., 2008), or that soluble signals including chemokines (Dominguez et al., 2003) and chorionic gonadogrophin (Cameo et al., 2004) pass locally through between the embryo and maternal receptors on the epithelium at the attachment site (Aplin, 2006). In the present study, immunocytochemical analysis of MUC1 clearance using BC2 antibody

which targets the extracellular domain indicates that cleavage of the extracellular domain by embryo-derived MMP14 or TACE results in the clearance of MUC1 at the embryo attachment site. There is also emerging evidence that the cytoplasmic domain of MUC1 contributes anti-adhesive properties. EGFR or c-Src induced interaction of the cytoplasmic domain from the MUC1 C-terminal subunit with β-catenin results in a reduction of β-catenin binding to E-cadherin and the subsequent suppression of E-cadherin-mediated cell-cell adhesion contributing to regulation of surface expression (Li et al., 2005; Kufe, 2008). This mechanism may loosen cell-cell interaction in the epithelium and allow the embryo to attach and penetrate through the epithelium. Further studies will be required to identify the signalling pathways for local MUC1 loss in the epithelium. It will also be interesting to test how signals diffuse between epithelial cells once these signals are secreted from the embryo to induce MUC1 regulation. Gap junctions containing connexins 26 and 43 are involved in transformation of the endometrum exhibiting reduced expression at implantation in rat *in vivo* (Grummer et al., 2004). This finding may suggest how the embryo-derived signals are transferred and diffused between epithelial cells.

3.3.4 Integrins of the αv family

Integrin αvβ3 is present in the luminal and glandular epithelium during the window of implantation in both the mouse and human (Lessey et al., 1992; Lessey et al., 1994; Merviel et al., 2001; Srinivasan et al., 2009). The results reported in this chapter demonstrated that integrin αvβ3 was expressed weakly but predominantly at the lateral side of control Ishikawa cells and 48 h after co-culture, was up-regulated locally near both mouse and human embryo attachment sites on either the 2D or 3D *in vitro* model.

Predominant expression at the lateral and apical side of cells suggests that integrin αvβ3 on the cell surface interacts with cell surface components on the embryo to mediate attachment. Western blot analysis demonstrated up-regulation of integrin β3 in lysates prepared from a culture with 5 mouse embryos in a single well from a 24-well plate compared to controls. This data set indicates that paracrine signals secreted from the embryo might increase levels of integrin αvβ3 level on endometrial epithelial cells when the embryo attaches to the endometrium, as previously suggested (Simon et al., 1997). Up-regulation of integrin αvβ3 observed in an *in vitro* model of embryo implantation is consistent with previous findings in baboon (Fazleabas et al., 1997; Lobo et al., 2001), mouse (Shiotani et al., 1993; Aplin et al., 1996b; Illera et al., 2000), rat (Srinivasan et al., 2009), rabbit (Harper et al., 1989; Illera et al., 2003), and sheep (Godkin et al., 1984; Kimmins et al., 2004) *in vivo.* Additionally, it has been suggested that up-regulation of epithelial integrin αvβ3 at the site of embryo attachment may be triggered by embryo-derived interleukin-1 (IL-1), which is secreted only when the embryo is co-cultured with endometrial epithelial cells *in vitro*, and subsequently binds and activates endometrial IL-1 receptor type I (De los Santos et al., 1996; Simon et al., 1997). Embryonic IL-1 may act as a paracrine factor to regulate epithelial integrin αvβ3 during implantation.

Furthermore, integrin αvβ3 was expressed in the blastocyst, consistent with previous observations in mouse and rat (Sutherland et al., 1993; Kaneko et al., 2011a). Kaneko, et al. (2011a) demonstrated the re-localisation of integrin β3 to the apical membrane from the cytoplasm of trophoblast cells in response to attachment to the endometrial epithelium *in vitro*, while no effect was observed during adherence onto glass coverslips suggesting that apical re-localisation of integrin β3 in trophoblast cells may be induced by crosstalk between the embryo and the luminal epithelium and that integrin β3

may be important in the initial embryo-endometrial interaction during implantation.

Although the current study does not address the parameters of maternal effect on embryo implantation, a number of earlier studies have reported that epithelial integrin αvβ3 is strongly related to the window of implantation and its absence in the endometrium is observed in infertility including luteal phase defects (Lessey et al., 1992; Castelbaum et al., 1994), endometriosis (Lessey et al., 1994; Lessey, 2002b; Wei et al., 2009; Casals et al., 2012b), and unexplained infertility (Lessey et al., 1995). Moreover, in immature ovariectomised rats, integrin αvβ3 was up-regulated by the exogenous application of progesterone or a combination of estrogen and progesterone (Srinivasan et al., 2009), indicating that epithelial integrin αvβ3 expression is under the influence of maternal hormones, especially progesterone. Collectively, these data suggest that maternal cycle-dependent integrin αvβ3 expression in the epithelium may be a prerequisite for endometrial receptivity and that embryo-derived signals might be essential factors for the mediation of local cell-cell interaction between the embryo and epithelium.

Knock-down of integrin αvβ3 in epithelial cells reduced embryo attachment at 24 h of co-culture *in vitro,* however, embryos were all stably attached by 48 h. This may suggest that both integrin αv and β3 subunits may be involved in the mechanism of initial embryo attachment phase and that deficiency of these subunits in the epithelium may induce delay of embryo attachment but may be compensated by other integrins which share ECM ligands with integrin αvβ3, such as integrin αvβ1, αvβ5, and α5β1, for the embryo to reach stable adhesion stages. The gaps appeared between Ishikawa cells with longer than 48 h of integrin αv or β3 siRNA transfection may be resulted by inhibition of lateral intercellular adhesion between cells or basal adhesion to the substrate. Upon binding to the ECM ligands including vitronectin, fibronectin, fibrinogen, collagen and osteopontin

(Hynes, 1992; Butler et al., 2003; Garcia et al., 2004; Maile et al., 2008), integrin αvβ3 is activated and mediates cell-cell interaction via intracellular signalling transduction. The significant reduction in the initial phase of embryo attachment observed following knock-down of integrin subunits αv and β3 in Ishikawa cells in the current study may have arisen from the inhibition of αvβ3 with an extracellular ligand. This finding can be supported by an earlier *in vivo* study by Illera et al. (2000) in which the functional blockage of integrin αvβ3 by the intrauterine injection of neutralising antibodies or disintegrin echistatin was shown to reduce the number of implantation sites in mouse uterus. The same research group demonstrated a reduction in the number of implantation sites following intrauterine injection of GRGDSP in the rabbit, while no effect was seen with GRGESP (Illera et al., 2003). However, mice with the deficiency of the integrin subunit αv or β3 are fertile but undergo fetal mortality despite successful implantation (Graham et al., 1990; Bader et al., 1998). Embryo-derived factors and their influence on integrin αvβ3 signalling are explored further in Chapter 4.

Compared to the alteration of integrin αvβ3 distribution upon the presence of embryo attachment, integrin αvβ5 showed an even distribution of immunostaining in Ishikawa cells near to and far from sites of both mouse and human embryo attachment *in vitro,* suggesting that this may be independent of the presence of an embryo. This has been reported in previous studies in which the integrin β5 subunit expresses at the apical surface of both glandular and luminal epithelium throughout the menstrual cycle in the human, and also at both apical and basal luminal epithelial cells in the mouse showing cycle-independency. However, integrin β5 null mice are also fertile but result in perinatal lethality due to major development defects (Hynes, 1996; Reynolds et al., 2002).

3.3.5 OPN in embryo attachment

OPN, a primary ligand of integrin αvβ3 appears during the early secretory phase of the menstrual cycle, shows co-expression with integrin αvβ3 in human endometrium (Apparao et al., 2001), and exhibits dramatic elevation at the time of initial embryo attachment in pig (White et al., 2005), sheep (Johnson et al., 2003b), rabbit (Apparao et al., 2003), and mouse (Weintraub et al., 2004; White et al., 2006) uteri, thereby supporting an important role in embryo implantation. In the present study, the 2D model revealed that OPN was predominantly cytoplasmic in control conditions but in the presence of embryos was up-regulated near to attachment sites displaying movement towards the surface of cells. Up-regulation of OPN expression was also observed by Western blotting using lysates from Ishikawa cells co-cultured with mouse embryos. Interestingly, Western blot analysis revealed that three predominant cleaved fragments that were 70, 45, and 25kDa in molecular weight were present in both control cells and cells exposed to embryos. In particular, increased levels of the 45kDa OPN fragment was detected after co-culture with embryos. It has been previously reported that the proteolytically cleaved 45kDa form of OPN is highly expressed at the apical surface of trophectoderm and along the placental interface throughout pregnancy in the ovine uterus, and is more active in terms of cell-cell adhesion and migration than parent 70kDa OPN (Johnson et al., 2003b). This may indicate that embryo-derived signals, possibly growth factors, stimulate OPN and promote production of the 45kDa fragment including its transport to the cell surface. Knock-down of the OPN reduced the stability of attachment compared to control cells. This finding suggests that OPN at the surface of Ishikawa cells is involved in regulating embryo attachment.

Although co-localisation of OPN with its receptor integrin αvβ3 has not been performed in this Chapter, the local up-regulation of both molecules appears to be detected in the area surrounding the embryo attachment site. Johnson et al. (2001) demonstrated that OPN-coated polystyrene beads induced the activation of integrin αvβ3 at focal adhesion sites, suggesting that binding of OPN to integrin αvβ3 promotes attachment of trophoblast cells onto the epithelium. There is emerging evidence that interaction between integrin αvβ3 and OPN regulates embryo implantation. Firstly, both integrin αvβ3 and OPN showed an increase of expression during the mid to late secretory phases in the endometrial epithelium indicating that both molecules may have roles in regulating endometrial receptivity (Apparao et al., 2001; von Wolff et al., 2001; Casals et al., 2012a; Casals et al., 2010). Secondly, studies in other systems have shown that integrin αvβ3 expressing smooth muscle cells adhered to an OPN substrate and that VEGF-induced integrin αvβ3 expression resulted in increased migration of endothelial cells towards OPN (Senger et al., 1996; Senger and Perruzzi, 1996; Standal et al., 2004). Finally, it has been reported that patients with unexplained infertility showed aberrant expression of integrin αvβ3 and OPN (Lessey et al., 1994; Lessey et al., 1995; Quenby et al., 2007; DuQuesnay et al., 2009)

In order to investigate a role for OPN as a bridging molecule of embryo-endometrial interaction, previous studies based on *in vivo* evidence in pigs, demonstrated that OPN was localised at the interface between the embryo and endometrial epithelium during implantation (Garlow et al., 2002; White et al., 2005). In pigs, the conceptus is in contact with the uterine luminal epithelium and OPN is seen in both the embryo and epithelium before and at stable adhesion occurs (Geisert and Yelich, 1997). OPN has been shown to bind to the luminal epithelium via integrin αvβ3 and to the trophectoderm via integrin αvβ6 indicating that integrin-OPN-integrin complex may mediate stable adhesion

of embryos to the epithelium (Erikson et al., 2009).

Despite the significant role of OPN in embryo implantation, it should be noted that mice with deficiency of the OPN gene are fertile (Liaw et al., 1998), suggesting the involvement of other factors which could compensate for the loss of OPN to ensure a higher likelihood of successful implantation. More details concerning the mechanism of integrin αvβ3-OPN interaction are explored further in Chapter 4.

3.3.6 HB-EGF in embryo attachment

In vivo, HB-EGF appears 6-7 h before embryo attachment in the mouse and induces signs of implantation including increased endometrial vascular permeability at the apposition site of the embryo, which is considered as the earliest and prerequisite sign of successful implantation (Das et al., 1994; Lim and Dey, 2009). Overlapping of this event with the timing and location of HB-EGF appearance may indicate its involvement in a molecular cascade that establishes an appropriate environment for embryo implantation (Psychoyos, 1973; Das et al., 1994).

In the present study, local up-regulation of HB-EGF was observed in epithelial cells near to the site of embryo attachment *in vitro* and additionally, HB-EGF was also expressed in the attached mouse embryo, as described for previously by *in vivo* in the mouse and rat (Das et al., 1994; Isaacs and Murphy, 2002). Comparing HB-EGF distribution with the nuclear expression of Ishikawa cells on 2D *in vitro* cultures, local up-regulation of HB-EGF has not been affected by the initial cell seeding density but signals secreted from the embryo during its attachment may cause HB-EGF up-regulation in the

epithelium.

In pseudopregnant mouse uteri with similar hormonal composition to normal pregnant mice, the initial expression of HB-EGF is not observed. However, beads carrying HB-EGF placed in the uterus of pseudopregnant mice induced local decidual responses that mimic those induced by the blastocyst, such as increased vascular permeability, decidualisation, and the appearance of implantation maker genes (Paria et al., 2001). These lines of evidence may raise the possibility that initial HB-EGF in the uterus may not be maternal hormone-dependent but is rather induced by paracrine signals from the embryo (Lim and Dey, 2009). Embryo-derived HB-EGF serves as an auto-inductive stimulus for local uterine HB-EGF during implantation (Barnard et al., 1994; Le et al., 2002).

HB-EGF expression at the time of embryo attachment on the epithelium and the expression of its corresponding receptor, ErbB4, on the surface of the trophectoderm of blastocyst provide more sound evidence that the direct binding of HB-EGF to ErbB4 may assist with the attachment of blastocyst to the uterine epithelium. Soluble HB-EGF stimulates mouse trophoblast differentiation to an adhesive phenotype via Ca^{2+} influx *in vitro* by accelerating the trafficking of integrin α5β1 to the surface of trophectoderm and promotes the translocation of ErbB4 to the apical surface of trophoblast cells (Wang et al., 2000; Chobotova et al., 2002; Armant, 2005). Furthermore, the localisation of HB-EGF on the apical surface of embryo and luminal epithelial expression of ErbB receptors suggest that HB-EGF-ErbBs serves as a two-way signalling system between the embryo and endometrium in order to mediate initial attachment (Hamatani et al., 2004b).

HB-EGF improves implantation in mice by accelerating the expression of embryonic integrin αvβ3 (Lim et al., 2006). The expression of HB-EGF has demonstrated

slightly prior to the expression of other potential markers for uterine receptivity, including integrin αvβ3, leukemia inhibitory factor (LIF) and homeobox gene (HOXA-10) (Lessey et al., 2002). This has been further affirmed by *in vitro* studies demonstrating that the expression of integrin β3, LIF and HOXA-10 was stimulated by HB-EGF. This work suggested that endometrial receptivity may be regulated by an HB-EGF-mediated paracrine mechanism (Lessey et al., 2002). However, the precise role that HB-EGF is involved with the cascade to establish successful implantation has yet to be reported. The role of HB-EGF as either a paracrine factor secreted from the apposing embryo, or as a juxtacrine factor from the epithelium, in regulating embryo attachment by interacting with other components will be explored further in Chapter 4.

3.3.7 Concluding remarks

Collectively, the data reported in this Chapter suggest that the embryo initiates crosstalk to the endometrial epithelium and reaches a stage of stable adhesion by 48 h. Embryo attachment induces alteration in the levels of MUC1, integrin αvβ3, OPN and HB-EGF distribution in the endometrial epithelium. The alteration of distribution of these molecules at the site of embryo attachment is similar to others in *in vitro* models. Links between these molecules are explored further in the next Chapter.



CHAPTER 4

Cell signalling at implantation

4.1 Introduction

Remarkable progress has been achieved in understanding the process underlying the complex process of embryo implantation. Studies using genomic and proteomic techniques which allow scientists to analyse the simultaneous expression of numerous endometrial genes throughout the menstrual cycle have reported genes that are strongly up- or down-regulated when the endometrium is receptive, indicating that controlled ovarian stimulation has a significant effect upon endometrial receptivity (Horcajadas et al., 2005; Simon et al., 2005; Burney et al., 2007; Van Vaerenbergh et al., 2010). As well as studying the molecular changes occurring in the endometrium, there is emerging evidence to emphasise the importance of molecular studies on the embryo to become implantation competent and mediate implantation (Dobson et al., 2004; Katz-Jaffe et al., 2006). Based on these investigations of important changes in gene transcription, intracellular signal transduction, growth factor and cytokine networks, signalling mechanisms mediating cell-cell and cell-extracellular matrix interactions that occur in maternal-fetal interface are beginning to be formulated.

At implantation, cell-cell and cell-matrix interactions directly modulate signal transduction to mediate embryo-endometrial interaction. In particular, up-regulation of both integrin αvβ3 and OPN close to the embryo attachment site, as demonstrated in Chapter 3, can alter the adhesion status of cells and affect cell signalling by associating with the cytoskeletal network (Gilcrease, 2007; Gahmberg et al., 2009; Barczyk et al., 2010).

I hypothesised that IGF-I and/or HB-EGF secreted from peri-implanting embryo (Spaventi et al., 1990; Paria et al., 2001) may increase levels of integrin αvβ3, and its ligand OPN locally in the epithelial layer and regulate down-stream factors mediating embryo implantation. Although the exact roles of IGF-I and HB-EGF in human embryo implantation have not been reported yet, there is emerging evidence that both growth factors secreted from the attaching embryo are involved in the mechanisms of regulating integrin αvβ3 in other systems. IGF-I has been reported to induce the activation of integrin αvβ3 upon binding to its ligand via autophosphorylation on the IGF-I receptor in order to transduce the signal to down-stream components in blood vessel cells (Maile and Clemmons, 2002), while HB-EGF has been shown to play a role in accelerating the expression of integrin αvβ3 in embryos (Lim and Dey, 2009).

In order to investigate the role of the IGF-I or HB-EGF axis in regulating integrin αvβ3 and OPN interaction to mediate embryo attachment, integrin αvβ3, OPN, and factors relating to IGF-I or HB-EGF were tested. To extend the 2-dimensional *in vitro* model of embryo implantation developed in Chapter 3, and to dissect various mechanisms from the whole system down to a single molecular interaction between the embryo and the endometrial epithelium, a new assay was developed herein using embryo-sized beads with high capacity for protein binding. Epithelial responses to beads loaded with IGF-I, HB-EGF, or OPN were subsequently tested.

4.2 Results

4.2.1 IGF-I and HB-EGF regulate the expression of integrin β3 and OPN in Ishikawa cells

In order to test the response to IGF-I or HB-EGF in soluble form, Ishikawa cells were treated for 0-48 h (0, 2, 4, 8, 24, and 48 h). Western blotting of lysates prepared from treated cells demonstrated that the expression of the integrin β3 subunit was increased in both cases. Cleaved OPN fragments, predominantly 45kDa in size, appeared as cells were treated for longer time periods with IGF-I while full-length OPN (70kDa) predominated in HB-EGF treated cells (Figure 4.1).

For immunofluorescence analysis Ishikawa cells were treated with IGF-I or HB-EGF for 8 h. Duration of treatment was determined based on Western blotting analysis by which marked cleavage of OPN was initially observed at 8 h of IGF-I treatment. Analysis of integrin αvβ3 demonstrated that in control conditions (without any growth factors) integrin αvβ3 was weakly expressed on the lateral side of cells and that most OPN was cytoplasmic. Following exposure of cells to either IGF-I or HB-EGF (8 h), notably increased integrin αvβ3 staining was observed compared to untreated cells; staining was predominantly punctate on the lateral side of the cell membrane (Figure 4.2). After 8 h exposure to IGF-I, OPN expression was increased, exhibiting more staining on the apical cell surface compared to control cells, while there was no significant change in OPN staining between control and HB-EGF treated cells (Figure 4.3).

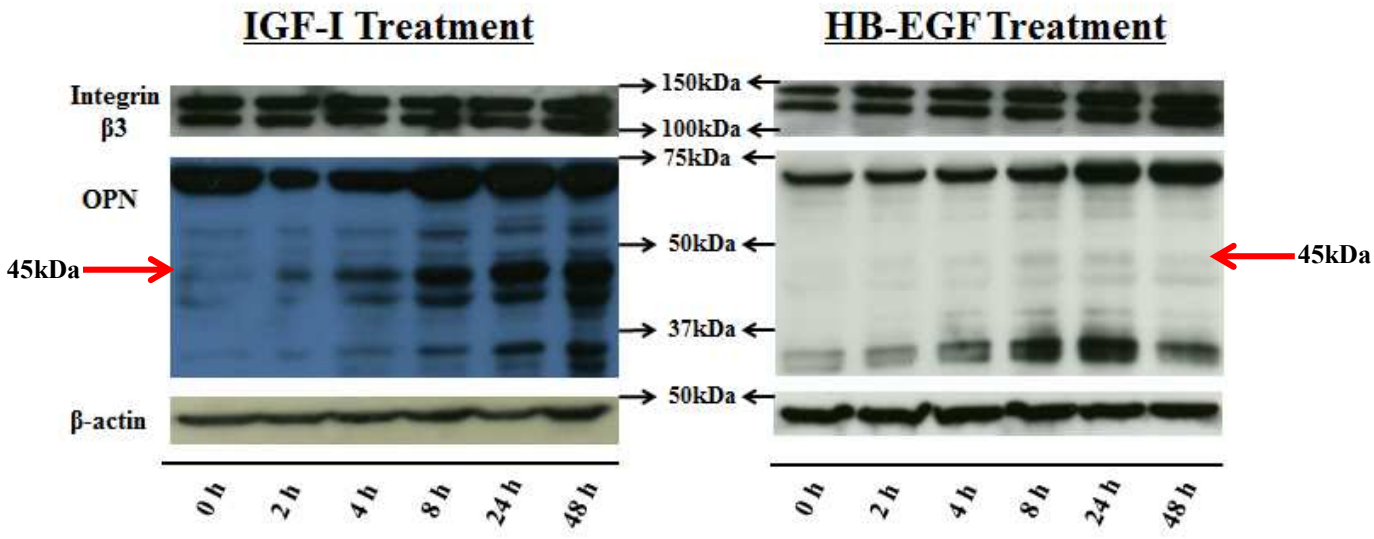


Figure 4.1: The effect of IGF-I or HB-EGF treatment upon integrin β3 subunit and OPN expression

Representative immunoblots of 3 experiments using an anti-integrin β3 subunit polyclonal antibody and an anti-OPN monoclonal antibody with purified lysates prepared from Ishikawa cells at each time point after 0-48 h of IGF-I or HB-EGF soluble treatment (50ng/ml). Bands corresponding to ~110/130kDa and 20~70kDa were successfully detected, which were the expected size for the expressed integrin β3 or OPN protein, respectively. A β-actin antibody was used to demonstrate equal loading.

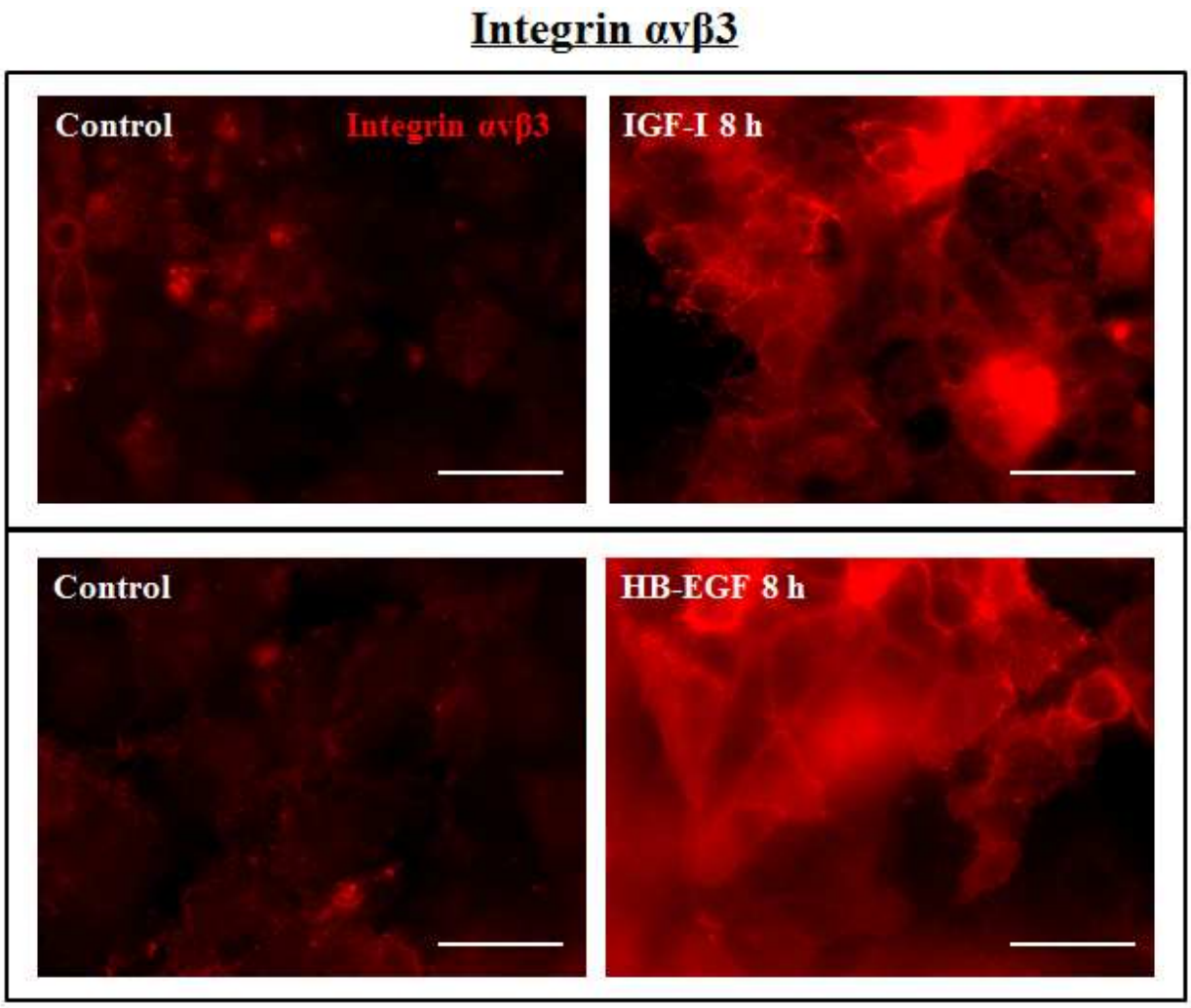


Figure 4.2: Localisation of integrin αvβ3 in IGF-I or HB-EGF treated Ishikawa cells

Representative immunofluorescence microscopy images taken across 0 h and 8 h time points for Ishikawa cells treated with IGF-I or HB-EGF (50ng/ml). Cells were immunostained for integrin αvβ3 without permeabilisation. Images were captured at a magnification of 40X with oil. Red: integrin αvβ3, Scale bar = 50 µm

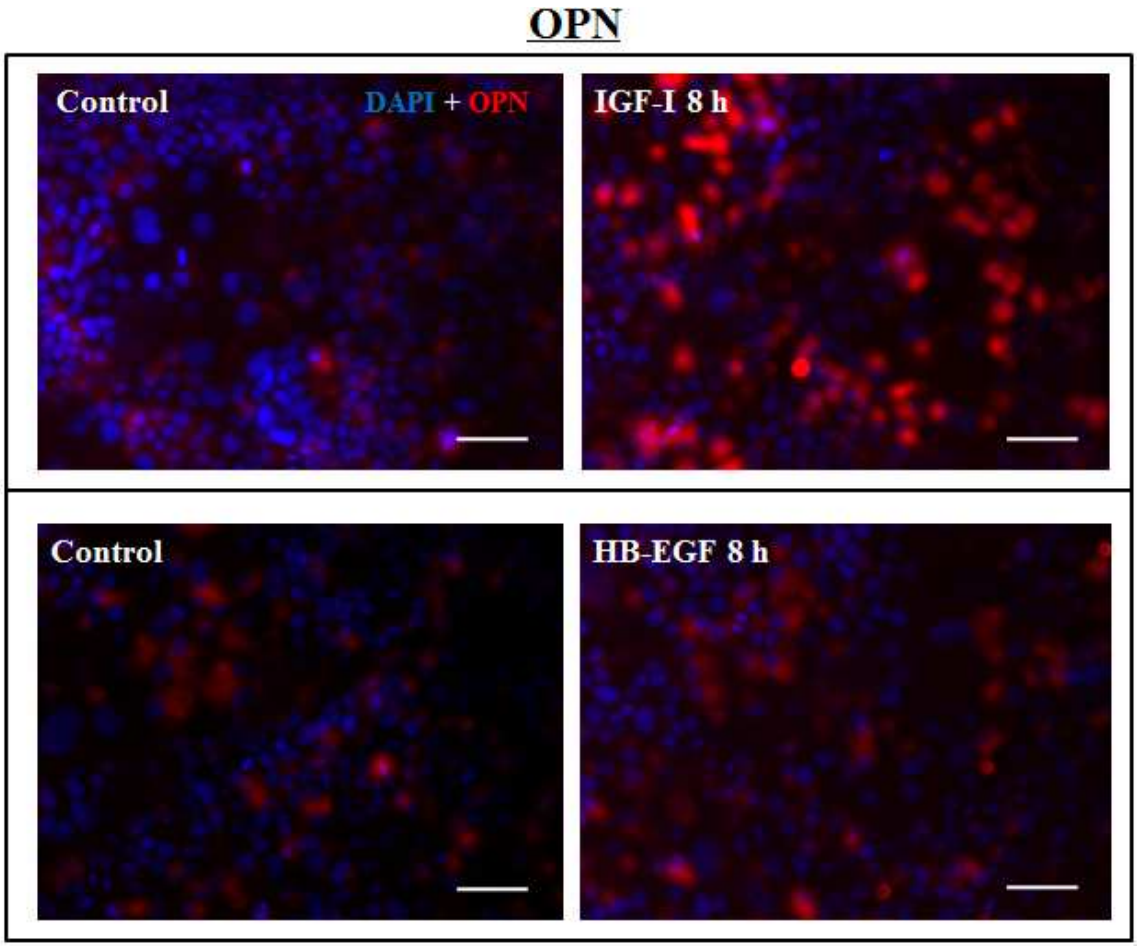


Figure 4.3: Localisation of OPN in IGF-I or HB-EGF treated Ishikawa cells

Representative immunofluorescence microscopy images taken across 0 h and 8 h time points for Ishikawa cells treated with IGF-I or HB-EGF (50ng/ml). Cells were immunostained for OPN without permeabilisation. The diagonal black stripe was caused from a cracked element in the fluorescence light path on nuclear staining. Images were captured at a magnification of 20X. Blue: Nucleus (DAPI), Red: OPN, Scale bar = 50 µm

4.2.2 Cleaved OPN is localised on the apical surface of Ishikawa cells

In order to confirm the localisation and distributional change of OPN in response to IGF-I or HB-EGF, the surface proteins of intact Ishikawa cells were selectively biotinylated after 8 h of IGF-I or HB-EGF treatment. Cell lysates were then immunoprecipitated with neutroavidin and probed for OPN using the protocol described in Section 2.11. Western blotting demonstrated cleaved forms of OPN (70/45/25kDa) in lysates from IGF-I treated cells, while lysates from HB-EGF treated and control cells expressed predominantly 70kDa OPN, with very weak expression of both 45 and 25kDa fragments (Figure 4.4).

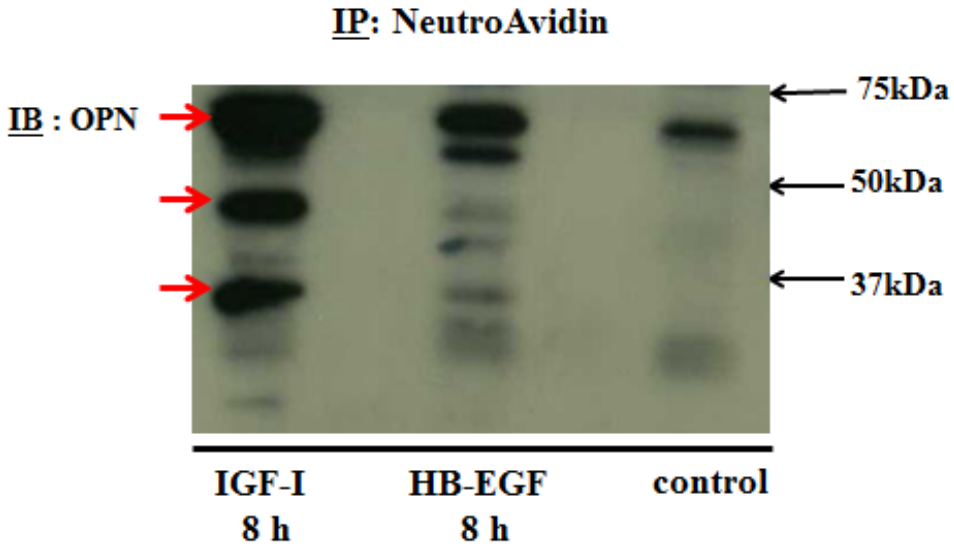


Figure 4.4: OPN on the surface of Ishikawa cells in response to IGF-I or HB-EGF

Representative immunoblots using an anti-OPN monoclonal antibody with purified samples from immunoprecipitation with neutroavidin after biotinylation. Bands corresponding to 20~70kDa were successfully detected, which were the expected size for the expressed OPN protein.

To examine the mechanism by which OPN cleavage is induced, Ishikawa cells were exposed to an inhibitor for serine protease, broad matrix metalloproteinase, serine and cysteine protease, or caspase, prior to IGF-I (50ng/ml) soluble treatment. Cells maintained in serum-free culture medium, or soluble HB-EGF (50ng/ml), acted as negative controls.

Prior to the exposure to IGF-I, cells were treated with protease inhibitor AEBSF (10μM), broad MMP inhibitor NNGH (50μM), serine and cystien inhibitor Leupeptin (50μM), or caspase inhibitor ZVAD-fmk (50μM) for 30 min respectively. After 8 h of IGF-I treatment including individual enzyme inhibitors, cell lysates were extracted and separated by SDS-PAGE.

Western blotting showed that lysates extracted from all pre-treated cells showed cleavage of OPN, similar to the pattern of cleavage observed with IGF-I alone (Figure 4.5). Interestingly, cells pretreated with ZVAD-fmk (shown as ★ in Figure 4.5) demonstrated a distinct pattern of cleavage, exhibiting markedly higher expression of 45kDa OPN and another cleaved fragment which was approximately 15kDa.

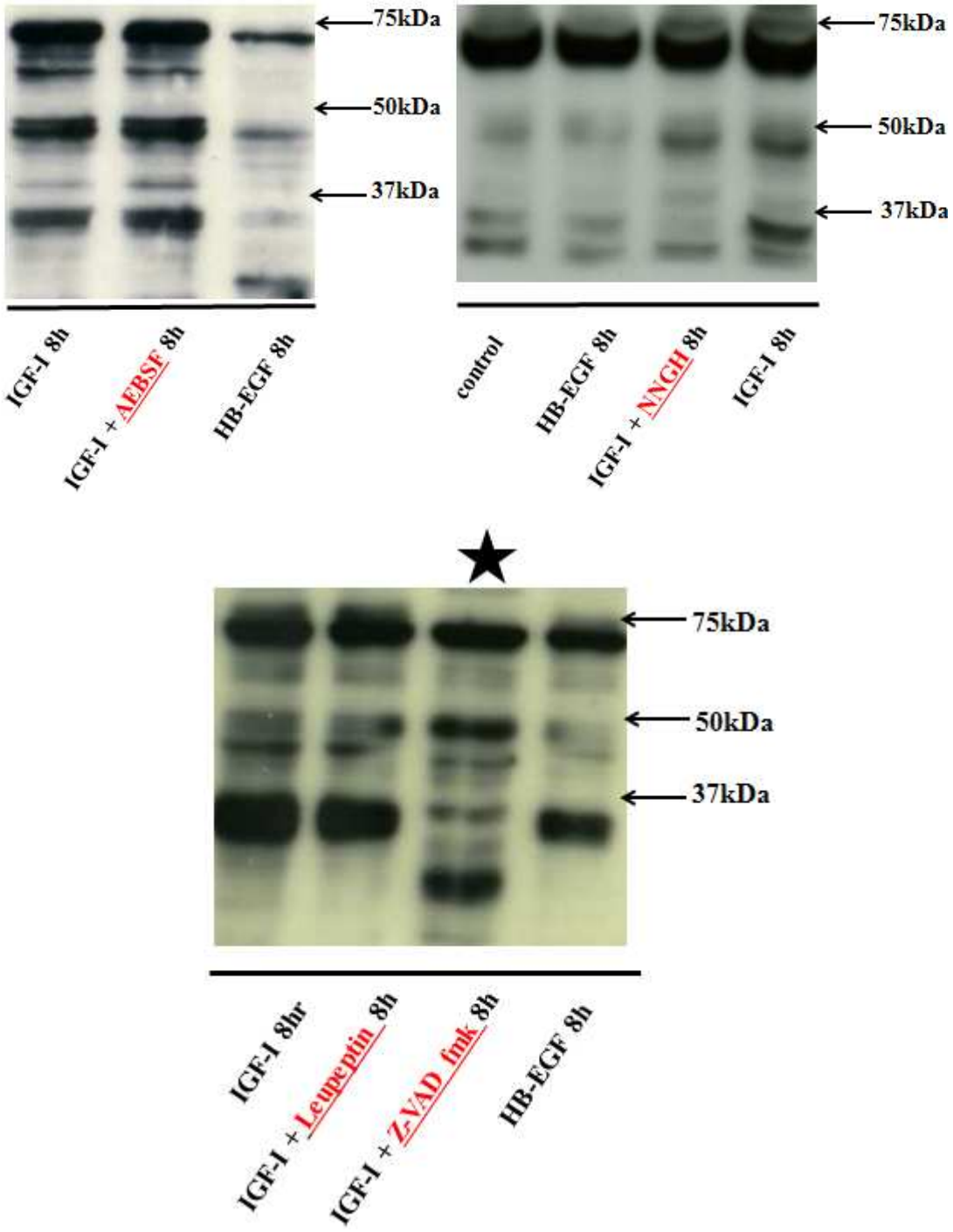


Figure 4.5: Cleavage of OPN in response to AEBSF, NNGH, Leupeptin, and ZVAD-fmk treatment prior to IGF-I

Representative immunoblots of 3 experiments using an anti-OPN monoclonal antibody with purified lysates from Ishikawa cells pre-treated with AEBSF (10μM), NNGH (50μM), Leupeptin (50μM), or ZVAD-fmk (50μM) for 30 min prior to 8 h of exposure to IGF-I. Bands corresponding to 20~70kDa were successfully detected, which were the expected size for the expressed OPN protein.

4.2.3 OPN promotes cell adhesion

To study the role of OPN in regulating cell adhesion Ishikawa cells were plated onto an OPN-coated microwell plate. As a negative control the same number of cells was plated on BSA-coated wells, and serum-coated wells were used for a positive control. After 24 h of culture, morphological changes of cells on each substrate were compared. Cells on the OPN-coated plate became flattened and were solidly attached. A few small colonies were observed. Cells on serum-coated wells were all flattened and seen in a compact colony. However, cells plated on BSA-coated wells remained as single cells and many detached during washing (Figure 4.6.A).

In addition, 9 day 5 hatched mouse embryos were cultured on OPN, serum, or BSA-coated microwells. Thirty hours after culture, embryos on OPN-coated wells were solidly attached and flattened with early signs of cell outgrowth. Embryos on serum-coated wells showed a more flattened shape and more outgrowth, while embryos on BSA-coated wells remained attached but there was no change in shape (Figure 4.6.B). Three different sets of experiments were shown similar morphological changes.

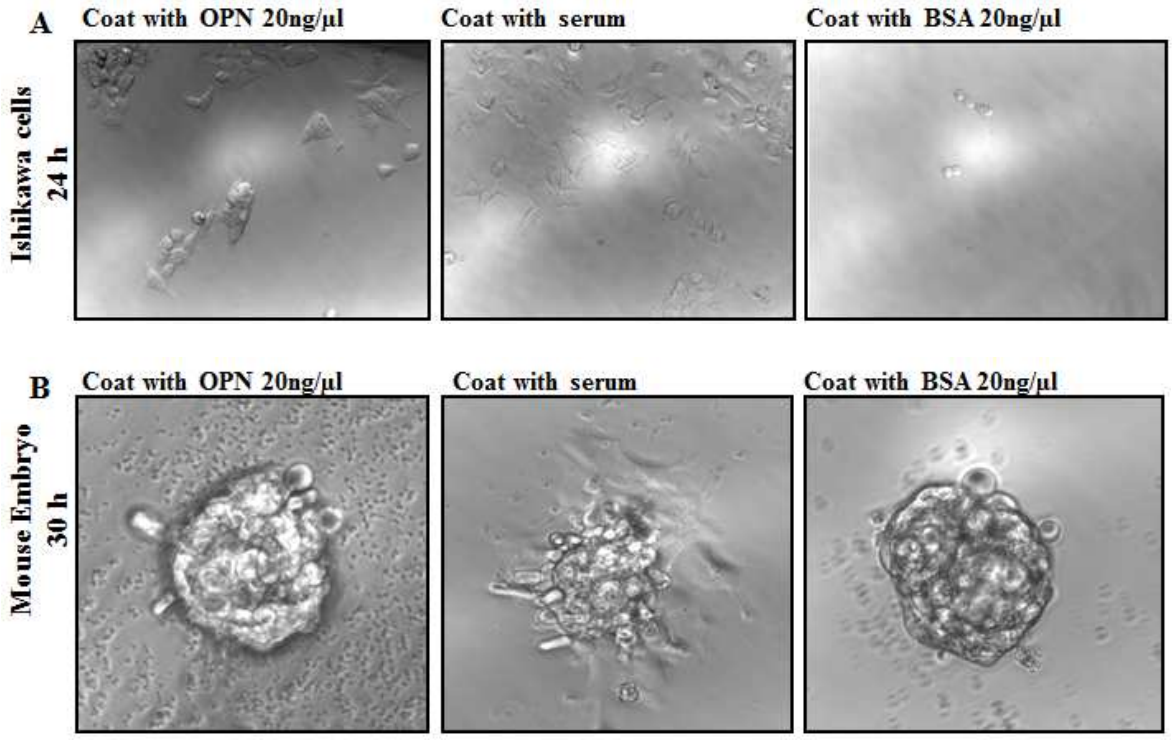


Figure 4.6: OPN promoted the adhesion of Ishikawa cells and mouse embryos

Representative phase contrast microscopic images of 3 experiments of Ishikawa cells (**A**) and day 5 hatched mouse embryos (**B**) plated on OPN (20ng/µl) -coated microwells. Cells or embryos plated on BSA (20ng/µl) -coated wells were used for negative controls and cells on serum-coated microwells were used as positive controls. The diagonal stripe on images (**A**) was caused from a cracked element in the fluorescence light path. Images were captured at 20X magnification and enlarged digitally.

Thrombin is suggested to cleave OPN to produce an active 45kDa fragment. Here, comparison was made between the morphology of cells plated on OPN-coated wells with or without thrombin exposure. After 24 h, more cells were attached on OPN-coated wells with thrombin compared to native OPN (Figure 4.7).

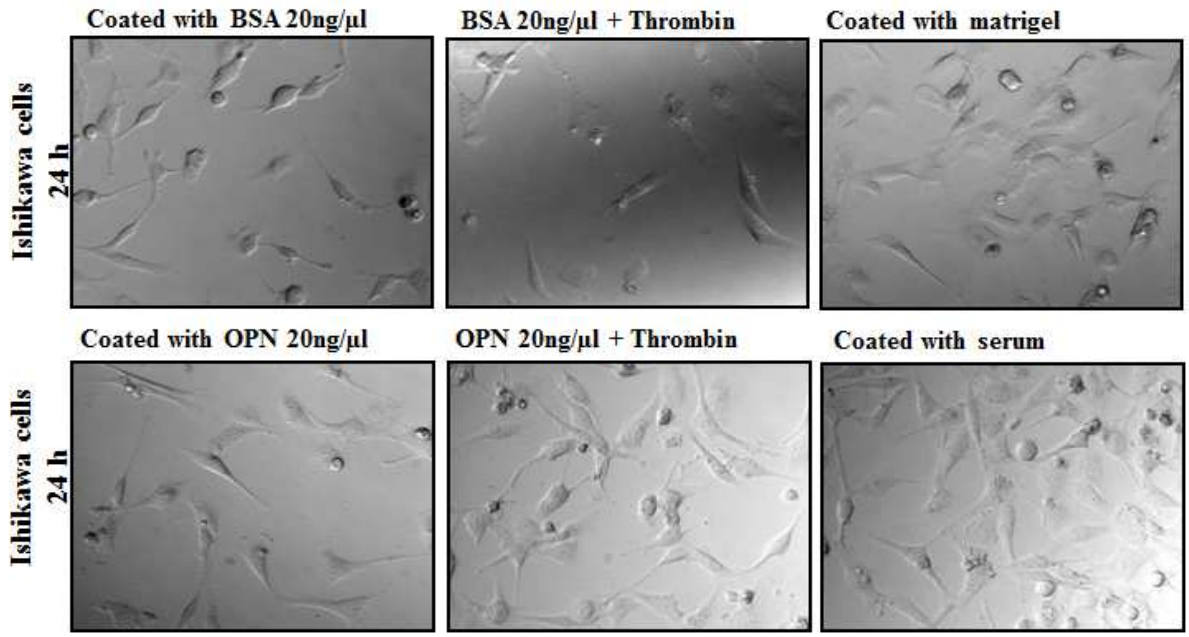


Figure 4.7: Thrombin enhanced OPN-mediated cell adhesion

Representative phase contrast microscopic images of 3 experiments of Ishikawa cells plated on OPN (20ng/µl) or OPN (20ng/µl) + thrombin (10NIH units/µg) -coated microwells. Cells plated on BSA (20ng/µl) or BSA (20ng/µl) + thrombin (10NIH units/µg) -coated wells were used for negative controls and cells on serum or matrigel (1 in 16 dilution) -coated microwells were used as positive controls. Images were captured at 20X magnification and enlarged digitally.

4.2.4 Factors down-stream of IGF-I and HB-EGF

Ishikawa cells were treated with IGF-I or HB-EGF (50ng/ml) for 0-48 h and cell lysates were extracted at each time point (0, 2, 4, 8, 24, and 48 h). Western blotting demonstrated the level of IGF-IR phosphorylation was dramatically elevated in response to IGF-I (Figure 4.8.A). Forty eight hours after HB-EGF treatment, the level of ErbB4 phosphorylation showed 1.5 x elevations (Figure 4.8.B). SHP-2 was weakly expressed by control cells, and was increased (2.5 x) by IGF-I, while there was no significant change in SHP-2 in response to HB-EGF (Figure 4.8.C).

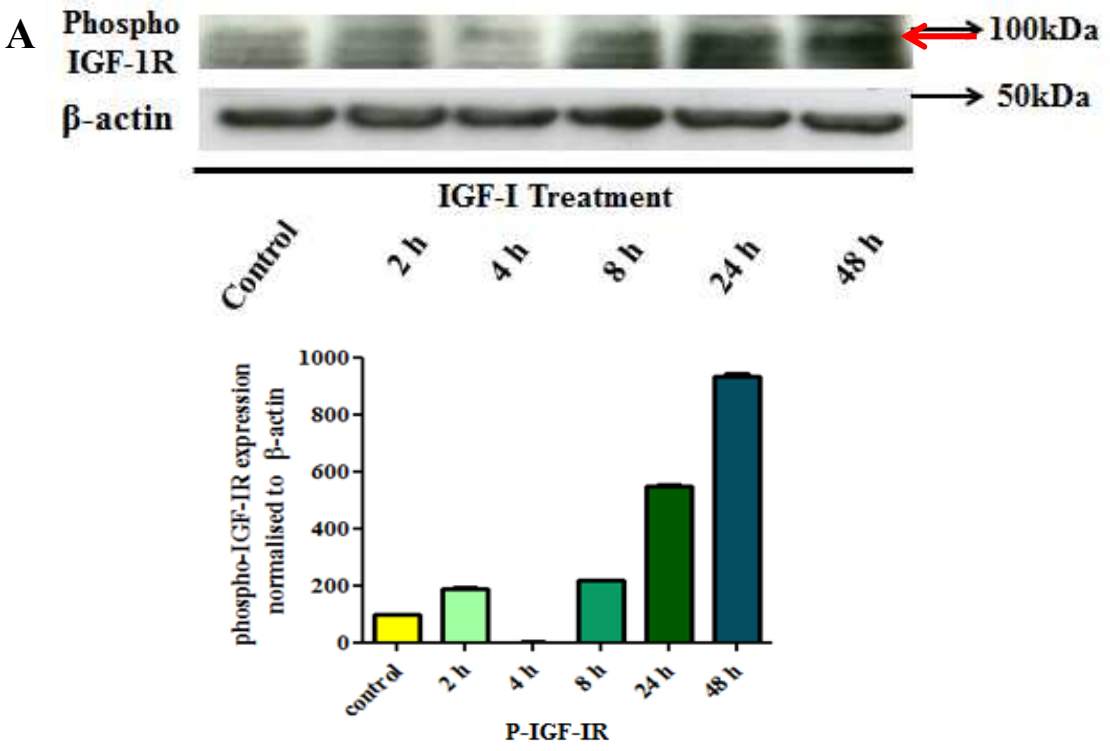


Figure 4.8: Phospho-IGF-IR expression in Ishikawa cells in response to IGF-I (Continued on page 165)

Representative immunoblots of 3 experiments using an anti-phospho IGF-IR (**A**) polyclonal antibody with purified lysates from Ishikawa cells at each time point after 0-48 h of IGF-I soluble treatment (50ng/ml). Bands corresponding to ~97kDa were successfully detected, which were the expected size for the expressed phospho-IGF-IR protein. A β-actin antibody was used to demonstrate equal loading.

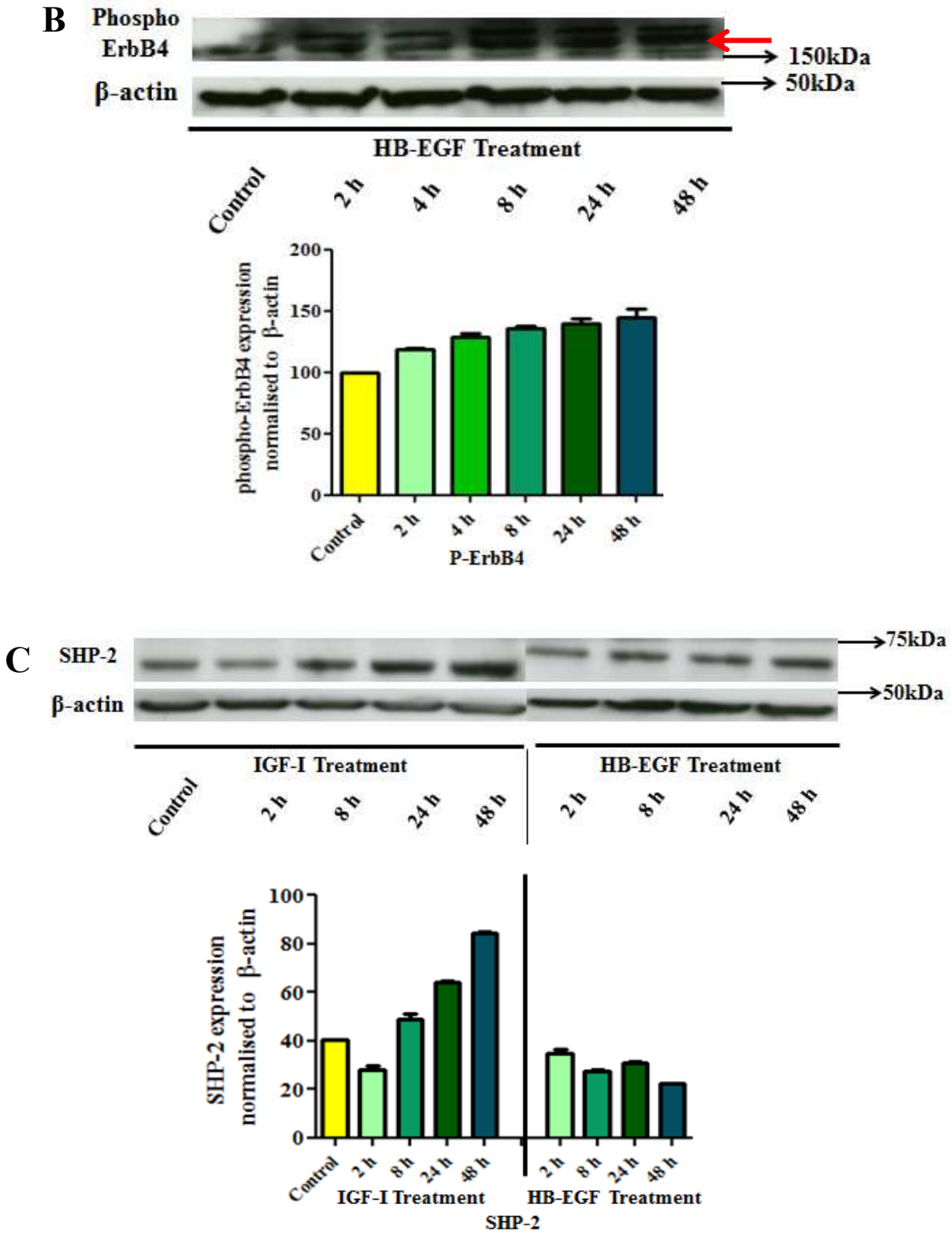


Figure 4.8 (continued): Phospho-ErbB4 and SHP-2 expression in Ishikawa cells in response to IGF-I or HB-EGF

Representative immunoblots of 3 experiments using an anti-phospho ErbB4 (**B**) or an anti-SHP-2 (**C**) polyclonal antibody with purified samples from Ishikawa cells at each time point after 0-48 h of IGF-I or HB-EGF soluble treatment (50ng/ml). Bands corresponding to ~180kDa or ~70kDa were successfully detected, which were the expected size for the expressed phospho-ErbB4, or SHP-2 protein respectively. A β-actin antibody was used to demonstrate equal loading.

Cell lysates were prepared from Ishikawa cells co-cultured with 5 mouse embryos for 72 h. Blots were probed for phospho-IGF-IR, IGF-IR (Figure 4.9.A), phospho-ErbB4 (Figure 4.9.B), and SHP-2 (Figure 4.9.C).

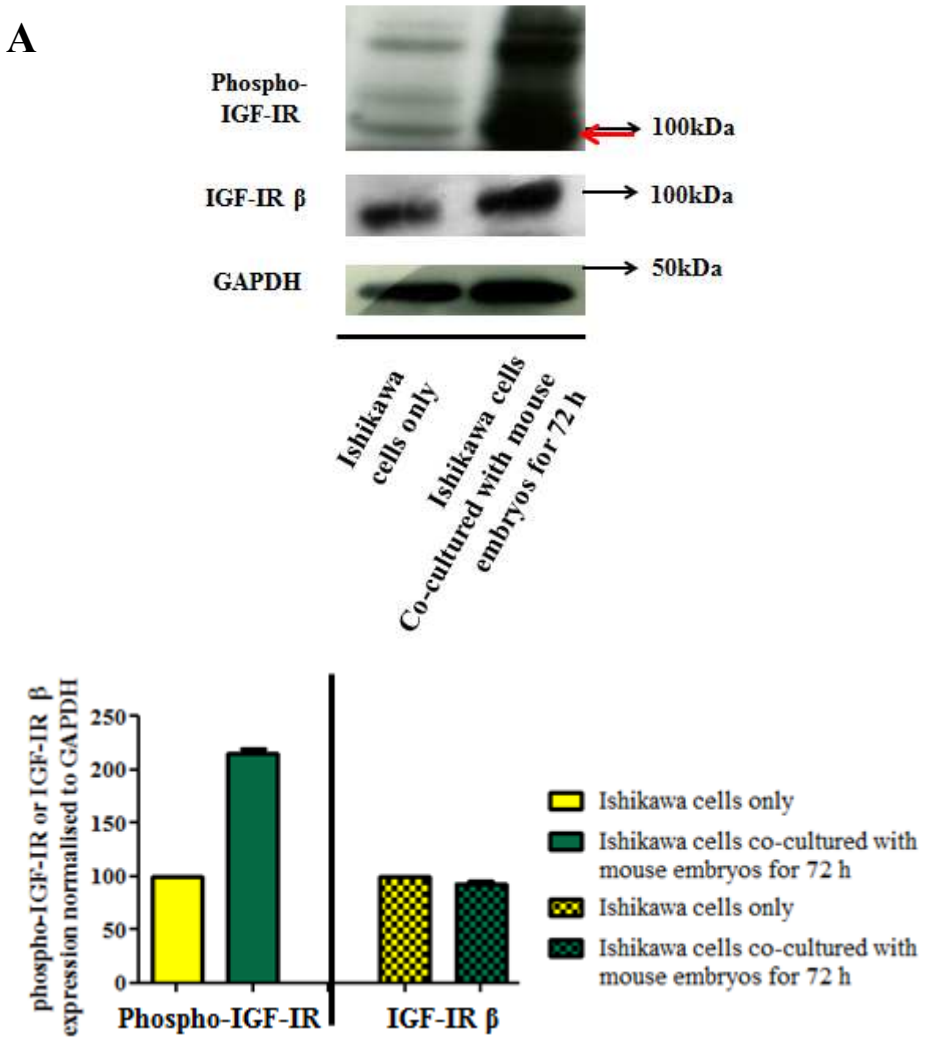


Figure 4.9: Western blotting analysis of phospho-IGF-IR and IGF-IR β in Ishikawa cells co-cultured with mouse embryos (Continued on page 167)

Representative immunoblots of 3 experiments (**A**) using an anti-phospho IGF-IR or anti-IGF-IR β polyclonal antibody with purified lysates from Ishikawa cells alone or in the presence of attached mouse embryos. Bands corresponding to ~97kDa were successfully detected, which were the expected size for the expressed phospho-IGF-IR and IGF-IR β protein. GAPDH was used to demonstrate equal loading.

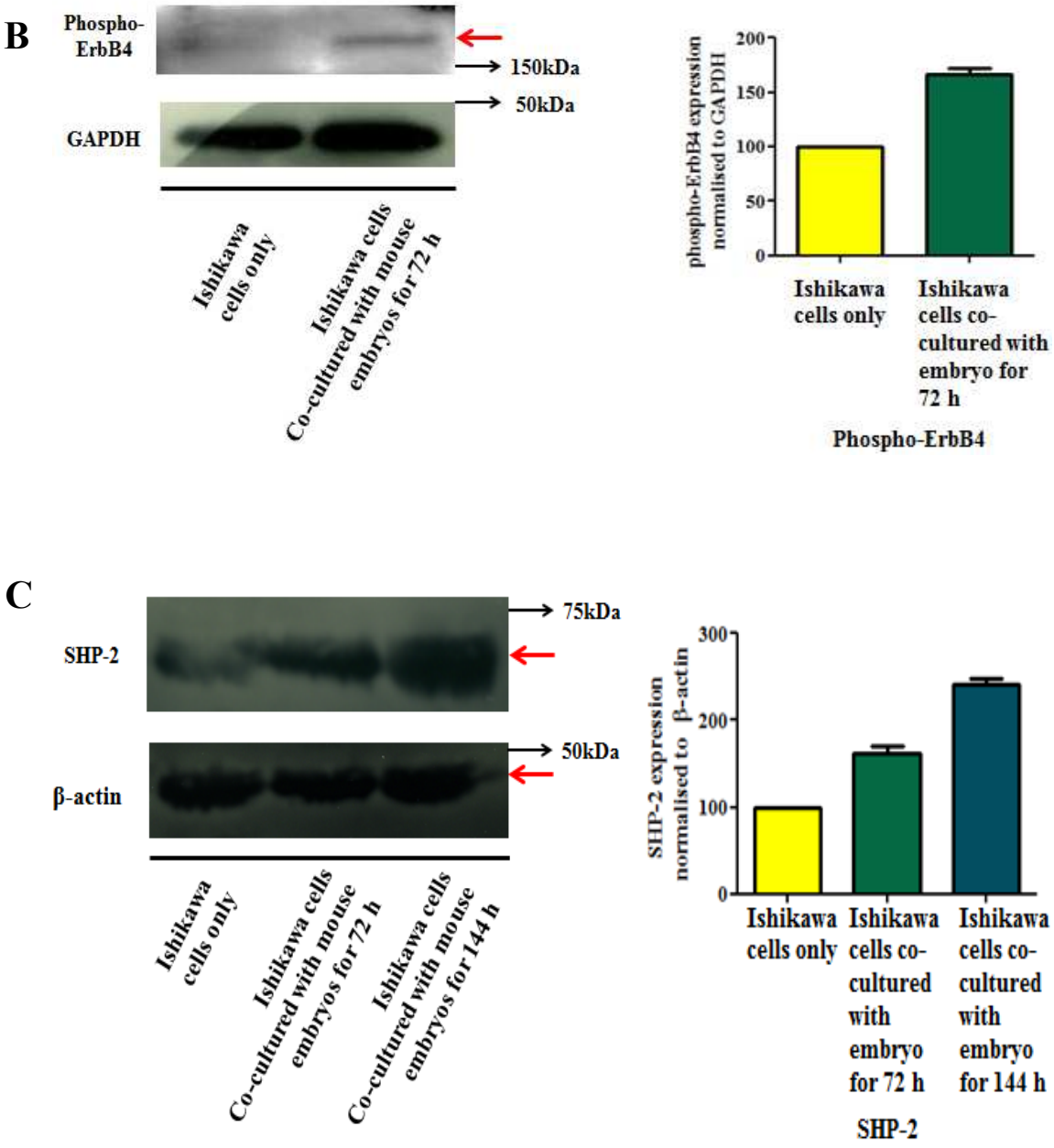


Figure 4.9 (continued): Western blotting analysis of phospho-ErbB4 and SHP-2 in Ishikawa cells co-cultured with mouse embryos

Representative immunoblots of 3 experiments using an anti-phospho ErbB4 (**B**) or anti-SHP-2 (**C**) polyclonal antibody with purified lysates from Ishikawa cells alone or in the presence of attached mouse embryos. Bands corresponding to ~180kDa or ~70kDa, respectively, were successfully detected, which were the expected size for the expressed phospho-ErbB4 or SHP-2 protein respectively. A GAPDH (**B**) or β-actin (**C**) antibody was used to demonstrate equal loading.

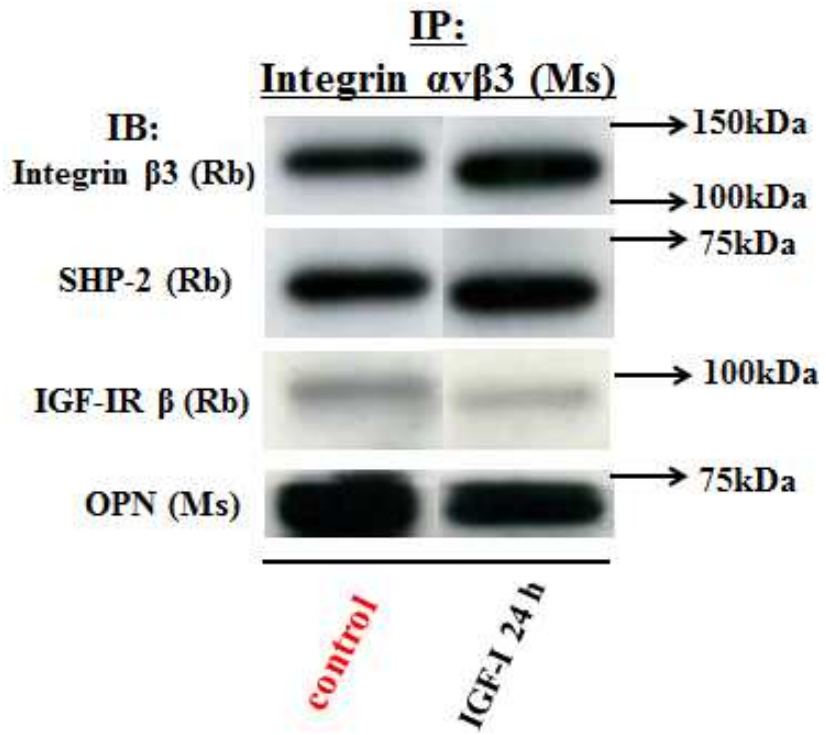
In the presence of embryos, the level of IGF-IR phosphorylation was increased to approximately double that of the basal level (Figure 4.9.A). In addition, the level of ErbB4 phosphorylation was highly increased (1.6 x the basal level) (Figure 4.9.B). Increased SHP-2 was observed with mouse embryos. After 72 h of co-culture, a 1.5 x elevation in SHP-2 was detected and a 2.5 x elevation after 144 h (Figure 4.9.C).

4.2.5 Protein-protein interaction in response to IGF-I

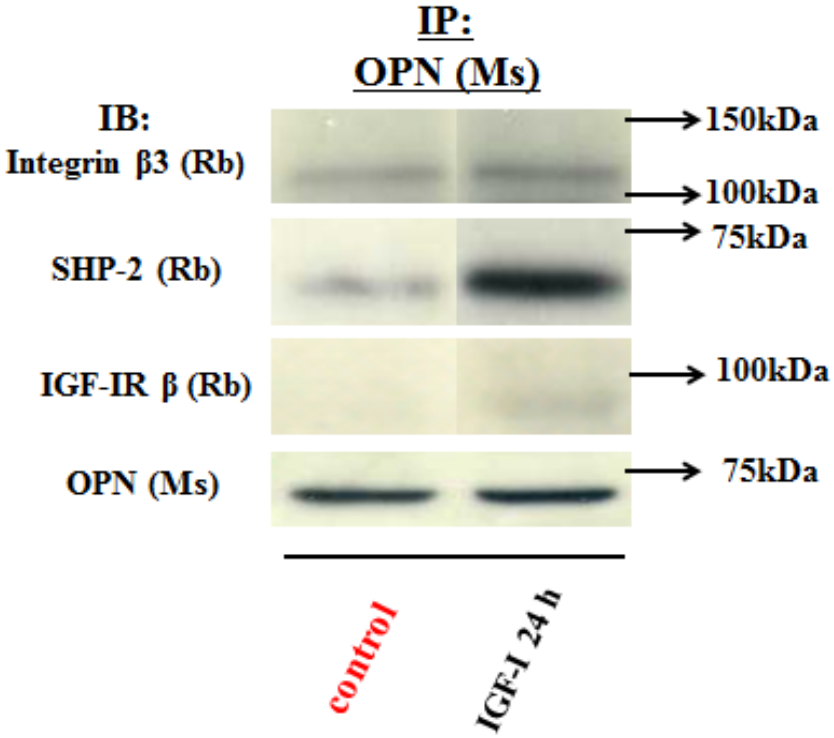
Multiple co-immunoprecipitation experiments were carried out to test the possibility that direct or indirect association occurs in Ishikawa cells between OPN, integrin αvβ3, the IGF-I receptor, and SHP-2, and its dependency upon IGF-I. Previous experiments have shown that OPN moves from intracellular locations (Quenby et al., 2007) to the cell surface during exposure to IGF-I as described in Figure 4.3 and Figure 4.4, however, it should be noted that the approach used in the current study would not distinguish complexes that are intracellular from those present at the surface.

Integrin αvβ3, OPN, or SHP-2 was immunoprecipitated from cell lysates prepared from the control and IGF-I treated cells, and blots were probed for integrin β3, SHP-2, IGF-IR β, or OPN respectively.

A


IP:
Integrin αvβ3 (Ms)
IB:
Integrin β3 (Rb)
150kDa
100kDa
SHP-2 (Rb)
75kDa
IGF-IR β (Rb)
100kDa
OPN (Ms)
75kDa
control
IGF-I 24 h

B


IP:
OPN (Ms)
IB:
Integrin β3 (Rb)
150kDa
100kDa
SHP-2 (Rb)
75kDa
IGF-IR β (Rb)
100kDa
OPN (Ms)
75kDa
control
IGF-I 24 h

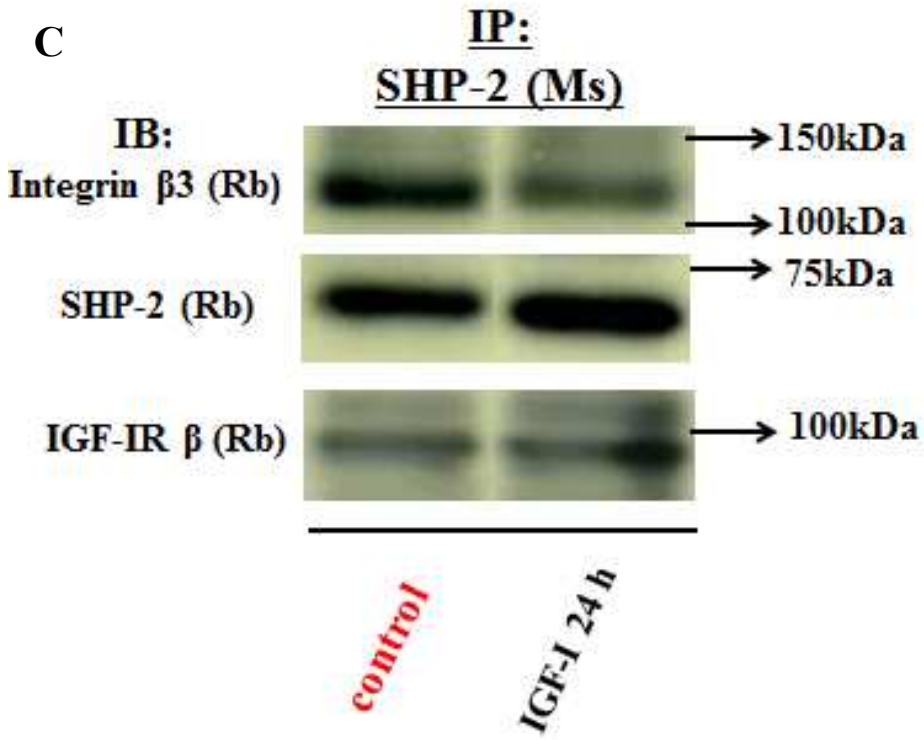


Figure 4.10: Protein-protein interaction in response to IGF-I

Representative immunoblots of 3 experiments using an anti-integrin β3, anti-SHP-2, anti-OPN or anti-IGF-IR β antibody with immunoprecipitates of integrin αvβ3 (**A**), OPN (**B**), or SHP-2 (**C**) from control and IGF-I (50ng/ml) exposed Ishikawa cells. Bands corresponding to ~110/130kDa, ~70kDa, ~97kDa, or ~70kDa were successfully detected, which were the expected size for the expressed integrin β3, SHP-2, IGF-IR β or OPN protein respectively.

SHP-2, IGF-IR, and OPN all co-precipitated with integrin αvβ3 in both control and IGF-I treated cells (Figure 4.10.A). The level of integrin β3 was increased modestly after 24 h of IGF-I treatment with slightly increased SHP-2 and decreased IGF-IR β in the complex. The association of integrin αvβ3 with native OPN (70kDa) did not appear to be IGF-I-dependent, thereby suggesting that OPN is constitutively associated with integrin αvβ3.

Under control conditions, immunoprecipitation with an antibody to OPN demonstrated co-precipitation of integrin β3 and SHP-2. Upon IGF-I treatment, stable levels of co-precipitation with integrin β3 and increased levels with SHP-2 were observed compared to control, but IGF-IR β was only weakly detectable after exposure to IGF-I (Figure 4.10.B). When SHP-2 was used as the precipitating antibody, IGF-IR β and integrin β3 were pulled down as expected revealing a reduction in integrin β3 and a slight elevation in IGF-IR β in the complex (Figure 4.10.C). The present data may suggest that only a fraction of the total population of αvβ3 integrin is associated with OPN, though this would need independent confirmation.

4.2.6 IGF-IR regulates embryo attachment

Given that IGF-IR is phosphorylated in response to either IGF-I or attached embryos (Section 4.2.4), I next investigated the localisation of IGF-IR near the embryo attachment site in an *in vitro* model and the role of IGF-IR in embryo attachment.

4.2.6.1 Up-regulation of IGF-IR at the site of embryo attachment in a 2D heterologous *in vitro* model

For immunofluorescence analysis on 2D *in vitro* cultures, three day 5 mouse embryos were transferred onto confluent Ishikawa cells. Forty eight hours after co-culture, the gel was fixed and immunostained for IGF-IR β using the protocol described in Section 2.8.1. Staining of IGF-IR β was examined adjacent to the embryo attachment sites.

IGF-IR β was locally elevated adjacent to the attachment site of the embryo, exhibiting marked vesicular expression at the apical cell surface with a low magnification (Figure 4.11.A), while intracellular mosaic staining was observed away from the attachment site (Figure 4.11.B). Furthermore, the mouse embryo expressed IGF-IR β. The vesicular signal from IGF-IR β staining was not observed in a rabbit IgG negative control (Figure 4.11.C). The heterogeneous IGF-IR β staining in the cytoplasm and nucleus of Ishikawa cells was clearly demonstrated in enlarged images obtained from two independent 2D gels (Set I and II) with a higher magnification, as well as by intensity profiling of IGF-IR β at the embryo attachment site or in areas away from the mouse embryo (Figure 4.12).

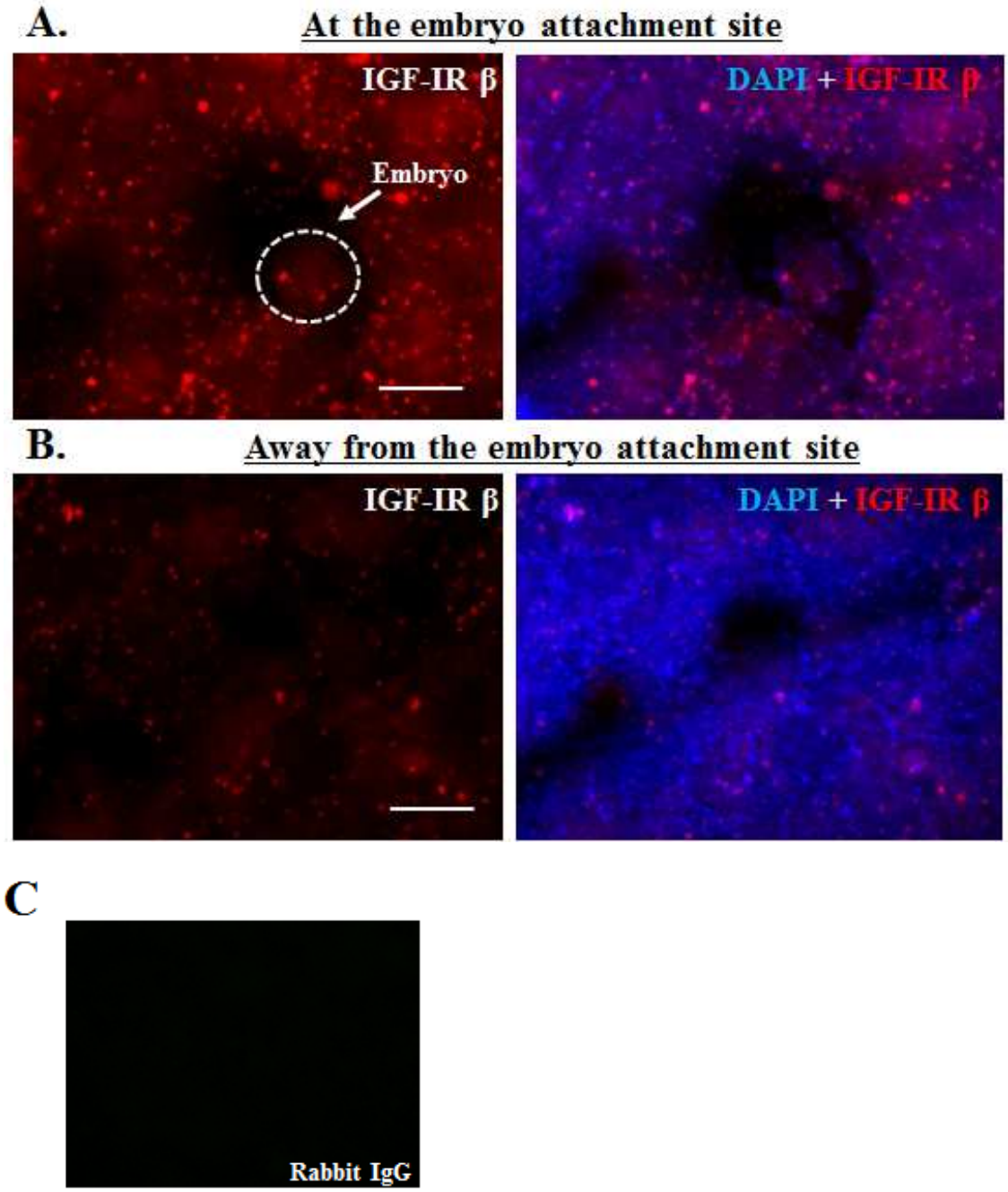
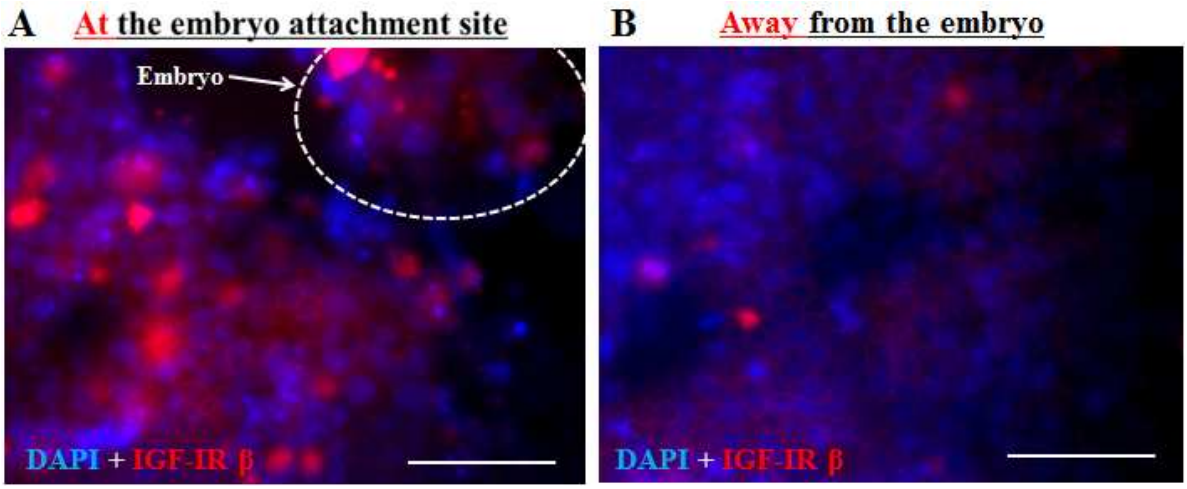
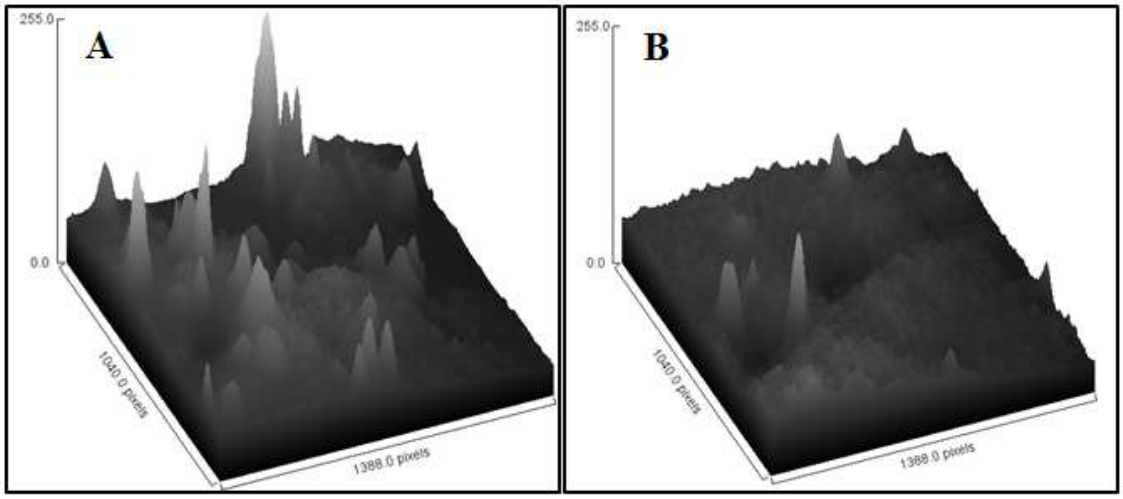


Figure 4.11: Localisation of IGF-IR β in Ishikawa cells co-cultured with the mouse embryo in a 2D *in vitro* model

Representative immunofluorescence microscopy images taken for IGF-IR β in Ishikawa cells co-cultured with a mouse embryo (white circle and arrow). Images were obtained from 2 different regions of coverslip, at the mouse embryo attachment site (**A**) and at the area away from the embryo (**B**). The diagonal black stripe is caused from a cracked element in the fluorescence light path on nuclear staining. A rabbit IgG was used as a negative control for IGF-IR β (**C**). Images were captured at a magnification of 10X. Red: IGF-IR β, Blue: Nucleus (DAPI), Scale bar = 200 µm

Set I


A
At the embryo attachment site
Embryo
DAPI + IGF-IR β
B
Away from the embryo
DAPI + IGF-IR β


255.0
A
0.0
1040.0 pixels
1388.0 pixels
255.0
B
0.0
1040.0 pixels
1388.0 pixels

Set II

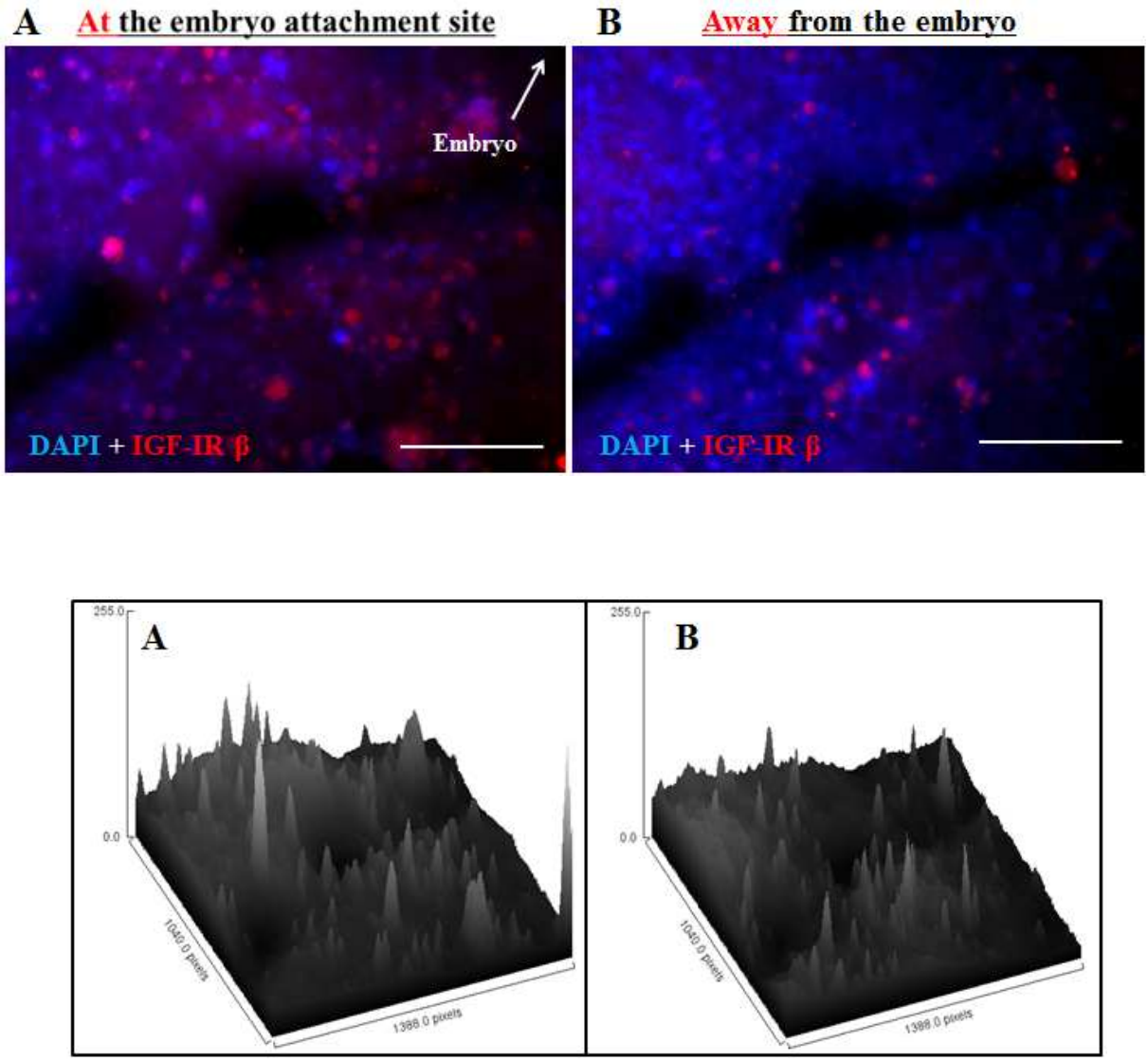


Figure 4.12: Localisation of IGF-IR β in Ishikawa cells co-cultured with the mouse embryo in a 2D *in vitro* model with a higher magnification

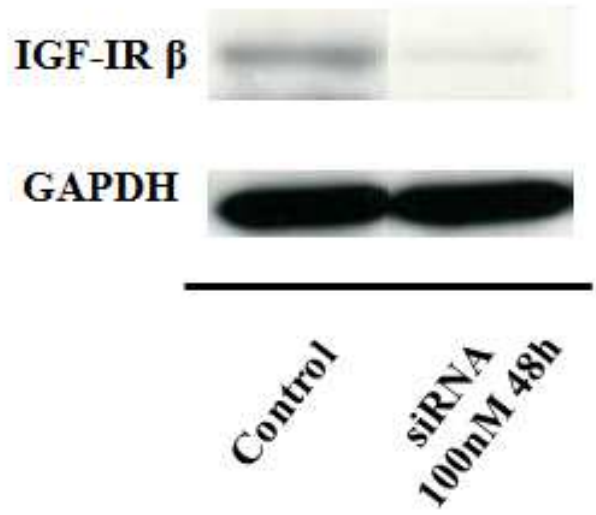
Representative immunofluorescence microscopy images taken for IGF-IR β in Ishikawa cells co-cultured with mouse embryos. Images were obtained from 2 different regions of each coverslip of two independent 2D gels (Set I and II), at the mouse embryo attachment sites (white arrow and circle) (**A**) and at the area away from the embryo (**B**). The diagonal black stripe was caused from a cracked element in the fluorescence light path on nuclear staining. Intensity of IGF-IR β of each image was profiled. Images were captured at a magnification of 40X in Set I and 20X in Set II. Red: IGF-IR β, Blue: Nucleus (DAPI), Scale bar = 50 (Set I) and 200 (Set II) µm

4.2.6.2 SiRNA-mediated knock-down of IGF-IR suppresses embryo attachment

Various concentrations and transfection times of an siRNA that targets IGF-IR mRNA (Details of sequences are stated in Table 2.9) were tested on Ishikawa cells up to 48 h. Western blotting demonstrated significant reduction (80%) of IGF-IR expression at the protein level after 48 h of 100nM transfection compared to the basal level (Figure 4.13).

Eighteen day 5 mouse embryos were transferred on Ishikawa cells transfected with IGF-IR siRNA. The stability of embryo attachment was measured after 24 h of co-culture followed the standard as described in Section 3.2.1.4. It was observed that embryos on control cells (P=0.0009), non-targeting siRNA (P=0.0007), or mock (P=0.0006) transfected cells were significantly more stably attached than on IGF-IR siRNA transfected cells. However, 48 h after transfer, all embryos were stably attached (Figure 4.14).

A **IGF-IR β expression at the protein level**



B

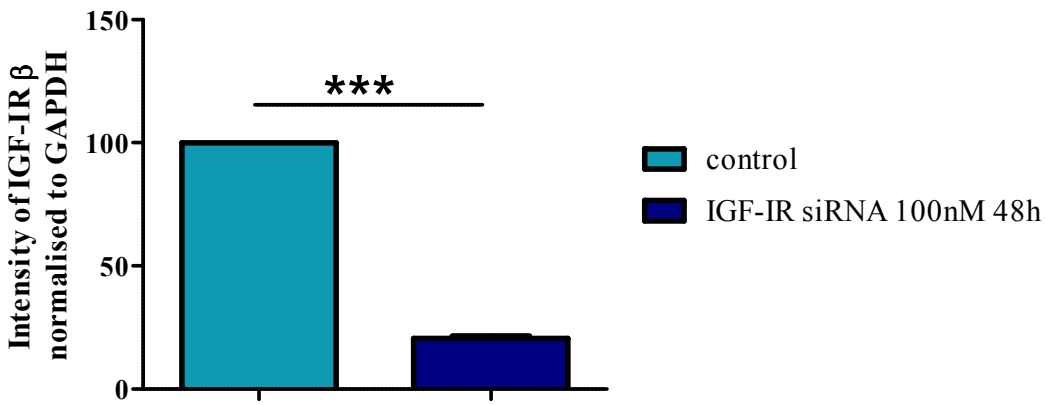


Figure 4.13: Knock-down of IGF-IR mediated by siRNA transfection

Immunoblot using an anti-IGF-IR β antibody with purified samples from control or IGF-IR siRNA (100nM, 48h) transfected Ishikawa cells. Bands corresponding to ~97kDa were successfully detected, which were the expected size for the expressed IGF-IR β protein (**A**). Relative densitometry values illustrating the intensity of IGF-IR β bands obtained for control or cells transfected with IGF-IR siRNA. Asterisk (***) denotes a statistically significant difference ($P \leq 0.0001$) as determined by the student's t-test. Data are represented as mean ± S.E.M (**B**).

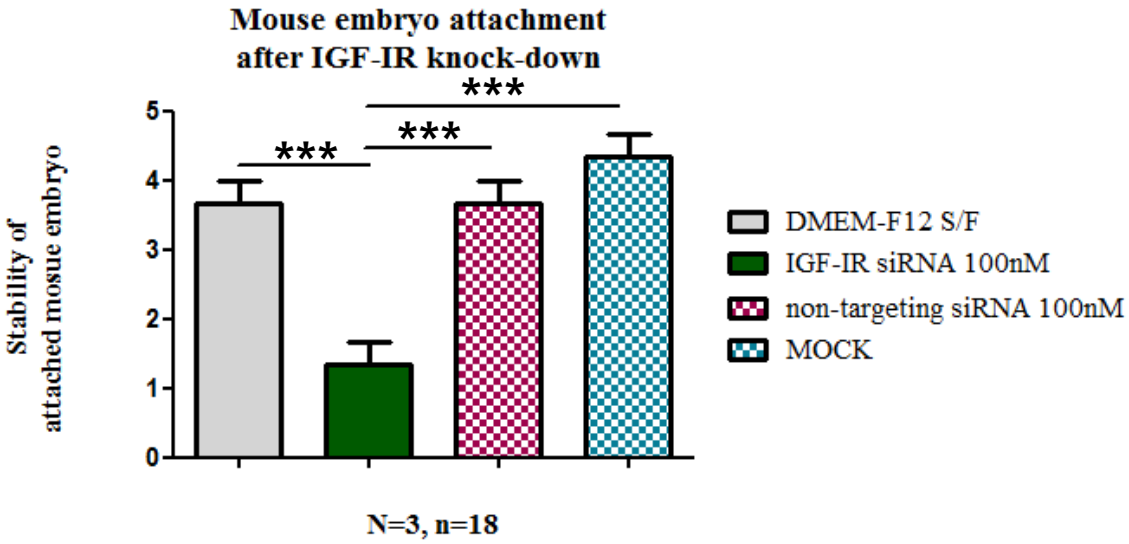


Figure 4.14: Knock-down of IGF-IR in Ishikawa cells reduced embryo attachment

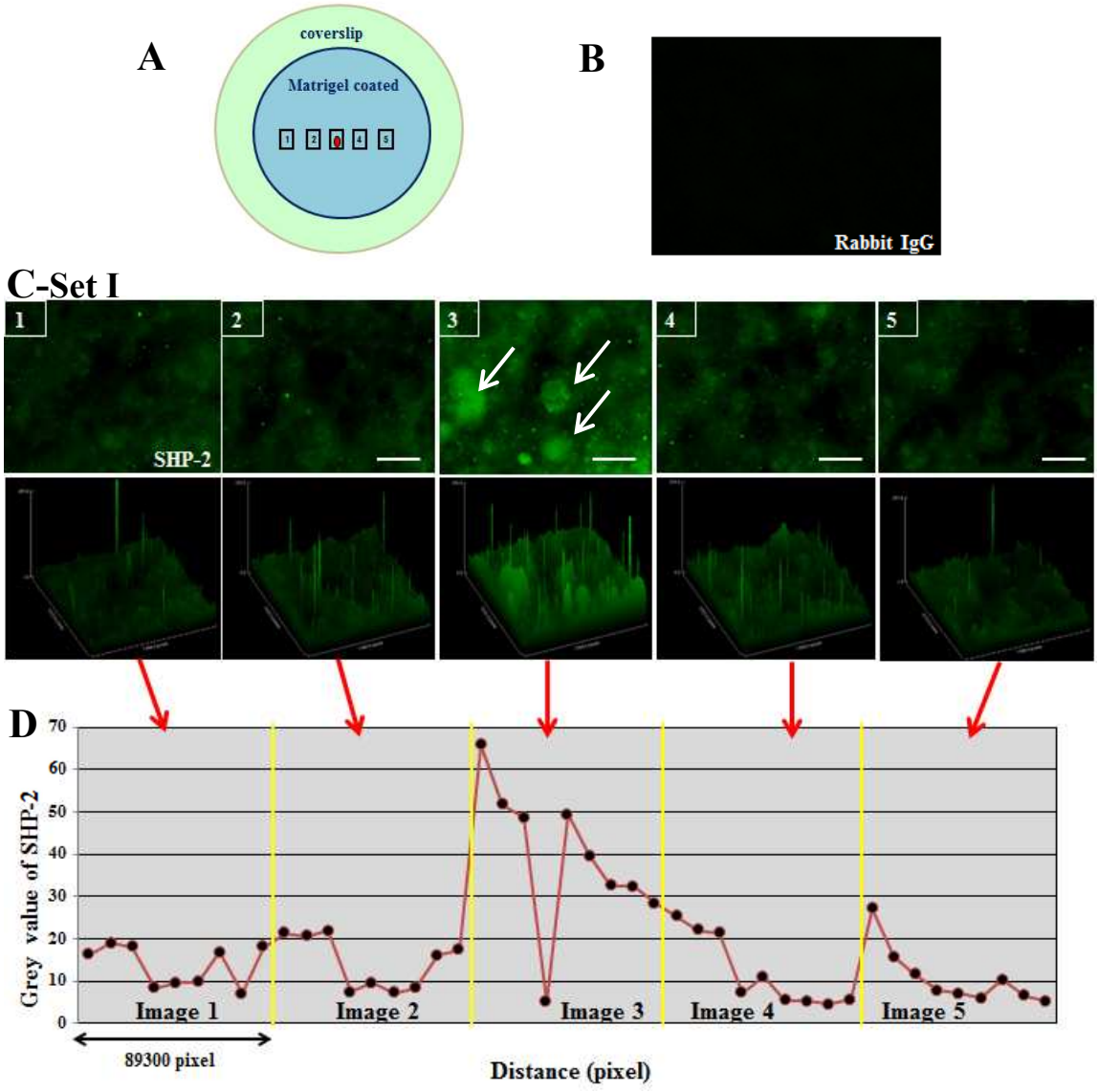
Mean proportions (from 3 different sets of experiments using 18 mouse embryos in total) of the stability of embryo attachment after 24 h of co-culture on control, IGF-IR, non-target siRNA (100nM), and mock transfected cells. Asterisks (***) on the histograms denote statistically significant differences ($P<0.0001$). Data are shown as mean ± SEM.

4.2.7 SHP-2 regulates embryo attachment

Given that SHP-2 increased in Ishikawa cells in the presence of attached embryos (Section 4.2.4, Figure 4.9.C) and in response to soluble IGF-I treatment (Section 4.2.4, Figure 4.8.C), I next investigated the localisation of SHP-2 near the site of embryo attachment and the role of SHP-2 in embryo attachment.

4.2.7.1 Up-regulation of SHP-2 at the site of embryo attachment

Six day 5 mouse embryos were co-cultured on confluent Ishikawa cells for 48 h. The gel was fixed and immunostained for SHP-2. SHP-2 was locally elevated adjacent to the attachment site of embryos, while unaffected mosaic staining was observed away from the embryo (Figure 4.15-Set I and Set II). Furthermore, mouse embryos expressed SHP-2. Intensity of SHP-2 expression across the gel was profiled and quantified in each graph illustrating the distributional change of SHP-2 across the whole region. The signal from SHP-2 staining was greater than that from a rabbit IgG negative control. SHP-2 staining in Ishikawa cells was clearly demonstrated in an enlarged image with a higher magnification (Figure 4.16). SHP-2 was highly stained in the cytoplasm showing prominent staining at the periphery of cells, which is consistent with the association of a fraction of SHP-2 with a cell surface component, such as integrin αvβ3. A few patches of Ishikawa cells were stained with SHP-2 with greater intensity than others.


A
coverslip
Matrigel coated
1
2
3
4
5
B
Rabbit IgG
C-Set I
SHP-2
D
Grey value of SHP-2
Image 1
Image 2
Image 3
Image 4
Image 5
89300 pixel
Distance (pixel)

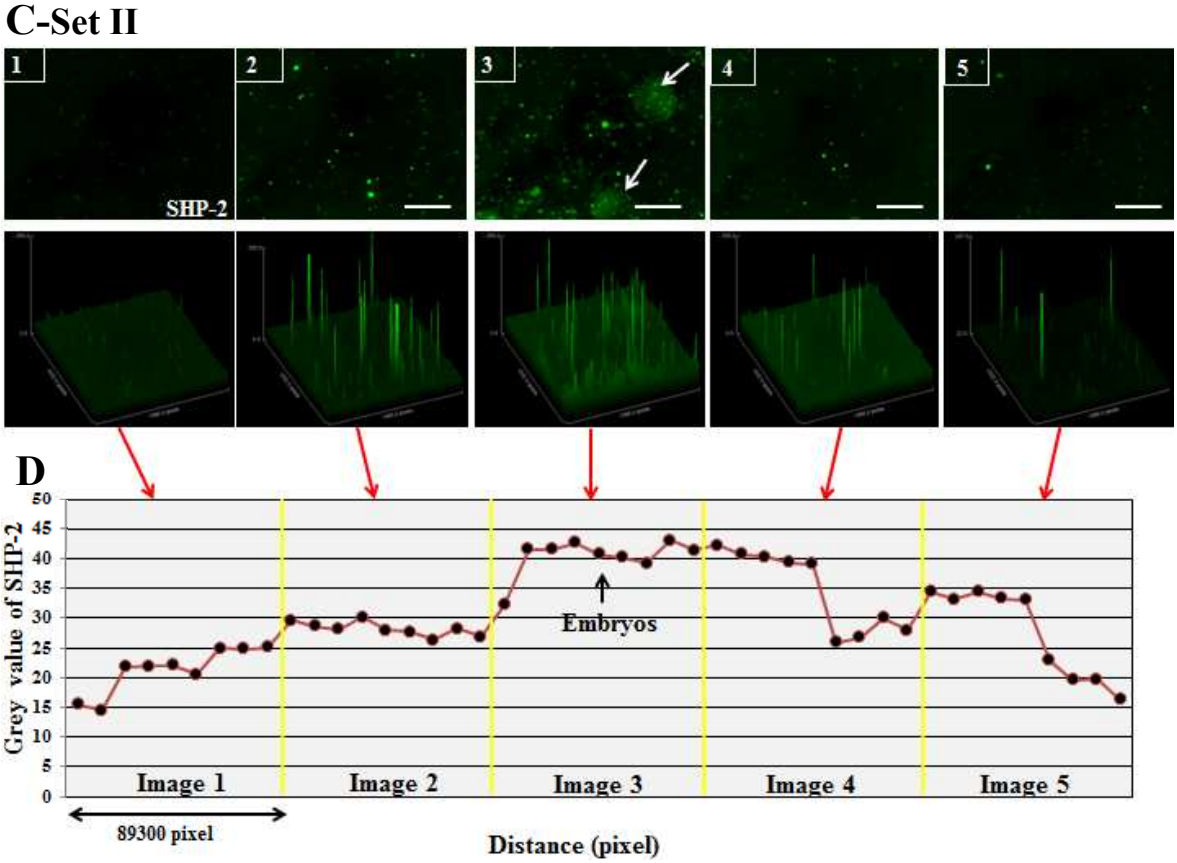


Figure 4.15: Locally increased SHP-2 in Ishikawa cells co-cultured with mouse embryos

Representative immunofluorescence microscopy images taken for SHP-2 in Ishikawa cells co-cultured with mouse embryos (white arrows) (**C-Set I and II**). Images were obtained from 5 different regions of each coverslip of two independent gels, as described (**A**). The diagonal black stripe was caused from a cracked element in the fluorescence light path. A rabbit IgG was used as a negative control for SHP-2 (**B**). Images were captured at a magnification of 10X. Intensity of SHP-2 staining across the gel was profiled and quantified. The X-axis indicates the distance (pixel) of each image, while the Y-axis shows grey value of SHP-2 expression. Each point on the graph shows the average of SHP-2 at every 10000 pixel of each image (Each image was 89300 pixels in width). Quantified intensity profiling showed that SHP-2 was gradually elevated towards the mouse embryo attachment sites (white arrows) from the outside of coverslip (**D-Set I and Set II**). Green: SHP-2, Scale bar = 200 µm

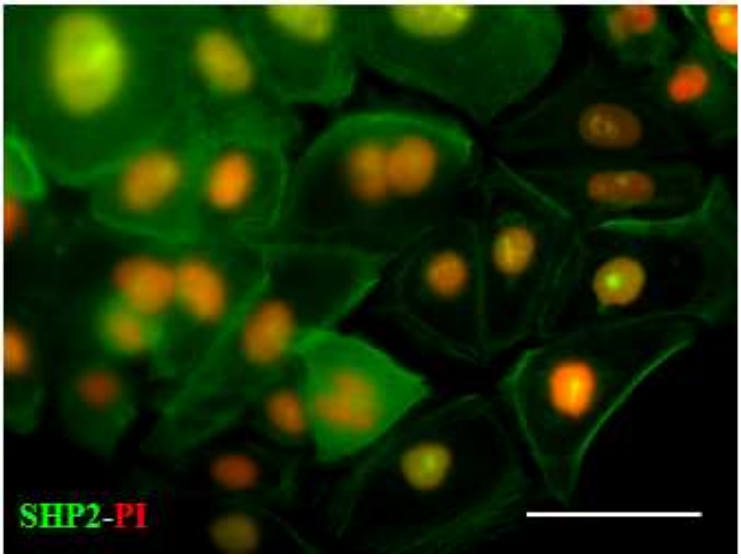


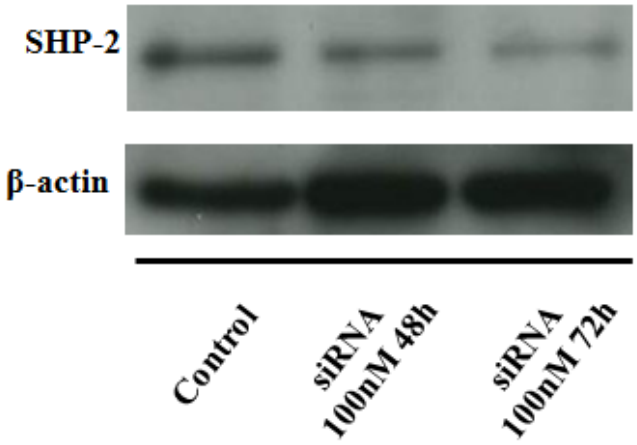
Figure 4.16: Localisation of SHP-2 in Ishikawa cells

Representative immunofluorescence microscopy image taken for the localisation of SHP-2 in Ishikawa cells. Images were captured at a magnification of 40X with oil. Green: SHP-2, Red: Nucleus (propidium iodide), Scale bar = 50 µm

4.2.7.2 SiRNA-mediated knock-down of SHP-2 suppresses embryo attachment

Cells were exposed to SHP-2 siRNA for up to 72 h and Western blotting demonstrated a reduction of expression (50% at 48 h and 80% at 72 h) (Figure 4.17). After 72 h of transfection with SHP-2 siRNA, small gaps had started to appear between the cells. Therefore, the optimal duration of transfection used for the embryo attachment assay was determined to be 48 h.

A SHP-2 expression at the protein level



B

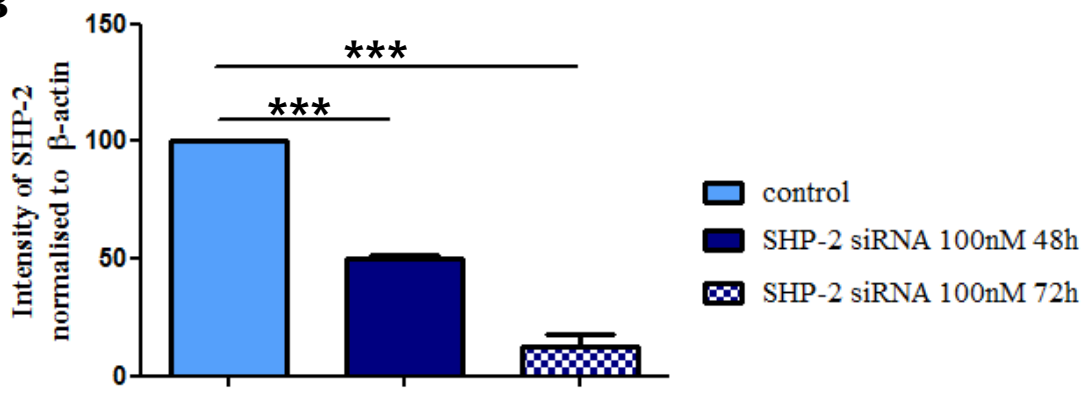


Figure 4.17: Knock-down of SHP-2 mediated by siRNA

Immunoblot using an anti-SHP-2 antibody with purified samples from control or SHP-2 siRNA (100nM, 48/72 h) transfected Ishikawa cells. Bands corresponding to ~70kDa were successfully detected, which were the expected size for the expressed SHP-2 protein. A β-actin antibody was used to normalise SHP-2 expression (**A**). Relative densitometry values illustrating the intensity of SHP-2 bands obtained for control or cells transfected with SHP-2 siRNA. Asterisk (***) denotes a statistically significant difference ($P \leq 0.0001$) as determined by the student's t-test. Data are represented as mean ± S.E.M (**B**).

After 48 h of transfection with SHP-2 siRNA, day 5 mouse embryos (n=28) were transferred to Ishikawa cells in microwell plates. The stability of embryo attachment was scored at 24 h using standard criteria described in Section 3.2.1.4. The stability of embryo attachment on control cells was significantly higher than that on cells transfected with SHP-2 siRNA (P=0.0003). The stability of embryo attachment on non-targeting siRNA transfected cells was similar to the level of embryo attachment on control cells (Figure 4.18).

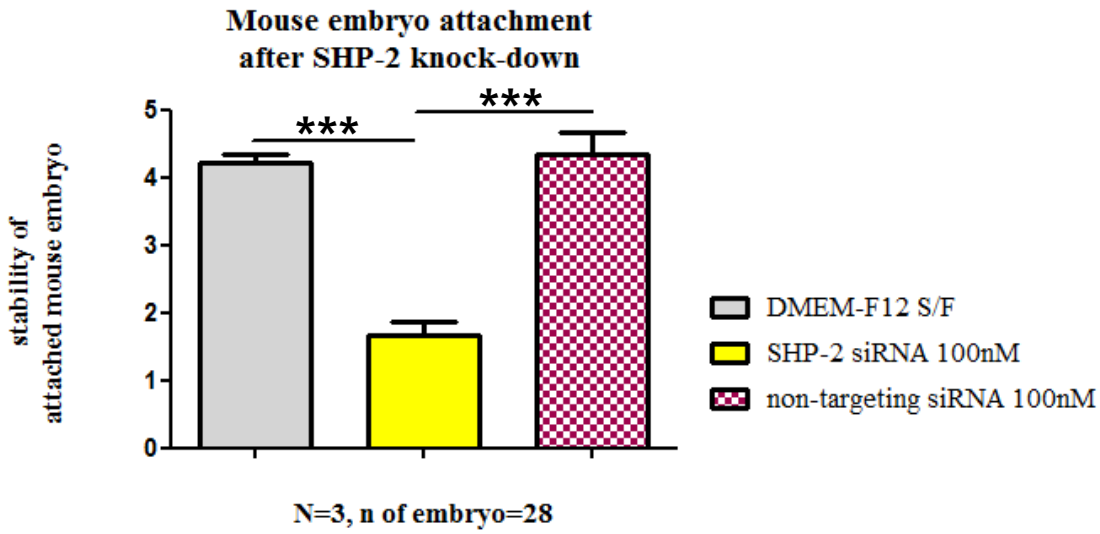


Figure 4.18: Knock-down of SHP-2 suppressed embryo attachment

Mean proportions (from 3 different sets of experiments using 28 mouse embryos in total) of the stability of embryo attachment after 24 h of co-culture on control, SHP-2 siRNA (100nM) transfected, and non-targeting siRNA (100nM) transfected cells. Asterisks (***) on the histograms denote statistically significant differences (p=0.0003). Data are shown as mean ± SEM.

4.2.8 Attachment of bead carrying proteins *in vitro*

Some of the growth factors thought to be involved in implantation are of embryonic origin and are probably confined to cells near the site of implantation. In order to investigate local growth factor influences and the possibility that growth factor receptors might play roles in attachment to the epithelium, I developed an assay in which embryo-sized beads loaded with growth factors attach to epithelial monolayers. The beads were conjugated to a blue dye that binds growth factor (IGF-I or HB-EGF) or OPN. Beads were incubated within a 20µl drop of IGF-I, HB-EGF, OPN, or BSA respectively for 2 h and transferred to confluent Ishikawa cells in a 2D gel. Forty eight hours after co-culture, gels were fixed. Beads were firstly loosely attached and lost their-original positions easily but at 48 h growth factor or OPN-coated beads remained solidly attached onto cells during washing and fixation steps (Figure 4.19).

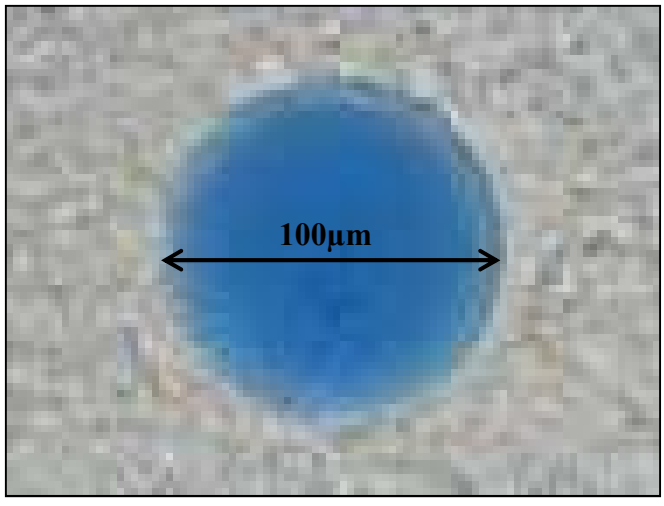


Figure 4.19: Attachment of bead carrying growth factor

An attached embryo-sized bead-loaded with growth factor (IGF-I) on Ishikawa cells after 48 h of co-culture.

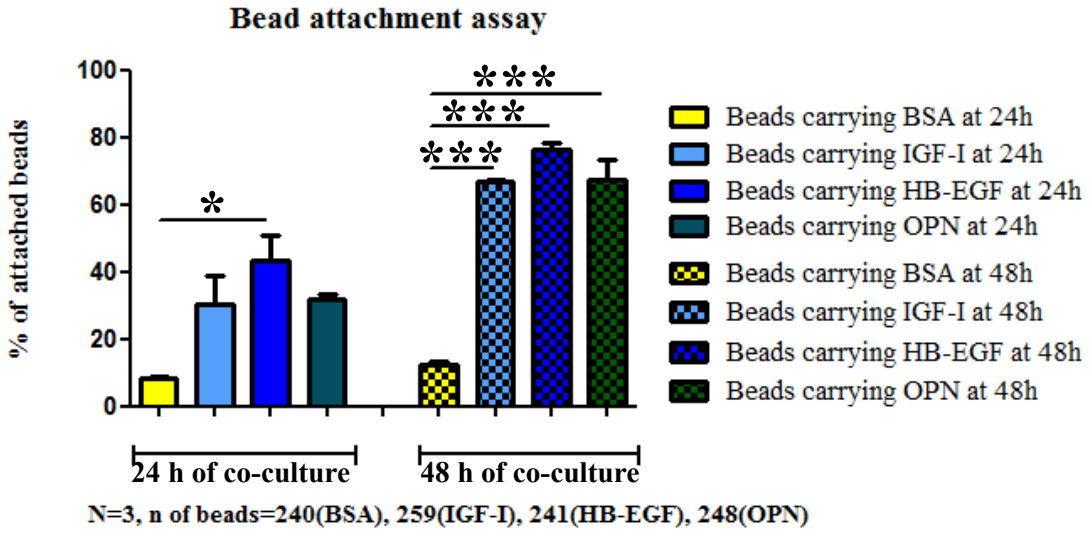


Figure 4.20: Bead attachment assay

Mean proportions of attached beads carrying BSA, IGF-I, HB-EGF, or OPN (100ng/µl) after 24 h or 48 h of co-culture on Ishikawa cells. Asterisks (*; **; ***) on the histograms denote statistically significant differences ($P<0.05$). Data are shown as mean ± SEM.

The bead attachment assay was performed by scoring the number of attached beads against the total number of beads originally transferred. Approximately 50 beads were transferred per well. The total number of beads used was 989 (BSA (240), IGF-I (259), HB-EGF (241), and OPN (248)). At 24 h of co-culture, 8% of beads bearing BSA remained attached on the gel, while around 30% of beads carrying IGF-I or OPN, and 45% of beads carrying HB-EGF, were solidly attached to Ishikawa cells. Forty eight hours after co-culture, 12% of beads bearing BSA were attached on the gel, while approximately 65% of beads carrying IGF-I or OPN, and 80% of beads carrying HB-EGF, remained solidly attached to cells (Figure 4.20). Compared to the number of attached beads bearing BSA,

only beads carrying HB-EGF showed significantly higher attachment rate at 24 h of co-culture (P=0.0354). Beads carrying IGF-I (P<0.0001), HB-EGF (P<0.0001), or OPN (P=0.0001) exhibited significantly higher attachment rates at 48 h.

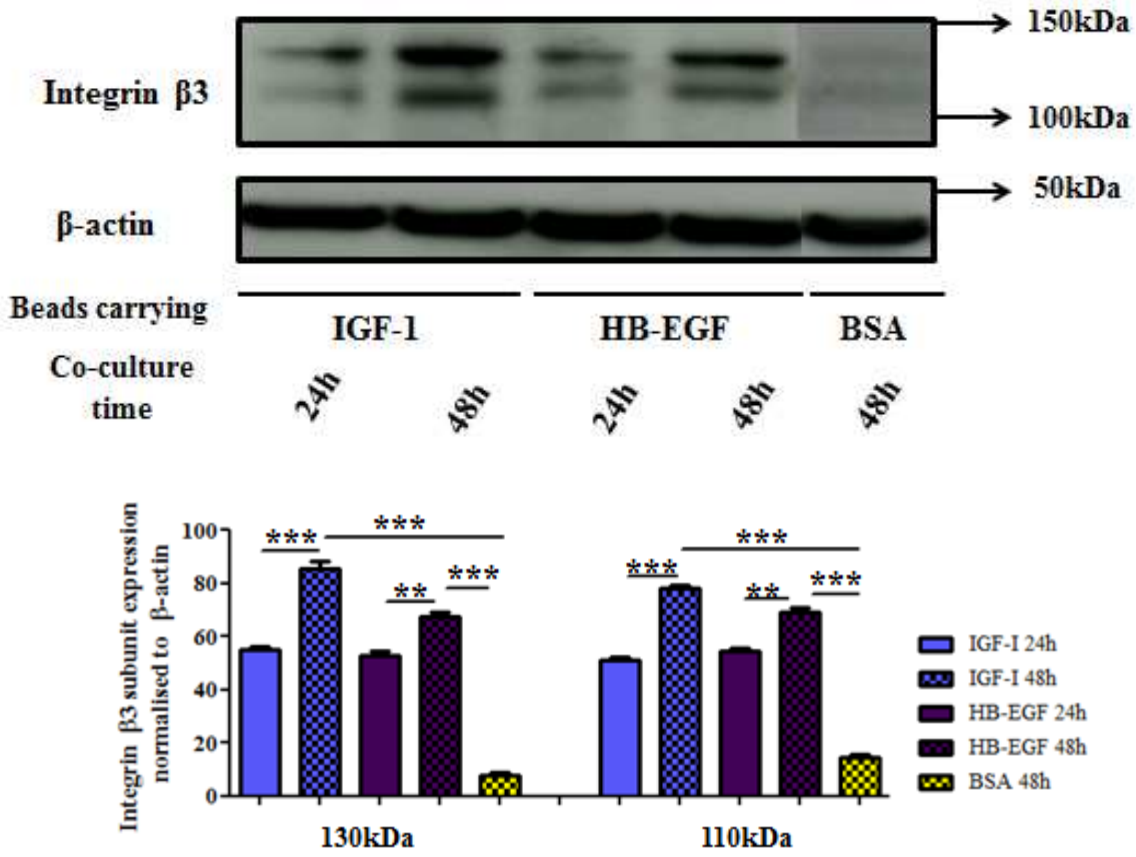


Figure 4.21: Western blotting analysis of integrin β3 subunit in Ishikawa cells co-cultured with beads carrying IGF-I or HB-EGF

Representative immunoblot of 3 experiments using an anti-integrin β3 polyclonal antibody with purified lysates from Ishikawa cells co-cultured with beads carrying either IGF-I or HB-EGF (50 beads per well) for 24 h or 48 h respectively. Bands corresponding to ~110/130kDa were successfully detected, which was the expected size for the expressed integrin β3 protein. β-actin was used to demonstrate equal loading. Asterisks (**; ***) on the histograms denote statistically significant differences (P<0.05). Data are shown as mean ± SEM.

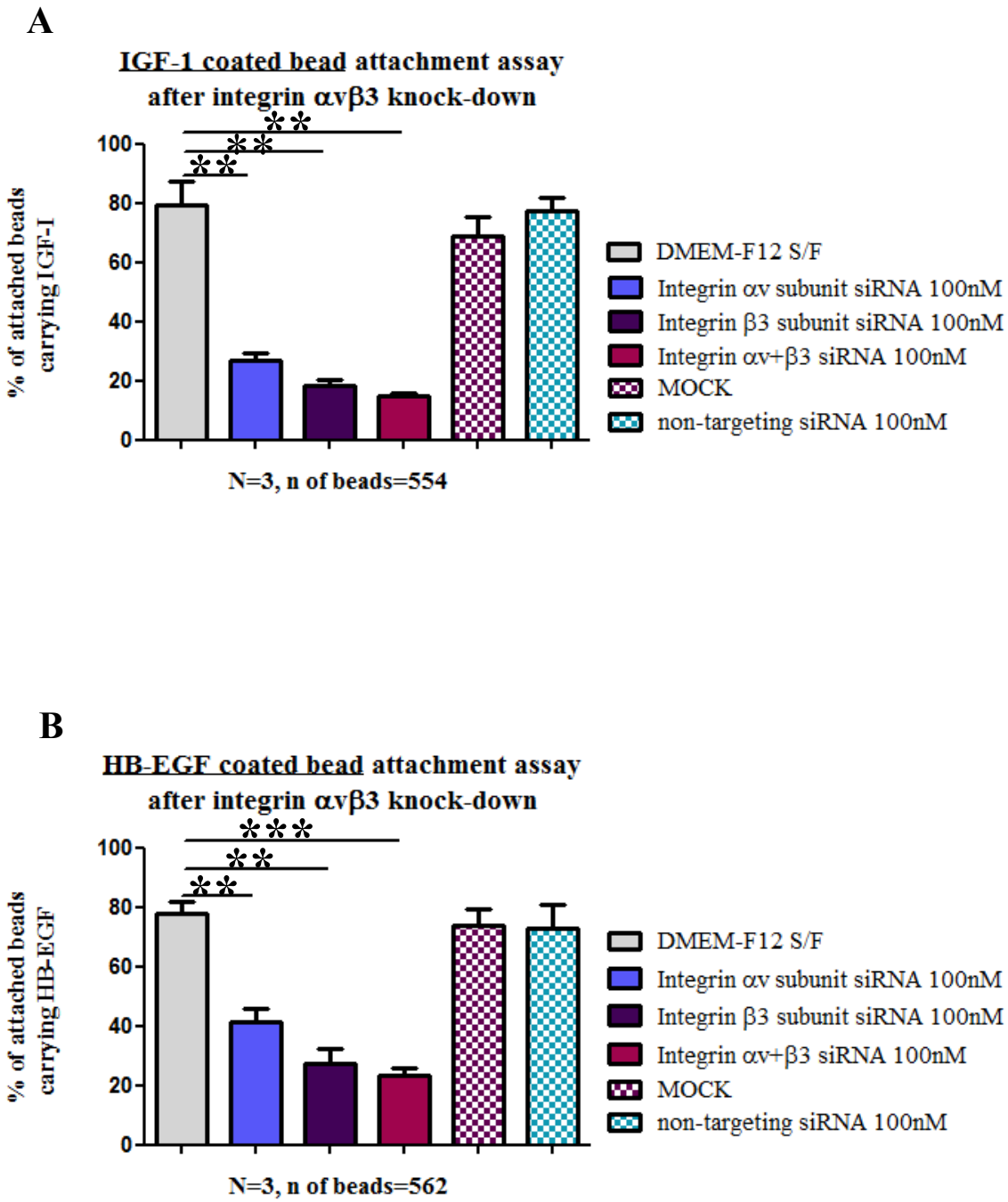
Cell lysates from Ishikawa cells that were co-cultured with beads bearing IGF-I, HB-EGF, or BSA, for 24 h or 48 h respectively, demonstrated increased expression of integrin β3 with advancing time of co-culture with beads (Figure 4.21). Integrin β3 expression of cells co-cultured with beads bearing BSA was used as a negative control. This showed a similar pattern as previous Western blotting data demonstrating that integrin β3 was elevated when co-cultured with mouse embryos (Section 3.2.2.2.4, Figure 3.23).

4.2.8.1 SiRNA-mediated knock-down of integrin αvβ3 suppresses the attachment of beads bearing IGF-I, HB-EGF, or OPN

Ishikawa cells were transfected with integrin αv, β3, or αvβ3 siRNA for 48 h and beads bearing IGF-I (n=554), HB-EGF (n=562), or OPN (n=662) were transferred onto 2D gels. Knock-down validation data are shown in Section 3.2.2.6. The number of attached beads carrying IGF-I on transfected cells with siRNA integrin αv (P=0.0029), β3 (P=0.0016), or αvβ3 (P=0.0012) was significantly reduced relative to controls (DMEM-F12 S/F). However, there was no significant difference between the number of attached beads on cells transfected with non-targeting siRNA or untreated cells. Furthermore, the rate of attachment of beads carrying IGF-I on mock-transfected cells was very similar to the level of attachment rate on control cells (Figure 4.22.A).

Similar patterns were observed in the attachment assay with beads carrying HB-EGF or OPN. A significantly reduced number of beads bearing HB-EGF on integrin αv (P=0.0039), β3 (P=0.0016), or αvβ3 (P=0.0004) siRNA transfected cells remained attached as compared with cells in serum-free medium (Figure 4.22.B). In addition, the rate of attached beads carrying OPN on integrin αv (P<0.0001), β3 (P=0.0006), or αvβ3

(P<0.0001) siRNA transfected cells was significantly reduced compared to that of beads on control cells (Figure 4.22.C). In both cases, the bead attachment rate on non-targeting siRNA, or mock-transfected cells was similar to the rate of attached beads on cells in serum-free medium.



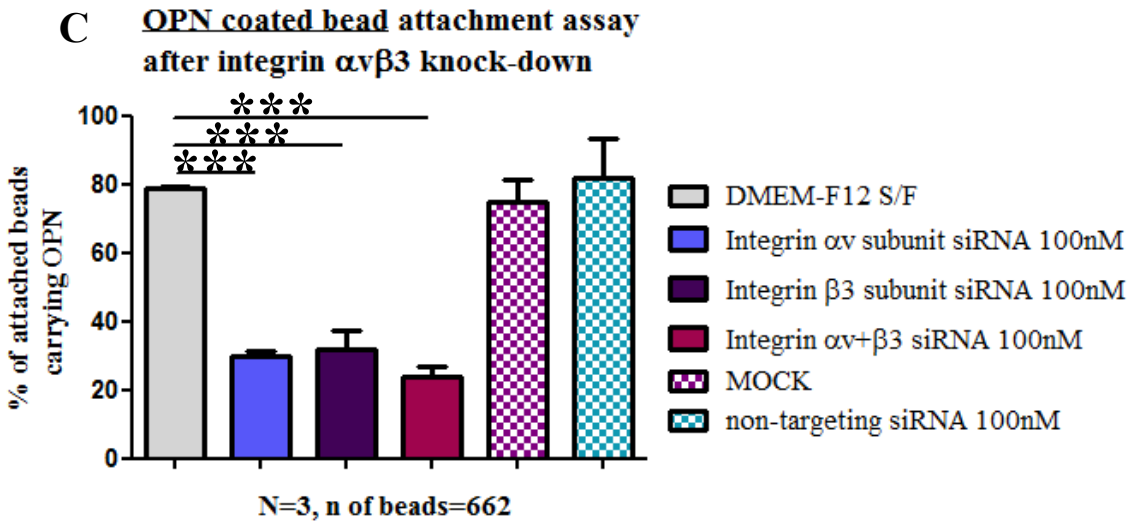
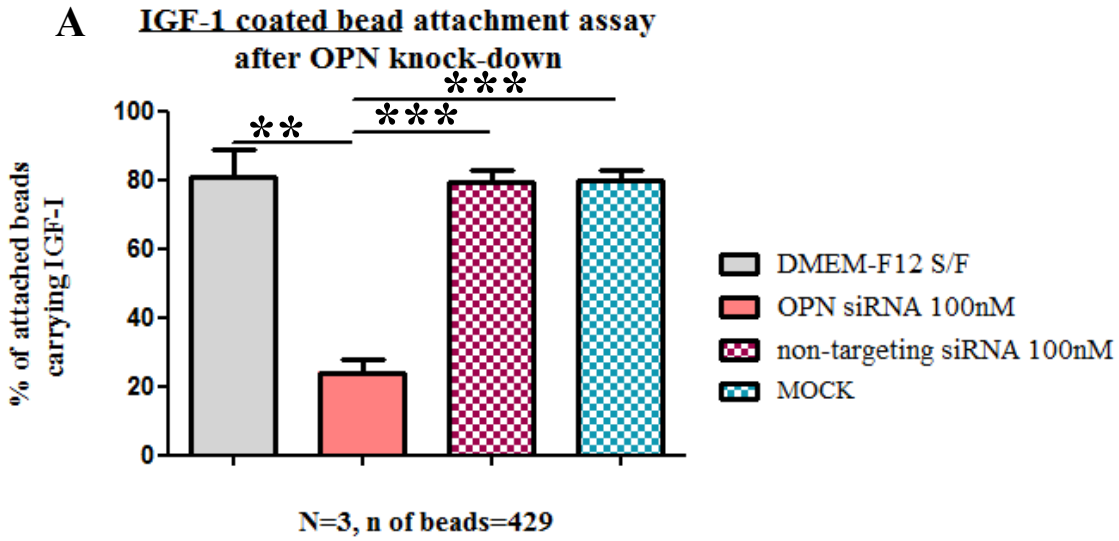


Figure 4.22: Attachment assays of beads carrying IGF-I, HB-EGF, or OPN after knock-down of integrin αv, β3, or αvβ3

Mean proportions (3 different sets of experiments using 554 (IGF-I coated beads), 562 (HB-EGF coated beads) and 662 (OPN coated beads)) of attached beads after 48 h of co-culture on control, integrin subunit αv, β3, or αvβ3 siRNA (100nM) transfected, and cells transfected with non-targeting siRNA (100nM). Asterisks (**; ***) on the histograms denote statistically significant differences ($P<0.05$) as determined by the student's t-test. Data are shown as mean ± SEM.

4.2.8.2 SiRNA-mediated knock-down of OPN suppresses the attachment of beads bearing IGF-I or OPN but not beads bearing HB-EGF

Ishikawa cells were transfected with OPN siRNA for 48 h and beads carrying IGF-I (n=429), HB-EGF (n=426), or OPN (n=470) were transferred. The number of attached beads was assessed after a further 48 h of co-culture. The rate of attachment of beads bearing IGF-I (P=0.0029, Figure 4.23.A) or OPN (P=0.0001, Figure 4.23.C) on OPN siRNA transfected Ishikawa cells was significantly reduced compared to the attachment rate of beads carrying IGF-I or OPN on control cells (DMEM-F12 S/F). However, the attachment rate of beads bearing HB-EGF on OPN siRNA transfected cells (P=0.1451) remained at a similar level to the rate on Ishikawa cells maintained in serum-free medium (Figure 4.23.B). The rate of attachment of beads carrying IGF-I, HB-EGF or OPN on non-targeting siRNA and mock-transfected cells was similar to that observed in control cells.



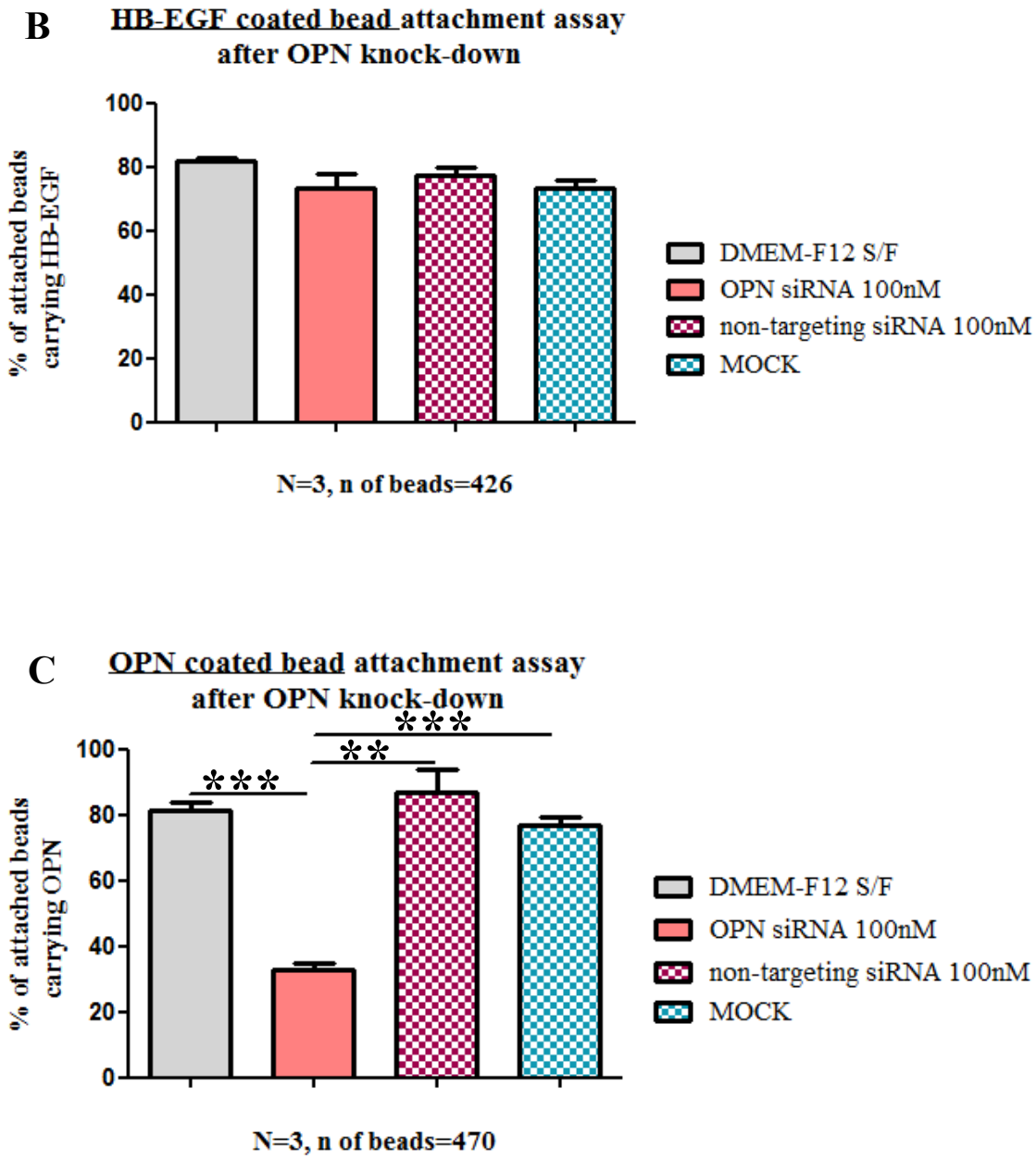


Figure 4.23: Attachment assays of beads carrying IGF-I, HB-EGF, or OPN after knock-down of OPN

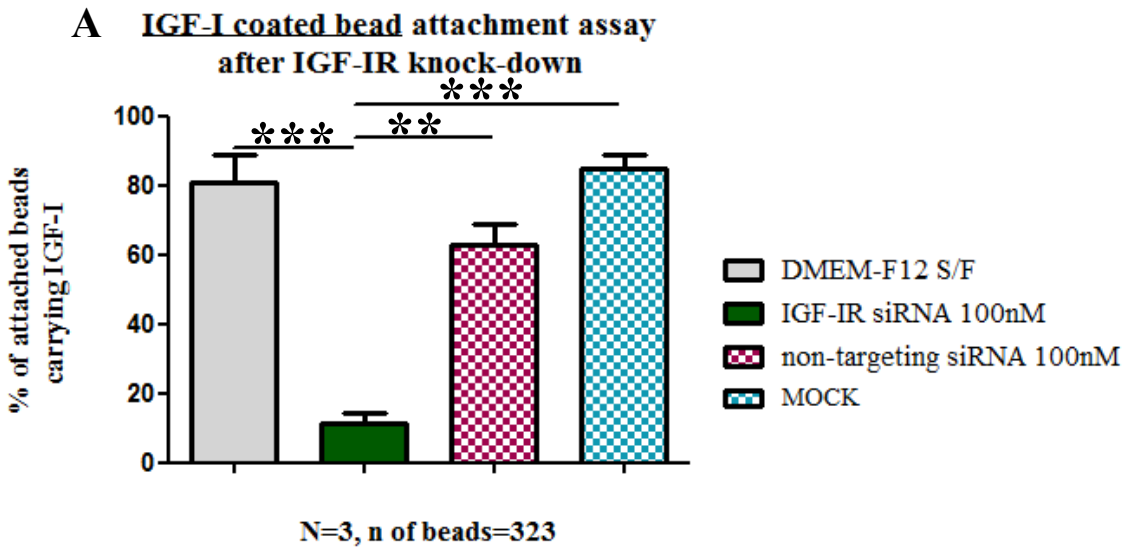
Mean proportions (3 different sets of experiments using 429 (IGF-I coated beads), 426 (HB-EGF coated beads) and 470 (OPN coated beads)) of attached beads after 48 h of co-culture on control, OPN siRNA (100nM) transfected, non-targeting siRNA (100nM), or mock transfected cells. Asterisks (**; ***) on the histograms denote statistically significant differences ($P<0.05$) as determined by the student's t-test. Data are shown as mean ± SEM.

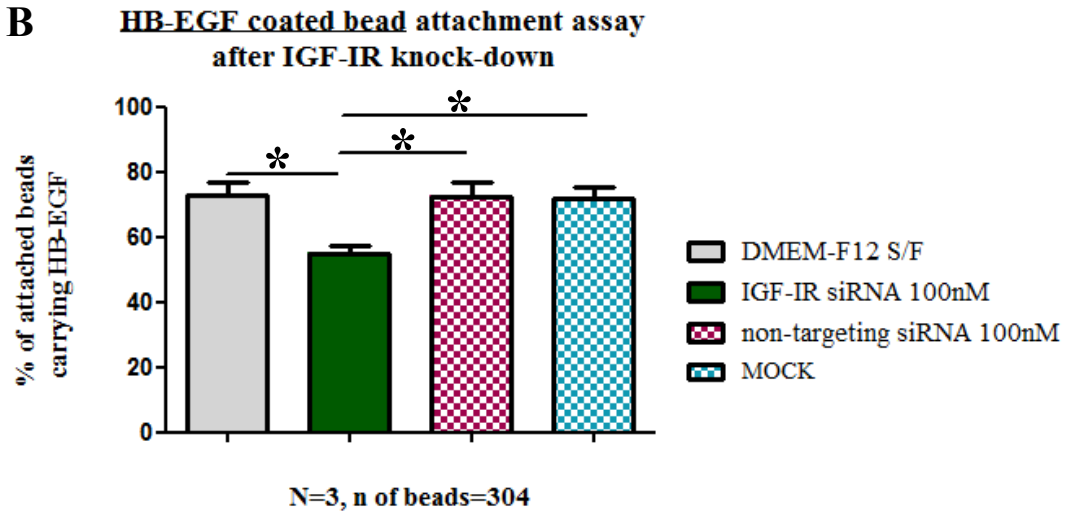
4.2.8.3 SiRNA-mediated knock-down of IGF-IR suppresses the attachment of beads bearing IGF-I, HB-EGF, or OPN

IGF-I (n=323), HB-EGF (n=304), or OPN (n=281) pre-absorbed beads were transferred and co-cultured with Ishikawa cells transfected with IGF-IR siRNA for 48 h. Knock-down validation data are shown in Section 4.2.6.2. After 48 h of co-culture, the number of attached beads was scored. For comparison, the rate of bead attachment on control cells (DMEM-F12 S/F), non-targeting siRNA transfected, or mock transfected cells was used for negative controls.

The number of attached beads carrying IGF-I ($P=0.0002$) or OPN ($P<0.0001$) on IGF-IR siRNA transfected Ishikawa cells was significantly lower than that on control cells (Figure 4.24.A, C).

The rate of attachment of beads carrying HB-EGF on IGF-IR knocked-down Ishikawa cells was approximately 50% of the total number of beads originally transferred to the gel. Around 70% of beads bearing HB-EGF remained attached on cells in serum-free medium, non-targeting siRNA, or mock transfected cells. There was a significant reduction between the attachment rate on IGF-IR siRNA transfected cells and the rate on control ($P=0.0134$), non-targeting ($P=0.0208$), or mock (0.0149) transfected cells. However, these differences were lower than that observed with IGF-I or OPN-loaded beads (Figure 4.24.B).


A
IGF-I coated bead attachment assay
after IGF-IR knock-down
% of attached beads
carrying IGF-I
100
80
60
40
20
0
***
***
**
DMEM-F12 S/F
IGF-IR siRNA 100nM
non-targeting siRNA 100nM
MOCK
N=3, n of beads=323


B
HB-EGF coated bead attachment assay
after IGF-IR knock-down
% of attached beads
carrying HB-EGF
100
80
60
40
20
0
*
*
*
DMEM-F12 S/F
IGF-IR siRNA 100nM
non-targeting siRNA 100nM
MOCK
N=3, n of beads=304

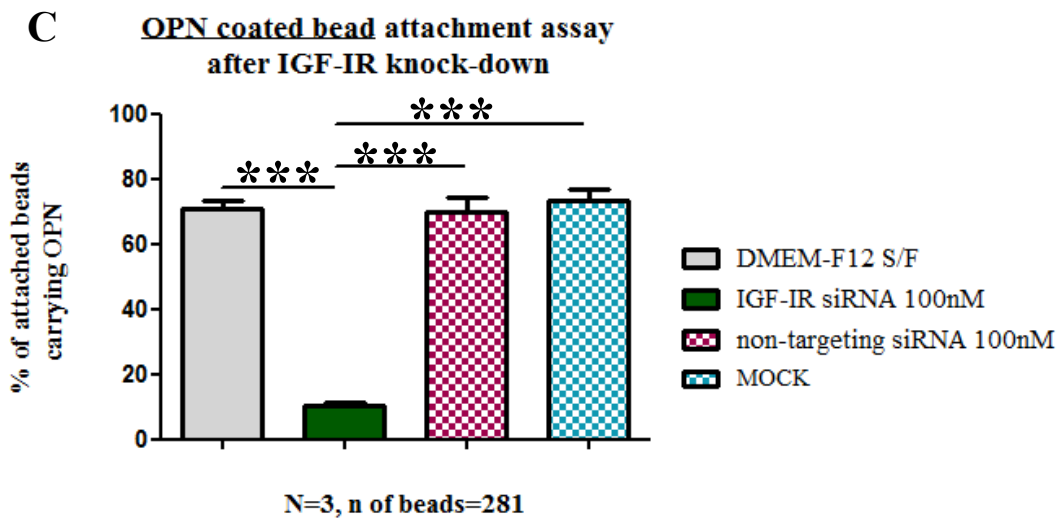


Figure 4.24: Attachment assay of beads carrying IGF-I, HB-EGF, or OPN on Ishikawa cells after knock-down of IGF-IR

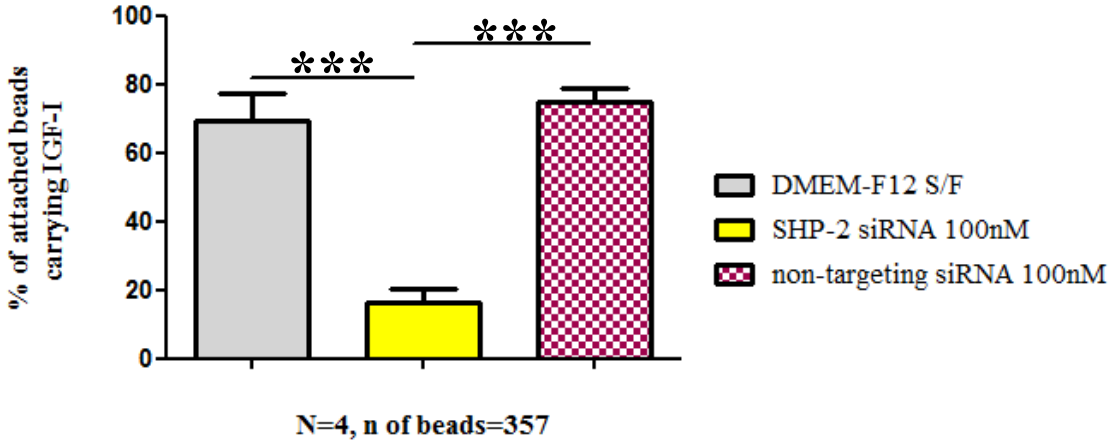
Mean proportions (3 different sets of experiments using 323 (IGF-I coated beads), 304 (HB-EGF coated beads) and 281 (OPN coated beads)) of attached beads after 48 h of co-culture on control, IGF-IR siRNA (100nM), non-targeting siRNA (100nM), or mock transfected cells. Asterisks (*; **; ***) on the histograms denote statistically significant differences ($P<0.05$) as determined by the student's t-test. Data are shown as mean ± SEM.

4.2.8.4 SiRNA-mediated knock-down of SHP-2 suppresses the attachment of beads bearing IGF-I, HB-EGF, or OPN

Bead attachment assays were performed on Ishikawa cells after the knock-down of SHP-2. Knock-down validation data are shown in Section 4.2.7.2. IGF-I (n=357), HB-EGF (n=386), or OPN (n=319) loaded beads were transferred to confluent Ishikawa cells transfected with SHP-2 siRNA. Forty eight hours after co-culture, an attachment assay was carried out.

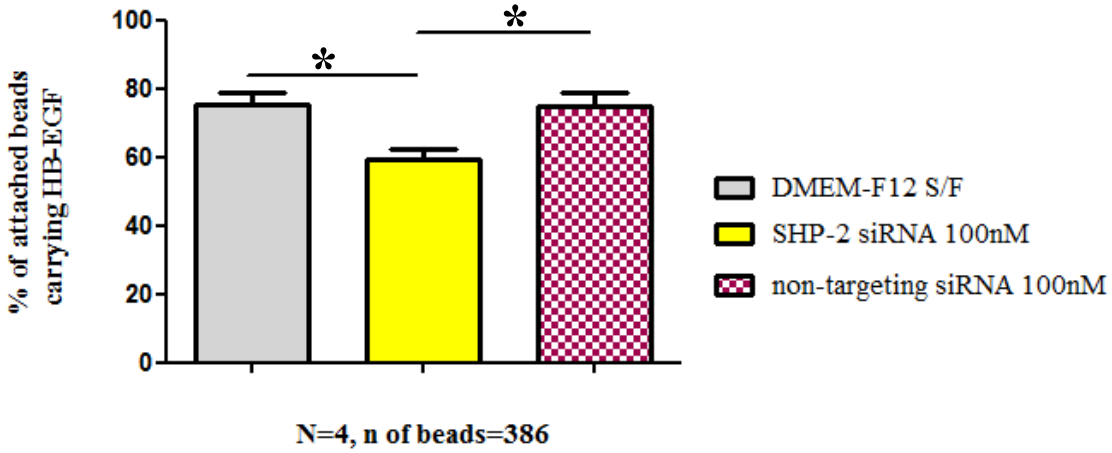
It was observed that the rate of attached beads bearing IGF-I ($P=0.0007$, Figure 4.25.A) or OPN ($P<0.0001$, Figure 4.25.C) on SHP-2 knocked-down cells was significantly lower than that on control cells. Furthermore, the number of attached beads bearing HB-EGF ($P=0.0167$, Figure 4.25.B) on SHP-2 siRNA transfected cells was significantly reduced compared to control cells. However, the significance in differences between the attachment rate of beads carrying IGF-I or OPN on SHP-2 siRNA transfected cells and the rate on control cells was higher than the significance for reduction in the attachment rate of beads carrying HB-EGF.

A **IGF-1 coated bead attachment assay after SHP-2 knock-down**



N=4, n of beads=357

B **HB-EGF coated bead attachment assay after SHP-2 knock-down**



N=4, n of beads=386

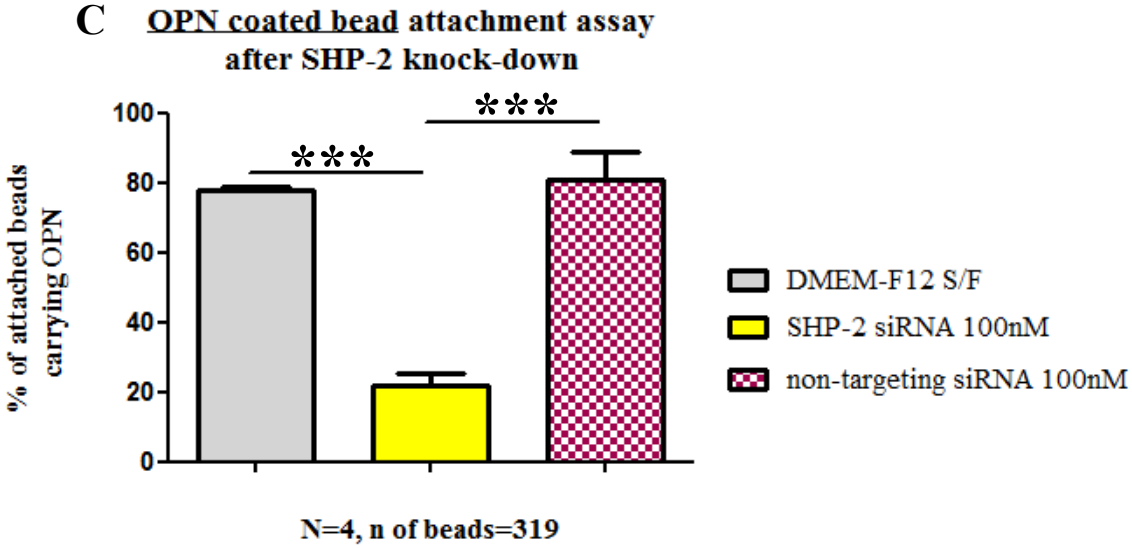


Figure 4.25: Attachment of beads carrying IGF-I, HB-EGF, or OPN, after knock-down of SHP-2

Mean proportions (4 different sets of experiments using 357 (IGF-I coated beads), 386 (HB-EGF coated beads) and 319 (OPN coated beads)) of attached beads after 48 h of co-culture on control, SHP-2 siRNA (100nM) transfected, or non-targeting siRNA (100nM) transfected cells. Asterisks (*;***) on the histograms denote statistically significant differences ($P<0.05$) as determined by the student's t-test. Data are shown as mean ± SEM.

4.3 Discussion

4.3.1 General summary of main results

Integrin αvβ3 was weakly expressed at the lateral side of Ishikawa cells and elevated in response to IGF-I or HB-EGF. Intracellular OPN moved toward the cell surface in response to IGF-I producing 70/45/25 kDa cleavage fragments, while no significant change in OPN was observed in response to HB-EGF. In order to investigate the localisation of OPN after cleavage events, the surface proteins of Ishikawa cells were biotinylated and isolated by co-immunoprecipitation. Cleaved OPN after IGF-I treatment was localised at the surface of cells and caspase, serine protease, cysteine protease, or MMP was not involved in the cleavage mechanism. However, a distinct pattern of cleavage was observed in the cells pre-treated with an inhibitor of caspase. OPN-coating promoted cell adhesion and thrombin enhanced OPN-induced cell adhesion and migration.

IGF-I receptor and ErbB4, a receptor for HB-EGF, were phosphorylated in Ishikawa cells in the presence of attaching embryos or in response to IGF-I or HB-EGF, respectively. SHP-2 was elevated when the cells were exposed to embryos or IGF-I, while no change was observed in response to HB-EGF. Multiple co-immunoprecipitation experiments demonstrated either direct or indirect association between integrin αvβ3, OPN, IGF-IR, and SHP-2 in response to IGF-I. IGF-IR was locally up-regulated near the embryo attachment site in Ishikawa cells, exhibiting vesicular localisation. SHP-2 was also locally elevated adjacent to attached embryos. Knock-down of either IGF-IR or SHP-2 suppressed

embryo attachment.

In order to investigate embryo-derived local growth factor effects in embryo attachment, embryo-sized beads were pre-absorbed with IGF-I, HB-EGF, or OPN and transferred onto Ishikawa cells. Ligand-conjugated beads were stably attached at 48 h of co-culture, while BSA-loaded beads were not attached. Co-culture with IGF-I or HB-EGF bearing beads induced increase of epithelial integrin β3 expression. IGF-I, HB-EGF, or OPN bearing beads were transferred onto the cells transfected with siRNA targeting integrin αvβ3, OPN, IGF-IR, or SHP-2, respectively.

Knock-down of integrin αvβ3 inhibited IGF-I, HB-EGF, or OPN-conjugated bead attachment and OPN knock-down in the cells suppressed attachment of IGF-I or OPN carrying beads, while HB-EGF carrying beads were not affected. Furthermore, knock-down of IGF-IR or SHP-2 suppressed attachment of all ligand conjugated beads, however, the extent of the reduction of attachment rates was different among IGF-I, HB-EGF, or OPN carrying beads.

4.3.2 The role of OPN in embryo attachment

It has been described that OPN has roles in the adhesion and migration of various cell types by interacting with different cell surface receptors of the integrin family, primarily integrin αvβ3 (Senger et al., 1989b; Brown et al., 1992; Liaw et al., 1998; Johnson et al., 2000; Apparao et al., 2001; Hotte et al., 2002; Quenby et al., 2007; Imano et al., 2009; Singh and Aplin, 2009). In the endometrium, OPN is modulated by progesterone, while integrin αvβ3 is regulated by estrogen or EGF, demonstrating increased expression in

both glandular and luminal epithelium during the mid to late secretory phase of the menstrual cycle (Somkuti et al., 1997; Apparao et al., 2001; Singh and Aplin, 2009). Since these molecules co-express in the human endometrium (Apparao et al., 2001), it has been suggested that OPN and integrin αvβ3 are very likely to be involved in the process of implantation (Apparao et al., 2001; von Wolff et al., 2001; Casals et al., 2010; Casals et al., 2012b).

Ishikawa cells express both integrin αvβ3 and OPN. Predominant expression of integrin αvβ3 at the lateral side, and cytoplasmic OPN expression in Ishikawa cells, is consistent with earlier findings from *in vivo* studies exhibiting basolateral and apical expression of integrin αvβ3, and the intercellular cytoplasmic expression of OPN (Quenby et al., 2007). Collectively, these data support the use of this cell line as an appropriate model of the normal epithelium of the endometrium.

Upon embryo attachment, OPN was locally increased near to the attached mouse embryo and up-regulation was observed in Ishikawa cells following IGF-I treatment. Interestingly, immunocytochemistry revealed translocation of OPN to the cell surface with prominent vesicle expression. Increased levels of IGF-I-induced OPN was predominantly observed at the surface of endometrial epithelial cells suggesting intracellularly localised OPN may have to move towards the apical cell surface. This pattern has been reported in *in vivo* studies showing the expression of apical secretory vesicles in the epithelium during the mid-secretory phase (Apparao et al., 2001; Hannan et al., 2011). Previous functional studies of OPN have shown that it promotes both the adhesion and migration of aortic smooth muscle cells which accompany the increased formation of focal adhesion plaques (Liaw et al., 2011). Consequently, it follows that cell surface OPN may interact with other cell surface receptors and mediate cell-cell adhesion or migration. Consistent with previous

studies, it was observed OPN promotes cell attachment exhibiting more cell colonies and outgrowth.

Western blot analysis of OPN revealed that in response to IGF-I, but not HB-EGF treatment, OPN is proteolytically cleaved predominantly producing 70, 45, and 25kDa fragments. Since IGF-I also promotes the movement of OPN to the cell surface, this may suggest that OPN cleavage products may be mediating the functional effects of OPN at the cell surface. This can be supported by Western blotting analysis with isolated extracts from the cell surface after biotinylation showing cleaved OPN product at the external side of cells during IGF-I stimulation. Biotinylation and affinity enrichment of proteins have been previously carried out in intestinal epithelial cells (Orru et al., 2003), primary trophoblast cells (Robinson et al., 2007), and brain tumour cells (Emerman et al., 2010). In this study, a similar approach was adopted to identify glycoproteins expressed on the apical cell surface. Thus, cleavage and translocation of OPN to the cell surface may be correlated and both events are related to cell attachment. Even though there is no record of the precise mechanism of OPN cleavage in the regulation of IGF-I, it has been reported that OPN promotes metastasis formation in cooperation with IGF-I in pulmonary cancer cells (Weber, 2001). It may be useful in future to develop an antibody which specifically detects the 45kDa OPN cleavage fragment in order to investigate its specific role during internalisation or translocation.

Johnson et al. (2003c) demonstrated that the 45kDa OPN fragment, a proteolytic cleavage fragment containing the RGD sequence is more biologically active and more stimulatory to cell attachment and migration than the native 70kDa OPN. In ovine endometrial epithelial cells, OPN cleavage following post-translational modification has been suggested to occur via thrombin or matrix metalloproteinases (MMPs) with cleaved

products binding to cell surface integrins to promote cell adhesion and migration (Agnihotri et al., 2001; Johnson et al., 2003b). Although the mechanism of OPN cleavage has not yet been studied specifically, the present finding that thrombin enhanced OPN-induced cell attachment and migration, producing stronger adhesion of Ishikawa cells, suggests that cleavage of OPN may be mediated by thrombin. This can be supported by a previous study of the role of thrombin cleavage site of OPN in cell adhesion and migration demonstrating that mutant OPN lacking the thrombin cleavage site in human breast tumour cells reduced OPN-mediated metastasis (Beausoleil et al., 2011). Furthermore, data demonstrating that MMP, serine, and caspase inhibitors were unable to block OPN cleavage suggests that some other, more complicated mechanisms may be involved in OPN cleavage, other than a simple thrombin-related mechanism.

Further complexity of the role of OPN in Ishikawa cells comes from experiments with OPN bearing beads attached to cells which suggested that OPN on beads binds to other molecules localised on the cell surface. The current findings showing that knock-down of integrin αvβ3 in cells inhibited OPN-coated bead attachment prove that integrin αvβ3 acts as a receptor of OPN. Surprisingly, OPN-coated bead attachment is also suppressed by knock-down of the OPN gene in Ishikawa cells. This may suggest that OPN can interact with itself in order to adopt an OPN-OPN homotypic dimerised configuration in order to mediate cell attachment with higher tensile strength (Goldsmith et al., 2002).

Taken together, a local growth factor, possibly IGF-I (Spaventi et al., 1990; Fluhr et al., 2008), may stimulate the cleavage of OPN and its transport to the cell surface in order to create a receptive state in the endometrium and at the same time to promote interaction between the two different integrins of the endometrial epithelium and embryo, respectively, thus acting as a bridging molecule. It would be interesting to investigate the

role of each cleaved OPN fragment in regulating cell-cell interaction in *in vitro* and also *in vivo* studies using intrauterine injection of the OPN 45kDa cleaved fragment. Such studies would be valuable in confirming the biological activity of OPN cleavage product in embryo implantation.

4.3.3 The role of IGF-I-integrin αvβ3-SHP-2 in embryo attachment

During implantation, IGF-I is considered as one of the paracrine factors secreted from the embryo when it attaches to the endometrial epithelium. It has been shown previously that increased levels of IGF-I in culture media surrounding developing mouse embryos suggesting that embryos secrete IGF-I during embryogenesis (Spaventi et al., 1990; Pavelic et al., 1991). The autocrine and paracrine activities of IGF-I have been suggested to mediate cell growth and proliferation in mouse blastocyst (Pantaleon and Kaye, 1996). Moreover, IGF-I-loaded beads transferred to pseudopregnant mouse uteri induced local implantation-like responses (Paria et al., 2001).

Although the specific role of IGF-I in regulating embryo implantation has not yet been reported, IGF-I is a well-known potent regulator of stimulating cell proliferation and inhibiting apoptosis in various cell types (Galvan et al., 2003; Shukla et al., 2009) and is mediated by the binding of IGF-I to IGF-IR tyrosine kinase resulting in phosphorylation and activation of the receptor (Lammers et al., 1989; Jones et al., 1996; Gan et al., 2010) and recruitment of SHP-2 to IGF-IR in order to activate down-stream molecules such as MAPK (Maile and Clemmons, 2002), thus suggesting that this process may also occur during embryo attachment.

This hypothesis is supported by observations that cells co-cultured with mouse embryos induced local up-regulation of IGF-IR exhibiting movement to the cell surface adjacent to the attachment site, while increased expression of SHP-2 was also observed near attached embryos. Western blotting analysis also revealed that higher levels of IGF-IR phosphorylation, and greater expression of SHP-2, were induced in cells exposed to 5 mouse embryos in a single well from a 24-well plate compared to that of control cells. Similarly, the individual reactions observed in Ishikawa cells exposed to IGF-I exhibited increased levels of IGF-IR phosphorylation and elevated levels of SHP-2.

In addition to enhanced expression and activation of IGF-IR and SHP-2 in endometrial epithelial cells, the IGF-I-conjugated beads attached to cells; this suggests that IGF-I on the surface of beads binds to cell surface receptors on the endometrium in order to mediate attachment. Knock-down of IGF-IR inhibited the attachment of both mouse embryos and beads bearing IGF-I while these attachments were also suppressed by knock-down of SHP-2. This might imply that IGF-I secreted from the implanting embryo activates IGF-IR and that IGF-I-transmitted signals to down-stream factors via IGF-IR activation are involved in mechanisms which regulate attachment and adhesion of the embryo to the endometrial epithelium. Furthermore, this suggests that SHP-2 seems to have a role in regulating embryo attachment during implantation directly via the IGF-I-IGF-IR axis.

In vitro studies of smooth muscle cells have demonstrated that the occupancy of integrin αvβ3 upon binding to its ligand regulates the duration and extent of activation on IGF-IR in response to IGF-I by altering the rate of recruitment of SHP-2 phosphatase to IGF-IR (Kuemmerle, 2006). In the present study, IGF-I stimulation induced an increase of integrin αvβ3 and the cleavage of OPN in Ishikawa cells while also promoting both

integrin αvβ3 and OPN movement towards the apical cell surface. This is consistent with the findings that both integrin αvβ3 and the 45kDa OPN cleavage product were increased in cells including embryo attachment and exhibiting translocation to the surface. It may be postulated that IGF-I promotes interaction between integrin αvβ3 and the cleaved OPN fragment by transporting them to the cell surface. Evidence for this comes from observations that co-culture with IGF-I-loaded beads induced increased levels of integrin β3 expression and that the attachment of IGF-I carrying beads was suppressed following knock-down of integrin αvβ3 or OPN in endometrial cells. Although further work will be required to clarify the exact role of IGF-I in the mutual interaction between the embryo and endometrium by *in vitro* studies using embryos depleted of the IGF-I gene, this may also imply that IGF-I requires the activation of integrin αvβ3 upon binding to an active form of OPN at the cell surface in order to transmit its signal and activate down-stream molecules and mediate embryo attachment.

4.3.4 The role of HB-EGF-ErbB4-integrin αvβ3 in embryo attachment

It is well established that HB-EGF is involved in the mechanism of embryo implantation, and appears on the apical cell surface of the receptive endometrial epithelium immediately prior to implantation (Das et al., 1994). Paria et al. (2001) demonstrated that HB-EGF-loaded beads transferred into mouse uterine horns induced local responses elicited by the blastocyst, including increased vascular permeability, decidualisation, and the appearance of Bmp-2 at the site of beads attachment. It can therefore be hypothesised that HB-EGF is secreted from both the attaching embryo and the receptive endometrium acting as a juxtacrine or paracrine signalling mediator to mediate the primary event of

embryo attachment by binding to its receptors, ErbB1 or ErbB4 and to activate additional molecules required for the initiation of down-stream processes (Raab et al., 1996; Nishi and Klagsbrun, 2004). This is supported by current observations showing that upon embryo attachment, HB-EGF was up-regulated near the attachment site with an increased level of ErbB4 phosphorylation. Cells stimulated by soluble HB-EGF also induced the phosphorylation of ErbB4 in Ishikawa cells. The expression of both HB-EGF and its receptor ErbB4 on the surface of endometrial epithelial cells and trophectoderm of the embryo (Chobotova et al., 2002; Wang et al., 2002) may suggest its orchestral "two-way" molecular signalling between the embryo and the endometrium.

Immunofluorescence analysis of integrin αvβ3 and OPN in response to HB-EGF showing increased integrin αvβ3 at the apical and lateral side of cells, and along with persistent weak cytoplasmic OPN staining compared to controls, may suggest that integrin αvβ3 is regulated in response to HB-EGF by transporting it to the cell surface but that OPN is not affected by HB-EGF. This is supported by the findings that cleaved OPN was not produced in response to HB-EGF compared to the cleavage and translocation of OPN to the cell surface in response to IGF-I. This indicates that the interaction between integrin αvβ3 and OPN at the cell surface is not directly regulated by the HB-EGF-ErbB4 axis.

HB-EGF-loaded beads successfully attached to Ishikawa cells. HB-EGF on the surface of beads may be secreted and bound to cell surface components in order to mediate attachment. Consistent with the previous findings, knock-down of integrin αvβ3 in cells suppressed the attachment of bead bearing HB-EGF, while attachment of HB-EGF-loaded beads was not interrupted in cells in which OPN was knocked-down. Although the mechanism of how HB-EGF associates with adhesion molecules has yet to be studied in the endometrium, it has been reported that HB-EGF modulates epithelial integrins in breast

cancer cells to mediate metastasis by enhancing the transmigration of cancer cells to extravascular tissues (Narita et al., 1996). It can be postulated then that the local increase of HB-EGF secreted from the attaching embryo binds to its receptor resulting in receptor activation and the subsequent elevation of epithelial integrin αvβ3 on the apical site of cells in order to promote interaction with other adhesion molecules on the surface of embryo that transmit signals and activate down-stream molecules including MAPK and AKT to mediate embryo attachment. Indeed, Yarden and Sliwkowski (2001) hypothesised that HB-EGF activates further down-stream pathways including PI3K/AKT and/or MAPK signalling by activating its receptors, ErbB1/4, in order to promote cell growth, survival and proliferation. Furthermore, metalloprotease-mediated ectodomain shedding of HB-EGF and its binding to ErbB receptors have been demonstrated to be critical to activate PI3K/AKT pathways regulating both cell-cell adhesion and migration in ovarian cancer cells (Tsujioka et al., 2011) as well as to activate the mammalian target of mTOR pathway through ERK1/2 phosphorylation (Li et al., 2012).

4.3.5 The role of molecular crosstalk regulating embryo attachment

In the present study, data suggest that the interaction between integrin αvβ3 and OPN is regulated by IGF-I and/or HB-EGF and that such interaction is strongly involved in the mechanisms mediating embryo attachment. The interaction between integrin αvβ3 and OPN remains stable in the presence of either IGF-I or HB-EGF. This may indicate that integrin αvβ3 acts as a ligand for OPN as a primary receptor in any conditions. The level of association between IGF-IR and integrin αvβ3 was reduced, while the interaction between

IGF-IR and SHP-2 was slightly elevated in response to IGF-I. Furthermore, the association of IGF-IR with OPN appears following IGF-I exposure. Although further clarification is crucial, protein-protein interaction analysis might suggest that IGF-I secreted by the attaching embryo activates IGF-IR and dissociates it from the complex with integrin αvβ3 in order to activate down-stream signalling by recruiting more SHP-2 to IGF-IR to eventually mediate embryo attachment. The level of association of OPN with SHP-2 was increased with IGF-I stimulation. This was supported by observations that OPN-loaded bead attachment is inhibited by the knock-down of SHP-2 in cells. An explanation for this might be that depletion of the SHP-2 gene inhibits embryo attachment by blocking its association with the integrin αvβ3-OPN complex as well as its recruitment to the IGF-IR. Despite the lack of association between OPN and IGF-IR, OPN-loaded bead attachment was suppressed by the knock-down of IGF-IR in Ishikawa cells, suggesting that both OPN and IGF-IR are regulated by IGF-I as discussed earlier. However, these two mechanisms may be related via some other, as yet unknown mediators. Interestingly, the knock-down of IGF-IR or SHP-2 suppressed the attachment of beads carrying HB-EGF. This may be consistent with previous preliminary data reporting that the level of association between integrin αvβ3 and IGF-IR altered in response to HB-EGF stimulation. This can be supported by the studies of Mulligan et al. (2002) who described a novel pathway by demonstrating that IGF-I-induced IGF-IR activation stimulates transcription of the HB-EGF gene resulting in HB-EGF protein that is capable of stimulating MAPK phosphorylation and cell proliferation via activation of EGFR (ErbB1). Furthermore, a previous study investigating crosstalk between the IGF-I and EGF receptor was mediated by a mechanism involving the MMP-dependent release of HB-EGF in an autocrine manner in response to IGF-I and showing that IGF-I-mediated MAPK activation is inhibited by an

inhibitor of HB-EGF (Roudabush et al., 2000). This may also suggest the role of HB-EGF as a mediator of the MAPK cascade in response to IGF-I via the activation of IGF-IR as well as IGF-I-stimulated Shc phosphorylation in order to mediate cell proliferation.

4.3.6 Concluding remarks

Collectively, evidence now supports the roles of both IGF-I-IGF-IR and HB-EGF-ErbB4 axes during embryo attachment regulating the interaction between integrin αvβ3 and OPN. Presumably, embryo-derived IGF-I and HB-EGF are crucial in mediating the orchestral mechanisms regulating embryo attachment, although further studies will be required to clarify this beyond doubt. The most interesting results however, were observed in examining the regulation of OPN in response to IGF-I and/or HB-EGF and its association with down-stream molecules of IGF-I or HB-EGF signalling. Further work will be essential to investigate down-stream networks activated by the ligation of integrin αvβ3 with either IGF-I or HB-EGF signalling as well as the molecular reactions involved in the local response to combined stimulation by IGF-I and HB-EGF. Additionally, it will be of interest to examine the potential impact of other growth factors and other adhesion molecules on this process.



CHAPTER 5

General Discussion & Future Work

5.1 General discussion

Extensive research has been performed to investigate the mechanisms by which infertility is caused in women; altered folliculogenesis, poor oocyte quality, reduced fertilisation, abnormal embryogenesis, or aberrant endometrial receptivity (Gupta et al., 2008; Casals et al., 2012b). All of these factors are known to reduce the capacity of implantation, fundamental biological events.

Despite phenomenal improvements in assisted reproductive technology (ART) over recent years, only 25-30% of cycles result in successful pregnancy (de los Santos et al., 2003; de Mouzon et al., 2010). A predominant factor underlying poor ART success rates is considered to be implantation failure (Margalioth et al., 2006; Marhuenda-Egea et al., 2010). In order to improve the probability for a successful ART procedure, many clinicians have used more than one embryo per cycle (Lukassen et al., 2005; Grady et al., 2012a). However, this caused increased rates of maternal and fetal complications associated with multiple-infant births including higher rates of caesarean section, prematurity, low birth weight, and infant disability or death (van Montfoort et al., 2006; Grady et al., 2012b). Recent report suggested that elective single embryo transfer lowers the risk of poor perinatal outcomes associated with ART and addressed the importance of research to improve implantation rate for a single embryo transfer (Min et al., 2010; Grady et al., 2012a). Furthermore, many techniques have been developed over recent years to improve embryo quality and to assist embryo hatching in order to maximise the chances of successful implantation during ART treatment. However, the efficacy of these techniques is

still insufficient (Marhuenda-Egea et al., 2010). Although studies to examine the mechanism of implantation are limited by the inaccessibility of the implantation site, such studies may both enhance our understanding of normal embryo implantation while also increasing our understanding of how this process is altered in infertility.

Therefore, this study attempted to address crosstalk between the attaching embryo and receptive endometrium by establishing *in vitro* models and investigating individual molecular mechanisms which mediate embryo attachment in order to provide potential therapeutic applications to improve the rate of implantation.

5.2 Recapitulation of the key phases of embryo attachment *in vitro*

Both mouse and human embryos exhibit sequential stages of embryo attachment beginning with a weak initial attachment and subsequent to this, stable adhesion. Shiotani et al. (1993) suggested that cell surface glycoconjugates may play an important role in mediating initial attachment of the embryo onto epithelium by demonstrating the attachment of mouse embryo without direct membrane-membrane contact. In Chapter 3 of the current study, embryos showed initial weak interaction with epithelial cells but this was not always strong enough for the embryo to maintain position. This was described as Stage 2 stability in accordance with a standard classification scheme for embryo attachment and modified from (Carver et al., 2003). Subsequent adhesion stages exhibiting persistence of attachment position and clear outgrowth of the embryonic trophectoderm, described as Stage 3, 4, and 5, were also clearly observed. Apposition of the embryo has not been

observed in the human (Hertig et al., 1956) and other primates (Enders et al., 1983) due to the highly transient and tenuous interaction between the embryo and endometrial epithelium. High rates of stable embryo attachment observed in the *in vitro* models developed during the current study suggested the involvement of multiple ligand interactions between the embryo and endometrium.

Both mouse and human embryos induced alterations in local epithelial phenotypes by exhibiting the clearance of MUC1 and increased expression of integrin αvβ3, OPN, SHP-2, IGF-IR and HB-EGF adjacent to embryo attachment sites. Interestingly, the alteration of distribution for these molecules occurred across a similar area in all *in vitro* models suggesting that the links may exist between these molecules and that all molecular distributional changes may occur in response to common embryonic signals.

5.3 Embryo-uterine crosstalk

I hypothesised the embryo-derived paracrine factors, IGF-I and/or HB-EGF (Spaventi et al., 1990; Paria et al., 2001; Wang et al., 2002; Fluhr et al., 2008), may stimulate the local expression of epithelial integrin αvβ3 and OPN and also promote their interaction at the apical cell surface. In the current study, it was determined that OPN produced a biologically active fragment after post-translational modification events, possibly thrombin-derived proteolytic cleavage (Senger et al., 1995; Senger and Perruzzi, 1996; Mi et al., 2007; Beausoleil et al., 2011). The 45kD fragment of OPN, which was observed at the apical cell surface, appears to be an important mediator of cell-cell adhesion and migration by interacting with integrin αvβ3. Elevation in the levels of both integrin αvβ3 and OPN expression, and translocation of both molecules to the apical cell

surface, strongly indicates that integrin αvβ3-OPN interaction at the cell surface plays an important role in creating endometrial receptivity, as well as embryo attachment.

OPN, and its association with integrin αvβ3, may be involved in the initiation of uterine epithelial cell remodelling at the embryo attachment site, therby inducing epithelial displacement, as illustrated in Figure 1.3, Stage 5. Restructuring of numerous actin cytoskeleton and membrane-binding proteins are known to be involved in uterine epithelial cell remodellings (Terry et al., 1996; Lecce et al., 2011). Lecce et al. (2011) reported the involvement of cytoskeletal proteins including ezrin and ezrin-radixin-moesin-binding protein 50-kDa (EBP50) in the plasma membrane transformation of uterine epithelial cells. These authours demonstrated increased expression of ezrin and EBP-50 in abundance at the rat embryo implantation site in response to embryo attachment, thereby facilitating uterine receptivity and embryo-epithelial adhesion. Such effects were absent at inter-implantation sites, thereby permitting subsequent invasion to the stroma. Heng et al. (2011) suggested that proprotein convertase 5/6 (PC6), a serine protease of the proprotein convertase family, plays an important role in regulating the mechanisms of epithelial remodelling, such as plasma membrane transformation and reorganisation of the membrane-cytoskeletal interface, during implantation. This enzyme is known to cause its effect by causing cleavage of a scaffolding protein, EBP50 and by regulating interaction between ezrin and EBP50. Distribution of other cytoskeletal proteins, such as talin, paxillin, and vinculin are also involved in epithelial tissue integrity (DeMali et al., 2003; Kaneko et al., 2009). Additionally, adhesion molecules are redistributed in order to mediate embryo-epithelial adhesion (Aplin, 1997); the current study observed in Chapter 4 that both integrin αvβ3 and OPN were translocated to the apical membrane. Upon ligand occupancy of integrin αvβ3 with OPN, intracellular components may be stimulated via actin

cytoskeletal activation to promote the migration of both uterine epithelial and embryonic cells. IGF-I stimulation may also allow the initiation of cytoskeletal interactions by dissociation of the IGF-IR-SHP-2 complex from the integrin αvβ3-OPN complex.

ADAM 17 or MMP 14 has been reported as a MUC 1 sheddase, a membrane-bound enzyme, which cleaves MUC1 into two fragments and subsequently inducing release of the extracellular domain of MUC1 (Aplin, 2006), as discussed in Chapter 3. ADAM 17 has previously been shown at increased levels near the attachment site of rabbit embryos *in vivo* coincident with the loss of MUC1, suggesting the involvement of ADAM 17 in local MUC1 regulation (Olson et al., 1998; Aplin, 2006). It has also been demonstrated that IGF-I caused an increase in MMP 14 expression and promoted its proteolytic cleavage activity to secrete mucin in epithelial cells of the human airway (Deshmukh et al., 2009). This may indicate that embryo-derived IGF-I is involved in the mechanisms underlying local MUC1 clearance at the embryo attachment site by boosting the activity of embryo-derived MMP 14. Further work is required to elucidate the mechanisms by which surface clearance of MUC1 is stimulated locally by attaching embryos.

5.4 A novel *in vitro* embryo attachment assay

In order to gain more evidence of the molecular mechanisms underlying successful implantation, a novel *in vitro* model was devised in which implanting embryos were replaced by microbeads carrying several candidate embryo-derived paracrine factors, IGF-I or HB-EGF, or OPN; a primary ligand to integrin αvβ3. This *in vitro* model allowed the study of early tenuous attachment and subsequent stable adhesion, which remarkably

resembled the behaviour of embryos. This novel system permitted dissection of the whole molecular system mediating embryo attachment down to individual mechanisms relating to growth factors such as IGF-I or HB-EGF and extracellular molecules. In each case, ligand-conjugated beads first became tenuously attached, and then stably attached, to the apical surface of confluent epithelial cells. The functionality of ligand-conjugated beads *in vitro* has been confirmed by *in vivo* mouse studies. IGF-I- or HB-EGF-soaked beads transferred to mouse uterine horns induced local responses elicited by the implanting embryo, such as increased vascular permeability and decidualisation at the attachment site (Paria et al., 2001).

5.5 IGF-integrin αvβ3-HB-EGF signalling

SiRNA-mediated knock-down of αvβ3 drastically inhibited the attachment of embryos or beads bearing either IGF-I, HB-EGF or OPN. Embryo attachment was highly suppressed by OPN knock-down in cells and the same pattern of inhibition was observed with attachment of IGF-I or OPN-loaded beads, but not with beads bearing HB-EGF. When IGF-IR or SHP-2 was knocked down, mouse embryo attachment was significantly suppressed. Beads bearing IGF-I or OPN were also inhibited from attaching to cells, while beads bearing HB-EGF showed less significant reduction in the rate of attachment, compared to IGF-I or OPN-loaded beads.

Parallel protein-protein interaction studies further revealed that integrin αvβ3 is associated with OPN, IGF-IR, and SHP-2 and that the level of association between these molecules was altered in response to IGF-I stimulation. This may suggest that embryo-derived factor, IGF-I, activates IGF-IR and dissociates it from the integrin αvβ3-OPN

complex to activate downstream signalling by recruiting SHP-2 to IGF-IR in order to mediate embryo attachment. Further work is required to clarify and overcome the limitations of signalling studies caused by the wide time window that embryos or beads need with which pass through the stages occurring from weak to stable attachment.

It may be postulated that embryo-derived IGF-I and/or HB-EGF stimulate the interaction between integrin αvβ3 and OPN by increasing in abundance and triggering the translocation of both molecules to the apical cell surface following OPN cleavage to produce a biologically active 45kDa fragment. Binding of OPN to integrin αvβ3 mediates intracellular signal transduction through actin cytoskeletal activation. Upon IGF-I and/or HB-EGF stimulation, their respective receptors are activated and signal transmission to down-stream components, including PI3K/AKT or MAP kinase via receptor activation, and recruitment of the IGF-IR-SHP-2 complex to the membrane, facilitates the motility of both embryonic and endometrial cells and ultimately regulates attachment and adhesion of the embryo to the uterine epithelium. Further understanding of the molecular factors inducing the association between these molecules as well as the localisation of these complexes, will be crucial. A summary of the findings from the current study is illustrated in Figure 5.1.

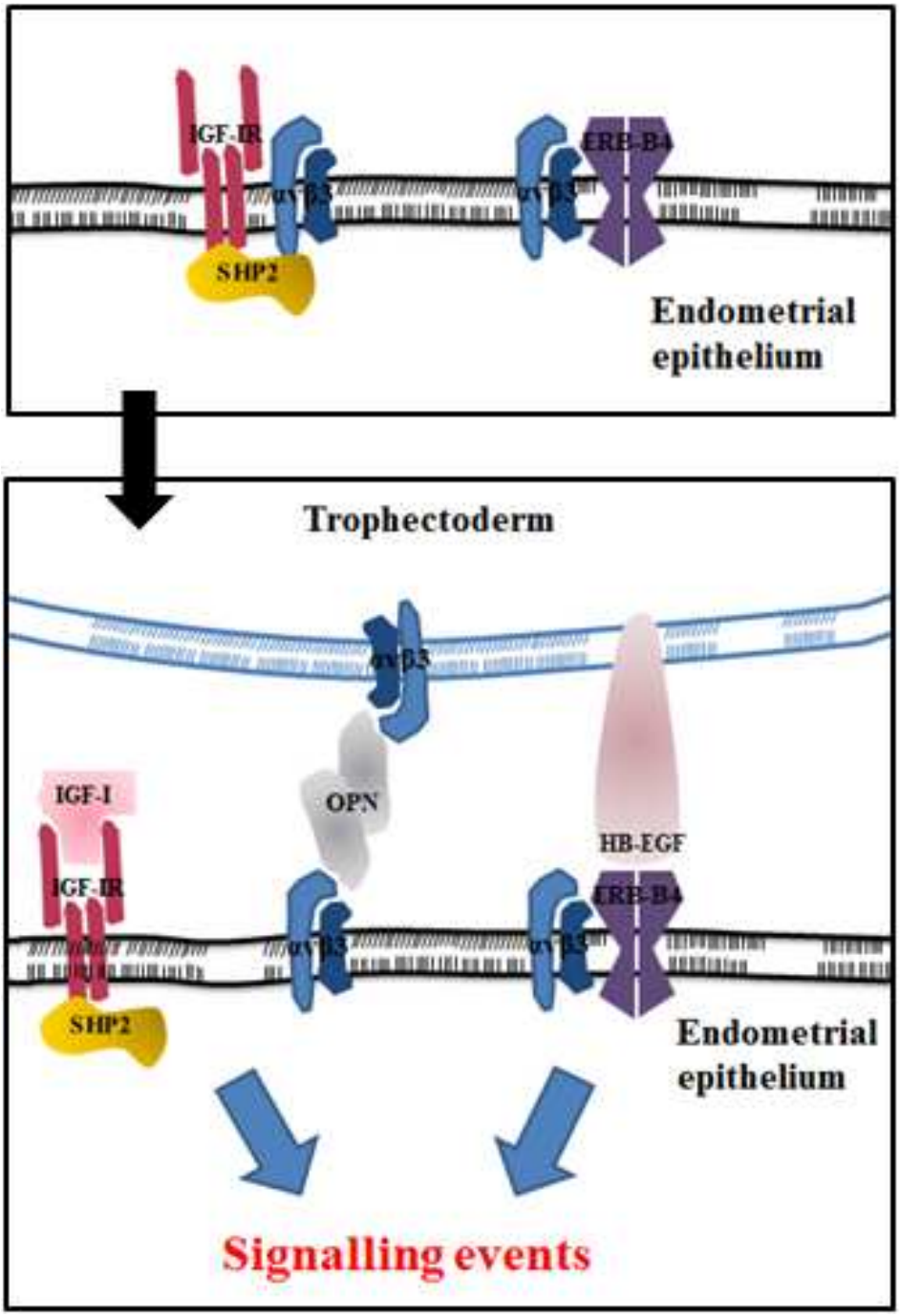


Figure 5.1: Schematic summary of key findings from the present study

Schematic diagrams illustrating two independent signalling pathways, including IGF-I-integrin αvβ3-OPN and integrin αvβ3-HB-EGF axes, to mediate embryo-epithelial adhesion at implantation, created by Professor John Aplin and modified by the Author.

5.6 Clinical implications of integrin αvβ3-OPN as a potential biomarker for infertility

Implantation failure has been reported as a major contributor to the low rate of successful outcomes of both normal pregnancies and pregnancies from ART (Margalioth et al., 2006; Ly et al., 2010). There are several factors leading to the failure of implantation, including embryonic defects, aberrantly differentiated or unreceptive endometrium, and unsuccessful interaction between the embryo and endometrium (Levi Setti et al., 2004; Quenby et al., 2007; Ly et al., 2010).

Abnormal endometrial receptivity accounts for a significant proportion of cases of unexplained infertility in women. Lack of integrin β3 (Graham et al., 1990; Lessey et al., 1995), IGF-IR (Wu and Zhou, 2002), or HB-EGF-ErbB4 (Aghajanova et al., 2008), in the endometrium has been reported to be associated with unexplained infertility.

Polycystic ovary syndrome (PCOS) has also been reported as a cause of infertility in women who undergo oligo-ovulation or anovulation (Adams et al., 2004). Furthermore, IGF-I has been reported to play an important role during oocyte maturation in the PCOS condition (Schoyer et al., 2007). Additionally, chronically elevated levels of androgen induced by the excessive activity of insulin and IGFs via IGF-IR (Lopes et al., 2011) may result in endometrial defects with significant reduction in OPN expression and cell-cell adhesion during implantation. Moreover, samples of an infertile endometrium with PCOS showed reduced levels of HOXA-10, a potential up-stream regulator of integrin αvβ3, during the mid-secretory phase (Apparao et al., 2003; Cermik et al., 2003). This may indicate aberrant interaction of IGF-integrin αvβ3-OPN as a main cause of infertility in PCOS.

Moreover, failure to achieve on-time implantation caused by luteal phase deficiency is another risk factor for normal pregnancy outcome, resulting in spontaneous pregnancy losses (Wilcox et al., 1999). Luteal phase deficiency is asynchronous timing between progesterone-induced endometrial differentiation leading to the delay of endometrial maturation and arrival of the embryo into the uterine cavity (Lessey, 1998). Progesterone responsive integrin αvβ3 and OPN are therefore delayed and consequently fail to establish the endometrial receptivity in time for the implanting embryo.

Considering the evidence from recent studies together, collectively, it follows that aberrant expression of integrin αvβ3-OPN in the endometrium is highly associated with impaired implantation, as it was observed in the present study that deficiency of integrin αvβ3 or OPN in endometrial epithelial cells suppressed embryo attachment *in vitro*. This suggests that improving integrin αvβ3-OPN interaction in the endometrium during the window of implantation could be a potential therapeutic option and indicates that acquiring more detailed understanding of intracellular signalling events derived from αvβ3-OPN interaction will be crucial in improving pregnancy rates. Although preliminary, and in need of more extensive study, the present data highlighted the potential roles of IGF-IR and SHP-2 in regulating embryo implantation and therefore suggests that these molecules may represent useful novel biomarkers to assist the advancement of ART.

5.7 Future directives and general conclusion

Despite the phenomenal growth, and technological development of ART, emerging evidence of implantation rate continues to be modest at best. It is therefore critical to gain further understanding of the micro-environment created by the endometrium, and the

biological processes and signalling pathways between the embryo and endometrium that occur during the window of implantation. Data arising from such studies are vital if implantation rates are to be improved in the future.

The present study utilised siRNA technology to determine the effect of knocking-down specific genes in the IGF-I-integrin αvβ3-OPN and integrin αvβ3-HB-EGF axes. Application of selectable plasmid-based shRNA constructs targeting integrin αvβ3, OPN, SHP-2, IGF-IR, or ErbB4, could achieve full or partial, but stable knock-down of interesting genes compared to the outcomes from the utilisation of siRNA, and thus generate endometrial defects with strong or mild impairment to simulate clinical conditions. Embryo or ligand-conjugated bead attachment assays following shRNA transfection will provide more details of individual molecular mechanisms in regulating embryo attachment, as well as providing opportunities to develop patient-tailored therapeutic methods.

Although, the bead attachment assay developed herein provides a highly useful tool with which to investigate molecular mechanisms associated with implantation, it does not allow us to investigate mutual interaction between the embryo and epithelium. One way to overcome this limitation would be to use mouse embryos deficient in the IGF-I or HB-EGF gene. Such embryos could be transferred onto either normal endometrial cells or those modified by knock-down of specific genes.

As observed, soluble IGF-I and/or HB-EGF stimulation promote interaction between integrin αvβ3 and cleaved OPN at the cell surface, therefore, the addition of soluble IGF-I and/or HB-EGF, or the cleaved OPN fragment to cells impaired by gene manipulation would help us to test the capacity for improvement in embryo attachment. Intrauterine delivery of candidate additives, such as IGF-I or HB-EGF would promote

adhesion factors in the epithelium. For example, cationised gelatin nanoparticles have been confirmed as an efficient delivery method of plasmids including IGF-I in other systems (Xu et al., 2008). Delivery of constructs including the integrin αvβ3-OPN complex or SHP-2 to the endometrium using nanoparticles (Feng, 2006; Liang et al., 2011) to overcome the lack of their expression on uterine epithelium could possibly boost the process of implantation by shortening the duration taken for the embryo to attach stably on the endometrium and ultimately increase the rate of implantation, especially in patients with repeated implantation failure.

To our knowledge, the present study describes a novel mechanism mediating embryo attachment. The use of *in vitro* models developed herein provides an excellent opportunity for further research targeting an increased understanding of embryo implantation. Such studies could yield improvements to the treatment of female infertility and permit the development of novel diagnostic biomarkers for evaluating uterine receptivity.



References

ACHACHE, H. & REVEL, A. 2006. Endometrial receptivity markers, the journey to successful embryo implantation. *Hum Reprod Update,* 12**,** 731-46.

ADAMS, J. M., TAYLOR, A. E., CROWLEY, W. F., JR. & HALL, J. E. 2004. Polycystic ovarian morphology with regular ovulatory cycles: insights into the pathophysiology of polycystic ovarian syndrome. *J Clin Endocrinol Metab,* 89**,** 4343-50.

AGHAJANOVA, L., BJURESTEN, K., ALTMAE, S., LANDGREN, B. M. & STAVREUS-EVERS, A. 2008. HB-EGF but not amphiregulin or their receptors HER1 and HER4 is altered in endometrium of women with unexplained infertility. *Reprod Sci,* 15**,** 484-92.

AGNIHOTRI, R., CRAWFORD, H. C., HARO, H., MATRISIAN, L. M., HAVRDA, M. C. & LIAW, L. 2001. Osteopontin, a novel substrate for matrix metalloproteinase-3 (stromelysin-1) and matrix metalloproteinase-7 (matrilysin). *J Biol Chem,* 276**,** 28261-7.

AHMED, M., BEHERA, R., CHAKRABORTY, G., JAIN, S., KUMAR, V., SHARMA, P., BULBULE, A., KALE, S., KUMAR, S., MISHRA, R., RAJA, R., SARASWATI, S., KAUR, R., SOUNDARARAJAN, G., KUMAR, D., THORAT, D., SANYAL, M., RAMDASI, A., GHOSH, P. & KUNDU, G. C. 2011. Osteopontin: a potentially important therapeutic target in cancer. *Expert Opin Ther Targets,* 15**,** 1113-26.

ANTHIS, N. J. & CAMPBELL, I. D. 2011. The tail of integrin activation. *Trends Biochem Sci,* 36**,** 191-8.

APLIN, J. D. 1997. Adhesion molecules in implantation. *Rev Reprod,* 2**,** 84-93.

APLIN, J. D. 2006. Embryo implantation: the molecular mechanism remains elusive. *Reprod Biomed Online,* 13**,** 833-9.

APLIN, J. D. & HEY, N. A. 1995. MUC1, endometrium and embryo implantation. *Biochem Soc Trans,* 23**,** 826-31.

APLIN, J. D., HEY, N. A. & GRAHAM, R. A. 1998. Human endometrial MUC1 carries keratan sulfate: characteristic glycoforms in the luminal epithelium at receptivity. *Glycobiology,* 8**,** 269-76.

APLIN, J. D., HEY, N. A. & LI, T. C. 1996a. MUC1 as a cell surface and secretory component of endometrial epithelium: reduced levels in recurrent miscarriage. *Am J Reprod Immunol,* 35**,** 261-6.

APLIN, J. D. & KIMBER, S. J. 2004. Trophoblast-uterine interactions at implantation. *Reprod Biol Endocrinol,* 2**,** 48.

APLIN, J. D., MESEGUER, M., SIMON, C., ORTIZ, M. E., CROXATTO, H. & JONES, C. J. 2001. MUC1, glycans and the cell-surface barrier to embryo implantation. *Biochem Soc Trans,* 29**,** 153-6.

APLIN, J. D., SEIF, M. W., GRAHAM, R. A., HEY, N. A., BEHZAD, F. & CAMPBELL, S. 1994. The endometrial cell surface and implantation. Expression of the polymorphic mucin MUC-1 and adhesion molecules during the endometrial cycle. *Ann N Y Acad Sci,* 734**,** 103-21.

APLIN, J. D. & SINGH, H. 2008. Bioinformatics and transcriptomics studies of early implantation. *Ann N Y Acad Sci,* 1127**,** 116-20.

APLIN, J. D., SPANSWICK, C., BEHZAD, F., KIMBER, S. J. & VICOVAC, L. 1996b. Integrins beta 5, beta 3 and alpha v are apically distributed in endometrial epithelium. *Mol Hum Reprod,* 2**,** 527-34.

APPARAO, K. B., ILLERA, M. J., BEYLER, S. A., OLSON, G. E., OSTEEN, K. G., CORJAY, M. H., BOGGESS, K. & LESSEY, B. A. 2003. Regulated expression of osteopontin in the peri-implantation rabbit uterus. *Biol Reprod,* 68**,** 1484-90.

APPARAO, K. B., LOVELY, L. P., GUI, Y., LININGER, R. A. & LESSEY, B. A. 2002. Elevated endometrial androgen receptor expression in women with polycystic ovarian syndrome. *Biol Reprod,* 66**,** 297-304.

APPARAO, K. B., MURRAY, M. J., FRITZ, M. A., MEYER, W. R., CHAMBERS, A. F., TRUONG, P. R. & LESSEY, B. A. 2001. Osteopontin and its receptor alphavbeta(3) integrin are coexpressed in the human endometrium during the menstrual cycle but regulated differentially. *J Clin Endocrinol Metab,* 86**,** 4991-5000.

ARMANT, D. R. 2005. Blastocysts don't go it alone. Extrinsic signals fine-tune the intrinsic developmental program of trophoblast cells. *Dev Biol,* 280**,** 260-80.

ASKARI, J. A., BUCKLEY, P. A., MOULD, A. P. & HUMPHRIES, M. J. 2009. Linking integrin conformation to function. *J Cell Sci,* 122**,** 165-70.

BADER, B. L., RAYBURN, H., CROWLEY, D. & HYNES, R. O. 1998. Extensive vasculogenesis, angiogenesis, and organogenesis precede lethality in mice lacking all alpha v integrins. *Cell,* 95**,** 507-19.

BAKER, R. K. & LYONS, G. E. 1996. Embryonic stem cells and in vitro muscle development. *Curr Top Dev Biol,* 33**,** 263-79.

BANERJEE, P. & FAZLEABAS, A. T. 2010. Endometrial responses to embryonic signals in the primate. *Int J Dev Biol,* 54**,** 295-302.

BARCZYK, M., CARRACEDO, S. & GULLBERG, D. 2010. Integrins. *Cell Tissue Res,* 339**,** 269-80.

BARNARD, J. A., GRAVES-DEAL, R., PITTELKOW, M. R., DUBOIS, R., COOK, P., RAMSEY, G. W., BISHOP, P. R., DAMSTRUP, L. & COFFEY, R. J. 1994. Auto- and cross-induction within the mammalian epidermal growth factor-related peptide family. *J Biol Chem,* 269**,** 22817-22.

BARRY, S. T., LUDBROOK, S. B., MURRISON, E. & HORGAN, C. M. 2000. A regulated interaction between alpha5beta1 integrin and osteopontin. *Biochem Biophys Res Commun,* 267**,** 764-9.

BASAK, S., DHAR, R. & DAS, C. 2002. Steroids modulate the expression of alpha4 integrin in mouse blastocysts and uterus during implantation. *Biol Reprod,* 66**,** 1784-9.

BAYLESS, K. J., MEININGER, G. A., SCHOLTZ, J. M. & DAVIS, G. E. 1998. Osteopontin is a ligand for the alpha4beta1 integrin. *J Cell Sci,* 111 (Pt 9)**,** 1165-74.

BAZER, F. W., SPENCER, T. E., JOHNSON, G. A., BURGHARDT, R. C. & WU, G. 2009. Comparative aspects of implantation. *Reproduction,* 138**,** 195-209.

BEAUSOLEIL, M. S., SCHULZE, E. B., GOODALE, D., POSTENKA, C. O. & ALLAN, A. L. 2011. Deletion of the thrombin cleavage domain of osteopontin mediates breast cancer cell adhesion, proteolytic activity, tumorgenicity, and metastasis. *BMC Cancer,* 11**,** 25.

BENTIN-LEY, U. & LOPATA, A. 2000. In vitro models of human blastocyst implantation. *Baillieres Best Pract Res Clin Obstet Gynaecol,* 14**,** 765-74.

BENTIN-LEY, U., SJOGREN, A., NILSSON, L., HAMBERGER, L., LARSEN, J. F. & HORN, T. 1999. Presence of uterine pinopodes at the embryo-endometrial interface during human implantation in vitro. *Hum Reprod,* 14**,** 515-20.

BIRDSALL, M. A., HOPKISSON, J. F., GRANT, K. E., BARLOW, D. H. & MARDON, H. J. 1996. Expression of heparin-binding epidermal growth factor messenger RNA in the human endometrium. *Mol Hum Reprod,* 2**,** 31-4.

BLOOR, D. J., METCALFE, A. D., RUTHERFORD, A., BRISON, D. R. & KIMBER, S. J. 2002. Expression of cell adhesion molecules during human preimplantation embryo development. *Mol Hum Reprod,* 8**,** 237-45.

BLUNDELL, T. L. & HUMBEL, R. E. 1980. Hormone families: pancreatic hormones and homologous growth factors. *Nature,* 287**,** 781-7.

BOSHELL, M., LALANI, E. N., PEMBERTON, L., BURCHELL, J., GENDLER, S. & TAYLOR-PAPADIMITRIOU, J. 1992. The product of the human MUC1 gene when secreted by mouse cells transfected with the full-length cDNA lacks the cytoplasmic tail. *Biochem Biophys Res Commun,* 185**,** 1-8.

BOWEN, J. A. & HUNT, J. S. 2000. The role of integrins in reproduction. *Proc Soc Exp Biol Med,* 223**,** 331-43.

BRAKEBUSCH, C., HIRSCH, E., POTOCNIK, A. & FASSLER, R. 1997. Genetic analysis of beta1 integrin function: confirmed, new and revised roles for a crucial family of cell adhesion molecules. *J Cell Sci,* 110 (Pt 23)**,** 2895-904.

BRAYMAN, M., THATHIAH, A. & CARSON, D. D. 2004. MUC1: a multifunctional cell surface component of reproductive tissue epithelia. *Reprod Biol Endocrinol,* 2**,** 4.

BRIESE, J., CHENG, S., EZZAT, S., LIU, W., WINER, D., WAGENER, C., BAMBERGER, A. M. & ASA, S. L. 2010. Osteopontin (OPN) expression in thyroid carcinoma. *Anticancer Res,* 30**,** 1681-8.

BRIESE, J., OBERNDORFER, M., SCHULTE, H. M., LONING, T. & BAMBERGER, A. M. 2005. Osteopontin expression in gestational trophoblastic diseases: correlation with expression of the adhesion molecule, CEACAM1. *Int J Gynecol Pathol,* 24**,** 271-6.

BROWN, L. F., BERSE, B., VAN DE WATER, L., PAPADOPOULOS-SERGIOU, A., PERRUZZI, C. A., MANSEAU, E. J., DVORAK, H. F. & SENGER, D. R. 1992. Expression and distribution of osteopontin in human tissues: widespread association with luminal epithelial surfaces. *Mol Biol Cell,* 3**,** 1169-80.

BURGESS, A. W., CHO, H. S., EIGENBROT, C., FERGUSON, K. M., GARRETT, T. P., LEAHY, D. J., LEMMON, M. A., SLIWKOWSKI, M. X., WARD, C. W. & YOKOYAMA, S. 2003. An open-and-shut case? Recent insights into the activation of EGF/ErbB receptors. *Mol Cell,* 12**,** 541-52.

BURNEY, R. O., TALBI, S., HAMILTON, A. E., VO, K. C., NYEGAARD, M., NEZHAT, C. R., LESSEY, B. A. & GIUDICE, L. C. 2007. Gene expression analysis of endometrium reveals progesterone resistance and candidate susceptibility genes in women with endometriosis. *Endocrinology,* 148**,** 3814-26.

BUTLER, B., WILLIAMS, M. P. & BLYSTONE, S. D. 2003. Ligand-dependent activation of integrin alpha vbeta 3. *J Biol Chem,* 278**,** 5264-70.

CAKMAK, H. & TAYLOR, H. S. 2011. Implantation failure: molecular mechanisms and clinical treatment. *Hum Reprod Update,* 17**,** 242-53.

CALDERWOOD, D. A., SHATTIL, S. J. & GINSBERG, M. H. 2000. Integrins and actin filaments: reciprocal regulation of cell adhesion and signaling. *J Biol Chem,* 275**,** 22607-10.

CAMARERO, G., AVENDANO, C., FERNANDEZ-MORENO, C., VILLAR, A., CONTRERAS, J., DE PABLO, F., PICHEL, J. G. & VARELA-NIETO, I. 2001. Delayed inner ear maturation and neuronal loss in postnatal Igf-1-deficient mice. *J Neurosci,* 21**,** 7630-41.

CAMEO, P., SRISUPARP, S., STRAKOVA, Z. & FAZLEABAS, A. T. 2004. Chorionic gonadotropin and uterine dialogue in the primate. *Reprod Biol Endocrinol,* 2**,** 50.

CAMPBELL, I. D. & HUMPHRIES, M. J. 2011. Integrin structure, activation, and interactions. *Cold Spring Harb Perspect Biol,* 3.

CARSON, D. D., BAGCHI, I., DEY, S. K., ENDERS, A. C., FAZLEABAS, A. T., LESSEY, B. A. & YOSHINAGA, K. 2000. Embryo implantation. *Dev Biol,* 223**,** 217-37.

CARSON, D. D., LAGOW, E., THATHIAH, A., AL-SHAMI, R., FARACH-CARSON, M. C., VERNON, M., YUAN, L., FRITZ, M. A. & LESSEY, B. 2002. Changes in gene expression during the early to mid-luteal (receptive phase) transition in human endometrium detected by high-density microarray screening. *Mol Hum Reprod,* 8**,** 871-9.

CARTER, A. M. 2007. Animal models of human placentation--a review. *Placenta,* 28 Suppl A**,** S41-7.

CARVER, J., MARTIN, K., SPYROPOULOU, I., BARLOW, D., SARGENT, I. & MARDON, H. 2003. An in-vitro model for stromal invasion during implantation of the human blastocyst. *Hum Reprod,* 18**,** 283-90.

CASALS, F., IDAGHDOUR, Y., HUSSIN, J. & AWADALLA, P. 2012a. Next-generation sequencing approaches for genetic mapping of complex diseases. *J Neuroimmunol*.

CASALS, G., ORDI, J., CREUS, M., FABREGUES, F., CARMONA, F., CASAMITJANA, R. & BALASCH, J. 2010. Osteopontin and alphavbeta3 integrin as markers of endometrial receptivity: the effect of different hormone therapies. *Reprod Biomed Online,* 21**,** 349-59.

CASALS, G., ORDI, J., CREUS, M., FABREGUES, F., CARMONA, F., CASAMITJANA, R. & BALASCH, J. 2012b. Expression pattern of osteopontin and alphavbeta3 integrin during the implantation window in infertile patients with early stages of endometriosis. *Hum Reprod,* 27**,** 805-13.

CASTELBAUM, A. J., WHEELER, J., COUTIFARIS, C. B., MASTROIANNI, L., JR. & LESSEY, B. A. 1994. Timing of the endometrial biopsy may be critical for the accurate diagnosis of luteal phase deficiency. *Fertil Steril,* 61**,** 443-7.

CASTELBAUM, A. J., YING, L., SOMKUTI, S. G., SUN, J., ILESANMI, A. O. & LESSEY, B. A. 1997. Characterization of integrin expression in a well differentiated endometrial adenocarcinoma cell line (Ishikawa). *J Clin Endocrinol Metab,* 82**,** 136-42.

CERMIK, D., SELAM, B. & TAYLOR, H. S. 2003. Regulation of HOXA-10 expression by testosterone in vitro and in the endometrium of patients with polycystic ovary syndrome. *J Clin Endocrinol Metab,* 88**,** 238-43.

CHAKRABORTY, G., JAIN, S., BEHERA, R., AHMED, M., SHARMA, P., KUMAR, V. & KUNDU, G. C. 2006. The multifaceted roles of osteopontin in cell signaling, tumor progression and angiogenesis. *Curr Mol Med,* 6**,** 819-30.

CHO, S., AHN, Y. S., CHOI, Y. S., SEO, S. K., NAM, A., KIM, H. Y., KIM, J. H., PARK, K. H., CHO, D. J. & LEE, B. S. 2009. Endometrial osteopontin mRNA expression and plasma osteopontin levels are increased in patients with endometriosis. *Am J Reprod Immunol,* 61**,** 286-93.

CHOBOTOVA, K., SPYROPOULOU, I., CARVER, J., MANEK, S., HEATH, J. K., GULLICK, W. J., BARLOW, D. H., SARGENT, I. L. & MARDON, H. J. 2002. Heparin-binding epidermal growth factor and its receptor ErbB4 mediate implantation of the human blastocyst. *Mech Dev,* 119**,** 137-44.

CHRISTENSEN, B., NIELSEN, M. S., HASELMANN, K. F., PETERSEN, T. E. & SORENSEN, E. S. 2005. Post-translationally modified residues of native human osteopontin are located in clusters: identification of 36 phosphorylation and five O-glycosylation sites and their biological implications. *Biochem J,* 390**,** 285-92.

CLARK, K., PANKOV, R., TRAVIS, M. A., ASKARI, J. A., MOULD, A. P., CRAIG, S. E., NEWHAM, P., YAMADA, K. M. & HUMPHRIES, M. J. 2005. A specific alpha5beta1-integrin conformation promotes directional integrin translocation and fibronectin matrix formation. *J Cell Sci,* 118**,** 291-300.

CLARKE, C. L., FEIL, P. D. & SATYASWAROOP, P. G. 1987. Progesterone receptor regulation by 17 beta-estradiol in human endometrial carcinoma grown in nude mice. *Endocrinology,* 121**,** 1642-8.

CLEMMONS, D. R. & MAILE, L. A. 2005. Interaction between insulin-like growth factor-I receptor and alphaVbeta3 integrin linked signaling pathways: cellular responses to changes in multiple signaling inputs. *Mol Endocrinol,* 19**,** 1-11.

D'ERCOLE, A. J., APPLEWHITE, G. T. & UNDERWOOD, L. E. 1980. Evidence that somatomedin is synthesized by multiple tissues in the fetus. *Dev Biol,* 75**,** 315-28.

DAFTARY, G. S., TROY, P. J., BAGOT, C. N., YOUNG, S. L. & TAYLOR, H. S. 2002. Direct regulation of beta3-integrin subunit gene expression by HOXA10 in endometrial cells. *Mol Endocrinol,* 16**,** 571-9.

DAS, S. K., WANG, X. N., PARIA, B. C., DAMM, D., ABRAHAM, J. A., KLAGSBRUN, M., ANDREWS, G. K. & DEY, S. K. 1994. Heparin-binding EGF-like growth factor gene is induced in the mouse uterus temporally by the blastocyst solely at the site of its apposition: a possible ligand for interaction with blastocyst EGF-receptor in implantation. *Development,* 120**,** 1071-83.

DATTA, A., HUBER, F. & BOETTIGER, D. 2002. Phosphorylation of beta3 integrin controls ligand binding strength. *J Biol Chem,* 277**,** 3943-9.

DE LOS SANTOS, M. J., MERCADER, A., FRANCES, A., PORTOLES, E., REMOHI, J., PELLICER, A. & SIMON, C. 1996. Role of endometrial factors in regulating secretion of components of the immunoreactive human embryonic interleukin-1 system during embryonic development. *Biol Reprod,* 54**,** 563-74.

DE LOS SANTOS, M. J., MERCADER, A., GALAN, A., ALBERT, C., ROMERO, J. L. & PELLICER, A. 2003. Implantation rates after two, three, or five days of embryo culture. *Placenta,* 24 Suppl B**,** S13-9.

DE MOUZON, J., GOOSSENS, V., BHATTACHARYA, S., CASTILLA, J. A., FERRARETTI, A. P., KORSAK, V., KUPKA, M., NYGREN, K. G., NYBOE ANDERSEN, A., EUROPEAN IVF-MONITORING CONSORTIUM, F. T. E. S. O. H. R. & EMBRYOLOGY 2010. Assisted reproductive technology in Europe, 2006: results generated from European registers by ESHRE. *Hum Reprod,* 25**,** 1851-62.

DEMALI, K. A., WENNERBERG, K. & BURRIDGE, K. 2003. Integrin signaling to the actin cytoskeleton. *Curr Opin Cell Biol,* 15**,** 572-82.

DENDA, S., REICHARDT, L. F. & MULLER, U. 1998. Identification of osteopontin as a novel ligand for the integrin alpha8 beta1 and potential roles for this integrin-ligand interaction in kidney morphogenesis. *Mol Biol Cell,* 9**,** 1425-35.

DESHMUKH, H. S., MCLACHLAN, A., ATKINSON, J. J., HARDIE, W. D., KORFHAGEN, T. R., DIETSCH, M., LIU, Y., DI, P. Y., WESSELKAMPER, S. C., BORCHERS, M. T. & LEIKAUF, G. D. 2009. Matrix metalloproteinase-14 mediates a phenotypic shift in the airways to increase mucin production. *Am J Respir Crit Care Med,* 180**,** 834-45.

DEY, S. K., LIM, H., DAS, S. K., REESE, J., PARIA, B. C., DAIKOKU, T. & WANG, H.

2004. Molecular cues to implantation. *Endocr Rev,* 25**,** 341-73.

DHARMARAJ, N., WANG, P. & CARSON, D. D. 2010. Cytokine and progesterone receptor interplay in the regulation of MUC1 gene expression. *Mol Endocrinol,* 24**,** 2253-66.

DIEDRICH, K., FAUSER, B. C., DEVROEY, P., GRIESINGER, G. & EVIAN ANNUAL REPRODUCTION WORKSHOP, G. 2007. The role of the endometrium and embryo in human implantation. *Hum Reprod Update,* 13**,** 365-77.

DOBSON, A. T., RAJA, R., ABEYTA, M. J., TAYLOR, T., SHEN, S., HAQQ, C. & PERA, R. A. 2004. The unique transcriptome through day 3 of human preimplantation development. *Hum Mol Genet,* 13**,** 1461-70.

DOMINGUEZ, F., GALAN, A., MARTIN, J. J., REMOHI, J., PELLICER, A. & SIMON, C. 2003. Hormonal and embryonic regulation of chemokine receptors CXCR1, CXCR4, CCR5 and CCR2B in the human endometrium and the human blastocyst. *Mol Hum Reprod,* 9**,** 189-98.

DUC-GOIRAN, P., MIGNOT, T. M., BOURGEOIS, C. & FERRE, F. 1999. Embryo-maternal interactions at the implantation site: a delicate equilibrium. *Eur J Obstet Gynecol Reprod Biol,* 83**,** 85-100.

DUQUESNAY, R., WRIGHT, C., AZIZ, A. A., STAMP, G. W., TREW, G. H., MARGARA, R. A. & WHITE, J. O. 2009. Infertile women with isolated polycystic ovaries are deficient in endometrial expression of osteopontin but not alphavbeta3 integrin during the implantation window. *Fertil Steril,* 91**,** 489-99.

ELENIUS, K., PAUL, S., ALLISON, G., SUN, J. & KLAGSBRUN, M. 1997. Activation of HER4 by heparin-binding EGF-like growth factor stimulates chemotaxis but not proliferation. *EMBO J,* 16**,** 1268-78.

EMERMAN, A. B., ZHANG, Z. R., CHAKRABARTI, O. & HEGDE, R. S. 2010. Compartment-restricted biotinylation reveals novel features of prion protein metabolism in vivo. *Mol Biol Cell,* 21**,** 4325-37.

ENDERS, A. C. 1975. The implantation chamber, blastocyst and blastocyst imprint of the rat; a scanning electron microscope study. *Anat Rec,* 182**,** 137-49.

ENDERS, A. C. 1989. Trophoblast differentiation during the transition from trophoblastic plate to lacunar stage of implantation in the rhesus monkey and human. *Am J Anat,* 186**,** 85-98.

ENDERS, A. C. 2000. Trophoblast-uterine interactions in the first days of implantation: models for the study of implantation events in the human. *Semin Reprod Med,* 18**,**

255-63.

ENDERS, A. C., HENDRICKX, A. G. & SCHLAFKE, S. 1983. Implantation in the rhesus monkey: initial penetration of endometrium. *Am J Anat,* 167**,** 275-98.

ENDERS, A. C. & KING, B. F. 1991. Early stages of trophoblastic invasion of the maternal vascular system during implantation in the macaque and baboon. *Am J Anat,* 192**,** 329-46.

ENDERS, A. C., LANTZ, K. C., PETERSON, P. E. & HENDRICKX, A. G. 1997. From blastocyst to placenta: the morphology of implantation in the baboon. *Hum Reprod Update,* 3**,** 561-73.

ENDERS, A. C. & SCHLAFKE, S. 1969. Cytological aspects of trophoblast-uterine interaction in early implantation. *Am J Anat,* 125**,** 1-29.

ENDERS, A. C. & SCHLAFKE, S. 1971. Penetration of the uterine epithelium during implantation in the rabbit. *Am J Anat,* 132**,** 219-30.

ERIKSON, D. W., BURGHARDT, R. C., BAYLESS, K. J. & JOHNSON, G. A. 2009. Secreted phosphoprotein 1 (SPP1, osteopontin) binds to integrin alpha v beta 6 on porcine trophectoderm cells and integrin alpha v beta 3 on uterine luminal epithelial cells, and promotes trophectoderm cell adhesion and migration. *Biol Reprod,* 81**,** 814-25.

FAZLEABAS, A. T., BELL, S. C., FLEMING, S., SUN, J. & LESSEY, B. A. 1997. Distribution of integrins and the extracellular matrix proteins in the baboon endometrium during the menstrual cycle and early pregnancy. *Biol Reprod,* 56**,** 348-56.

FENG, G. S. 2006. Shp2 as a therapeutic target for leptin resistance and obesity. *Expert Opin Ther Targets,* 10**,** 135-42.

FITZGERALD, J. S., POEHLMANN, T. G., SCHLEUSSNER, E. & MARKERT, U. R. 2008. Trophoblast invasion: the role of intracellular cytokine signalling via signal transducer and activator of transcription 3 (STAT3). *Hum Reprod Update,* 14**,** 335-44.

FLUHR, H., CARLI, S., DEPERSCHMIDT, M., WALLWIENER, D., ZYGMUNT, M. & LICHT, P. 2008. Differential effects of human chorionic gonadotropin and decidualization on insulin-like growth factors-I and -II in human endometrial stromal cells. *Fertil Steril,* 90**,** 1384-9.

FORBES, K., WESTWOOD, M., BAKER, P. N. & APLIN, J. D. 2008. Insulin-like growth factor I and II regulate the life cycle of trophoblast in the developing human

placenta. *Am J Physiol Cell Physiol,* 294**,** C1313-22.

FRANZEN, A. & HEINEGARD, D. 1985. Isolation and characterization of two sialoproteins present only in bone calcified matrix. *Biochem J,* 232**,** 715-24.

FUJIOKA, Y., MATOZAKI, T., NOGUCHI, T., IWAMATSU, A., YAMAO, T., TAKAHASHI, N., TSUDA, M., TAKADA, T. & KASUGA, M. 1996. A novel membrane glycoprotein, SHPS-1, that binds the SH2-domain-containing protein tyrosine phosphatase SHP-2 in response to mitogens and cell adhesion. *Mol Cell Biol,* 16**,** 6887-99.

GAHMBERG, C. G., FAGERHOLM, S. C., NURMI, S. M., CHAVAKIS, T., MARCHESAN, S. & GRONHOLM, M. 2009. Regulation of integrin activity and signalling. *Biochim Biophys Acta,* 1790**,** 431-44.

GALAN, A., O'CONNOR, J. E., VALBUENA, D., HERRER, R., REMOHI, J., PAMPFER, S., PELLICER, A. & SIMON, C. 2000. The human blastocyst regulates endometrial epithelial apoptosis in embryonic adhesion. *Biol Reprod,* 63**,** 430-9.

GALBRAITH, C. G., YAMADA, K. M. & SHEETZ, M. P. 2002. The relationship between force and focal complex development. *J Cell Biol,* 159**,** 695-705.

GALVAN, V., LOGVINOVA, A., SPERANDIO, S., ICHIJO, H. & BREDESEN, D. E. 2003. Type 1 insulin-like growth factor receptor (IGF-IR) signaling inhibits apoptosis signal-regulating kinase 1 (ASK1). *J Biol Chem,* 278**,** 13325-32.

GAN, Y., ZHANG, Y., DIGIROLAMO, D. J., JIANG, J., WANG, X., CAO, X., ZINN, K. R., CARBONE, D. P., CLEMENS, T. L. & FRANK, S. J. 2010. Deletion of IGF-I receptor (IGF-IR) in primary osteoblasts reduces GH-induced STAT5 signaling. *Mol Endocrinol,* 24**,** 644-56.

GAO, J. G., ZHU, H. H., FAN, J., MAZELLA, J. & TSENG, L. 1995. Progestin and antiprogestin differentially regulate the expression of insulin-like growth factors (IGF-I and IGF-II) messenger ribonucleic acid in human endometrial stromal cells. *Biol Reprod,* 53**,** 355-60.

GARCIA, P., NIETO, A., SANCHEZ, M. A., PIZARRO, M. & FLORES, J. M. 2004. Expression of alphav, alpha4, alpha5 and beta3 integrin subunits, fibronectin and vitronectin in goat peri-implantation. *Anim Reprod Sci,* 80**,** 91-100.

GARLOW, J. E., KA, H., JOHNSON, G. A., BURGHARDT, R. C., JAEGER, L. A. & BAZER, F. W. 2002. Analysis of osteopontin at the maternal-placental interface in pigs. *Biol Reprod,* 66**,** 718-25.

GARRIDO-GOMEZ, T., DOMINGUEZ, F. & SIMON, C. 2010. Proteomics of embryonic

implantation. *Handb Exp Pharmacol*, 67-78.

GEIGER, B., SPATZ, J. P. & BERSHADSKY, A. D. 2009. Environmental sensing through focal adhesions. *Nat Rev Mol Cell Biol,* 10, 21-33.

GEISERT, R. D. & YELICH, J. V. 1997. Regulation of conceptus development and attachment in pigs. *J Reprod Fertil Suppl,* 52, 133-49.

GENDLER, S. J., COHEN, E. P., CRASTON, A., DUHIG, T., JOHNSTONE, G. & BARNES, D. 1990. The locus of the polymorphic epithelial mucin (PEM) tumour antigen on chromosome 1q21 shows a high frequency of alteration in primary human breast tumours. *Int J Cancer,* 45, 431-5.

GHAHARY, A., CHAKRABARTI, S. & MURPHY, L. J. 1990. Localization of the sites of synthesis and action of insulin-like growth factor-I in the rat uterus. *Mol Endocrinol,* 4, 191-5.

GILCREASE, M. Z. 2007. Integrin signaling in epithelial cells. *Cancer Lett,* 247, 1-25.

GINSBERG, M. H., LOFTUS, J. C., D'SOUZA, S. & PLOW, E. F. 1990. Ligand binding to integrins: common and ligand specific recognition mechanisms. *Cell Differ Dev,* 32, 203-13.

GIUDICE, L. C., DSUPIN, B. A., JIN, I. H., VU, T. H. & HOFFMAN, A. R. 1993. Differential expression of messenger ribonucleic acids encoding insulin-like growth factors and their receptors in human uterine endometrium and decidua. *J Clin Endocrinol Metab,* 76, 1115-22.

GIUDICE, L. C., MARK, S. P. & IRWIN, J. C. 1998. Paracrine actions of insulin-like growth factors and IGF binding protein-1 in non-pregnant human endometrium and at the decidual-trophoblast interface. *J Reprod Immunol,* 39, 133-48.

GODKIN, J. D., BAZER, F. W. & ROBERTS, R. M. 1984. Ovine trophoblast protein 1, an early secreted blastocyst protein, binds specifically to uterine endometrium and affects protein synthesis. *Endocrinology,* 114, 120-30.

GOISHI, K., HIGASHIYAMA, S., KLAGSBRUN, M., NAKANO, N., UMATA, T., ISHIKAWA, M., MEKADA, E. & TANIGUCHI, N. 1995. Phorbol ester induces the rapid processing of cell surface heparin-binding EGF-like growth factor: conversion from juxtacrine to paracrine growth factor activity. *Mol Biol Cell,* 6, 967-80.

GOLDSMITH, H. L., LABROSSE, J. M., MCINTOSH, F. A., MAENPAA, P. H., KAARTINEN, M. T. & MCKEE, M. D. 2002. Homotypic interactions of soluble and immobilized osteopontin. *Ann Biomed Eng,* 30, 840-50.

GOMEZ, E., TARIN, J. J. & PELLICER, A. 1993. Oocyte maturation in humans: the role of gonadotropins and growth factors. *Fertil Steril,* 60**,** 40-6.

GRADY, R., ALAVI, N., VALE, R., KHANDWALA, M. & MCDONALD, S. D. 2012a. Elective single embryo transfer and perinatal outcomes: a systematic review and meta-analysis. *Fertil Steril,* 97**,** 324-31.

GRADY, R., ALAVI, N., VALE, R., KHANDWALA, M. & MCDONALD, S. D. 2012b. Elective single embryo transfer and perinatal outcomes: a systematic review and meta-analysis. *Fertil Steril,* 97**,** 324-331 e8.

GRAHAM, R. A., SEIF, M. W., APLIN, J. D., LI, T. C., COOKE, I. D., ROGERS, A. W. & DOCKERY, P. 1990. An endometrial factor in unexplained infertility. *BMJ,* 300**,** 1428-31.

GREWAL, S., CARVER, J. G., RIDLEY, A. J. & MARDON, H. J. 2008. Implantation of the human embryo requires Rac1-dependent endometrial stromal cell migration. *Proc Natl Acad Sci U S A,* 105**,** 16189-94.

GRUMMER, R., HEWITT, S. W., TRAUB, O., KORACH, K. S. & WINTERHAGER, E. 2004. Different regulatory pathways of endometrial connexin expression: preimplantation hormonal-mediated pathway versus embryo implantation-initiated pathway. *Biol Reprod,* 71**,** 273-81.

GUPTA, S., GOLDBERG, J. M., AZIZ, N., GOLDBERG, E., KRAJCIR, N. & AGARWAL, A. 2008. Pathogenic mechanisms in endometriosis-associated infertility. *Fertil Steril,* 90**,** 247-57.

GUZELOGLU-KAYISLI, O., KAYISLI, U. A. & TAYLOR, H. S. 2009. The role of growth factors and cytokines during implantation: endocrine and paracrine interactions. *Semin Reprod Med,* 27**,** 62-79.

HAMATANI, T., CARTER, M. G., SHAROV, A. A. & KO, M. S. 2004a. Dynamics of global gene expression changes during mouse preimplantation development. *Dev Cell,* 6**,** 117-31.

HAMATANI, T., DAIKOKU, T., WANG, H., MATSUMOTO, H., CARTER, M. G., KO, M. S. & DEY, S. K. 2004b. Global gene expression analysis identifies molecular pathways distinguishing blastocyst dormancy and activation. *Proc Natl Acad Sci U S A,* 101**,** 10326-31.

HANISCH, F. G. & MULLER, S. 2000. MUC1: the polymorphic appearance of a human mucin. *Glycobiology,* 10**,** 439-49.

HANNAN, N. J., EVANS, J. & SALAMONSEN, L. A. 2011. Alternate roles for immune

regulators: establishing endometrial receptivity for implantation. *Expert Rev Clin Immunol,* 7**,** 789-802.

HARPER, M. J., JONES, M. A., NORRIS, C. J. & WOODARD, D. S. 1989. Prostaglandin synthesis by day-6 rabbit blastocysts in vitro. *J Reprod Fertil,* 86**,** 315-25.

HENG, S., CERVERO, A., SIMON, C., STEPHENS, A. N., LI, Y., ZHANG, J., PAULE, S., RAINCZUK, A., SINGH, H., QUINONERO, A., TAPIA, A., VELASQUEZ, L., SALAMONSEN, L., ROMBAUTS, L. J. & NIE, G. 2011. Proprotein convertase 5/6 is critical for embryo implantation in women: regulating receptivity by cleaving EBP50, modulating ezrin binding, and membrane-cytoskeletal interactions. *Endocrinology,* 152**,** 5041-52.

HERTIG, A. T., ROCK, J. & ADAMS, E. C. 1956. A description of 34 human ova within the first 17 days of development. *Am J Anat,* 98**,** 435-93.

HERTIG, A. T., ROCK, J., ADAMS, E. C. & MENKIN, M. C. 1959. Thirty-four fertilized human ova, good, bad and indifferent, recovered from 210 women of known fertility; a study of biologic wastage in early human pregnancy. *Pediatrics,* 23**,** 202-11.

HEY, N. A. & APLIN, J. D. 1996. Sialyl-Lewis x and Sialyl-Lewis a are associated with MUC1 in human endometrium. *Glycoconj J,* 13**,** 769-79.

HEY, N. A., LI, T. C., DEVINE, P. L., GRAHAM, R. A., SARAVELOS, H. & APLIN, J. D. 1995. MUC1 in secretory phase endometrium: expression in precisely dated biopsies and flushings from normal and recurrent miscarriage patients. *Hum Reprod,* 10**,** 2655-62.

HIEDA, M., ISOKANE, M., KOIZUMI, M., HIGASHI, C., TACHIBANA, T., SHUDOU, M., TAGUCHI, T., HIEDA, Y. & HIGASHIYAMA, S. 2008. Membrane-anchored growth factor, HB-EGF, on the cell surface targeted to the inner nuclear membrane. *J Cell Biol,* 180**,** 763-9.

HIGASHIYAMA, S., ABRAHAM, J. A., MILLER, J., FIDDES, J. C. & KLAGSBRUN, M. 1991. A heparin-binding growth factor secreted by macrophage-like cells that is related to EGF. *Science,* 251**,** 936-9.

HIGASHIYAMA, S., IWAMOTO, R., GOISHI, K., RAAB, G., TANIGUCHI, N., KLAGSBRUN, M. & MEKADA, E. 1995. The membrane protein CD9/DRAP 27 potentiates the juxtacrine growth factor activity of the membrane-anchored heparin-binding EGF-like growth factor. *J Cell Biol,* 128**,** 929-38.

HIKITA, S. T., KOSIK, K. S., CLEGG, D. O. & BAMDAD, C. 2008. MUC1* mediates the growth of human pluripotent stem cells. *PLoS One,* 3**,** e3312.

HILKENS, J., LIGTENBERG, M. J., VOS, H. L. & LITVINOV, S. V. 1992. Cell membrane-associated mucins and their adhesion-modulating property. *Trends Biochem Sci,* 17**,** 359-63.

HO, H., SINGH, H., ALJOFAN, M. & NIE, G. 2012. A high-throughput in vitro model of human embryo attachment. *Fertil Steril*.

HOFFMAN, L. H., OLSON, G. E., CARSON, D. D. & CHILTON, B. S. 1998. Progesterone and implanting blastocysts regulate Muc1 expression in rabbit uterine epithelium. *Endocrinology,* 139**,** 266-71.

HOLBRO, T. & HYNES, N. E. 2004. ErbB receptors: directing key signaling networks throughout life. *Annu Rev Pharmacol Toxicol,* 44**,** 195-217.

HONDA, S., SHIROTANI-IKEJIMA, H., TADOKORO, S., MAEDA, Y., KINOSHITA, T., TOMIYAMA, Y. & MIYATA, T. 2009. Integrin-linked kinase associated with integrin activation. *Blood,* 113**,** 5304-13.

HORCAJADAS, J. A., RIESEWIJK, A., POLMAN, J., VAN OS, R., PELLICER, A., MOSSELMAN, S. & SIMON, C. 2005. Effect of controlled ovarian hyperstimulation in IVF on endometrial gene expression profiles. *Mol Hum Reprod,* 11**,** 195-205.

HORNE, A. W., LALANI, E. N., MARGARA, R. A. & WHITE, J. O. 2006. The effects of sex steroid hormones and interleukin-1-beta on MUC1 expression in endometrial epithelial cell lines. *Reproduction,* 131**,** 733-42.

HORTON, M. A. 1997. The alpha v beta 3 integrin "vitronectin receptor". *Int J Biochem Cell Biol,* 29**,** 721-5.

HOTTE, S. J., WINQUIST, E. W., STITT, L., WILSON, S. M. & CHAMBERS, A. F. 2002. Plasma osteopontin: associations with survival and metastasis to bone in men with hormone-refractory prostate carcinoma. *Cancer,* 95**,** 506-12.

HU, D. D., HOYER, J. R. & SMITH, J. W. 1995a. Characterization of the interaction between integrins and recombinant human osteopontin. *Ann N Y Acad Sci,* 760**,** 312-4.

HU, D. D., LIN, E. C., KOVACH, N. L., HOYER, J. R. & SMITH, J. W. 1995b. A biochemical characterization of the binding of osteopontin to integrins alpha v beta 1 and alpha v beta 5. *J Biol Chem,* 270**,** 26232-8.

HUANG, L., REN, J., CHEN, D., LI, Y., KHARBANDA, S. & KUFE, D. 2003. MUC1 cytoplasmic domain coactivates Wnt target gene transcription and confers transformation. *Cancer Biol Ther,* 2**,** 702-6.

HUGHES, P. E., DIAZ-GONZALEZ, F., LEONG, L., WU, C., MCDONALD, J. A., SHATTIL, S. J. & GINSBERG, M. H. 1996. Breaking the integrin hinge. A defined structural constraint regulates integrin signaling. *J Biol Chem,* 271**,** 6571-4.

HUMBEL, R. E. 1990. Insulin-like growth factors I and II. *Eur J Biochem,* 190**,** 445-62.

HUMPHRIES, J. D., WANG, P., STREULI, C., GEIGER, B., HUMPHRIES, M. J. & BALLESTREM, C. 2007. Vinculin controls focal adhesion formation by direct interactions with talin and actin. *J Cell Biol,* 179**,** 1043-57.

HUTTENLOCHER, A. & HORWITZ, A. R. 2011. Integrins in cell migration. *Cold Spring Harb Perspect Biol,* 3**,** a005074.

HUVENEERS, S. & DANEN, E. H. 2009. Adhesion signaling - crosstalk between integrins, Src and Rho. *J Cell Sci,* 122**,** 1059-69.

HYNES, R. O. 1992. Integrins: versatility, modulation, and signaling in cell adhesion. *Cell,* 69**,** 11-25.

HYNES, R. O. 1996. Targeted mutations in cell adhesion genes: what have we learned from them? *Dev Biol,* 180**,** 402-12.

HYNES, R. O. 2002. Integrins: bidirectional, allosteric signaling machines. *Cell,* 110**,** 673-87.

IHNEN, M., WIRTZ, R. M., KALOGERAS, K. T., MILDE-LANGOSCH, K., SCHMIDT, M., WITZEL, I., ELEFTHERAKI, A. G., PAPADIMITRIOU, C., JANICKE, F., BRIASSOULIS, E., PECTASIDES, D., RODY, A., FOUNTZILAS, G. & MULLER, V. 2010. Combination of osteopontin and activated leukocyte cell adhesion molecule as potent prognostic discriminators in HER2- and ER-negative breast cancer. *Br J Cancer,* 103**,** 1048-56.

ILLERA, M. J., CULLINAN, E., GUI, Y., YUAN, L., BEYLER, S. A. & LESSEY, B. A. 2000. Blockade of the alpha(v)beta(3) integrin adversely affects implantation in the mouse. *Biol Reprod,* 62**,** 1285-90.

ILLERA, M. J., LORENZO, P. L., GUI, Y. T., BEYLER, S. A., APPARAO, K. B. & LESSEY, B. A. 2003. A role for alphavbeta3 integrin during implantation in the rabbit model. *Biol Reprod,* 68**,** 766-71.

IMANO, M., SATOU, T., ITOH, T., SAKAI, K., ISHIMARU, E., YASUDA, A., PENG, Y. F., SHINKAI, M., AKAI, F., YASUDA, T., IMAMOTO, H., OKUNO, K., ITO, H., SHIOZAKI, H. & OHYANAGI, H. 2009. Immunohistochemical expression of osteopontin in gastric cancer. *J Gastrointest Surg,* 13**,** 1577-82.

ISAACS, J. & MURPHY, C. R. 2002. Heparin-binding EGF-like growth factor is seen on the extracellular surface of uterine epithelial cells only after the initial stages of blastocyst attachment. *Histochem J,* 34**,** 339-43.

IWAMOTO, R., HANDA, K. & MEKADA, E. 1999. Contact-dependent growth inhibition and apoptosis of epidermal growth factor (EGF) receptor-expressing cells by the membrane-anchored form of heparin-binding EGF-like growth factor. *J Biol Chem,* 274**,** 25906-12.

IWAMOTO, R. & MEKADA, E. 2000. Heparin-binding EGF-like growth factor: a juxtacrine growth factor. *Cytokine Growth Factor Rev,* 11**,** 335-44.

IZUMI, Y., HIRATA, M., HASUWA, H., IWAMOTO, R., UMATA, T., MIYADO, K., TAMAI, Y., KURISAKI, T., SEHARA-FUJISAWA, A., OHNO, S. & MEKADA, E. 1998. A metalloprotease-disintegrin, MDC9/meltrin-gamma/ADAM9 and PKCdelta are involved in TPA-induced ectodomain shedding of membrane-anchored heparin-binding EGF-like growth factor. *EMBO J,* 17**,** 7260-72.

JESSMON, P., LEACH, R. E. & ARMANT, D. R. 2009. Diverse functions of HBEGF during pregnancy. *Mol Reprod Dev,* 76**,** 1116-27.

JIANG, S., LEE, B. C., FU, Y., AVRAHAM, S., LIM, B. & AVRAHAM, H. K. 2010. Reconstitution of mammary epithelial morphogenesis by murine embryonic stem cells undergoing hematopoietic stem cell differentiation. *PLoS One,* 5**,** e9707.

JOHNSON, G. A., BAZER, F. W., JAEGER, L. A., KA, H., GARLOW, J. E., PFARRER, C., SPENCER, T. E. & BURGHARDT, R. C. 2001. Muc-1, integrin, and osteopontin expression during the implantation cascade in sheep. *Biol Reprod,* 65**,** 820-8.

JOHNSON, G. A., BURGHARDT, R. C., BAZER, F. W. & SPENCER, T. E. 2003a. Osteopontin: roles in implantation and placentation. *Biol Reprod,* 69**,** 1458-71.

JOHNSON, G. A., BURGHARDT, R. C., JOYCE, M. M., SPENCER, T. E., BAZER, F. W., GRAY, C. A. & PFARRER, C. 2003b. Osteopontin is synthesized by uterine glands and a 45-kDa cleavage fragment is localized at the uterine-placental interface throughout ovine pregnancy. *Biol Reprod,* 69**,** 92-8.

JOHNSON, G. A., BURGHARDT, R. C., JOYCE, M. M., SPENCER, T. E., BAZER, F. W., PFARRER, C. & GRAY, C. A. 2003c. Osteopontin expression in uterine stroma indicates a decidualization-like differentiation during ovine pregnancy. *Biol Reprod,* 68**,** 1951-8.

JOHNSON, G. A., BURGHARDT, R. C., SPENCER, T. E., NEWTON, G. R., OTT, T. L. & BAZER, F. W. 1999. Ovine osteopontin: II. Osteopontin and alpha(v)beta(3)

integrin expression in the uterus and conceptus during the periimplantation period. *Biol Reprod,* 61**,** 892-9.

JOHNSON, G. A., SPENCER, T. E., BURGHARDT, R. C., TAYLOR, K. M., GRAY, C. A. & BAZER, F. W. 2000. Progesterone modulation of osteopontin gene expression in the ovine uterus. *Biol Reprod,* 62**,** 1315-21.

JONES, C. J., ENDERS, A. C. & FAZLEABAS, A. T. 2001. Early implantation events in the baboon (Papio anubis) with special reference to the establishment of anchoring villi. *Placenta,* 22**,** 440-56.

JONES, J. I., PREVETTE, T., GOCKERMAN, A. & CLEMMONS, D. R. 1996. Ligand occupancy of the alpha-V-beta3 integrin is necessary for smooth muscle cells to migrate in response to insulin-like growth factor. *Proc Natl Acad Sci U S A,* 93**,** 2482-7.

KAARTINEN, M. T., EL-MAADAWY, S., RASANEN, N. H. & MCKEE, M. D. 2002. Tissue transglutaminase and its substrates in bone. *J Bone Miner Res,* 17**,** 2161-73.

KANEKO, Y., DAY, M. L. & MURPHY, C. R. 2011a. Integrin beta3 in rat blastocysts and epithelial cells is essential for implantation in vitro: studies with Ishikawa cells and small interfering RNA transfection. *Hum Reprod,* 26**,** 1665-74.

KANEKO, Y., LECCE, L., DAY, M. L. & MURPHY, C. R. 2011b. beta(1) and beta(3) integrins disassemble from basal focal adhesions and beta(3) integrin is later localised to the apical plasma membrane of rat uterine luminal epithelial cells at the time of implantation. *Reprod Fertil Dev,* 23**,** 481-95.

KANEKO, Y., LECCE, L. & MURPHY, C. R. 2009. Ovarian hormones regulate expression of the focal adhesion proteins, talin and paxillin, in rat uterine luminal but not glandular epithelial cells. *Histochem Cell Biol,* 132**,** 613-22.

KAO, L. C., TULAC, S., LOBO, S., IMANI, B., YANG, J. P., GERMEYER, A., OSTEEN, K., TAYLOR, R. N., LESSEY, B. A. & GIUDICE, L. C. 2002. Global gene profiling in human endometrium during the window of implantation. *Endocrinology,* 143**,** 2119-38.

KAPUR, S., TAMADA, H., DEY, S. K. & ANDREWS, G. K. 1992. Expression of insulin-like growth factor-I (IGF-I) and its receptor in the peri-implantation mouse uterus, and cell-specific regulation of IGF-I gene expression by estradiol and progesterone. *Biol Reprod,* 46**,** 208-19.

KATAGIRI, Y. U., SLEEMAN, J., FUJII, H., HERRLICH, P., HOTTA, H., TANAKA, K., CHIKUMA, S., YAGITA, H., OKUMURA, K., MURAKAMI, M., SAIKI, I., CHAMBERS, A. F. & UEDE, T. 1999. CD44 variants but not CD44s cooperate

with beta1-containing integrins to permit cells to bind to osteopontin independently of arginine-glycine-aspartic acid, thereby stimulating cell motility and chemotaxis. *Cancer Res,* 59**,** 219-26.

KATZ-JAFFE, M. G., GARDNER, D. K. & SCHOOLCRAFT, W. B. 2006. Proteomic analysis of individual human embryos to identify novel biomarkers of development and viability. *Fertil Steril,* 85**,** 101-7.

KIM, S., LEE, G. S., LEE, S. H., KIM, H. S., JEONG, Y. W., KIM, J. H., KANG, S. K., LEE, B. C. & HWANG, W. S. 2005. Embryotropic effect of insulin-like growth factor (IGF)-I and its receptor on development of porcine preimplantation embryos produced by in vitro fertilization and somatic cell nuclear transfer. *Mol Reprod Dev,* 72**,** 88-97.

KIMMINS, S., LIM, H. C. & MACLAREN, L. A. 2004. Immunohistochemical localization of integrin alpha V beta 3 and osteopontin suggests that they do not interact during embryo implantation in ruminants. *Reprod Biol Endocrinol,* 2**,** 19.

KLIMAN, H. J., FEINBERG, R. F. & HAIMOWITZ, J. E. 1990. Human trophoblast-endometrial interactions in an in vitro suspension culture system. *Placenta,* 11**,** 349-67.

KON, S., YOKOSAKI, Y., MAEDA, M., SEGAWA, T., HORIKOSHI, Y., TSUKAGOSHI, H., RASHID, M. M., MORIMOTO, J., INOBE, M., SHIJUBO, N., CHAMBERS, A. F. & UEDE, T. 2002. Mapping of functional epitopes of osteopontin by monoclonal antibodies raised against defined internal sequences. *J Cell Biochem,* 84**,** 420-32.

KUEMMERLE, J. F. 2006. Occupation of alphavbeta3-integrin by endogenous ligands modulates IGF-I receptor activation and proliferation of human intestinal smooth muscle. *Am J Physiol Gastrointest Liver Physiol,* 290**,** G1194-202.

KUFE, D. W. 2008. Targeting the human MUC1 oncoprotein: a tale of two proteins. *Cancer Biol Ther,* 7**,** 81-4.

KUHN, K. & EBLE, J. 1994. The structural bases of integrin-ligand interactions. *Trends Cell Biol,* 4**,** 256-61.

KUMAR, C. C. 1998. Signaling by integrin receptors. *Oncogene,* 17**,** 1365-73.

KURAMOTO, H., TAMURA, S. & NOTAKE, Y. 1972. Establishment of a cell line of human endometrial adenocarcinoma in vitro. *Am J Obstet Gynecol,* 114**,** 1012-9.

LACKEY, B. R., GRAY, S. L. & HENRICKS, D. M. 1999. The insulin-like growth factor (IGF) system and gonadotropin regulation: actions and interactions. *Cytokine*

Growth Factor Rev, 10**,** 201-17.

LAMMERS, R., GRAY, A., SCHLESSINGER, J. & ULLRICH, A. 1989. Differential signalling potential of insulin- and IGF-1-receptor cytoplasmic domains. *EMBO J,* 8**,** 1369-75.

LANDGREN, B. M., JOHANNISSON, E., STAVREUS-EVERS, A., HAMBERGER, L. & ERIKSSON, H. 1996. A new method to study the process of implantation of a human blastocyst in vitro. *Fertil Steril,* 65**,** 1067-70.

LE, M. N., KOHANSKI, R. A., WANG, L. H. & SADOWSKI, H. B. 2002. Dual mechanism of signal transducer and activator of transcription 5 activation by the insulin receptor. *Mol Endocrinol,* 16**,** 2764-79.

LEACH, R. E., KHALIFA, R., ARMANT, D. R., BRUDNEY, A., DAS, S. K., DEY, S. K. & FAZLEABAS, A. T. 2001. Heparin-binding EGF-like growth factor modulation by antiprogestin and CG in the baboon (Papio anubis). *J Clin Endocrinol Metab,* 86**,** 4520-8.

LEACH, R. E., KHALIFA, R., RAMIREZ, N. D., DAS, S. K., WANG, J., DEY, S. K., ROMERO, R. & ARMANT, D. R. 1999. Multiple roles for heparin-binding epidermal growth factor-like growth factor are suggested by its cell-specific expression during the human endometrial cycle and early placentation. *J Clin Endocrinol Metab,* 84**,** 3355-63.

LECCE, L., LINDSAY, L. A. & MURPHY, C. R. 2011. Ezrin and EBP50 redistribute apically in rat uterine epithelial cells at the time of implantation and in response to cell contact. *Cell Tissue Res,* 343**,** 445-53.

LEE, K. Y. & DEMAYO, F. J. 2004. Animal models of implantation. *Reproduction,* 128**,** 679-95.

LESSEY, B. A. 1994. The use of integrins for the assessment of uterine receptivity. *Fertil Steril,* 61**,** 812-4.

LESSEY, B. A. 1998. Endometrial integrins and the establishment of uterine receptivity. *Hum Reprod,* 13 Suppl 3**,** 247-58; discussion 259-61.

LESSEY, B. A. 2002a. Adhesion molecules and implantation. *J Reprod Immunol,* 55**,** 101-12.

LESSEY, B. A. 2002b. Implantation defects in infertile women with endometriosis. *Ann N Y Acad Sci,* 955**,** 265-80; discussion 293-5, 396-406.

LESSEY, B. A. 2011. Assessment of endometrial receptivity. *Fertil Steril,* 96**,** 522-9.

LESSEY, B. A. & CASTELBAUM, A. J. 2002. Integrins and implantation in the human. *Rev Endocr Metab Disord,* 3**,** 107-17.

LESSEY, B. A., CASTELBAUM, A. J., SAWIN, S. W., BUCK, C. A., SCHINNAR, R., BILKER, W. & STROM, B. L. 1994. Aberrant integrin expression in the endometrium of women with endometriosis. *J Clin Endocrinol Metab,* 79**,** 643-9.

LESSEY, B. A., CASTELBAUM, A. J., SAWIN, S. W. & SUN, J. 1995. Integrins as markers of uterine receptivity in women with primary unexplained infertility. *Fertil Steril,* 63**,** 535-42.

LESSEY, B. A., DAMJANOVICH, L., COUTIFARIS, C., CASTELBAUM, A., ALBELDA, S. M. & BUCK, C. A. 1992. Integrin adhesion molecules in the human endometrium. Correlation with the normal and abnormal menstrual cycle. *J Clin Invest,* 90**,** 188-95.

LESSEY, B. A., GUI, Y., APPARAO, K. B., YOUNG, S. L. & MULHOLLAND, J. 2002. Regulated expression of heparin-binding EGF-like growth factor (HB-EGF) in the human endometrium: a potential paracrine role during implantation. *Mol Reprod Dev,* 62**,** 446-55.

LESSEY, B. A., ILESANMI, A. O., LESSEY, M. A., RIBEN, M., HARRIS, J. E. & CHWALISZ, K. 1996. Luminal and glandular endometrial epithelium express integrins differentially throughout the menstrual cycle: implications for implantation, contraception, and infertility. *Am J Reprod Immunol,* 35**,** 195-204.

LEVI SETTI, P. E., COLOMBO, G. V., SAVASI, V., BULLETTI, C., ALBANI, E. & FERRAZZI, E. 2004. Implantation failure in assisted reproduction technology and a critical approach to treatment. *Ann N Y Acad Sci,* 1034**,** 184-99.

LI, M., YEE, D., MAGNUSON, T. R., SMITHIES, O. & CARON, K. M. 2006. Reduced maternal expression of adrenomedullin disrupts fertility, placentation, and fetal growth in mice. *J Clin Invest,* 116**,** 2653-62.

LI, Q., HOSAKA, T., SHIKAMA, Y., BANDO, Y., KOSUGI, C., KATAOKA, N., NAKAYA, Y. & FUNAKI, M. 2012. Heparin-binding EGF-like growth factor (HB-EGF) mediates 5-HT-induced insulin resistance through activation of EGF receptor-ERK1/2-mTOR pathway. *Endocrinology,* 153**,** 56-68.

LI, X., WANG, L., NUNES, D. P., TROXLER, R. F. & OFFNER, G. D. 2005. Suppression of MUC1 synthesis downregulates expression of the epidermal growth factor receptor. *Cancer Biol Ther,* 4**,** 968-73.

LIANG, C., YANG, Y., LING, Y., HUANG, Y., LI, T. & LI, X. 2011. Improved therapeutic effect of folate-decorated PLGA-PEG nanoparticles for endometrial carcinoma.

Bioorg Med Chem, 19**,** 4057-66.

LIAW, L., ALMEIDA, M., HART, C. E., SCHWARTZ, S. M. & GIACHELLI, C. M. 1994. Osteopontin promotes vascular cell adhesion and spreading and is chemotactic for smooth muscle cells in vitro. *Circ Res,* 74**,** 214-24.

LIAW, L., BIRK, D. E., BALLAS, C. B., WHITSITT, J. S., DAVIDSON, J. M. & HOGAN, B. L. 1998. Altered wound healing in mice lacking a functional osteopontin gene (spp1). *J Clin Invest,* 101**,** 1468-78.

LIAW, L., LINDNER, V., SCHWARTZ, S. M., CHAMBERS, A. F. & GIACHELLI, C. M. 1995a. Osteopontin and beta 3 integrin are coordinately expressed in regenerating endothelium in vivo and stimulate Arg-Gly-Asp-dependent endothelial migration in vitro. *Circ Res,* 77**,** 665-72.

LIAW, L., SKINNER, M. P., RAINES, E. W., ROSS, R., CHERESH, D. A., SCHWARTZ, S. M. & GIACHELLI, C. M. 1995b. The adhesive and migratory effects of osteopontin are mediated via distinct cell surface integrins. Role of alpha v beta 3 in smooth muscle cell migration to osteopontin in vitro. *J Clin Invest,* 95**,** 713-24.

LIAW, L. J., HSU, M. J., LIAO, C. F., LIU, M. F. & HSU, A. T. 2011. The relationships between inter-recti distance measured by ultrasound imaging and abdominal muscle function in postpartum women: a 6-month follow-up study. *J Orthop Sports Phys Ther,* 41**,** 435-43.

LIGTENBERG, M. J., KRUIJSHAAR, L., BUIJS, F., VAN MEIJER, M., LITVINOV, S. V. & HILKENS, J. 1992. Cell-associated episialin is a complex containing two proteins derived from a common precursor. *J Biol Chem,* 267**,** 6171-7.

LIGTENBERG, M. J., VOS, H. L., GENNISSEN, A. M. & HILKENS, J. 1990. Episialin, a carcinoma-associated mucin, is generated by a polymorphic gene encoding splice variants with alternative amino termini. *J Biol Chem,* 265**,** 5573-8.

LIM, H. J. & DEY, S. K. 2009. HB-EGF: a unique mediator of embryo-uterine interactions during implantation. *Exp Cell Res,* 315**,** 619-26.

LIM, J. J., LEE, D. R., SONG, H. S., KIM, K. S., YOON, T. K., GYE, M. C. & KIM, M. K. 2006. Heparin-binding epidermal growth factor (HB-EGF) may improve embryonic development and implantation by increasing vitronectin receptor (integrin alphanubeta3) expression in peri-implantation mouse embryos. *J Assist Reprod Genet,* 23**,** 111-9.

LING, Y., MAILE, L. A., BADLEY-CLARKE, J. & CLEMMONS, D. R. 2005a. DOK1 mediates SHP-2 binding to the alphaVbeta3 integrin and thereby regulates insulin-like growth factor I signaling in cultured vascular smooth muscle cells. *J Biol Chem,*

280**,** 3151-8.

LING, Y., MAILE, L. A., LIESKOVSKA, J., BADLEY-CLARKE, J. & CLEMMONS, D. R. 2005b. Role of SHPS-1 in the regulation of insulin-like growth factor I-stimulated Shc and mitogen-activated protein kinase activation in vascular smooth muscle cells. *Mol Biol Cell,* 16**,** 3353-64.

LITVINOV, S. V. & HILKENS, J. 1993. The epithelial sialomucin, episialin, is sialylated during recycling. *J Biol Chem,* 268**,** 21364-71.

LOBO, S. C., SRISUPARP, S., PENG, X. & FAZLEABAS, A. T. 2001. Uterine receptivity in the baboon: modulation by chorionic gonadotropin. *Semin Reprod Med,* 19**,** 69-74.

LOPATA, A., BENTIN-LEY, U. & ENDERS, A. 2002. "Pinopodes" and implantation. *Rev Endocr Metab Disord,* 3**,** 77-86.

LOPES, I. M., BARACAT, M. C., SIMOES MDE, J., SIMOES, R. S., BARACAT, E. C. & SOARES, J. M., JR. 2011. Endometrium in women with polycystic ovary syndrome during the window of implantation. *Rev Assoc Med Bras,* 57**,** 702-9.

LOUHIO, H., HOVATTA, O., SJOBERG, J. & TUURI, T. 2000. The effects of insulin, and insulin-like growth factors I and II on human ovarian follicles in long-term culture. *Mol Hum Reprod,* 6**,** 694-8.

LUEDTKE, C. C., MCKEE, M. D., CYR, D. G., GREGORY, M., KAARTINEN, M. T., MUI, J. & HERMO, L. 2002. Osteopontin expression and regulation in the testis, efferent ducts, and epididymis of rats during postnatal development through to adulthood. *Biol Reprod,* 66**,** 1437-48.

LUKASSEN, H. G., BRAAT, D. D., WETZELS, A. M., ZIELHUIS, G. A., ADANG, E. M., SCHEENJES, E. & KREMER, J. A. 2005. Two cycles with single embryo transfer versus one cycle with double embryo transfer: a randomized controlled trial. *Hum Reprod,* 20**,** 702-8.

MAHANTA, S., FESSLER, S. P., PARK, J. & BAMDAD, C. 2008. A minimal fragment of MUC1 mediates growth of cancer cells. *PLoS One,* 3**,** e2054.

MAILE, L. A., ADAY, A. W., BUSBY, W. H., SANGHANI, R., VELUVOLU, U. & CLEMMONS, D. R. 2008. Modulation of integrin antagonist signaling by ligand binding of the heparin-binding domain of vitronectin to the alphaVbeta3 integrin. *J Cell Biochem,* 105**,** 437-46.

MAILE, L. A., BUSBY, W. H., SITKO, K., CAPPS, B. E., SERGENT, T., BADLEY-CLARKE, J. & CLEMMONS, D. R. 2006. Insulin-like growth factor-I signaling in

smooth muscle cells is regulated by ligand binding to the 177CYDMKTTC184 sequence of the beta3-subunit of alphaVbeta3. *Mol Endocrinol,* 20**,** 405-13.

MAILE, L. A. & CLEMMONS, D. R. 2002. The alphaVbeta3 integrin regulates insulin-like growth factor I (IGF-I) receptor phosphorylation by altering the rate of recruitment of the Src-homology 2-containing phosphotyrosine phosphatase-2 to the activated IGF-I receptor. *Endocrinology,* 143**,** 4259-64.

MAILE, L. A., IMAI, Y., CLARKE, J. B. & CLEMMONS, D. R. 2002. Insulin-like growth factor I increases alpha Vbeta 3 affinity by increasing the amount of integrin-associated protein that is associated with non-raft domains of the cellular membrane. *J Biol Chem,* 277**,** 1800-5.

MARGALIOTH, E. J., BEN-CHETRIT, A., GAL, M. & ELDAR-GEVA, T. 2006. Investigation and treatment of repeated implantation failure following IVF-ET. *Hum Reprod,* 21**,** 3036-43.

MARHUENDA-EGEA, F. C., MARTINEZ-SABATER, E., GONSALVEZ-ALVAREZ, R., LLEDO, B., TEN, J. & BERNABEU, R. 2010. A crucial step in assisted reproduction technology: human embryo selection using metabolomic evaluation. *Fertil Steril,* 94**,** 772-4.

MARTIN, K. L., BARLOW, D. H. & SARGENT, I. L. 1998. Heparin-binding epidermal growth factor significantly improves human blastocyst development and hatching in serum-free medium. *Hum Reprod,* 13**,** 1645-52.

MCCARTY, J. H., MONAHAN-EARLEY, R. A., BROWN, L. F., KELLER, M., GERHARDT, H., RUBIN, K., SHANI, M., DVORAK, H. F., WOLBURG, H., BADER, B. L., DVORAK, A. M. & HYNES, R. O. 2002. Defective associations between blood vessels and brain parenchyma lead to cerebral hemorrhage in mice lacking alphav integrins. *Mol Cell Biol,* 22**,** 7667-77.

MERVIEL, P., EVAIN-BRION, D., CHALLIER, J. C., SALAT-BAROUX, J. & UZAN, S. 2001. The molecular basis of embryo implantation in humans. *Zentralbl Gynakol,* 123**,** 328-39.

MESEGUER, M., APLIN, J. D., CABALLERO-CAMPO, P., O'CONNOR, J. E., MARTIN, J. C., REMOHI, J., PELLICER, A. & SIMON, C. 2001. Human endometrial mucin MUC1 is up-regulated by progesterone and down-regulated in vitro by the human blastocyst. *Biol Reprod,* 64**,** 590-601.

MESEGUER, M., PELLICER, A. & SIMON, C. 1998. MUC1 and endometrial receptivity. *Mol Hum Reprod,* 4**,** 1089-98.

MI, Z., OLIVER, T., GUO, H., GAO, C. & KUO, P. C. 2007. Thrombin-cleaved COOH(-)

terminal osteopontin peptide binds with cyclophilin C to CD147 in murine breast cancer cells. *Cancer Res,* 67**,** 4088-97.

MIN, J. K., HUGHES, E., YOUNG, D., GYSLER, M., HEMMINGS, R., CHEUNG, A. P., GOODROW, G. J., SENIKAS, V., WONG, B. C., SIERRA, S., CARRANZA-MAMANE, B., CASE, A., DWYER, C., GRAHAM, J., HAVELOCK, J., LEE, F., LIU, K., VAUSE, T., JOINT SOCIETY OF, O., GYNAECOLOGISTS OF CANADA-CANADIAN, F. & ANDROLOGY SOCIETY CLINICAL PRACTICE GUIDELINES, C. 2010. Elective single embryo transfer following in vitro fertilization. *J Obstet Gynaecol Can,* 32**,** 363-77.

MIYAUCHI, A., ALVAREZ, J., GREENFIELD, E. M., TETI, A., GRANO, M., COLUCCI, S., ZAMBONIN-ZALLONE, A., ROSS, F. P., TEITELBAUM, S. L., CHERESH, D. & ET AL. 1991. Recognition of osteopontin and related peptides by an alpha v beta 3 integrin stimulates immediate cell signals in osteoclasts. *J Biol Chem,* 266**,** 20369-74.

MOISEEVA, E. P. 2001. Adhesion receptors of vascular smooth muscle cells and their functions. *Cardiovasc Res,* 52**,** 372-86.

MULLIGAN, C., ROCHFORD, J., DENYER, G., STEPHENS, R., YEO, G., FREEMAN, T., SIDDLE, K. & O'RAHILLY, S. 2002. Microarray analysis of insulin and insulin-like growth factor-1 (IGF-1) receptor signaling reveals the selective up-regulation of the mitogen heparin-binding EGF-like growth factor by IGF-1. *J Biol Chem,* 277**,** 42480-7.

MURATA, K., MARUO, T., MATSUO, H. & MOCHIZUKI, M. 1994. [Insulin-like growth factor-I (IGF-I) as a local regulator of proliferation and differentiation of villous trophoblasts in early pregnancy]. *Nihon Sanka Fujinka Gakkai Zasshi,* 46**,** 87-94.

MURRY, C. E., GIACHELLI, C. M., SCHWARTZ, S. M. & VRACKO, R. 1994. Macrophages express osteopontin during repair of myocardial necrosis. *Am J Pathol,* 145**,** 1450-62.

NAKAMURA, K., IWAMOTO, R. & MEKADA, E. 1995. Membrane-anchored heparin-binding EGF-like growth factor (HB-EGF) and diphtheria toxin receptor-associated protein (DRAP27)/CD9 form a complex with integrin alpha 3 beta 1 at cell-cell contact sites. *J Cell Biol,* 129**,** 1691-705.

NAM, T. J., BUSBY, W. H., JR., REES, C. & CLEMMONS, D. R. 2000. Thrombospondin and osteopontin bind to insulin-like growth factor (IGF)-binding protein-5 leading to an alteration in IGF-I-stimulated cell growth. *Endocrinology,* 141**,** 1100-6.

NARITA, T., KAWAKAMI-KIMURA, N., SATO, M., MATSUURA, N., HIGASHIYAMA, S., TANIGUCHI, N. & KANNAGI, R. 1996. Alteration of integrins by heparin-binding EGF-like growth factor in human breast cancer cells. *Oncology,* 53**,** 374-81.

NICHOLLS, P. K., SUN, Z., HENG, S., LI, Y., WANG, J. & NIE, G. 2011. Embryo implantation is closely associated with dynamic expression of proprotein convertase 5/6 in the rabbit uterus. *Reprod Biol Endocrinol,* 9**,** 43.

NIMBKAR-JOSHI, S., ROSARIO, G., KATKAM, R. R., MANJRAMKAR, D. D., METKARI, S. M., PURI, C. P. & SACHDEVA, G. 2009. Embryo-induced alterations in the molecular phenotype of primate endometrium. *J Reprod Immunol,* 83**,** 65-71.

NISHI, E. & KLAGSBRUN, M. 2004. Heparin-binding epidermal growth factor-like growth factor (HB-EGF) is a mediator of multiple physiological and pathological pathways. *Growth Factors,* 22**,** 253-60.

NISHIDA, M., KASAHARA, K., KANEKO, M., IWASAKI, H. & HAYASHI, K. 1985. [Establishment of a new human endometrial adenocarcinoma cell line, Ishikawa cells, containing estrogen and progesterone receptors]. *Nihon Sanka Fujinka Gakkai Zasshi,* 37**,** 1103-11.

NOLAN, M. K., JANKOWSKA, L., PRISCO, M., XU, S., GUVAKOVA, M. A. & SURMACZ, E. 1997. Differential roles of IRS-1 and SHC signaling pathways in breast cancer cells. *Int J Cancer,* 72**,** 828-34.

NORWITZ, E. R., SCHUST, D. J. & FISHER, S. J. 2001. Implantation and the survival of early pregnancy. *N Engl J Med,* 345**,** 1400-8.

OLAYIOYE, M. A., NEVE, R. M., LANE, H. A. & HYNES, N. E. 2000. The ErbB signaling network: receptor heterodimerization in development and cancer. *EMBO J,* 19**,** 3159-67.

OLSON, G. E., WINFREY, V. P., MATRISIAN, P. E., NAGDAS, S. K. & HOFFMAN, L. H. 1998. Blastocyst-dependent upregulation of metalloproteinase/disintegrin MDC9 expression in rabbit endometrium. *Cell Tissue Res,* 293**,** 489-98.

OMIGBODUN, A., ZIOLKIEWICZ, P., TESSLER, C., HOYER, J. R. & COUTIFARIS, C. 1997. Progesterone regulates osteopontin expression in human trophoblasts: a model of paracrine control in the placenta? *Endocrinology,* 138**,** 4308-15.

ONER, J. & ONER, H. 2007. Immunolocalization of insulin-like growth factor I (IGF-I) during preimplantation in rat uterus. *Growth Horm IGF Res,* 17**,** 271-8.

ORRU, S., CAPUTO, I., D'AMATO, A., RUOPPOLO, M. & ESPOSITO, C. 2003. Proteomics identification of acyl-acceptor and acyl-donor substrates for transglutaminase in a human intestinal epithelial cell line. Implications for celiac disease. *J Biol Chem,* 278**,** 31766-73.

OXLEY, C. L., ANTHIS, N. J., LOWE, E. D., VAKONAKIS, I., CAMPBELL, I. D. & WEGENER, K. L. 2008. An integrin phosphorylation switch: the effect of beta3 integrin tail phosphorylation on Dok1 and talin binding. *J Biol Chem,* 283**,** 5420-6.

PAMPFER, S. & DONNAY, I. 1999. Apoptosis at the time of embryo implantation in mouse and rat. *Cell Death Differ,* 6**,** 533-45.

PANTALEON, M. & KAYE, P. L. 1996. IGF-I and insulin regulate glucose transport in mouse blastocysts via IGF-I receptor. *Mol Reprod Dev,* 44**,** 71-6.

PARIA, B. C., ELENIUS, K., KLAGSBRUN, M. & DEY, S. K. 1999. Heparin-binding EGF-like growth factor interacts with mouse blastocysts independently of ErbB1: a possible role for heparan sulfate proteoglycans and ErbB4 in blastocyst implantation. *Development,* 126**,** 1997-2005.

PARIA, B. C., MA, W., TAN, J., RAJA, S., DAS, S. K., DEY, S. K. & HOGAN, B. L. 2001. Cellular and molecular responses of the uterus to embryo implantation can be elicited by locally applied growth factors. *Proc Natl Acad Sci U S A,* 98**,** 1047-52.

PATARCA, R., FREEMAN, G. J., SINGH, R. P., WEI, F. Y., DURFEE, T., BLATTNER, F., REGNIER, D. C., KOZAK, C. A., MOCK, B. A., MORSE, H. C., 3RD & ET AL. 1989. Structural and functional studies of the early T lymphocyte activation 1 (Eta-1) gene. Definition of a novel T cell-dependent response associated with genetic resistance to bacterial infection. *J Exp Med,* 170**,** 145-61.

PAVELIC, K., PECINA SLAUS, N. & SPAVENTI, R. 1991. Growth factors and proto-oncogenes in early mouse embryogenesis and tumorigenesis. *Int J Dev Biol,* 35**,** 209-14.

PETLEY, T., GRAFF, K., JIANG, W., YANG, H. & FLORINI, J. 1999. Variation among cell types in the signaling pathways by which IGF-I stimulates specific cellular responses. *Horm Metab Res,* 31**,** 70-6.

PLAISIER, M. 2011. Decidualisation and angiogenesis. *Best Pract Res Clin Obstet Gynaecol,* 25**,** 259-71.

POCHAMPALLI, M. R., EL BEJJANI, R. M. & SCHROEDER, J. A. 2007. MUC1 is a novel regulator of ErbB1 receptor trafficking. *Oncogene,* 26**,** 1693-701.

POPOVICI, R. M., KAO, L. C. & GIUDICE, L. C. 2000. Discovery of new inducible genes in in vitro decidualized human endometrial stromal cells using microarray technology. *Endocrinology,* 141**,** 3510-3.

PRINCE, R. N., SCHREITER, E. R., ZOU, P., WILEY, H. S., TING, A. Y., LEE, R. T. & LAUFFENBURGER, D. A. 2010. The heparin-binding domain of HB-EGF

mediates localization to sites of cell-cell contact and prevents HB-EGF proteolytic release. *J Cell Sci,* 123**,** 2308-18.

PSYCHOYOS, A. 1973. Hormonal control of ovoimplantation. *Vitam Horm,* 31**,** 201-56.

PSYCHOYOS, A. 1986. Uterine receptivity for nidation. *Ann N Y Acad Sci,* 476**,** 36-42.

QUENBY, S., ANIM-SOMUAH, M., KALUMBI, C., FARQUHARSON, R. & APLIN, J. D. 2007. Different types of recurrent miscarriage are associated with varying patterns of adhesion molecule expression in endometrium. *Reprod Biomed Online,* 14**,** 224-34.

RAAB, G. & KLAGSBRUN, M. 1997. Heparin-binding EGF-like growth factor. *Biochim Biophys Acta,* 1333**,** F179-99.

RAAB, G., KOVER, K., PARIA, B. C., DEY, S. K., EZZELL, R. M. & KLAGSBRUN, M. 1996. Mouse preimplantation blastocysts adhere to cells expressing the transmembrane form of heparin-binding EGF-like growth factor. *Development,* 122**,** 637-45.

RAMAIAH, S. K. & RITTLING, S. 2008. Pathophysiological role of osteopontin in hepatic inflammation, toxicity, and cancer. *Toxicol Sci,* 103**,** 4-13.

RAMASAMY, S., DURAISAMY, S., BARBASHOV, S., KAWANO, T., KHARBANDA, S. & KUFE, D. 2007. The MUC1 and galectin-3 oncoproteins function in a microRNA-dependent regulatory loop. *Mol Cell,* 27**,** 992-1004.

RANGASWAMI, H., BULBULE, A. & KUNDU, G. C. 2006. Osteopontin: role in cell signaling and cancer progression. *Trends Cell Biol,* 16**,** 79-87.

RECHLER, M. M. & NISSLEY, S. P. 1985. The nature and regulation of the receptors for insulin-like growth factors. *Annu Rev Physiol,* 47**,** 425-42.

REESE, J., WANG, H., DING, T. & PARIA, B. C. 2008. The hamster as a model for embryo implantation: insights into a multifaceted process. *Semin Cell Dev Biol,* 19**,** 194-203.

REGIMBALD, L. H., PILARSKI, L. M., LONGENECKER, B. M., REDDISH, M. A., ZIMMERMANN, G. & HUGH, J. C. 1996. The breast mucin MUCI as a novel adhesion ligand for endothelial intercellular adhesion molecule 1 in breast cancer. *Cancer Res,* 56**,** 4244-9.

REYNOLDS, L. E., WYDER, L., LIVELY, J. C., TAVERNA, D., ROBINSON, S. D., HUANG, X., SHEPPARD, D., HYNES, R. O. & HODIVALA-DILKE, K. M. 2002. Enhanced pathological angiogenesis in mice lacking beta3 integrin or beta3 and

beta5 integrins. *Nat Med,* 8**,** 27-34.

ROBINSON, N. J., BAKER, P. N., JONES, C. J. & APLIN, J. D. 2007. A role for tissue transglutaminase in stabilization of membrane-cytoskeletal particles shed from the human placenta. *Biol Reprod,* 77**,** 648-57.

ROSS, R. S. 2004. Molecular and mechanical synergy: cross-talk between integrins and growth factor receptors. *Cardiovasc Res,* 63**,** 381-90.

ROUDABUSH, F. L., PIERCE, K. L., MAUDSLEY, S., KHAN, K. D. & LUTTRELL, L. M. 2000. Transactivation of the EGF receptor mediates IGF-1-stimulated shc phosphorylation and ERK1/2 activation in COS-7 cells. *J Biol Chem,* 275**,** 22583-9.

RUTANEN, E. M. 1998. Insulin-like growth factors in endometrial function. *Gynecol Endocrinol,* 12**,** 399-406.

SASTRY, S. K. & HORWITZ, A. F. 1993. Integrin cytoplasmic domains: mediators of cytoskeletal linkages and extra- and intracellular initiated transmembrane signaling. *Curr Opin Cell Biol,* 5**,** 819-31.

SCHLAEPFER, D. D., BROOME, M. A. & HUNTER, T. 1997. Fibronectin-stimulated signaling from a focal adhesion kinase-c-Src complex: involvement of the Grb2, p130cas, and Nck adaptor proteins. *Mol Cell Biol,* 17**,** 1702-13.

SCHOU, M., HALLDIN, C., SOVAGO, J., PIKE, V. W., HALL, H., GULYAS, B., MOZLEY, P. D., DOBSON, D., SHCHUKIN, E., INNIS, R. B. & FARDE, L. 2004. PET evaluation of novel radiofluorinated reboxetine analogs as norepinephrine transporter probes in the monkey brain. *Synapse,* 53**,** 57-67.

SCHOYER, K. D., LIU, H. C., WITKIN, S., ROSENWAKS, Z. & SPANDORFER, S. D. 2007. Serum insulin-like growth factor I (IGF-I) and IGF-binding protein 3 (IGFBP-3) in IVF patients with polycystic ovary syndrome: correlations with outcome. *Fertil Steril,* 88**,** 139-44.

SCHROEDER, J. A., THOMPSON, M. C., GARDNER, M. M. & GENDLER, S. J. 2001. Transgenic MUC1 interacts with epidermal growth factor receptor and correlates with mitogen-activated protein kinase activation in the mouse mammary gland. *J Biol Chem,* 276**,** 13057-64.

SCHULZE, E. B., HEDLEY, B. D., GOODALE, D., POSTENKA, C. O., AL-KATIB, W., TUCK, A. B., CHAMBERS, A. F. & ALLAN, A. L. 2008. The thrombin inhibitor Argatroban reduces breast cancer malignancy and metastasis via osteopontin-dependent and osteopontin-independent mechanisms. *Breast Cancer Res Treat,* 112**,** 243-54.

SENGER, D. R., BROWN, L. F., PERRUZZI, C. A., PAPADOPOULOS-SERGIOU, A. & VAN DE WATER, L. 1995. Osteopontin at the tumor/host interface. Functional regulation by thrombin-cleavage and consequences for cell adhesion. *Ann N Y Acad Sci,* 760**,** 83-100.

SENGER, D. R., LEDBETTER, S. R., CLAFFEY, K. P., PAPADOPOULOS-SERGIOU, A., PERUZZI, C. A. & DETMAR, M. 1996. Stimulation of endothelial cell migration by vascular permeability factor/vascular endothelial growth factor through cooperative mechanisms involving the alphavbeta3 integrin, osteopontin, and thrombin. *Am J Pathol,* 149**,** 293-305.

SENGER, D. R. & PERRUZZI, C. A. 1996. Cell migration promoted by a potent GRGDS-containing thrombin-cleavage fragment of osteopontin. *Biochim Biophys Acta,* 1314**,** 13-24.

SENGER, D. R., PERRUZZI, C. A. & PAPADOPOULOS, A. 1989a. Elevated expression of secreted phosphoprotein I (osteopontin, 2ar) as a consequence of neoplastic transformation. *Anticancer Res,* 9**,** 1291-9.

SENGER, D. R., PERRUZZI, C. A., PAPADOPOULOS, A. & TENEN, D. G. 1989b. Purification of a human milk protein closely similar to tumor-secreted phosphoproteins and osteopontin. *Biochim Biophys Acta,* 996**,** 43-8.

SHARKEY, A. M. & SMITH, S. K. 2003. The endometrium as a cause of implantation failure. *Best Pract Res Clin Obstet Gynaecol,* 17**,** 289-307.

SHIOTANI, M., NODA, Y. & MORI, T. 1993. Embryo-dependent induction of uterine receptivity assessed by an in vitro model of implantation in mice. *Biol Reprod,* 49**,** 794-801.

SHISHIDO, Y., SHARMA, K. D., HIGASHIYAMA, S., KLAGSBRUN, M. & MEKADA, E. 1995. Heparin-like molecules on the cell surface potentiate binding of diphtheria toxin to the diphtheria toxin receptor/membrane-anchored heparin-binding epidermal growth factor-like growth factor. *J Biol Chem,* 270**,** 29578-85.

SHUKLA, A., GRISOUARD, J., EHEMANN, V., HERMANI, A., ENZMANN, H. & MAYER, D. 2009. Analysis of signaling pathways related to cell proliferation stimulated by insulin analogs in human mammary epithelial cell lines. *Endocr Relat Cancer,* 16**,** 429-41.

SIMMEN, R. C., SIMMEN, F. A., HOFIG, A., FARMER, S. J. & BAZER, F. W. 1990. Hormonal regulation of insulin-like growth factor gene expression in pig uterus. *Endocrinology,* 127**,** 2166-74.

SIMON, C., GIMENO, M. J., MERCADER, A., O'CONNOR, J. E., REMOHI, J., POLAN,

M. L. & PELLICER, A. 1997. Embryonic regulation of integrins beta 3, alpha 4, and alpha 1 in human endometrial epithelial cells in vitro. *J Clin Endocrinol Metab,* 82**,** 2607-16.

SIMON, C., MARTIN, J. C., MESEGUER, M., CABALLERO-CAMPO, P., VALBUENA, D. & PELLICER, A. 2000a. Embryonic regulation of endometrial molecules in human implantation. *J Reprod Fertil Suppl,* 55**,** 43-53.

SIMON, C., MARTIN, J. C. & PELLICER, A. 2000b. Paracrine regulators of implantation. *Baillieres Best Pract Res Clin Obstet Gynaecol,* 14**,** 815-26.

SIMON, C., OBERYE, J., BELLVER, J., VIDAL, C., BOSCH, E., HORCAJADAS, J. A., MURPHY, C., ADAMS, S., RIESEWIJK, A., MANNAERTS, B. & PELLICER, A. 2005. Similar endometrial development in oocyte donors treated with either high- or standard-dose GnRH antagonist compared to treatment with a GnRH agonist or in natural cycles. *Hum Reprod,* 20**,** 3318-27.

SINGH, H. & APLIN, J. D. 2009. Adhesion molecules in endometrial epithelium: tissue integrity and embryo implantation. *J Anat,* 215**,** 3-13.

SINGH, H., NARDO, L., KIMBER, S. J. & APLIN, J. D. 2010. Early stages of implantation as revealed by an in vitro model. *Reproduction,* 139**,** 905-14.

SINGH, M., CHAUDHRY, P. & ASSELIN, E. 2011. Bridging endometrial receptivity and implantation: network of hormones, cytokines, and growth factors. *J Endocrinol,* 210**,** 5-14.

SKRZYPCZAK, J., MIKOLAJCZYK, M. & SZYMANOWSKI, K. 2001. Endometrial receptivity: expression of alpha3beta1, alpha4beta1 and alphaVbeta1 endometrial integrins in women with impaired fertility. *Reprod Biol,* 1**,** 85-94.

SMITH, C. A., MOORE, H. D. & HEARN, J. P. 1987. The ultrastructure of early implantation in the marmoset monkey (Callithrix jacchus). *Anat Embryol (Berl),* 175**,** 399-410.

SODEK, J., GANSS, B. & MCKEE, M. D. 2000. Osteopontin. *Crit Rev Oral Biol Med,* 11**,** 279-303.

SOMKUTI, S. G., YUAN, L., FRITZ, M. A. & LESSEY, B. A. 1997. Epidermal growth factor and sex steroids dynamically regulate a marker of endometrial receptivity in Ishikawa cells. *J Clin Endocrinol Metab,* 82**,** 2192-7.

SPAVENTI, R., ANTICA, M. & PAVELIC, K. 1990. Insulin and insulin-like growth factor I (IGF I) in early mouse embryogenesis. *Development,* 108**,** 491-5.

SPENCER, T. E., JOHNSON, G. A., BAZER, F. W. & BURGHARDT, R. C. 2004. Implantation mechanisms: insights from the sheep. *Reproduction,* 128**,** 657-68.

SRINIVASAN, K. R., BLESSON, C. S., FATIMA, I., KITCHLU, S., JAIN, S. K., MEHROTRA, P. K. & DWIVEDI, A. 2009. Expression of alphaVbeta3 integrin in rat endometrial epithelial cells and its functional role during implantation. *Gen Comp Endocrinol,* 160**,** 124-33.

STANDAL, T., BORSET, M. & SUNDAN, A. 2004. Role of osteopontin in adhesion, migration, cell survival and bone remodeling. *Exp Oncol,* 26**,** 179-84.

STAVREUS-EVERS, A., AGHAJANOVA, L., BRISMAR, H., ERIKSSON, H., LANDGREN, B. M. & HOVATTA, O. 2002. Co-existence of heparin-binding epidermal growth factor-like growth factor and pinopodes in human endometrium at the time of implantation. *Mol Hum Reprod,* 8**,** 765-9.

STRAUSS, R., LI, Z. Y., LIU, Y., BEYER, I., PERSSON, J., SOVA, P., MOLLER, T., PESONEN, S., HEMMINKI, A., HAMERLIK, P., DRESCHER, C., URBAN, N., BARTEK, J. & LIEBER, A. 2011. Analysis of epithelial and mesenchymal markers in ovarian cancer reveals phenotypic heterogeneity and plasticity. *PLoS One,* 6**,** e16186.

SURVEYOR, G. A., GENDLER, S. J., PEMBERTON, L., DAS, S. K., CHAKRABORTY, I., JULIAN, J., PIMENTAL, R. A., WEGNER, C. C., DEY, S. K. & CARSON, D. D. 1995. Expression and steroid hormonal control of Muc-1 in the mouse uterus. *Endocrinology,* 136**,** 3639-47.

SUTHERLAND, A. E., CALARCO, P. G. & DAMSKY, C. H. 1993. Developmental regulation of integrin expression at the time of implantation in the mouse embryo. *Development,* 119**,** 1175-86.

TABIBZADEH, S. 1998. Molecular control of the implantation window. *Hum Reprod Update,* 4**,** 465-71.

TADOKORO, S., SHATTIL, S. J., ETO, K., TAI, V., LIDDINGTON, R. C., DE PEREDA, J. M., GINSBERG, M. H. & CALDERWOOD, D. A. 2003. Talin binding to integrin beta tails: a final common step in integrin activation. *Science,* 302**,** 103-6.

TAKADA, Y., YE, X. & SIMON, S. 2007. The integrins. *Genome Biol,* 8**,** 215.

TEKLENBURG, G. & MACKLON, N. S. 2009. Review: in vitro models for the study of early human embryo-endometrium interactions. *Reprod Sci,* 16**,** 811-8.

TERRY, V., SHAW, T. J., SHOREY, C. D. & MURPHY, C. R. 1996. Actin-binding proteins undergo major alterations during the plasma membrane transformation in

uterine epithelial cells. *Anat Rec,* 246**,** 71-7.

THATHIAH, A., BLOBEL, C. P. & CARSON, D. D. 2003. Tumor necrosis factor-alpha converting enzyme/ADAM 17 mediates MUC1 shedding. *J Biol Chem,* 278**,** 3386-94.

THATHIAH, A. & CARSON, D. D. 2002. Mucins and blastocyst attachment. *Rev Endocr Metab Disord,* 3**,** 87-96.

TOZER, E. C., HUGHES, P. E. & LOFTUS, J. C. 1996. Ligand binding and affinity modulation of integrins. *Biochem Cell Biol,* 74**,** 785-98.

TSUJIOKA, H., YOTSUMOTO, F., HIKITA, S., UEDA, T., KUROKI, M. & MIYAMOTO, S. 2011. Targeting the heparin-binding epidermal growth factor-like growth factor in ovarian cancer therapy. *Curr Opin Obstet Gynecol,* 23**,** 24-30.

UCHIDA, H., MARUYAMA, T., NISHIKAWA-UCHIDA, S., ODA, H., MIYAZAKI, K., YAMASAKI, A. & YOSHIMURA, Y. 2012. Studies using an in vitro model show evidence of involvement of epithelial-mesenchymal transition of human endometrial epithelial cells in human embryo implantation. *J Biol Chem,* 287**,** 4441-50.

VAN DER FLIER, A. & SONNENBERG, A. 2001. Function and interactions of integrins. *Cell Tissue Res,* 305**,** 285-98.

VAN MONTFOORT, A. P., FIDDELERS, A. A., JANSSEN, J. M., DERHAAG, J. G., DIRKSEN, C. D., DUNSELMAN, G. A., LAND, J. A., GERAEDTS, J. P., EVERS, J. L. & DUMOULIN, J. C. 2006. In unselected patients, elective single embryo transfer prevents all multiples, but results in significantly lower pregnancy rates compared with double embryo transfer: a randomized controlled trial. *Hum Reprod,* 21**,** 338-43.

VAN VAERENBERGH, I., MCINTIRE, R., VAN LOMMEL, L., DEVROEY, P., GIUDICE, L. & BOURGAIN, C. 2010. Gene expression during successful implantation in a natural cycle. *Fertil Steril,* 93**,** 268 e15-8.

VON WOLFF, M., STROWITZKI, T., BECKER, V., ZEPF, C., TABIBZADEH, S. & THALER, C. J. 2001. Endometrial osteopontin, a ligand of beta3-integrin, is maximally expressed around the time of the "implantation window". *Fertil Steril,* 76**,** 775-81.

WANG, H. & DEY, S. K. 2006. Roadmap to embryo implantation: clues from mouse models. *Nat Rev Genet,* 7**,** 185-99.

WANG, J., MAYERNIK, L., SCHULTZ, J. F. & ARMANT, D. R. 2000. Acceleration of

trophoblast differentiation by heparin-binding EGF-like growth factor is dependent on the stage-specific activation of calcium influx by ErbB receptors in developing mouse blastocysts. *Development,* 127**,** 33-44.

WANG, X., WANG, H., MATSUMOTO, H., ROY, S. K., DAS, S. K. & PARIA, B. C. 2002. Dual source and target of heparin-binding EGF-like growth factor during the onset of implantation in the hamster. *Development,* 129**,** 4125-34.

WEBER, G. F. 2001. The metastasis gene osteopontin: a candidate target for cancer therapy. *Biochim Biophys Acta,* 1552**,** 61-85.

WEBER, G. F., ASHKAR, S., GLIMCHER, M. J. & CANTOR, H. 1996. Receptor-ligand interaction between CD44 and osteopontin (Eta-1). *Science,* 271**,** 509-12.

WEI, Q., ST CLAIR, J. B., FU, T., STRATTON, P. & NIEMAN, L. K. 2009. Reduced expression of biomarkers associated with the implantation window in women with endometriosis. *Fertil Steril,* 91**,** 1686-91.

WEI, X., XU, H. & KUFE, D. 2005. Human MUC1 oncoprotein regulates p53-responsive gene transcription in the genotoxic stress response. *Cancer Cell,* 7**,** 167-78.

WEINTRAUB, A. S., LIN, X., ITSKOVICH, V. V., AGUINALDO, J. G., CHAPLIN, W. F., DENHARDT, D. T. & FAYAD, Z. A. 2004. Prenatal detection of embryo resorption in osteopontin-deficient mice using serial noninvasive magnetic resonance microscopy. *Pediatr Res,* 55**,** 419-24.

WESSELING, J., VAN DER VALK, S. W. & HILKENS, J. 1996. A mechanism for inhibition of E-cadherin-mediated cell-cell adhesion by the membrane-associated mucin episialin/MUC1. *Mol Biol Cell,* 7**,** 565-77.

WHITE, F. J., BURGHARDT, R. C., HU, J., JOYCE, M. M., SPENCER, T. E. & JOHNSON, G. A. 2006. Secreted phosphoprotein 1 (osteopontin) is expressed by stromal macrophages in cyclic and pregnant endometrium of mice, but is induced by estrogen in luminal epithelium during conceptus attachment for implantation. *Reproduction,* 132**,** 919-29.

WHITE, F. J., ROSS, J. W., JOYCE, M. M., GEISERT, R. D., BURGHARDT, R. C. & JOHNSON, G. A. 2005. Steroid regulation of cell specific secreted phosphoprotein 1 (osteopontin) expression in the pregnant porcine uterus. *Biol Reprod,* 73**,** 1294-301.

WILCOX, A. J., BAIRD, D. D. & WEINBERG, C. R. 1999. Time of implantation of the conceptus and loss of pregnancy. *N Engl J Med,* 340**,** 1796-9.

WIMSATT, W. A. 1975. Some comparative aspects of implantation. *Biol Reprod,* 12**,** 1-40.

WOODWARD, T. L., XIE, J., FENDRICK, J. L. & HASLAM, S. Z. 2000. Proliferation of mouse mammary epithelial cells in vitro: interactions among epidermal growth factor, insulin-like growth factor I, ovarian hormones, and extracellular matrix proteins. *Endocrinology,* 141**,** 3578-86.

WU, R. J. & ZHOU, F. Z. 2002. [Endometrial insulin-like growth factor II and type I receptor in unexplained infertility and its steroid regulation]. *Zhejiang Da Xue Xue Bao Yi Xue Ban,* 31**,** 163-166.

XIE, H., WANG, H., TRANGUCH, S., IWAMOTO, R., MEKADA, E., DEMAYO, F. J., LYDON, J. P., DAS, S. K. & DEY, S. K. 2007. Maternal heparin-binding-EGF deficiency limits pregnancy success in mice. *Proc Natl Acad Sci U S A,* 104**,** 18315-20.

XIE, Y., SAKATSUME, M., NISHI, S., NARITA, I., ARAKAWA, M. & GEJYO, F. 2001. Expression, roles, receptors, and regulation of osteopontin in the kidney. *Kidney Int,* 60**,** 1645-57.

XIONG, J. P., STEHLE, T., ZHANG, R., JOACHIMIAK, A., FRECH, M., GOODMAN, S. L. & ARNAOUT, M. A. 2002. Crystal structure of the extracellular segment of integrin alpha Vbeta3 in complex with an Arg-Gly-Asp ligand. *Science,* 296**,** 151-5.

XU, X., CAPITO, R. M. & SPECTOR, M. 2008. Delivery of plasmid IGF-1 to chondrocytes via cationized gelatin nanoparticles. *J Biomed Mater Res A,* 84**,** 73-83.

XU, X., RAO, G., QUIROS, R. M., KIM, A. W., MIAO, H. Q., BRUNN, G. J., PLATT, J. L., GATTUSO, P. & PRINZ, R. A. 2007. In vivo and in vitro degradation of heparan sulfate (HS) proteoglycans by HPR1 in pancreatic adenocarcinomas. Loss of cell surface HS suppresses fibroblast growth factor 2-mediated cell signaling and proliferation. *J Biol Chem,* 282**,** 2363-73.

YAHATA, Y., SHIRAKATA, Y., TOKUMARU, S., YANG, L., DAI, X., TOHYAMA, M., TSUDA, T., SAYAMA, K., IWAI, M., HORIUCHI, M. & HASHIMOTO, K. 2006. A novel function of angiotensin II in skin wound healing. Induction of fibroblast and keratinocyte migration by angiotensin II via heparin-binding epidermal growth factor (EGF)-like growth factor-mediated EGF receptor transactivation. *J Biol Chem,* 281**,** 13209-16.

YAMAMOTO, M., BHARTI, A., LI, Y. & KUFE, D. 1997. Interaction of the DF3/MUC1 breast carcinoma-associated antigen and beta-catenin in cell adhesion. *J Biol Chem,* 272**,** 12492-4.

YARDEN, Y. & SLIWKOWSKI, M. X. 2001. Untangling the ErbB signalling network. *Nat Rev Mol Cell Biol,* 2**,** 127-37.

YLANNE, J., HUUSKONEN, J., O'TOOLE, T. E., GINSBERG, M. H., VIRTANEN, I. & GAHMBERG, C. G. 1995. Mutation of the cytoplasmic domain of the integrin beta 3 subunit. Differential effects on cell spreading, recruitment to adhesion plaques, endocytosis, and phagocytosis. *J Biol Chem,* 270**,** 9550-7.

YOKOSAKI, Y., MATSUURA, N., SASAKI, T., MURAKAMI, I., SCHNEIDER, H., HIGASHIYAMA, S., SAITOH, Y., YAMAKIDO, M., TAOOKA, Y. & SHEPPARD, D. 1999. The integrin alpha(9)beta(1) binds to a novel recognition sequence (SVVYGLR) in the thrombin-cleaved amino-terminal fragment of osteopontin. *J Biol Chem,* 274**,** 36328-34.

YOKOSAKI, Y., TANAKA, K., HIGASHIKAWA, F., YAMASHITA, K. & EBOSHIDA, A. 2005. Distinct structural requirements for binding of the integrins alphavbeta6, alphavbeta3, alphavbeta5, alpha5beta1 and alpha9beta1 to osteopontin. *Matrix Biol,* 24**,** 418-27.

YOO, H. J., BARLOW, D. H. & MARDON, H. J. 1997. Temporal and spatial regulation of expression of heparin-binding epidermal growth factor-like growth factor in the human endometrium: a possible role in blastocyst implantation. *Dev Genet,* 21**,** 102-8.

YUE, Z. P., YANG, Z. M., LI, S. J., WANG, H. B. & HARPER, M. J. 2000. Epidermal growth factor family in rhesus monkey uterus during the menstrual cycle and early pregnancy. *Mol Reprod Dev,* 55**,** 164-74.

ZHANG, R. J., ZOU, L. B., ZHANG, D., TAN, Y. J., WANG, T. T., LIU, A. X., QU, F., MENG, Y., DING, G. L., LU, Y. C., LV, P. P., SHENG, J. Z. & HUANG, H. F. 2012. Functional expression of large-conductance calcium-activated potassium channels in human endometrium: a novel mechanism involved in endometrial receptivity and embryo implantation. *J Clin Endocrinol Metab,* 97**,** 543-53.

ZHANG, Z., FUNK, C., GLASSER, S. R. & MULHOLLAND, J. 1994a. Progesterone regulation of heparin-binding epidermal growth factor-like growth factor gene expression during sensitization and decidualization in the rat uterus: effects of the antiprogestin, ZK 98.299. *Endocrinology,* 135**,** 1256-63.

ZHANG, Z., FUNK, C., ROY, D., GLASSER, S. & MULHOLLAND, J. 1994b. Heparin-binding epidermal growth factor-like growth factor is differentially regulated by progesterone and estradiol in rat uterine epithelial and stromal cells. *Endocrinology,* 134**,** 1089-94.

ZHENG, B. & CLEMMONS, D. R. 1998. Blocking ligand occupancy of the alphaVbeta3 integrin inhibits insulin-like growth factor I signaling in vascular smooth muscle cells. *Proc Natl Acad Sci U S A,* 95**,** 11217-22.

ZHOU, J., DSUPIN, B. A., GIUDICE, L. C. & BONDY, C. A. 1994. Insulin-like growth

factor system gene expression in human endometrium during the menstrual cycle. *J Clin Endocrinol Metab,* 79**,** 1723-34.

ZOHAR, R., SUZUKI, N., SUZUKI, K., ARORA, P., GLOGAUER, M., MCCULLOCH, C. A. & SODEK, J. 2000. Intracellular osteopontin is an integral component of the CD44-ERM complex involved in cell migration. *J Cell Physiol,* 184**,** 118-30.

ZOTTER, S., HAGEMAN, P. C., LOSSNITZER, A., VAN DEN TWEEL, J., HILKENS, J., MOOI, W. J. & HILGERS, J. 1988. Monoclonal antibodies to epithelial sialomucins recognize epitopes at different cellular sites in adenolymphomas of the parotid gland. *Int J Cancer Suppl,* 3**,** 38-44.



Supplementary Appendices

Supplementary Appendix 1

Buffers and solutions

Standard solutions

Phosphate Buffered Saline (PBS)

171mM NaCl, 3.35mM KCl, 10.1mM Na_2HPO_4, 18.83mM KH_2PO_4, pH 7.6 with NaOH

Tris-Buffered Saline (TBS)

150mM NaCl, 10mM Tris, pH 8.0 with HCl

Tris-Buffered Saline with Tween (TBS/T)

150mM NaCl, 10mM Tris, pH 8.0 with HCl 0.05% (v/v) Tween 20 added after pH adjustment.

Tris-HCL (pH 8.3/6.5)

150mM NaCl, 10mM Tris, pH 8.3/6.5 with HCl

Immunocytochemistry

Fixative

4% Paraformaldehyde in 100ml dH_2O, dissolved on a heat block with stirring in a fume hood; stored at -20°C in 4ml aliquots.

Permeablisation

0.05% Triton-X in PBS

Western Blotting

SDS-PAGE Buffers

- Resolving gel buffer : 1.5M Tris HCL pH 8.8
- Stacking gel buffer : 0.5M Tris HCL pH 6.8
- Sample buffer (4x) : 63mM Tris-HCL, Ph6.8, 2mM NA4P2O7, 5mM EDTA, 10% (v/v) glycerol, 2% (w/v) SDS, 50mM DTT, 0.007% (w/v) bromophenol blue
- Bis-Acryamide : 30% bis-Acrylamide
- TEMED : N, N, N', N' –Tetramethyl Ethylenediamine
- APS (10%) : 1g Ammonium Persulphate; dH_2O up to 10ml
- Running buffer : 6g Tris Base, 28.8g Glycine, 2g SDS; dH_2O up to 2 litre
- Transfer buffer : 6g Tris Base, 28.8g Glycine, 400ml methanol; dH_2O up to 2 litre

Blocking buffer

5% Bovine Serum Albumin in TBS/T

ECL reagent 1

1ml 250mM Luminol, 0.44ml 250mM p-coumaric acid, 10ml 1M Tris pH 8.5, made up to 100ml with dH_2O

ECL reagent 2

10ml 1M Tris, pH 8.5, 64µl 30% hydrogen peroxide, make up to 100ml with dH_2O

Stripping buffer

0.1M glycine, pH 5.2

Embryo culture

Pregnant Mare Serum Gonadotrophin (PMSG)

1 vial lyophilised PMSG, 1000 IU (Calbiochem, Nottingham, UK) in 20ml normal saline (Baxter Healthcare Ltd, Norfolk, UK), stored at -20°C in 1ml aliquots

Human Chorionic Gonadotrophin (hCG)

1 vial 'Chorulon', 1500 IU lyophilised hCG (Intervet, UK Ltd, Cambridge, UK) in 30 ml normal saline (Baxter Healthcare Ltd, Norfolk, UK), stored at -20°C in 1ml aliquots

M2 media

M2 media (Sigma, UK) was supplemented with 4mg/ml bovine serum albumin and stored at 4°C. The solution was placed on a heat block at 37°C prior to use.

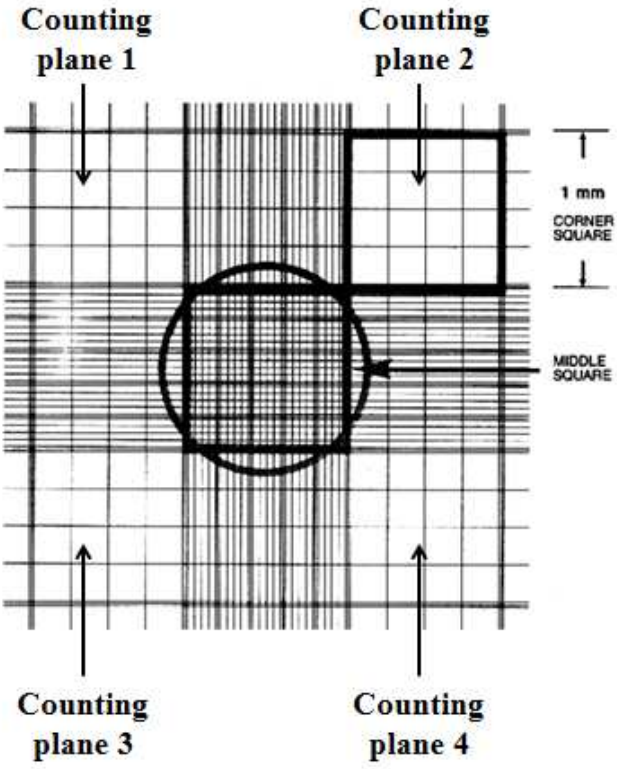
KSOM (EmbryoMax KSOM Embryo Culture (1x), Powder, w/o Phenol Red)

Stored at -20°C in 5 ml aliquots. Prior to use, the solution was thawed at 37°C and placed on a heat block at 37°C.

Supplementary Appendix 2

Cell counting

Following resuspension of pelletes of 1 ml of media, cells were diluted in Trypan Blue dye exclusion medium (1 in 10 dilutions). 20 µl of diluted cells were transferred evenly to a hemacytometer chamber. Cells on the counting plane of four large corner squares were counted under a microscope. It should be noted that dead cells appeared blue while live cells were birefringent. Each square had a surface area of $1mm^2$ and a depth of 0.1 mm, giving a volume of 0.1 mm^3. For example, if 100 cells were counted from 4 counting planes, it follows that 25 cells were in one counting plane (25 cells per 0.1 mm^3). Thus, it could be determined that the total cell number per 1 ml was $2.5x10^5$ by the number of cells in one square by $1x10^4$.



Supplementary Appendix 3

Clinical procedures of ovarian stimulation, oocyte retrieval and insemination prior to embryo classification for IVF treatment

Ovarian stimulation was achieved by Nafarelin (Searle, High Wycombe, UK) to induce pituitary down-regulation starting on day 21 of the luteal phase of the menstrual cycle, followed by Metrodin (Serono, Welwyn Garden City, UK) administration for 9-13 days. Cycles were monitored biochemically, and follicular development was assessed by vaginal ultrasound. Oocyte retrieval was performed 35 h following human chorionic gonadotrophin (HCG) administration by vaginal ultrasound-guided aspiration. Oocytes were incubated for 5-6 h prior to insemination and checked 12-18 h following insemination for fertilisation by the presence of pronuclei. Embryos following insemination were initially maintained individually in 1 ml of Tyrode's 6 (T6) culture medium supplemented with 10% of human serum albumin (HSA) at 5% CO_2, 37°C.

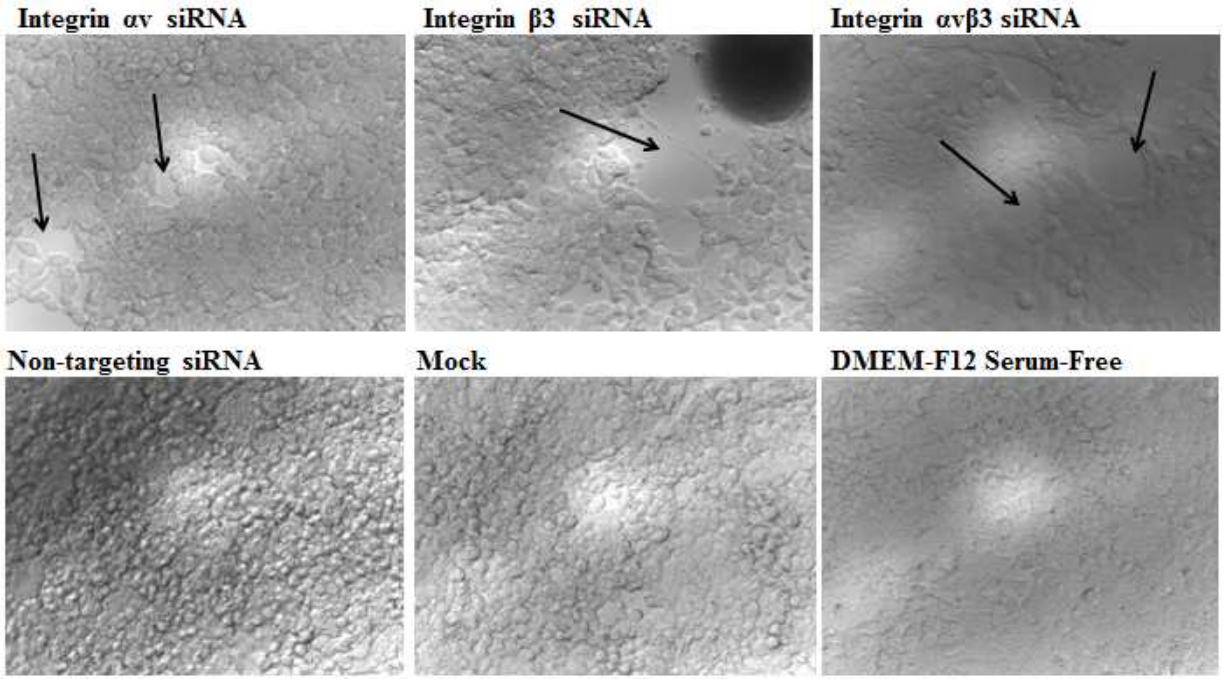
Supplementary Appendix 4

Studies of each molecule on heterologous and homologous *in vitro* models

	Mouse Embryo (N)				Human Embryo (N)	
	2D Model		3D Model		2D Model	
	Gel (N)	Data shown (Y/N)	Gel (N)	Data shown (Y/N)	Gel (N)	Data shown (Y/N)
MUC1	√ (31)		√ (6)		√ (9)	
	13	Y	3	Y	9	Y
Integrin αvβ3	√ (55)		√ (6)		√ (8)	
	31	Y	3	Y	8	Y
Integrin αvβ5	√ (17)		√ (6)		√ (5)	
	8	N	3	Y	5	Y
OPN	√ (6)		-		-	
	6	Y	-	-	-	-
HB-EGF	√ (35)		√ (6)		√ (4)	
	16	Y	4	N	4	N
IGF-IR β	√ (3)		-		-	
	3	Y	-	-	-	-
SHP-2	√ (6)		-		-	
	3	Y	-	-	-	-

(√ : Number of embryos studied)

Supplementary Appendix 5



Morphological alterations resulting from 72 h of transfection with siRNA targeting integrin αvβ3

Phase contrast images demonstrating morphology of Ishikawa cells transfected with siRNA targeting integrin αv, β3, αvβ3, non-target, or mock transfection for 72 h. Morphological alterations (marked with black arrows) were observed in cells transfected with integrin αv, β3, or αvβ3 siRNA compared to control or non-targeting siRNA or mock-transfected cells. The diagonal stripe on images was caused from a cracked element in the fluorescence light path. Images were captured at a magnification of 10X.



List of publications

International peer-reviewed articles

1. H. Singh, **YJ Kang** and JD Aplin (2012) Apical glycoproteomic analysis reveals roles for cadherin 6 in endometrial epithelial integrity, and integrin αvβ3 in embryo implantation. Journal of Cell Science (reviewed, revision in progress in response to Referee comments)

2. **YJ Kang**, K. Forbes, J. Carver, SJ Kimber and JD Aplin (2012) Synergy between integrin αvβ3, osteopontin and growth factor pathways in embryo-epithelial adhesion at implantation (in preparation)

3. **YJ Kang**, K. Forbes and JD Aplin (2012) MicroRNA 145 overexpression suppresses embryo-epithelial juxtacrine communication at implantation by modulating maternal IGF1R expression (in preparation)

Presentations at international and university conferences

1. Kang YJ et al. (2011) **Embryo-epithelial adhesion mediated by integrin αvβ3, osteopontin and growth factors.** Get Connected 2 Welcome Trust Matrix Meeting, Manchester, UK (poster presentation)

2. Kang YJ et al. (2011) **Synergy between integrin αvβ3, osteopontin and growth factor pathways in embryo-epithelial adhesion at implantation.** British Society of Matrix Biology Meeting, Newcastle, UK (poster & oral presentation, best poster prize awarded)

3. Kang YJ et al. (2012) **Synergy between integrin αvβ3, osteopontin and growth factor pathways in embryo-epithelial adhesion at implantation.** Research Symposium of the University of Oxford, Oxford, UK (24, Jan, 2012)

4. Kang YJ et al. (2012) **Short-interfering RNA mediated knock-down of integrin αvβ3**

or its ligand osteopontin suppresses embryo-epithelial adhesion at implantation. RNAi Meeting. Oxford, UK (poster & oral presentation, 27-29, Mar, 2012)

5. Kang YJ et al. (2012) **MicroRNA 145 overexpression suppresses embryo-epithelial juxtacrine communication at implantation by modulating maternal IGF1R expression.** RNAi Meeting. Oxford, UK (poster presentation, 27-29, Mar, 2012)

6. Kang YJ et al. (2012) **Integrin-growth factor cross-talk during embryo implantation**. 25th UK Adhesion Society Meeting "Cell trafficking; new directions". Sheffield, UK (poster & oral presentation, 17, Apr, 2012)

7. Kang YJ et al. (2012) **IGF-1 mediates embryo-epithelial juxtacrine communication at implantation through the osteopontin-integrin αvβ3 system.** GRS and IGF meeting. Munich, Germany (17-20, Oct, 2012)

8. Kang YJ et al. (2012) **MicroRNA 145 overexpression suppresses embryo-epithelial juxtacrine communication at implantation by modulating maternal IGF1R expression.** GRS and IGF meeting. Munich, Germany (17-20, Oct, 2012)

Popular science articles

1. Junaid Kashir, Celine Jones, Walaa Ramadan, **Youn-Jung Kang**, Janet Carver, Tracey Griffiths, Karen Turner and Kevin Coward (2012). **Magnifying human fertility: microscopy and assisted reproductive technology. 'In Focus'** – Journal of the Royal Microscopy Society (Invited Article), 25,4-23

Prizes and awards

Best Poster Prize: British Society of Matrix Biology Meeting. 2010. Newcastle